THE UNIVERSITY OF AUCKLAND

Stability Analysis and Controller Synthesis for Networked Control Systems

by

Faiz Rasool

A thesis submitted in partial fulfillment
of the requirements for the degree of
Doctor of Philosophy

in the
FACULTY OF ENGINEERING
DEPARTMENT OF ELECTRICAL AND COMPUTER ENGINEERING

October 2013

Declaration of Authorship

I, Faiz Rasool, declare that this thesis titled, 'Stability Analysis and Controller Synthesis for Networked Control Systems' and the work presented in it are my own. I confirm that:

- This work was done wholly or mainly while in candidature for a research degree at this University.

- Where any part of this thesis has previously been submitted for a degree or any other qualification at this University or any other institution, this has been clearly stated.

- Where I have consulted the published work of others, this is always clearly attributed.

- Where I have quoted from the work of others, the source is always given. With the exception of such quotations, this thesis is entirely my own work.

- I have acknowledged all main sources of help.

- Where the thesis is based on work done by myself jointly with others, I have made clear exactly what was done by others and what I have contributed myself.

Signed:
_____

Date:
_____

Abstract

In recent years, Networked Control Systems (NCSs) are recognized as a new research frontier in the advanced control engineering, theory and applications due to various advantages such as higher reliability, more flexibility, design modularity, and easier deployment and maintenance. An NCS refers to a system controlled remotely by a digital controller over a wired or wireless network. Networks can be either dedicated such as control area network (CAN), or shared such as Internet. In the NCSs, system components such as plant, sensor, controller and actuator are spatially distributed over the networks and each component represents a network node. Several design constraints have also emerged due to insertion of networks and distributed system components. Recently, two research approaches, 1) scheduling algorithms, and 2) control designs, are used to cater for the constraints in the NCSs. The scheduling algorithm approach is used to reduce the effect of network-induced constraints on the system performance, whereas control design approach covers novel control methodologies that compensate for the inherited constraints.

In this thesis, control design approach is investigated to improve quality of control in the NCSs. It requires identification and modelling of the constraints before their incorporation in the system designs. Therefore, the potential constraints, induced by a network, are identified with a detailed literature survey and by a comparison of two sampling mechanisms: 1) time triggered (TT), and 2) event triggered (ET). Both mechanisms are compared through qualitative analysis and simulations, and effect of these mechanisms is analyzed on the system performance. The constraints identified in this research include: 1) time delays, 2) packet dropouts, 3) quantization error, and 4) limited bandwidth.

Time delays that cause performance degradation and system instability are mostly time varying or random in shared networks. In this thesis, time delays are considered as stochastic processes, which follow a finite state Markov chain. The transitions in the Markov chain take values from a transition probability matrix obtained by performing experiments on a cellular network. Packet dropouts that adversely affect the system performance can be single or successive. This work presents the modelling of single and successive packet dropouts using Bernoulli random distribution and Poisson distribution, respectively. In the NCSs, networks and controllers are digital which require quantization of data before transmission of data from sensor to controller over a network. Quantization process not only adds up quantization error in the system design, but is also useful in the NCSs designs as an information coder. In this thesis, both characteristics of the quantizers are investigated. Firstly, a sector bound approach is used to bound the quantization error and robust state and output feedback controllers are proposed to mitigate its effect. In case of multiple quantizers, errors are bounded by

the sector bound approach and are represented as poly-topic uncertainties. Secondly, an adaptive quantizer is proposed to explore its advantages as an information coder. The quantizer adapts its quantization densities according to network load conditions, hence is used to adjust data rate. Since components are directly connected in classic control systems, bandwidth is therefore infinite, whereas components are spatially distributed in the NCSs, bandwidth is therefore limited. To cater for this issue, robust state and output feedback controllers are proposed with a novel congestion control mechanism. In this mechanism, data is transmitted when required which helps in the optimization of bandwidth utilization. In addition to congestion control mechanism, this work also investigates ET sampling mechanism to optimize the bandwidth consumption. Various NCSs frameworks are considered which incorporate one or more constraints. For each framework, the constraints are properly modelled before proposing stability criterion and control design.

This thesis proposes detailed Lyapunov-Krasovskii (L-K) functionals to obtain new sufficient conditions for the stability of NCSs. On the basis of stability criteria, state of the art control laws are proposed in terms of bilinear matrix inequalities (BMIs). Furthermore, an iterative cone complementarity algorithm is suggested to convert the BMIs into quasi-convex linear matrix inequalities (LMIs). Numerical values of the proposed controllers are obtained by solving the LMIs with the help of MATLAB based LMI and YALMIP toolboxes.

Simulation examples, performed using Simulink and Simulink based toolbox TrueTime, elaborate the effectiveness of the proposed designs. Simulation results are also used to analyze the effects of the NCSs constraint on system stability, $\mathcal{H}_\infty$ performance, and bandwidth utilization.

Acknowledgements

First and above all, I praise Omnipresent ALLAH, the Almighty, for providing me with this opportunity and granting me the capability and strength to strive successfully in seeking knowledge. This thesis appears in its current form due to the assistance and/or guidance of several people and organizations. I would therefore like to offer my sincere thanks to all of them, especially the following:

Contents

List of Figures

List of Tables

Abbreviations

NCSs   Networked Control Systems

TDSs   Time-Delayed Systems

CAN   Control Area Network

TT   Time Triggered

ET   Event Triggered

ST   Self Triggered

QoC   Quality of Control

MATI   Maximum Allowable Transmission Interval

TD   Time Delays

L-K   Lyapunov-Krasovskii

L-R   Lyapunov-Razumikhin

ZOH   Zero Order Hold

LTI   Linear Time Invariant

LMI   Linear Matrix Inequality

BMI   Bilinear Matrix Inequality

Notations

The notations used in this thesis are quite standard. R^n and $R^{n \times m}$ denote the set of $n \times 1$ vectors, and the set of all $n \times m$ matrices, respectively. The superscript T denotes the transpose and $*$ represents the transposed symmetric entries in the matrix inequalities. The I represents the identity matrix, and $\mathcal{L}_2[0, \infty)$, the space of square summable vector sequence over $[0, \infty)$. The $\|.\|_{[0,\infty)}$ denotes the $\mathcal{L}_2[0, \infty)$ norm over $[0, \infty)$ defined as $\|f(x)\|^2_{[0,\infty)} = \sum_0^\infty \|f(x)\|^2$. $Q > 0$ and $Q < 0$ denote the positive and negative definiteness of the Q, respectively. The $diag(A_1; ....; A_n)$ denotes a block-diagonal matrix with the elements $A_1; ...; A_n$ on the diagonal.

Dedicated to Islam, my way of living

Chapter 1

Introduction

1.1 Networked Control Systems

Today's large scale and complex systems integrate communication, computing and control on the different levels of their operational and informational processes [1]. The integration of these fields results in two new research fields, 1) control of the networks and 2) Networked Control Systems (NCSs). The former field addresses the application of control methods to improve the quality of networks e.g., congestion control, routing control and queue management etc. The latter field talks about the insertion of a network in the closed-loop of a control system. This thesis is a detailed study on the NCSs.

The control systems in which components e.g., plants and controllers are spatially distributed and communicate with each other, with the help of sensors and actuators, over a network are called NCSs. A large number of the industrial control systems such as displacement control in a motor are discrete in nature [3]. On the other hand, the evolution of the digital controllers in $1970s$ added new horizons in the control systems. The focus of the research are discrete-time systems controlled by the digital controllers over a network. In the NCSs, each system component can be recognised as a node. At least two network nodes are required to describe a single loop of a discrete-time NCS. In a simple NCS configuration, as shown in Figure 1.1, the plant output is sensed and transmitted by the channel encoder. The encoder node includes a quantizer and a triggering mechanism. The data is received with the help of a channel decoder by the controller that calculates the control input and transmits it over the network. The control input is received by the chancel decoder at the plant side which is applied to the plant by the actuator.
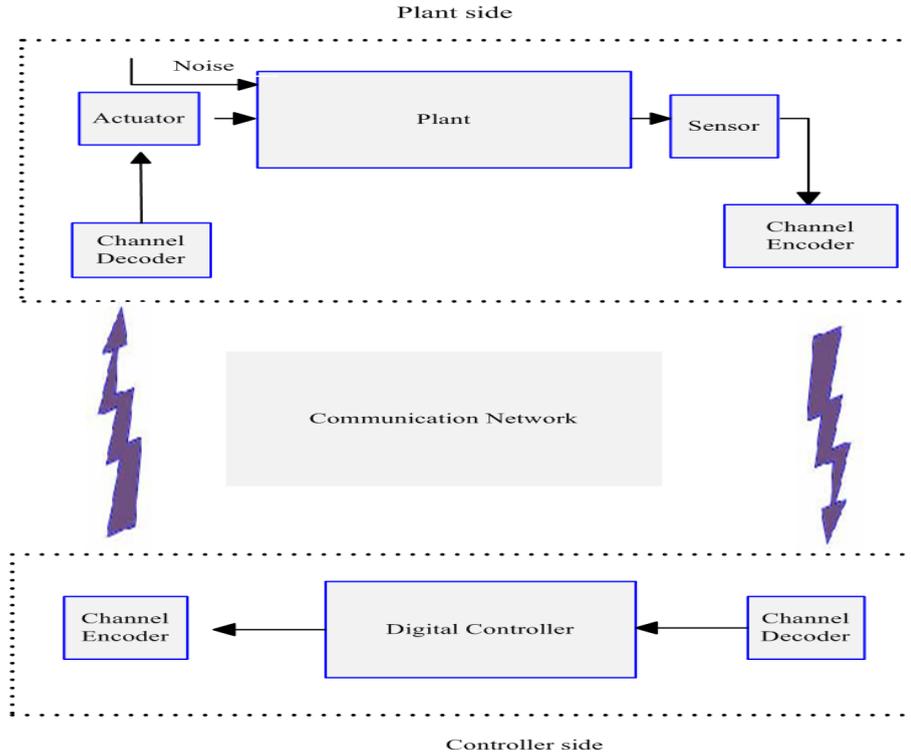
FIGURE 1.1: Networked control systems

The architecture of the NCSs is called common-bus network architecture and can be classified into 1) direct, and 2) hierarchical structures. In the direct structure, a single loop is closed over the network as shown in Figure 1.2(a). In this structure, sensors and actuators communicate with the controller through a network. In the hierarchical structure, there are local loops which are connected with the main controller over the network. The main controller provides the set-point for the local loops and local controllers try to achieve this goal. This configuration is shown in Figure 1.2(b). Due to their architectures, the NCSs improve the system flexibility, efficiency, modularity and reliability. The NCSs also reduce the installation, reconfiguration, and maintenance costs and time. The advantages of the NCSs make them highly popular in the academia and industry [2, 3, 5–7, 10, 12–18].

The traditional point to point control systems have been used in the industry for decades. In the traditional control systems, the system components are connected with help of dedicated wires which do not provide the advantages of the common-bus network [1]. However, the use of the common-bus network introduces new design constraints in the NCSs e.g., time delays due to shared bus and node priorities, quantization process due to digital networks, limited bandwidth due to packet-switched networks, and packet dropouts due to buffer overflows. The NCSs constraints can then be compensated for either by improving the network scheduling algorithms or by proposing novel control

(a) Direct structures   (b) Hierarchical structures
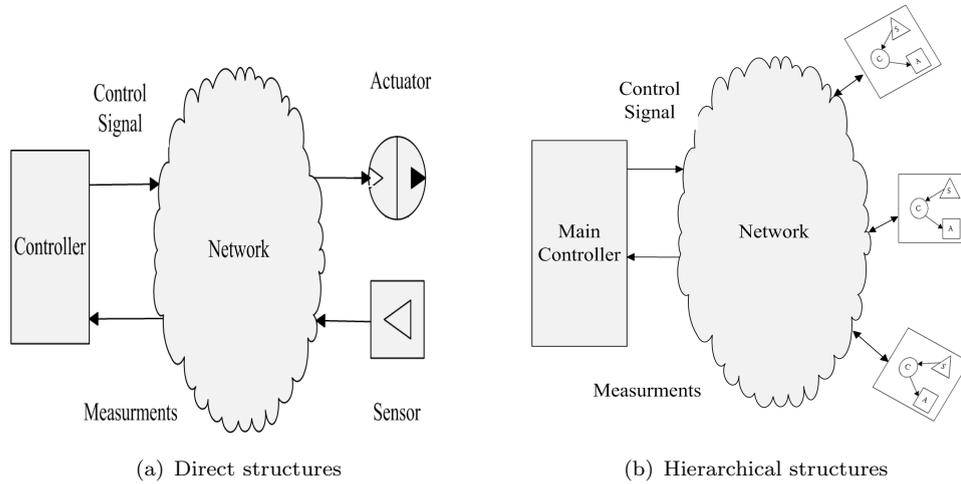
FIGURE 1.2: NCSs architectures

methodologies [14]. In this thesis, the second approach is adopted and various stability criteria and controller designs are proposed.

In the NCSs, the network-induced time delays are one of the major constraints, therefore the NCSs are considered as a sub class of time-delayed systems (TDSs). The TDSs are infinitely dimensional and can reduce the system performance and can even unstablize it [4]. On the basis of the Lyapunov stability methods, the two approaches have been proposed to cater for the time delays; 1) delay independent approach and 2) delay dependent approach. The first approach calculates the control law for the system stability without considering the time delays in the system dynamics. It also talks about maximum allowable transmission interval (MATI) in which the system remains stable. The second approach provides the stability conditions and the control law, allowing the delays in the system dynamics. The latter approach reduces the design overhead allowed in the former approach, hence it is better. Therefore, it is adopted here for stability analysis and synthesis. The Lyapunov stability methods are classified in 1) Lyapunov-Krasovskii (L-K) functional and 2) Lyapunov-Razumikhin (L-R) function. In this thesis, the first approach is investigated to develop the stability criteria. Both approaches are discussed in detail in Chapter 2.

The NCSs are also called digital control systems due to the presence of digital networks and controllers. It requires the signal should be quantized before transmission. This process induces quantization error in the system. In the beginning, the research had been carried out to mitigate the effect of quantization error on the system performance [69, 70, 148]. However in the inspirational work of [72], it is proved that the quantizers are useful in the NCSs, to achieve the system stability with limited bandwidth. A lot of research has been done to achieve the stability results while considering the quantizers as

information coders [73, 75, 76, 78, 79]. The constraint of the limited bandwidth can also be catered for by using an event-triggered (ET) sampling mechanism [39, 42–44]. In this thesis, some other techniques are also proposed to cater for limited bandwidth constraint e.g., congestion control mechanisms in Chapters 4 and 5, adaptive quantization densities in Chapter 7, and ET sampling mechanism in Chapter 8.

It is not feasible to have the prefect information flow between the NCSs components due to shared networks. It is possible that some of the transmitted information can be missed or dropped due to overflow. This phenomenon is called packet dropouts. The packet dropouts occur in forward and backward channels of the closed-loop [8]. A lot of research has been carried out to incorporate the packet dropouts in the NCSs design [30, 119, 120, 132]. The packet dropouts are random in nature and are modelled with the help of Bernoulli distributions. Along with other NCSs constraints, the packet dropouts are compensated by using exclusively-proposed Poisson distribution in Chapter 3 and widely-used Bernoulli distribution in Chapter 7.

The $\mathcal{H}_\infty$ is a performance index of a control system in terms of better control and reduced cost. However, the reduced cost increases the parameter variation and makes the system uncertain [9]. Therefore, the purpose of a control system design is to minimize $\mathcal{H}_\infty$ norm with uncertainties. The $\mathcal{H}_\infty$ control is a robust design against unstructured uncertainties. On the other hand, the system may have parametric uncertainties in its structure. It is quite useful to evaluate $\mathcal{H}_\infty$ performance against structured and unstructured uncertainties. Therefore, most of the proposed designs are robust in terms of $\mathcal{H}_\infty$ against both types of uncertainties. In this study, the structured uncertainties are assumed in all system matrices and are norm bounded.

1.2   Research Motivation

The development of NCSs has accelerated the technological convergence of various research fields such as control, communication, signalling and computing, therefore the NCSs inherit huge research potential and technological challenges in them. In the NCSs, the plants are controlled over a network with the help of sensors, actuators and remote controllers. Therefore, the NCSs have a list of real-time applications such as industrial control [2], sensors web [5], unmanned automatic vehicles (UAVs) [10] etc. The NCSs facilitate these applications with modularity, flexibility, mobility and reduced wiring cost. All theses advantages make the NCSs research very attractive in the industry and the academia research groups.

Although, a considerable amount of research has been done on the NCSs, there are a lot of practical questions that require detailed investigation. These questions include, but are not limited to, 1) stable operation of the interconnected system components, 2) sampling mechanisms and 3) the effect of a network on the system performance [6]. It motivates me to conduct a literature survey to point out the potential NCSs constraints and research gaps. It is concluded from the literature survey that if the system components are connected over the network then the network-induced constraints such as time delays, limited bandwidth, packet dropout and quantization error are expected in the control loop. This fact motivated me to develop the control strategies for the different NCSs scenarios with realistic and practical constraints.

It is evaluated from the literature survey that most of the previous studies consider delays as fixed [67] or time varying [52]. However, the simulation performed in the literature survey tells that delays can be stochastic in nature. It is due to the random nature of the networks. It inspires me to model the delays stochastically with the help of the Markov chain. The time delays are the most important constraints of NCSs that can degrade the system performance and can cause system instability [53]. Therefore, the delays are compensated in all of the proposed control designs. Further motivation is to design a control strategy to cater successive packet dropouts and Poisson noise. It arises from the fact that packet dropouts are mostly modelled by the Bernoulli distribution [119], which is not capable of modelling successive packet dropouts. Therefore, I introduced Poisson distribution to cater for the issue. The phenomenon of Poisson noise can be described as random unwanted discontinuous pulses that can affect the system stability. It is introduced in the NCSs model that is controlled by the proposed control strategy.

Subsequent motivation comes from the introduction of shared networks in the control loops. The shared networks can only provide limited bandwidth. It requires such mechanisms that can sample the data on demand. Along with this, the novel control strategies are required which can achieve the system stability in the presence of such mechanisms.

Another motivation arises from the fact that mostly a single quantizer is assumed to transmit the data over the digital networks, however it is more natural to assume separate quantizer for each system input and output. A robust $\mathcal{H}_\infty$ dynamic output feedback control law is proposed for the NCSs with random time delay and multiple quantizers.

In the seminal work [72], it is evident that the quantizers can be used as information coders and are helpful to design a stabilizing feedback controller with limited communication resources. It prompts me to study a dynamic output feedback controller consisting of a quantizer with adaptive quantization densities. It helps to regulate the bandwidth utilization according to the network load conditions. Moreover, network-induced packet dropouts are investigated with the help of Bernoulli distribution.

In this thesis, most of the control strategies assume that the sampling mechanism is time triggered (TT). The theoretical results of the stability analysis and the controller designs with TT mechanisms are comparatively easy and more mature than that with the ET mechanism. It motivates me to study the stability analysis of ET NCSs with packet dropouts. In this thesis, all of the stability criteria and the controller designs are represented as LMIs . The motivation of formulating the problems in terms of the LMIs is the availability of MATLAB toolboxes that can efficiently solve these inequalities.

1.3   Scope and Objectives

The scope of this study comprises three main parts: identification and modelling of the network-induced constraints in the NCSs, the stability analysis and the controller designs to compensate the NCSs constraints, and validation of the proposed design using simulations.

The objectives of the research are:

- Identification of potential design constraints in the NCSs, induced by networks existing between system components

- Design of a state feedback control law to compensate Poisson noise, successive packet dropouts and random delays

- Design of a robust $\mathcal{H}_\infty$ state feedback control law with a congestion control mechanism

- Design of a robust $\mathcal{H}_\infty$ dynamic output feedback control law with congestion control mechanisms on system input and output

- Design of a robust $\mathcal{H}_\infty$ dynamic output feedback control law with multiple quantizers

- Design of a robust $\mathcal{H}_\infty$ dynamic output feedback based control law in the presence of time varying delays, packet dropouts and adaptive quantizer

- Stability analysis of ET distributed NCSs with packet dropouts.

Overall, the research consists of novel stability criteria and controller designs for the NCSs that have been verified by the simulations. The stability conditions are provided after modelling the NCSs constraints, identified through a detailed literature survey.

1.4   Contribution of Thesis

The focus of the thesis is to identify and compensate the NCSs constraints in the presence of networks and different sampling mechanisms. The NCSs are always affected by various constraints such as time delays, limited bandwidth, quantization errors and packet dropouts. This thesis presents various novel control methodologies, developed for linear time invariant (LTI) discrete time NCSs. The constraints are mathematically modelled before their incorporation in the designs. The random time delays are modelled with the help of Markov chain. The limited bandwidth is catered for by using adaptive quantization densities and by transmitting less samples than actual. The packet dropouts are modelled using Bernoulli and Poisson probability distributions. The quantization errors are bounded by a sector bound approach. Sufficient conditions for the system stability are achieved by using the L-K functional approach. On the basis of the stability conditions, the control laws are proposed in terms of BMIs that are converted into quasi-convex LMIs with the help of cone complimentarity algorithm. Furthermore, the proposed designs are verified with the help of simulation examples. The contributions of the thesis are :

- A literature survey to identify the potential constraints in a controller design for the NCSs due to existence of networks between system components and due to different sampling mechanisms

- Proposal of a novel methodology of state feedback controllers to compensate Poisson noise, successive packet dropouts and random delays

- Investigation of a robust $\mathcal{H}_\infty$ state feedback control law to provide congestion control with the help of a "sampling on demand" strategy

- Design of a robust $\mathcal{H}_\infty$ dynamic output feedback control law for the NCSs with congestion control mechanisms, available on both system input and output

- Design of a robust $\mathcal{H}_\infty$ output feedback control law in the presence of network-induced random delays and quantization errors due to multiple quantizers present on both system inputs and outputs

- Development of a robust $\mathcal{H}_\infty$ dynamic output feedback based control law in the presence of time varying delays, packet dropouts modelled by the Bernoulli distribution and a quantizer with adaptive quantization densities which is proved to be helpful to adjust bandwidth utilization according to the requirement

- The stability analysis of distributed ET NCSs, with packet dropouts

- Verification of all designs using MATLAB toolboxes such as LMI, YALMIP and Truetime.

1.5 Thesis Outline

This thesis is a deep insight on the stability analysis and the controller designs for the NCSs where different scenarios and related constraints are discussed. The NCSs constraints such as time delays, packet dropouts, quantization error, limited information and congestion control are modelled and incorporated in the closed-loop system. After modelling these constraints, the novel stability criteria and controller designs are proposed to compensate them. The proposed designs are also validated with the help of simulation examples. The contents of the thesis are as follows:

Chapter 2 presents a literature survey and analysis on the advanced topics in NCSs. This chapter discusses the NCSs background, sampling mechanisms, constraints and related research. The two NCSs classes, on the basis of sampling mechanisms i.e., TT NCSs and ET NCSs, are discussed in detail. Moreover, various NCSs constraints, their modelling and related researches are presented in the context of TT and ET NCSs. Both classes are also compared through qualitative analysis and simulations.

In **Chapter 3**, various constraints of NCSs such as network-induced random delays, successive packet dropouts and Poisson noise are examined. The time delays are represented as modes of a Markov chain and the successive packet dropouts are modelled using the Poisson probability distribution. For each of the delay-mode, separate Poisson distribution is used with the help of an indicator function. The Poisson noise is incorporated in the design to cater for sudden network link failures and power shutdowns. After incorporating all the constraints, the LMI conditions for the stochastic stability and robust $\mathcal{H}_\infty$ state feedback controller design are derived. The effects of successive packet dropouts and the Poisson noise on $\mathcal{H}_\infty$ performance are also analyzed with the help of simulations.

Chapter 4 examines the problem of robust $\mathcal{H}_\infty$ state feedback control for the NCSs with a congestion control scheme. This scheme is based on comparing current measurement with the last transmitted measurement. If their difference is less than a prescribed value of the current measurement, then no measurement will be transmitted to the controller. Otherwise, the current measurement will be transmitted over the network. On the controller side, the last transmitted measurement will be used as a feedback. The effectiveness of the scheme in terms of reducing the network bandwidth is elaborated using simulation examples.

In **Chapter 5**, the congestion control technique of Chapter 4 is incorporated in the design of a dynamic output feedback controller. The technique is applied to the controller output as well. The proposed designs are verified with the help of a simulation example.

Chapter 6 covers the stability and stabilizability problems of the NCSs with multiple quantizers. The resultant quantization errors are bounded by a sector bound approach and represented as the convex poly-topic uncertainties. The network-induced delays are modelled by a Markov chain. The L-K functional approach is used to develop the stability criteria. A quantized robust $\mathcal{H}_\infty$ output feedback control law is proposed in terms of BMIs. An iterative cone complementarity algorithm is used to convert these BMIs into a quasi-convex optimization problem that is solved by the available mathematical tools. A simulation example is provided to demonstrate the effectiveness of the proposed theorems.

Chapter 7 investigates the problem of designing a robust $\mathcal{H}_\infty$ output feedback controller for the discrete-time NCSs with limited information using adaptive quantization densities. These densities are designed to be a function of the network load conditions that are modelled by a Markov chain. A stability criterion is developed using L-K functional approach, and sufficient conditions for the existence of a dynamic quantized output feedback controller are given in terms of BMIs. A simulation is performed to illustrate the effectiveness of the proposed design.

The measurement is transmitted over the network after the occurrence of an event in the congestion control scheme proposed in Chapter 4 and 5. This phenomenon is similar to the ET control approach. However, the measurement error is treated just as an uncertainty. The stability analysis and synthesis is performed by considering the system as robust TT NCSs that are well established. These TT NCSs designs do not provide a formal stability analysis method for ET control systems. This issue is catered for in Chapter 8.

Chapter 8 proposes a formal stability criterion for the ET NCSs. In this chapter discrete time NCSs with ET mechanisms on system input and output are considered. This configuration helps to represent the ET NCSs as impulsive systems with network constraints. The stability condition and $\mathcal{H}_\infty$ performance objective are obtained in terms of LMIs. The simulation examples are provided to validate the design.

The concluding remarks and the future research interest are given in **Chapter 9**, followed by the references. The proofs for Lemmas and Theorems are provided in the **Appendices**.

Chapter 2

NCSs: A New Frontier in Control Systems

This chapter investigates the tradeoffs between time triggered and event triggered mechanisms in the framework of networked control systems (NCSs) using previous studies. Although deterministic in nature, TT mechanism based control designs result in hard real time lines. These time lines are difficult to complete by software developers due to network and operating system scheduling algorithms. On the other hand, ET mechanism based control designs result in unknown asynchronous events but do not require hard real time lines. Both TT and ET mechanism based control designs have their own particular features e.g., TT mechanisms are deterministic, easier for developing formal design theories and results in fixed jitter and latencies, whereas ET mechanisms are soft real time, priority based, and save communication, computational and power resources. In this chapter, the basic concepts of TT and ET mechanisms are presented. NCSs and their constraints, such as random time delays, packet dropouts and quantization errors are also discussed for both mechanisms. The comparison between both mechanisms is done qualitatively that is verified by the simulations [58].

2.1 Introduction

In Networked Control Systems (NCSs), the system components i.e., sensors, actuators and controllers are spatially distributed over a digital network [7]. A NCSs framework is shown in Figure 2.1. The networks in the NCSs range from dedicated real time networks (e.g., control area network (CAN), fieldbus etc) to shared networks (e.g., Internet). The motivation to develop the NCSs technology is to reduce wiring and installation cost, modularity, flexibility and remote control of hazardous area plants. These benefits make

u_{k-Tcp} D/A Actuator w_k Plant Sensor y_k A/D $Q(y_k)$

Plant side

N e t w o r k

$Q(y_{k-Tpc})$

u_k Digital Controller T_c

Controller side
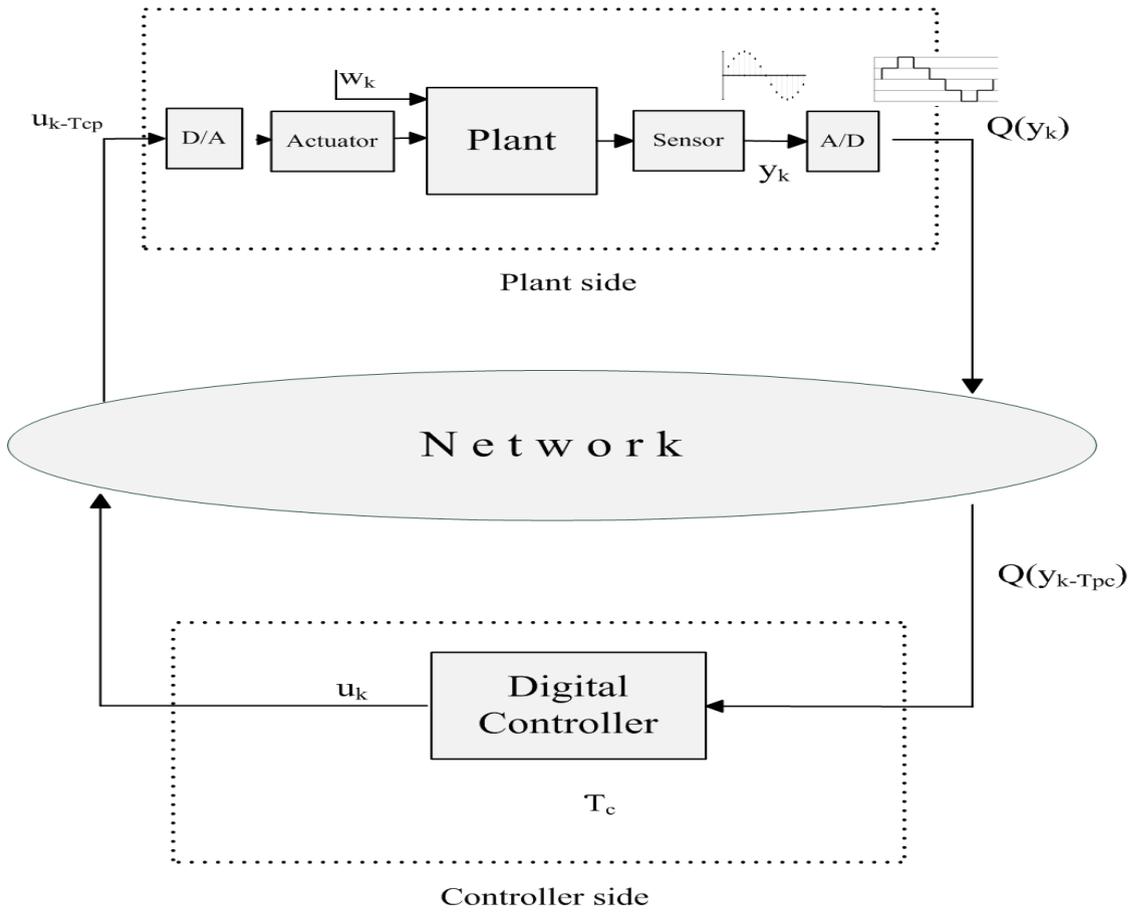
FIGURE 2.1: A NCSs framework

the NCSs technology indispensable in the various fields such as vehicle industry [10], process control [11], unmanned aerial vehicle (UAVs) [12] and signal power control in the communication systems [13]. Along with the advantages, the spatial distribution of the system components brings many new constraints in stability analysis and controller design of the NCSs. These network-induced imperfections include (1) limited bandwidth, (2) time delays, (3) packet dropouts, (4) quantization error, (5) variable sampling intervals and (6) network security etc. The modelling and the compensation of the former four constraints is the discussion of this thesis, whereas the latter two are beyond the scope of this thesis.

The quality of control (QoC) of the NCSs can be improved either by developing the network scheduling algorithms or by designing the novel control strategies that can compensate the network constraints. The main aim of the scheduling algorithms is to improve the network performance. The scheduling algorithms can be divided into (1) static scheduling algorithms, and (2) dynamic scheduling algorithms [14]. The static scheduling is done by pre-allocating the communication channel but it can not guarantee the system stability with the changes in the plant states or outputs. On the other

hand, the dynamic scheduling always has resource allocation priorities on the basis of system requirements. Various scheduling algorithms, to reduce the network constraints and achieve the system stability, are available in the literature [15–18, 149, 165]. Along with the improvements in the network scheduling algorithms, the necessity for the new control paradigms to cater for the communication imperfections can be deduced from the work of Chae [19]. He studied the behavior of classic LQR for mobile NCSs (moNCSs) and concluded that the traditional control strategies can not guarantee the system stability above a certain threshold of the time delays. Therefore, all the communication constraints such as limited bandwidth, time delays, packet dropouts and quantization errors should be properly modelled before proposing the stability criteria and the controller designs.

The stability of the NCSs with limited bandwidth or information can be achieved by different ways such as sampling on demand [60], quantizers or information coders [72], adaptive quantization densities [128]. The 'sampling on demand' is possible if the data sampling, i.e., the triggering of the communication between the plant and the remote controller, is controlled. The sampling mechanisms can either be time-scheduled, reactive or proactive. The first mechanism transmits the data on the elapsed of a fixed time interval and is uncontrolled. The second mechanism transmits the data on the occurrence of an event or when some conditions are violated, hence it is controlled. Similarly, the last approach pro-actively determines the violation of the conditions and sends the data accordingly. The basics of all three sampling mechanisms are discussed in detail in the section 2.2. The use of the quantizers as the information coders is discussed in the section 2.3.1.3. Chapter 7 discusses the use of the adaptive quantization densities to achieve the system stability with the limited information.

The study of the time delays belongs to a very important and enriched research field called time delayed systems (TDSs) [115, 141]. The time delays can vary in nature e.g., constant, successive, time varying, and random delays and can adversely affect the system performance [114]. The time delays are one of the main sources of the system instability and the performance degradation in the NCSs. Research on the TDSs stability analysis and controller synthesis can be classified into (1) time independent, and (2) time dependent approaches. The former approach assures the system stability and the controller gains that can stabilize the system in the presence of any arbitrary delay. The latter approach [96–98] considers time delays as a parameter in developing the stability criteria and the controller synthesis and is less conservative than the former approach [99, 100].

The packet dropout is another network constraint that increases the complexity of stability analysis and controller design of the NCSs [120]. Most of the studies considered

the packet dropout sequences as the stochastic processes and modelled them using the Bernoulli random distribution [30, 119, 120, 132]. A stochastic variable $\alpha(k)$, which follows the Bernoulli distribution, can be used of modelling any packet dropout sequence. The $\alpha(k) = 0$ denotes the occurrence of a packet dropout sequence while $\alpha(k) = 1$ show no packet dropouts. However, these packet dropout sequences can vary in real world networks and the Bernoulli distribution is not capable to model multiple and random packet dropout sequences. To cater for this issue, the Bernoulli distribution can be combined with other probability distributions such as Uniform and Poisson distributions [132]. An introduction to packet dropouts modelling using these probability distributions is given in the section 2.3.1.2. In Chapter 3 a new technique is suggested in which the multiple packet dropouts are modelled using the Poisson distribution with random delays and Poisson noise.

The use of the digital networks and the computers in the control systems introduce signal quantization because of their finite precision arithmetic and limited bandwidth. In the twentieth century the research had been carried out to diminish the quantization errors and their effects on the system performance [70, 71, 148]. However, modern research shows that the quantizers are the information coders [69, 72–74]. Here, the question of interest is: how much information is required for the system stability? The minimum information required for the system stability depends on the quantization density and the unstable poles of the plant. The static quantizers require an infinite number of quantization levels of providing the asymptotic stability, however they can provide practical quadratic stability. Especially the logarithmic quantizers, that is a class of static quantizers, assuring the quadratic system stability with the coarsest quantization densities [72]. For the logarithmic quantizers, Xie and Fu [75] proved that the quantization errors can be treated as sector bounded uncertainties. By doing this, they converted many quantized feedback problems into robust control problems. In their seminal work, the previous results (e.g., [72]), related to the system stability and stabilization, are extended to the MIMO case and various control objectives such as $\mathcal{H}_\infty$, guaranteed cost control and robustness are achieved in a unified framework. A less conservative approach for the quantized feedback, using poly-quadratic Lyapunov function, is proposed by [79]. On the other hand, the dynamic quantizers are capable to provide the asymptotic stability with a finite number of quantization levels. There are various dynamic quantization policies available in the literature e.g., ([59, 77, 78, 92]). A detailed discussion on the quantizers is given in the section 2.3.1.3.

This chapter investigates the differences between the TT and the ET mechanisms in the framework of the NCSs. The formal design and implementation of the NCSs has

multidisciplinary research aspects such as control theory, applied mathematics, embedded systems and software engineering etc. The design approaches for the TT mechanism based control system are comparatively easy and are well matured due to their deterministic nature. However, these designs result in hard real time-lines for the implementation. The hard real time-lines are difficult to follow, by the software developers, due to network and operating system scheduling algorithms. On the other hand, the ET mechanism based designs result in unknown asynchronous events but do not require hard real time-lines. Both types of designs have their own particular features; e.g., the TT mechanism is deterministic, easier for developing formal designs, and results in fixed jitters and latencies, whereas the ET mechanism is soft real time, priority based, and saves communication, computational and power resources. In this chapter, the TT and the ET mechanisms are assessed qualitatively and by the simulation.

The organization of the chapter can be followed from Figure 2.2. In the section 2.2, the basic concepts of the TT and the ET mechanisms are presented in the framework of general control systems. The section 2.3 extends this discussion to the NCSs. Various NCSs constraints such as random time delays, packet dropouts and quantization errors are discussed. The comparison between both approaches is done qualitatively and by the simulations in the context of the NCSs framework in the section 2.4. The qualitative comparison is based on the different NCSs requirements e.g., compensation for delays and jitters. In the simulations, the impact of both mechanisms on the system performance is analyzed in the sense of $\mathcal{H}_\infty$ and the resource utilization. It is deduced that the TT mechanism results in better $\mathcal{H}_\infty$ performance while the ET mechanism helps in reducing the resources utilization.

2.2 Sampling Mechanisms

In a control system communication between a plant and a controller can be seen as triggering of data sampling and transmission from one node to another node. The sampling/triggering mechanisms are of three types: 1) time triggered (TT) mechanism, 2) event triggered (ET) mechanism, and 3) self triggered (ST) mechanism. This section is comprised of an introduction to these mechanisms in the context of general control systems. In the next section the discussion on the triggering mechanisms is extended in the context of NCSs and their constraints. The control systems can be classified on the basis of the sampling mechanisms as: (1) TT control systems, 2) ET control systems, and 3) ST control systems.
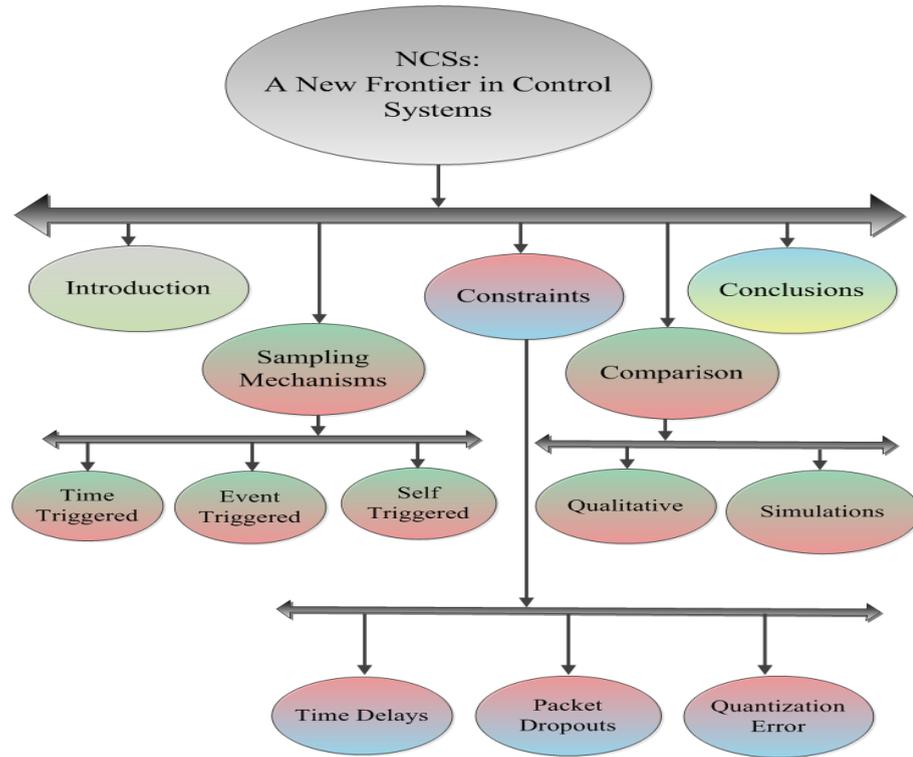
FIGURE 2.2: Tree architecture of the survey

2.2.1 TT Control Systems

The control systems with equidistant or periodic sampling mechanism are called the TT control systems. In this section the periodic discrete linear time invariant (LTI) control systems are discussed. This type of system can be obtained by doing the exact discretization of continuous LTI systems.

Consider state space representation of a continuous LTI plant:

$$
\begin{aligned}
\frac{d}{dt}x(t) &= A_p x(t) + B_p u(t) \\
y(t) &= C_p x(t)
\end{aligned}
\tag{2.1}
$$

where $x(t) \in R^n$, $u(t) \in R^{m_1}$, $y(t) \in R^{m_2}$, $t \in R_+$, are system states, control input, system output, and time, respectively. $A_p \in R^{n \times n}$, $B_p \in R^{n \times m_1}$, $C_p \in R^{m_2 \times n}$ are system, control and measurement matrices, respectively.

The discrete counterpart of the plant (2.1) can be obtained by applying the approximation techniques such as zero order hold, Tustin approximation and Euler method. For the different systems, different approximation methods can be used to get an exact discretization on a fixed sampling instance $\mathbf{T_s}$. By using zero order hold the state space

representation of discrete time version of the plant (2.1) is obtained as:

$$
\begin{aligned}
x(k+1) &= Ax(k) + Bu(k) \\
y(k) &= Cx(k)
\end{aligned}
\tag{2.2}
$$

where $x(k) \in R^n$, $u(k) \in R^{m_1}$, $y(k) \in R^{m_2}$, $k \in R_+$, are system states, control input, system output, and discrete time instance, respectively. $A = e^{A_p \cdot \mathbf{T_s}}$, $B = (\int_0^\infty e^{A_p \cdot \mathbf{T_s}} \, \mathrm{d}\tau) B_p$ and $C = C_p$ are system, control and measurement matrices, respectively.

Consider a dynamic output feedback controller of the following form:

$$
\begin{aligned}
\hat{x}(k+1) &= A_c \hat{x}(k) + B_c y(k) \\
u(k) &= C_c \hat{x}(k)
\end{aligned}
\tag{2.3}
$$

where A_c, B_c, C_c are the controller matrices.

In this representation next sampling instance $k+1$ can be determined as $k+1 = k + \hbar$, where $\hbar > 0$ and is fixed. Therefore, the distance between two consecutive sampling instances always remains the same. It results in the TT control systems in which the transmission of feedback information, $y(k)$, and control input, $u(k)$, between a plant and a controller, is done on each sampling instance k. This mechanism transmits the data as early as it is sampled. It results in the following closed-loop system representation:

$$
\begin{aligned}
\zeta(k+1) &= A_{cl} \zeta(k) \\
y(k) &= C_{cl} \zeta(k)
\end{aligned}
\tag{2.4}
$$

where $\zeta(k) = \begin{bmatrix} x(k) \\ \hat{x}(k) \end{bmatrix}$ is closed-loop system, and $A_{cl} = \begin{bmatrix} A & BC_c \\ B_c C & A_c \end{bmatrix}$, $C_{cl} = \begin{bmatrix} C & 0 \end{bmatrix}$ are closed-loop system and output matrices.

2.2.2 ET Control Systems

The ET control systems are the control systems with an ET mechanism. They are also called reactive control systems because their triggering mechanism determines the transmitting instance after the occurrence of an event instead of an elapsed time. The continuous ET control systems are called aperiodic control systems and require constant monitoring of the triggering conditions. However, in the case of discrete time, the ET control systems are called periodic ET control systems because their event triggering conditions are verified periodically instead of continuously [42]. The discrete ET control

systems have the advantage over the continuous ET control systems in a sense that they always result in a positive inter-event time and do not exhibit Zeno behavior.

Consider a class of discrete-time linear systems:

$$\begin{aligned} x(k+1) &= Ax(k) + B\bar{u}(k), \quad x(0) = 0 \\ y(k) &= Cx(k) \end{aligned} \tag{2.5}$$

where $x(k) \in \Re^n, \bar{u}(k) \in \Re^m, y(k) \in \Re^{m_2}$ are the state, event-based control input and measured output, respectively. The matrices A, B and C are of known dimensions. A dynamic output feedback controller of the following form is proposed:

$$\begin{aligned} \hat{x}(k+1) &= A_c\hat{x}(k) + B_c\bar{y}(k) \\ u(k) &= C_c\hat{x}(k) \end{aligned} \tag{2.6}$$

where A_c, B_c, C_c are the controller matrices. $\hat{x}(k) \in \Re^n$ and $\bar{y}(k) \in \Re^{m_2}$ are observer state and event-based feedback, respectively.

In the TT control system, $\bar{u}(k) = u(k)$ and $\bar{y}(k) = y(k)$. However, in the ET control systems, $\bar{u}(k)$ and $\bar{y}(k)$ are transmitted over the communication channel after the occurrence of an event on a particular discrete instance. The event is generated when the measured output or the control input will leave a set **C** around the origin. For the measured output this condition can be expressed mathematically as:

$$\bar{y}(k) = \begin{cases} y(k), & \text{if } \mathbf{C}(y(k), \bar{y}(k)) > 0 \\ \bar{y}(k), & \text{if } \mathbf{C}(y(k), \bar{y}(k)) \leq 0 \end{cases} \tag{2.7}$$

Similar conditions for the control input can be proposed as well. The different ET mechanisms are described as:

1. The event will be generated when the norm of the difference between the current and the previously transmitted output, termed as error and notated as $e(k)$, crosses a percentage σ of the current output. Therefore the next event triggering instance, proposed by [43], will be :

$$k_{n+1} = \inf\{k > k_n| \quad ||e(k)|| > \sigma||y(k)||\} \tag{2.8}$$

where k_{n+1} is the next event time, k_n is the current event time, $e(k) = \bar{y}(k) - y(k)$ and $\sigma > 0$.

2. The event will be generated when norm of the $e(k)$ crosses the sum of the percentage of the current output and a prescribed value. Therefore, the next event

triggering instance, proposed by [44], will be:

$$k_{n+1} = \inf\{k > k_n| \quad ||e(k)|| > \sigma||y(k)|| + \epsilon\} \tag{2.9}$$

where $\epsilon > 0$.

3. The event will be generated when $e(k)$ norm crosses the sum of the percentage of current output, previously accumulated error and a prescribed value. Therefore the next event triggering instance, proposed by the author, will be:

$$k_{n+1} = \inf\{k > k_n| \quad ||e(k)|| > \sigma||y(k)|| + \rho||e(k-1)|| + \epsilon\} \tag{2.10}$$

where $\rho > 0$.

4. The event triggering conditions can be provided on the basis of Lyapunov function. For example: consider a quadratic Lyapunov function:

$$V(x) = x^T(k)Px(k) \quad \text{with} \quad P > 0 \tag{2.11}$$

The next event triggering instances, proposed by [45], will be:

$$k_{n+1} = \inf\{k > k_n| \quad A_{cl}^T P A_{cl} > \sigma P\} \tag{2.12}$$

where P is positive definite symmetric matrix, and $\sigma > 0$.

2.2.3 ST Control Systems

The ST control systems are called proactive control systems because their triggering mechanism determines the transmitting instance in advance. It is useful in the cases when the dedicated hardware is not available for continuous monitoring of the event triggering conditions. The formal designs for ST control systems are still an open challenge. In this thesis, a brief introduction is included here only, whereas the detailed discussion is beyond the scope of the thesis.

Consider the system (2.5) with the control law (2.6). In ST control systems, the next triggering instance k_{n+1} depends upon the previous triggering instance k_n and the system state, $x(k_n)$, which is only dependent on the k_n. Mathematically:

$$k_{n+1} = k_n + \Gamma(x(k_n)) \tag{2.13}$$

where $\Gamma(x(k_n))$ is a mapping function. Once this mapping function is developed, the event triggering mechanism is able to determine the next triggering event in advance.

2.3   NCSs Constraints

In this section NCSs constraints such as 1) network induced time delays, 2) packet dropouts, and 3) quantization errors are discussed. These constraints not only degrade system performance but can also result in system instability. This section mostly focuses on the modelling of these constraints for the TT NCSs. After the modelling of the constraints, the various approaches to develop stability criteria are given. For the ET NCSs, only a brief introduction to these constraints is included here where as the detailed discussion is beyond the scope of the thesis.

2.3.1   Constraints in the TT NCSs

2.3.1.1   Time Delays

In the NCSs, the time delays are inevitable in the measurements and the control inputs due to the presence of network. It makes them a special class of the TDSs. In NCSs, the measurement delays are also denoted as sensor to controller delays (τ_{sc}) and the control input delays are called controller to actuator delays (τ_{ca}). Without loss of the generality, both τ_{sc} and τ_{ca} can be lumped together as one transmission delay τ [82]. This approach is adopted here. Mathematically:

$$\tau = \tau_{sc} + \tau_{ca} \tag{2.14}$$

Depending on the networks, the delays can be time invariant, time varying and random in nature. In the following, the delays are modelled for the plant (2.2). Among various types of the control laws proposed in the literature [47, 54, 55, 128], the dynamic observer-based output feedback is chosen for further discussion. These control laws, on the basis of formulation, can be divided into two types: 1) delay-independent, and 2) delay-dependent control laws. In the first type the stabilizing controllers are designed as independent of the delays. These designs assure the system stability even in the presence of the unbounded delays. The second type considers delay-dependent designs that are less conservative and reduce over-design. In this approach, the delays are properly modelled and are incorporated in the controller design [65]. Therefore, only delay-dependent controllers are discussed here.

Time invariant Delays and their Modelling: The constant or time invariant but unbounded delays were first considered by [67]. The networks with the time division multiplexing result in these types of delays. An overview of the system representation for the plant (2.2) with the constant delays is given below.

Consider a dynamic observer-based output feedback control law with the fixed delay τ as:

$$\begin{aligned}
\hat{x}(k+1) &= A_c\hat{x}(k) + B_c\bar{y}(k-\tau) \\
u(k) &= C_c\hat{x}(k)
\end{aligned} \tag{2.15}$$

After applying the controller (2.15) on the plant, the following closed-loop system is obtained:

$$\begin{aligned}
\zeta(k+1) &= A_{cl}\zeta(k) + B_{cl}\zeta(k-\tau) \\
y(k) &= C_{cl}\zeta(k)
\end{aligned} \tag{2.16}$$

where $A_{cl} = \begin{bmatrix} A & BC_c \\ 0 & A_c \end{bmatrix}$, $B_{cl} = \begin{bmatrix} 0 & 0 \\ B_c & 0 \end{bmatrix}$ and $C_{cl} = \begin{bmatrix} C & 0 \end{bmatrix}$.

Time Varying Delays and their Modelling: The delays which change with time are called time varying delays and are notated as $\tau(k)$. The networks with priority based transmission strategies result in these types of delays. These delays range from no delay to the maximum delays and can be bounded as $0 \leq \underline{\tau} \leq \tau(k) \leq \bar{\tau} < \infty$ where $\underline{\tau}$ and $\bar{\tau}$ are lower and upper bounds, respectively.

By applying the dynamic observer-based feedback controller on the plant, with time varying delay in the transmission link, the following closed-loop system is obtained:

$$\begin{aligned}
\zeta(k+1) &= A_{cl}(k)\zeta(k) + B_{cl}(k)\zeta(k-\tau(k)) \\
y(k) &= C_{cl}(k)\zeta(k)
\end{aligned} \tag{2.17}$$

where $A_{cl}(k) = \begin{bmatrix} A & BC_c(k) \\ 0 & A_c(k) \end{bmatrix}$, $B_{cl}(k) = \begin{bmatrix} 0 & 0 \\ B_c(k) & 0 \end{bmatrix}$ and $C_{cl}(k) = \begin{bmatrix} C & 0 \end{bmatrix}$.

Random Delays and their Modelling: The random or stochastic delays are special cases of time varying delays. The random delays are more natural in the networks with shared transmission mediums such as Internet. The random delays can be modelled with the help of statistical methods such as Bernoulli probability distributions and Markov chain [56, 96]. In this discussion, the network-induced random delays are modelled with the finite state Markov chain.

In the Markov chain method, the random delays can be treated as the stochastic processes and modelled by a finite state Markov chain as $\tau(k) = \tau(r_k)$ with $0 \leq \tau(1) < \tau(2) < \cdots < \tau(n) \leq \infty$, where r_k is the stochastic Markov process taking values from the finite set Markov chain $\mathcal{N} = \{1, 2, \cdots, n\}$, with the transition probability of the

form:

$$p_{ij} := \mathbf{Prob}\{r_{k+1} = j | r_k = i\}$$

where $i, j \in \mathcal{N}$ and the transition probability matrix for n processes is given as

$$P_\tau = \begin{bmatrix} p_{11} & p_{12} & \cdot & \cdot & \cdots & p_{1n} \\ p_{21} & p_{22} & \cdot & \cdot & \cdots & p_{2n} \\ \vdots & \vdots & \vdots & \vdots & \ddots & \vdots \\ \vdots & \vdots & \vdots & \vdots & \vdots & p_{(n-1)n} \\ p_{n1} & p_{n2} & \cdot & \cdot & \cdots & p_{nn} \end{bmatrix} \tag{2.18}$$

with $0 \le p_{ij} \le 1$ and $\sum_{j=1}^n p_{ij} = 1$.

A finite state machine (FSM) presentation of a Markov chain with three states is shown in the Figure 2.3.

Suppose that the measured output $y(k)$ is delayed by the time $\tau(k)$ which is modelled as a stochastic process $\tau(rk)$ taking values from the finite state Markov chain. The delayed $y(k)$ can be represented as:

$$y(k - \tau(k)) = y(k - \tau(r_k)) \tag{2.19}$$

where the transition from one delay to the other is governed by the transition probability as:

$$\tilde{\tau}(i) = \sum_{j=1}^n p_{ij} \tau(j) \tag{2.20}$$

By applying the dynamic observer-based feedback controller on the plant, with random delays modelled by Markov chain, the following closed-loop system is obtained:

$$\begin{aligned} \zeta(k+1) &= A_{cl}(r_k)\zeta(k) + B_{cl}(r_k)\zeta(k - \tau(r_k)) \\ y(k) &= C_{cl}(r_k)\zeta(k) \end{aligned} \tag{2.21}$$

where $A_{cl}(r_k) = \begin{bmatrix} A & BC_c(r_k) \\ 0 & A_c(r_k) \end{bmatrix}$, $B_{cl}(r_k) = \begin{bmatrix} 0 & 0 \\ B_c(r_k) & 0 \end{bmatrix}$ and $C_{cl}(r_k) = \begin{bmatrix} C & 0 \end{bmatrix}$.

2.3.1.2 Packet Dropouts

The transmission of the data between the plant and the controller is in the form of packets in the NCSs. The packets not only bear delays but sometimes are lost over the network [63]. The packet dropouts or the missing information are common in NCSs due to noise, fading and buffer overflows in the network nodes. They can degrade
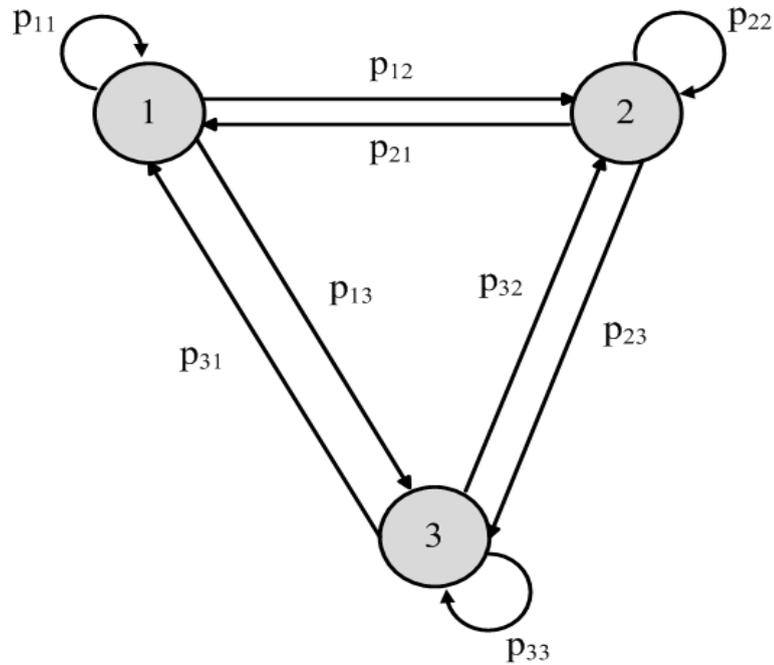
FIGURE 2.3: FSM representation of a three state Markov chain

the system performance and even result in system instability if they exceed a certain bound. The packet dropouts can be random due to the unreliable nature of the networks, therefore they can be molded as a stochastic process following a certain probability such as Bernoulli, Uniform and Poisson distributions [132].

Packet Dropout Modelling using Bernoulli Distribution:

Bernoulli distribution is useful to find out the occurrence of a packet dropout sequence as shown in Figure 2.4. However, it is not capable of telling how many packets are dropped in that particular sequence. Therefore, it is useful to model either a single packet dropout or a fixed sequence of packet dropouts. It can also be used with other probability distributions to model the random and successive packet dropouts.

In the following, a single packet dropout is molded using a stochastic variable $\alpha(k)$ following a Bernoulli random sequence as:

$$\alpha(k) = \begin{cases} 1, & \text{if packet dropout occurs} \\ 0, & \text{if packet dropout does not occur} \end{cases}$$

Assume that $\alpha(k)$ has the probability:

$$Prob\{\alpha(k) = 1\} = E\{\alpha(k)\} = \alpha, Prob\{\alpha(k) = 0\} = 1 - \alpha$$

(a) Packet Dropouts in Bernoulli Distribution

(b) Probability Mass Function
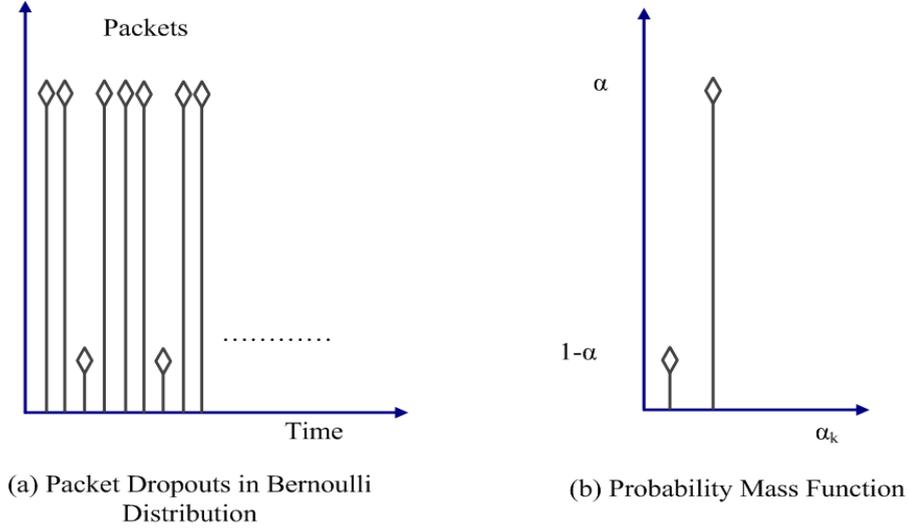
FIGURE 2.4: Packet dropouts following Bernoulli distribution and probability mass function

where $0 \leq \alpha \leq 1$ is a constant, and

$$E\{\alpha(k) - \alpha\} = 0, \beta^2 \equiv E\{(\alpha(k) - \alpha)^2\} = \alpha(1 - \alpha)$$

where $E(\cdot)$ is the expectation operator and β^2 is the variance.

Consider a dynamic output feedback controller with a single packet dropout compensation as:

$$
\begin{aligned}
\hat{x}(k+1) &= A_c(k)\hat{x}(k) + \alpha(k)B_c(k)y(k) + (1 - \alpha(k))B_c y(k-1) \\
u(k) &= C_c(k)\hat{x}(k)
\end{aligned}
$$
(2.22)

where $A_c(k)$, $B_c(k)$, $C_c(k)$ are the controller matrices.

The closed-loop system of (2.2) with (2.22) is given as follows:

$$
\begin{aligned}
\zeta(k+1) &= A_{cl}\zeta(k) + B_{cl}\zeta(k-1) \\
y(k) &= C_{cl}\zeta(k).
\end{aligned}
$$
(2.23)

where $\zeta(k) = [x(k) \ \hat{x}(k)]^T$ and

$$
A_{cl} = \begin{bmatrix} A & BC_c \\ \alpha(k)B_cC & A_c \end{bmatrix}, B_{cl} = \begin{bmatrix} 0 & 0 \\ (1 - \alpha(k))B_cC & 0 \end{bmatrix} \text{ and } C_{cl} = \begin{bmatrix} C & 0 \end{bmatrix}.
$$

Packet Dropout Modelling using Uniform Distribution:

The packet dropout sequences can be periodic, therefore they can be modelled by a stochastic variable $\beta(k)$. The $\beta(k)$ follows the Uniform probability distribution as shown in Figure 2.5. In this distribution, all the packet dropout sequences, $D_1, D_2...D_n$, are uniformly distributed with the probability:

$$p_i = \text{Prob}(\beta(k) = D_i) = \frac{1}{n} \tag{2.24}$$

It is already mentioned that the Bernoulli distribution can be combined with other probability distributions e.g., the Uniform or the Poisson probability distribution, to model different packet dropout sequences. In a hybrid probability distribution, the Bernoulli distribution tells the occurrence of a packet dropout event where the Uninform distribution can tell how many sequences occur in a given transmission. By using this approach, a dynamic output feedback controller is considered as:

$$
\begin{aligned}
\hat{x}(k+1) &= A_c \hat{x}(k) + \alpha(k) B_c y(k) + (1 - \alpha(k)) \sum_{i=1}^{n} \frac{1}{n} B_c y(k-i) \\
u(k) &= C_c \hat{x}(k)
\end{aligned} \tag{2.25}
$$

After applying (2.25) on (2.2), the following closed-loop representation is obtained:

$$
\begin{aligned}
\zeta(k+1) &= A_{cl}\zeta(k) + \alpha(k)B_{cl1}\zeta(k) + (1 - \alpha(k)) \sum_{i=1}^{n} \frac{1}{n} B_{cl2}\zeta(k-i) \\
y(k) &= C_{cl}\zeta(k).
\end{aligned} \tag{2.26}
$$

where

$$
A_{cl} = \begin{bmatrix} A & BC_c \\ 0 & A_c \end{bmatrix}, B_{cl1} = \begin{bmatrix} 0 & 0 \\ B_c C & 0 \end{bmatrix}, B_{cl2} = \begin{bmatrix} 0 & 0 \\ B_c C & 0 \end{bmatrix},
$$

$$
\text{and } C_{cl} = \begin{bmatrix} C & 0 \end{bmatrix}.
$$

Packet Dropout Modelling using Poisson Distribution

There can be a single or multiple/successive packet dropout random sequences in a network, existing between a plant and a controller. In the case of a single packet dropout sequence, the Bernoulli distribution is very effective and is adopted by many researchers [30, 119, 128]. However, the random sequences of the successive packet dropouts, occurring frequently in real time networks, got much less attention from the researchers. Both Bernoulli and Uniform distribution are not capable of modelling the random sequences of successive packet dropouts but the Poisson distribution can do so. Consider random sequences of multiple packet dropouts by a random variable $\sigma(k)$ following a Poisson

(a) Packet Dropouts in Uniform Distribution

(b) Probability Mass Function
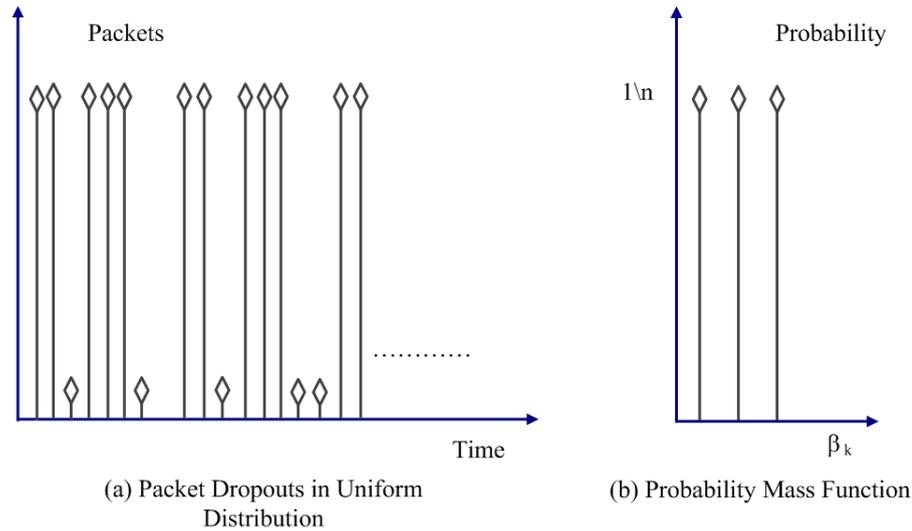
FIGURE 2.5: Packet dropouts following uniform distribution and probability mass function

distribution. Consider $\sigma(k)$ is with any n number of possible values $\kappa_1, \kappa_2 \cdots \kappa_m$. The probability of each outcome κ_d will follow the Poisson distribution as:

$$p_d = Prob\{\sigma(k) = \kappa_d\} = \frac{\lambda^{\kappa_d} e^{-\lambda}}{\kappa_d!} \quad d = 1, 2 \cdots m$$
$$Mean = E\{\sigma(k)\} = \lambda$$
$$E\{\sigma(k) - Mean\} = 0, \tag{2.27}$$

where m is the maximum packet dropouts.

The Bernoulli and the Uniform distributions result finite expectations while the Poisson distribution results infinite expectation. Therefore, the interval of any random sequence of the packet dropouts can range from 0 to ∞. The interval with ∞ value may occur when $m \to \infty$ and always has very low probability. Without loss of the generality, this low probability can be considered as 0. In this case, the current data will be used as the feedback. The probabilities of packet dropouts under the Poisson distribution and it probability mass function is shown in Figure 2.6. As discussed earlier, the Bernoulli distribution can be used with other distributions to model the packet dropouts. This approach is adopted here as well and the Bernoulli distribution used to determine the occurrence of any packet dropouts sequence whereas the Poisson distribution is used to model the random sequence of packet dropouts .

(a) Packet Dropouts in Poisson Distribution

(b) Probability Mass Function
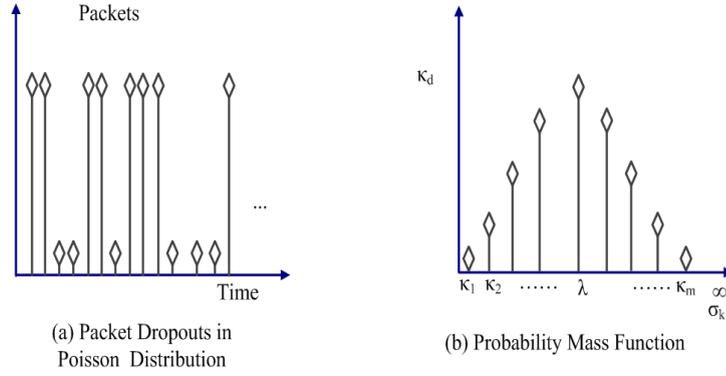
FIGURE 2.6: Packet dropouts following Poisson distribution and probability mass function

After modelling the random sequences of packet dropouts, a dynamic output feedback controller is proposed as:

$$
\begin{aligned}
\hat{x}(k+1) &= A_c\hat{x}(k) + \alpha(k)B_cy(k) + (1-\alpha(k))\left\{\sum_{\kappa_d=0}^{\kappa_m} p_dB_cy(k-\kappa_d)\right\} \\
u(k) &= C_c\hat{x}(k)
\end{aligned}
\tag{2.28}
$$

where κ_d is a packet dropouts sequence, κ_m is sequence with maximum dropouts, and p_d is the Poisson distribution based probabilities.

After applying (2.28) on (2.2), the following closed-loop representation is obtained:

$$
\begin{aligned}
\zeta(k+1) &= A_{cl}\zeta(k) + \alpha(k)B_{cl1}\zeta(k) + (1-\alpha(k))\left\{\sum_{\kappa_d=0}^{\kappa_m} p_dB_{cl2}\zeta(k-\kappa_d)\right\} \\
y(k) &= C_{cl}\zeta(k).
\end{aligned}
\tag{2.29}
$$

where

$$
A_{cl} = \begin{bmatrix} A & BC_c \\ 0 & A_c \end{bmatrix}, B_{cl1} = \begin{bmatrix} 0 & 0 \\ B_cC & 0 \end{bmatrix}, B_{cl2} = \begin{bmatrix} 0 & 0 \\ B_cC & 0 \end{bmatrix},
$$

$$
\text{and } C_{cl} = \begin{bmatrix} C & 0 \end{bmatrix}
$$

2.3.1.3 Quantization Process and Error

The evolution of the digital controllers and the NCSs resulted in the incorporation of the quantization in the feedback loops. The quantizer or quantization process can be described as the mapping of a real-valued function into a piecewise constant function i.e., $\mathbb{R} \rightarrow \mathbb{Z}$ taking values from a finite set e.g., $\mathbb{U} = \{\pm u_i, i = -, \pm 1, \pm 2....\} \cup \{0\}$.

The control system with quantizers are hybrid, i.e., continuous and symbolic, in nature [92]. In the beginning, the researchers mainly focused to mitigate the effect of quantization error on the system performance e.g., [70], however now a days, the quantizers are treated as the information coders to reduce the resource utilization such as computational and communication resources [72]. The design of quantized feedback control is a multidisciplinary research area and requires the integrated concepts of the control and the information theories. The research on the quantized feedback has been actively carried out recently [69, 75, 77]. On the basis of the quantization policy, the quantizers can be categorized as: (1) Static quantizers, (2) Dynamic quantizers.

Static Quantizers:

A static time invariant quantizer can be described as a memoryless nonlinear mapping function from $\mathbb{R} \to \mathbb{Z}$ [78]. The static quantizers require infinite number of levels to achieve asymptotic stability, therefore they only result in the practical quadratic stability of the control system. The static quantizers can be further classified as:

1. Uniform quantizer: It is nonlinear mapping function with uniform quantization levels as shown in the Figure 2.7. One of the quantization policy under this class of quantizers is given as

$$q_u(x(k)) = \begin{cases} M, & \text{if } x(k) > (S+0.5)\Delta \\ -M, & \text{if } x(k) \le -(S+0.5)\Delta \\ \lfloor \frac{x}{\Delta} + 0.5 \rfloor & \text{if } -(S+0.5)\Delta < x(k) \le (S+0.5)\Delta \end{cases} \qquad (2.30)$$

where $x(k), q_u(x(k)), S, \Delta$ are an actual signal, quantized signal, saturation region and quantization error, respectively.

A dynamic quantized output feedback of the form (2.3) is presented as:

$$\begin{aligned} \hat{x}(k+1) &= A_c \hat{x}(k) + B_c q_u(y(k)) \\ u(k) &= C_c \hat{x}(k) \end{aligned} \qquad (2.31)$$

where $q_u(y(k)$ is quantized feedback. By applying (2.31) on the plant (2.2):

$$\begin{aligned} \zeta(k+1) &= A_{cl}\zeta(k) \\ \text{and} y(k) &= C_{cl}\zeta(k) \end{aligned} \qquad (2.32)$$

where $A_{cl} = \begin{bmatrix} A & BC_c \\ B_c(\frac{C}{\Delta} + .5) & A_c \end{bmatrix}, \; C_{cl} = \begin{bmatrix} C & 0 \end{bmatrix}.$
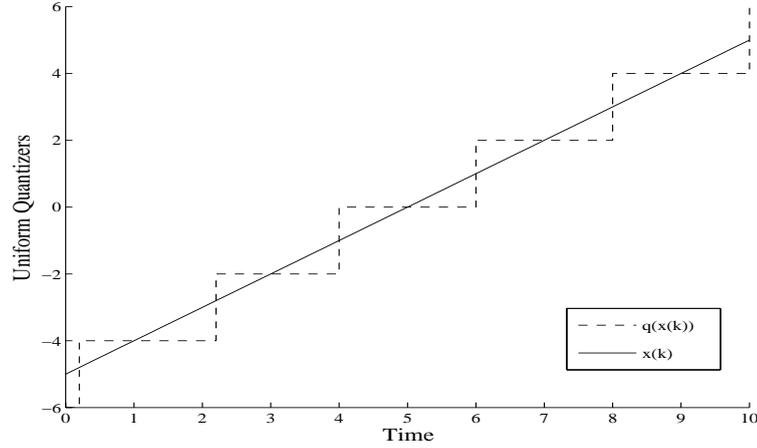
FIGURE 2.7: Uniform level quantization

2. Logarithmic quantizer: The static quantizers with coarsest quantization densities are logarithmic. In this type of quantizers, the time axis are linear where the signal axis are logarithmic as shown in Figure 2.8. It should be noted that the quantization density is directly proportional to the quantization levels. The logarithmic quantizers take values from the set $\mathbb{U} = \{\pm\rho^i, i = 0, \pm1, \pm2, \cdots\} \bigcup \{0\}$, where ρ is the quantization density and can be described as:

$$q_l(x(k)) = \begin{cases} \rho^i & \text{if } \frac{1}{1+\delta}\rho^i < x(k) \leq \frac{1}{1-\delta}\rho^i, \quad x(k) > 0, i = 0, \pm1, \pm2, \cdots \\ 0, & \text{if } x(k) = 0 \\ -q(-x(k)) & \text{if } x(k) < 0 \end{cases}$$

(2.33)

where δ is the sector, a bound on the quantization error Δ. The relationship between the quantization density and sector is given as follows:

$$\delta = \frac{1-\rho}{1+\rho}$$

The dynamic output feedback controller with quantized feedback is presented as:

$$\begin{aligned} \hat{x}(k+1) &= A_c\hat{x}(k) + B_cq_l(y(k)) \\ u(k) &= C_c\hat{x}(k) \end{aligned}$$

(2.34)

By applying (2.34) on the plant (2.2):

$$\begin{aligned} \zeta(k+1) &= A_{cl}\zeta(k) \\ y(k) &= C_{cl}\zeta(k) \end{aligned}$$

(2.35)
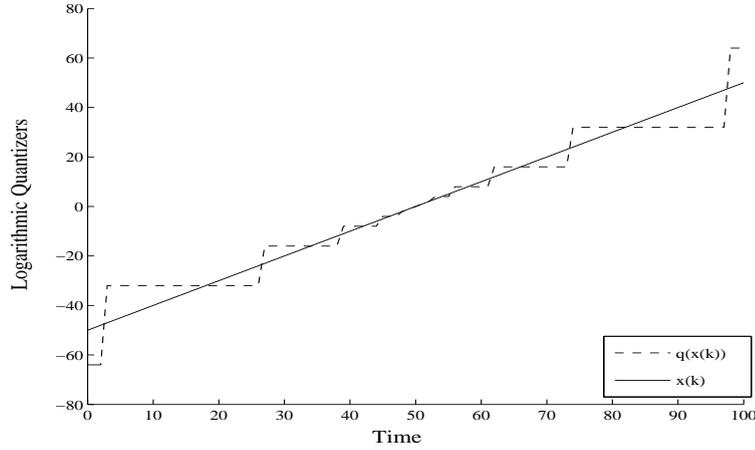
FIGURE 2.8: Logarithmic quantizers

where $A_{cl} = \begin{bmatrix} A & BC_c \\ B_cC(1+\Delta) & A_c \end{bmatrix}$, and $C_{cl} = \begin{bmatrix} C & 0 \end{bmatrix}$, $q(y(k)) = y(k) + \Delta y(k)$.

Dynamic Quantizers:

A dynamic quantizer uses memory and is complex to design, but is suitable to achieve the asymptotic stability with finite quantization levels or limited information. It helps in the optimized use of the computational and communication resources. The dynamic quantizers use both the current quantized signal and the previous quantized information in the calculation of control input [92]. There is a lot of active research going on the system stability and controller design with dynamic quantization policies [77, 78, 92, 138]. In the following, two types of the dynamic quantizers are discussed.

1. Static quantizers with dynamic scaling: A static for example logarithmic quantizer can be used as a dynamic quantizer with the help of dynamic scaling or zooming. The scaling parameter can be tuned online or dynamically for zooming in and out according to the signal size. Consider a logarithmic quantizer with truncated but finite $2N$ quantization levels:

$$q_{ld}(x(k)) = \begin{cases} \rho^i \mu_0 & \text{if } \frac{1}{1+\delta}\rho^i\mu_0 < x(k) \leq \frac{1}{1-\delta}\rho^i\mu_0, \quad 0 < i < N-1 \\ \rho^{N-1}\mu_0, & \text{if } 0 \leq x(k) \leq \frac{1}{1-\delta}\rho^{N-1}\mu_0 \\ \mu_0, & \text{if } \frac{1}{1+\delta}\mu_0 < x(k) \\ -q(-x(k)) & \text{if } x(k) < 0 \end{cases} \tag{2.36}$$

A out of the range feedback signal $y(k)$ can be scaled in the range of the logarithmic quantizer before the quantization and scaled back after the quantization

with the help of scaling parameter $s_k > 0$. Mathematically, this procedure can be expressed as $s_k^{-1} q_{ld}(s_k y(k))$. After applying the output feedback controller (2.3) on the system (2.2) with the 'scaled back' quantized signal, the following closed-loop system is obtained:

$$
\begin{aligned}
\zeta(k+1) &= A_{cl}\zeta(k) + B_{cl}s_k^{-1}q_{ld}(s_k C_{cl}x(k)) \\
y(k) &= C_{cl}\zeta(k)
\end{aligned}
\tag{2.37}
$$

where $A_{cl} = \begin{bmatrix} A & BC_c \\ 0 & A_c \end{bmatrix}$, $B_{cl} = \begin{bmatrix} 0 \\ B_c \end{bmatrix}$, and $C_{cl} = \begin{bmatrix} C & 0 \end{bmatrix}$, .

The dynamically adjustment of the parameter s_k can easily be done on the basis of the 'scaled' quantized signal $q_{ld}(s_k y(k))$ [78].

2. Logarithmic quantizer with dynamic input: In this type of dynamic quantizers, a logarithmic quantizer is used that quantize the difference between the current and the previous signal, i.e., $\bar{y}(k) = y(k) - y(k-1)$, instead of the current signal, $y(k)$. This quantization policy is proposed by the author in [59]. Consider a logarithmic quantizer of the form (2.33) with the proposed policy. By applying the output feedback controller (2.3) on the system (2.2):

$$
\begin{aligned}
\zeta(k+1) &= A_{cl}\zeta(k) + B_{cl}\zeta(k-1) \\
y(k) &= C_{cl}\zeta(k)
\end{aligned}
\tag{2.38}
$$

where $A_{cl} = \begin{bmatrix} A & BC_c \\ C(1+\delta) & A_c \end{bmatrix}$, $B_{cl} = \begin{bmatrix} 0 & 0 \\ C(1+\delta) & 0 \end{bmatrix}$, and $C_{cl} = \begin{bmatrix} C & 0 \end{bmatrix}$.

2.3.1.4 Stability Analysis Approaches

The time delays are the most important constraint of the NCSs that affects the system performance and the stability adversely. Moreover, the NCSs can also be considered as a subclass of the TDSs [53]. Therefore, the approaches to develop the stability criteria for the TDSs are also applicable to the NCSs. To obtain the quadratic stability, two state of the art approaches (Lyapunove-Krasovskii (L-K) functional and Lyapunove-Razumkhin (L-R) functions) are proposed in the literature. In this doctoral study, the L-K functional approach is adopted for stochastic stability and its various forms are proposed to cater for different NCSs constraints along with the time delays. In the following section, a brief introduction of both approaches is given.

L-K Functional Approach:

Consider the closed-loop system (2.17), a detailed L-K functional can be used to obtain the stochastic stability criteria:

$$V(\zeta_k, r_k) = V_1(\zeta_k, r_k) + V_2(\zeta_k, r_k) + V_3(\zeta_k, r_k) \tag{2.39}$$

with

$$V_1(\zeta_k, r_k) = \zeta_k^T P(r_k)\zeta_k \tag{2.40}$$

$V_1(\zeta_k, r_k)$ is a basic Lyapunov function to obtain the stability criteria for a simple closed-loop system without NCSs constraints.

$$V_2(\zeta_k, r_k) = \sum_{\ell=-\tau(r_k)}^{-1} \sum_{j=k+\ell}^{k-1} \bar{x}_j^T R_1 \bar{x}_j + \sum_{\ell=-\tau(s)}^{-1} \sum_{j=k+\ell}^{k-1} \bar{x}_j^T R_2 \bar{x}_j \tag{2.41}$$

$$V_3(\zeta_k, r_k) = \sum_{\ell=k-\tau(r_k)}^{k-1} \zeta_\ell^T Q \zeta_\ell + \sum_{\ell=-\tau(s)+2}^{-\tau(1)+1} \sum_{j=k+\ell-1}^{k-1} \zeta_j^T Q \zeta_j \tag{2.42}$$

$V_2(\zeta_k, r_k)$ and $V_3(\zeta_k, r_k)$ are the detailed L-K functionals which provide the closed-loop stability criteria while considering the each random delay, the minimum and the maximum delays and the average of the delays.

L-R Function Approach:

The L-R functions are the extension of Lyapunov quadratic function to achieve the system stability with the time delays. In the following discussion, L-R is explained briefly in the context of the closed-loop system 2.17. Let α_1, α_2 are positive numbers, $\rho \in R_{[-\tau(r_k),0)}$ and $\pi : R_+ \to R_+$ is a positive function with $\pi(s) > s$ for all $s \in R_+$ and $\pi(0) = 0$. Assume that there exists a Lyapunov function $V(\zeta(k), \tau(r_k)) : R^n \to R_+$ such that

$$\alpha_1||\zeta(k)||^2 < V(\zeta(k), \tau(r_k)) < \alpha_2||\zeta(k)||^2$$

where $\alpha_1 = \lambda_{min}(P)$, $\alpha_2 = \lambda_{max}(P)$ and for all $\zeta(k) \in R^n$ and $\tau(r_k) \in \mathcal{N}$, if $\pi(V(\zeta^+)) \geq max_{\theta \in Z[-\tau(r_k),0]} V(\zeta(\theta))$, then

$$V(\zeta^+) \leq \rho V(\zeta(0))$$

then the closed-loop system will be stochastically stable.

2.3.2 Current Research Trends in TT NCSs

Recently, various systematic stability analysis approaches of NCSs with networked-induced imperfections are proposed. For example, the constraint of time delays is discussed in [21, 22, 52], and of packet dropout effects in [23, 24, 26–28, 145], and

of quantization in [29, 30, 69], and communication constraints in [31–34], respectively. Although all the aforementioned constraints exist simultaneously in NCSs, however most of the research focuses on individual imperfections. In this thesis, I will focus on the modeling and stability of NCSs with multiple constraints.

Seminal works have been done on stability analysis and controller design for NCSs with time-varying, uncertain, large time, or random time delay, as presented in [21, 22, 52] (for more details, see references therein). To cater for the packet dropout, many approaches have been developed. Stabilization problem of NCSs with arbitrary and Markovian packet losses is considered in [23]. The $\mathcal{H}_\infty$ control problem for NCSs with packet dropouts is studied in [24, 27]. A new NCSs model is considered with single- and multiple-packet transmissions in [145]. The control problem for NCSs with Bernoulli-distributed stochastic packet losses is revisited in [28]. In real time, the time delay and packet dropout exist simultaneously in NCSs. Few results are also available that study both time delay and packet dropout [35, 37, 38, 118].

Recently, the problem of quantized feedback control has seen a growing research interest due to the emerging of computer based control and NCSs. The quantization effects can be investigated in two aspects: (1) reduction of the quantization effects to ensure the system performance and stability, and (2) considering quantizers as information coders. In the first approach, stability analysis and controller synthesis are done in the presence of a quantizer by [69, 70]. The second approach talks about the required information from a quantizer to ensure the system stability. It is proved by [72] that the minimum quantization information required for the system stability depends on the unstable poles of plant. The logarithmic quantizers can give minimum or coarsest quantization densities [75]. The similar research to use optimal quantizers and coarsest quantization densities is carried out by [76], while sustaining the system stability for Markovian jump systems (MJSs).

Various approaches are adopted to cater for NCSs constraint of limited bandwidth. For instance, the constraint of communication bus with limited capacity is handled with the help of a hold device and a communication sequence in [33]. Similar work are proposed in [31, 32, 34] to cater for limited communication bandwidth. The limited bandwidth is compensated in this thesis by proposing various techniques such as adaptive quantization densities, congestion control mechanism and event triggered control.

2.3.3 Constraints in ET NCSs

The incorporation of the ET mechanisms in the stability analysis and the controller design of the NCSs is a growing research area [60]. It is because of the capability of the

ET mechanisms to reduce the bandwidth consumption by ensuring data transmission on demand. However, this research area is not well developed and needs a lot of further investigation. Few researchers introduced the time-triggered mechanism for the NCSs framework in the presence of time delays [61, 62]. In Chapter 8, author developed a stochastic stability criteria and $\mathcal{H}_\infty$ performance is analyzed in the presence of packet dropouts. A detailed discussion on the ET NCSs while considering different NCSs constraints is beyond the scope of this doctoral study.

2.4 Comparison Between TT and ET NCSs

This section analyzes and compares the TT and the ET NCSs qualitatively and by the simulations using the MATLAB TrueTime toolbox and Simulink.

2.4.1 Qualitative Comparison

The TT and the ET triggering mechanisms are qualitatively compared on the basis of different requirements in the discrete time NCSs. These requirements are synchronization, the ability to react to asynchronous events and the compensation for the latencies and jitters in the worst case, and the regular operation of the control loops. The TT mechanism is quite useful in the NCSs framework due to its synchronization, quasi-deterministic nature and composability [41]. Due to these advantages the formal design theories are easy to develop but are time restrictive for the implementation. On the other hand, the ET mechanism is flexible for the implementation due to its quick response to the unknown asynchronous events [46]. It is the mechanism of choice, by implementation point of view, because of the optimized resource utilization. However, the formal designs for the ET mechanism are quite complex and are not developed as far. Therefore, the selection of either the TT or the ET mechanism is application dependent [39], and even some researchers also explored the advantages of their combination [47, 48]. It is intended to analyze the performance of TT and the ET mechanisms during the worst case scenario and regular operation of the NCSs. The worst case scenario requires a quick response from the system to a critical situation (an asynchronous event). In the regular operation three assumptions are normally made for NCSs. Firstly, the control law assumes that the transmission of the measured variable from the sensor to the controller and the control input from the controller to the actuator are perfectly periodic. Otherwise a time varying control law is required to achieve the stability and performance of the system. The time varying control law also assumes that the time information is available. Secondly, it is assumed that the controller variable is transmitted from sensor to controller with no delay or a constant delay (latency). There is the

same assumption for the control input transmission from controller to actuator. Otherwise, again, a time varying law is required to compensate the latencies and resulted jitter. Thirdly, the delays, either compensated or not, result in the degradation of the performance. Before proceeding further, it is worth mentioning that each component of a NCS can be considered as a network node.

2.4.1.1 Worst Case Scenario

The worst case scenario is defined as a critical situation which can occur at any node as an asynchronous event. The response to this event determines the performance of the TT and the ET mechanisms. Latency and jitter are two of the parameters that can measure the performance of the system's response to an asynchronous event. Latency can be defined as the round trip delay (delay in system's response to an event) between the plant and the controller nodes, while jitter is the variation in latency. The concept of latency and jitter is elaborated with the help of Figure 2.9. In this figure t_0 is the time on that a critical situation occurs at node A. In response, it transmits the message to node B at time t_1 that is received by node B at time t_2. After that, node B replies at time t_3 which is received by node A at time t_4. In this time framework, $t_0 - t_1$ is processing and wait delay at node A, $t_1 - t_2$ is the communication delay from node A to node B, $t_2 - t_3$ is again processing and wait time but at node B and $t_3 - t_4$ is the communication delay from node B to node A. The time from $t_0 - t_4$ is the system response time to the critical situation and is called latency. The right hand side of Figure 2.9 elaborates the concept of jitter that is variation in latencies.
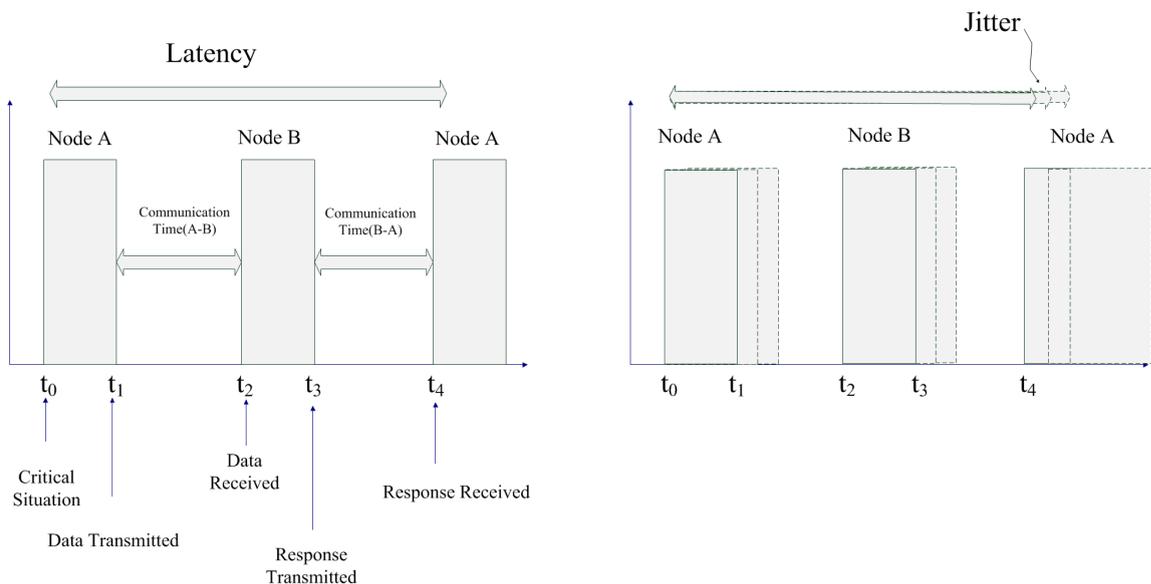
FIGURE 2.9: Latency and jitter

For the worst case scenario, the behavior of the TT and the ET is examined and it is found that the ET mechanism outperforms the TT mechanism in response to the asynchronous events. In the ET mechanism node A sends data as soon as the network is free. The performance of the ET mechanism solely depends upon network load, message priority and data rate. The ET mechanisms results in less latency and jitter for the reduced network load. However, higher network load reduces the efficiency of the mechanism. In the case of the TT mechanism, node A transmits its data to node B on its allocated time slot only, therefore its performance is totally invariant of the network load and depends on the cycle structure and data rate only. Although the TT mechanism is not capable to a quicker response to an asynchronous event, but it provides an upper bound on the response time due to its quasi-deterministic nature.

2.4.1.2 Regular Operation

For regular operation, the sampled data (discrete time) system, as shown in Figure 2.1, is considered. The discrete time system consists of two nodes i.e., the plant and the controller nodes. It is assumed that 1) the triggering mechanism, either the TT or the ET, is embedded in the nodes, and 2) all other system components such as sensors, actuators and quantizers (A/Ds), are part of the plant node. Both nodes are connected over the network. The round trip delay (latency) between nodes is divided into three main components: 1) communication delay between plant and controller, τ_{pc}, 2) processing delay at controller node, τ_c, and 3) communication delay between controller and plant, τ_{cp}. All other small delays, such as processing delays of sensors, actuators and quantizers are neglected without loss of generality. In this setup the TT and the ET mechanisms are compared with respect to their impact on the delays.

Communication Delays τ_{pc} and τ_{cp}

Both communication delays are same in nature, therefore they are considered together here. The effect of either the TT or the ET mechanism is the same on both delays. It is worth mentioning that communication networks are the main source of delays and jitters. Following are the impacts of the TT and the ET mechanisms on the communication delays:

TT Mechanism: In this mechanism, network-induced latencies remain constant, hence no jitter is produced. For this, it is required that all the network components should be globally synchronized, otherwise latencies and jitter will be worse than the ET mechanism.

ET Mechanism: In this mechanism, the data is sent as soon as the network is available. However, latencies and jitters are expected as they solely depend on the network load, message priority and data rate.

Computational Delay τ_c

This delay depends on the number of control tasks and their scheduling by the controller's operating system. Even the impact of the TT and the ET mechanisms, on the delay, depends on the number of the control tasks and their scheduling. The impact of both mechanisms is described as

TT Mechanism: If task synchronization is achieved, then the TT mechanism results in zero delay and jitter for the single control loop. However, if scheduling is required in the case of multiple control loops, then constant latencies are expected

ET Mechanism: It results in zero latency and jitter if the controller is catering for only one control loop. In the case of multiple loops, the performance of any particular loop can be achieved at the cost of other loop's performance.

In summary, it can be revealed that both the TT and the ET mechanisms can result in time varying delays. To cater for these jitters, a delay-dependent controller is required.

2.4.2 Comparison by Simulations

In this section, effect of the TT and the ET sampling mechanisms on the system performance, delays and jitters is analyzed. This analysis is performed by using the Simulink based toolbox, TrueTime [49]. The block diagram of the TrueTime toolbox is shown in Figure 2.10. This toolbox facilitates the simulation of real time processes such as DC servo system by presenting them with simple Simulink blocks. It also enables simulation of different communication networks as Simulink blocks. The toolbox is suitable for analyzing the temporal behavior of control processes, timing parameters and multi-task scheduling for real-time and NCSs.

2.4.2.1 Example: A DC Servo Control Over the Network

This example is taken from [50]. In this example, a DC servo motor is controlled over a general purpose Ethernet network as shown in Figure 2.11. It is natural in the NCSs framework that the sensor node is considered as TT, while network, controller and actuator nodes are considered as ET. In this example, however, the sensor node is considered as both TT and ET mechanisms, to analyze the effect of both sampling
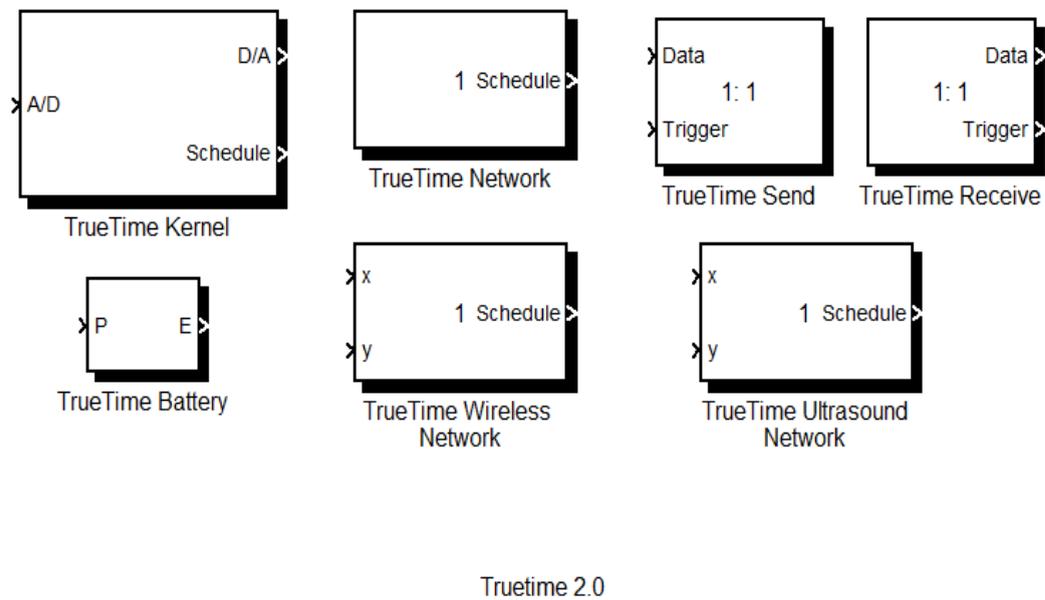
FIGURE 2.10: A Simulink based toolbox for real-time and networked control systems:
TrueTime

mechanisms. In addition to this, the control law is proposed without delay compensation so that the impact of the sampling mechanisms on the delays and jitters can be realized properly.

Consider the transfer function of a DC servo motor:

$$G(s) = \frac{100}{s(s+1)} \tag{2.43}$$

It is discretized at the sampling rate of 1 ms, with $w(k) = 0$. According to the equation (2.2), the state space representation of the system is:

$$
\begin{aligned}
x(k+1) &= \begin{bmatrix} 1.3680 & -0.3679 \\ 1.0000 & 0 \end{bmatrix} x(k) + \begin{bmatrix} 1 \\ 0 \end{bmatrix} u(k) \\
y(k) &= \begin{bmatrix} 36.79 & 26.42 \end{bmatrix} x(k)
\end{aligned}
\tag{2.44}
$$
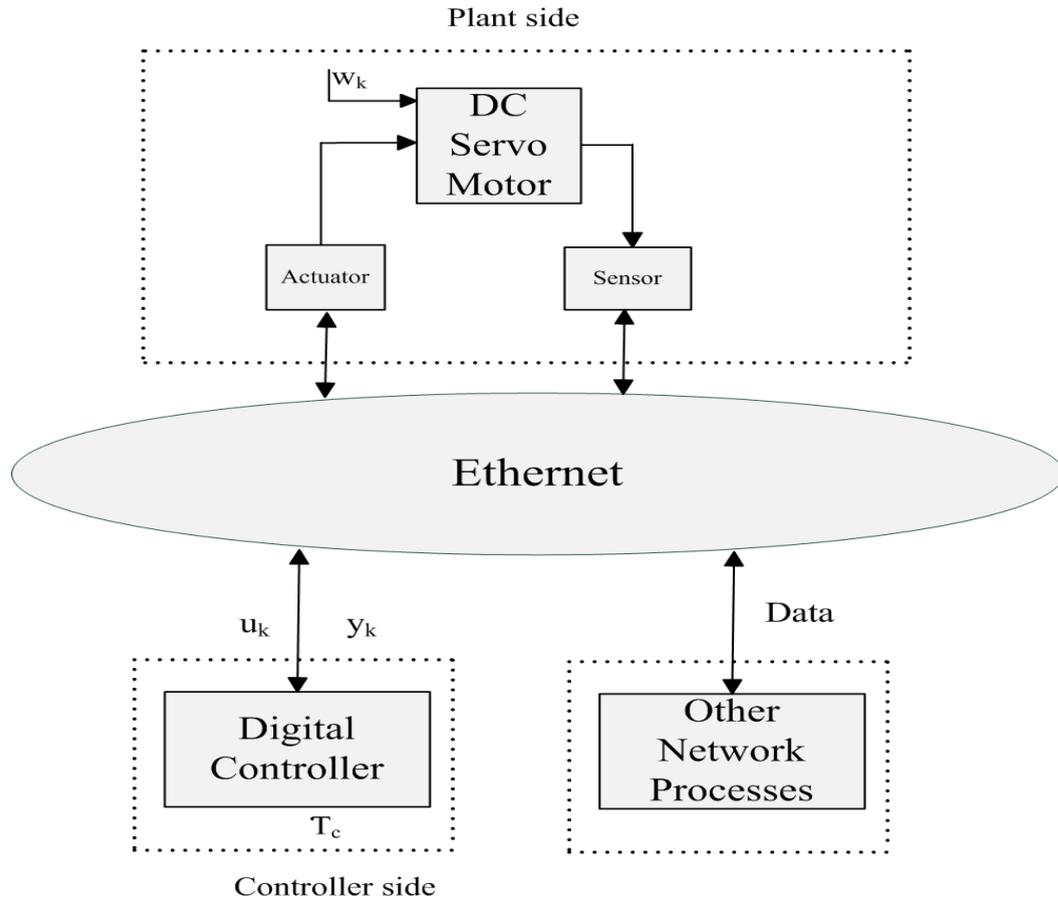
FIGURE 2.11: A servo motor control in NCSs Framework

In this example, a dynamic output feedback controller of the form (2.3) is proposed. The controller gains are obtained using LMI toolbox:

$$
\begin{aligned}
A_c &= \begin{bmatrix} 0.9424 & -0.5566 \\ 0.9510 & -0.0490 \end{bmatrix}, \quad B_c = 1.0e + 003 * \begin{bmatrix} 1.1430 \\ 0.9798 \end{bmatrix} \\
C_c &= \begin{bmatrix} -0.9995 & 0.4995 \end{bmatrix}
\end{aligned}
$$

The motor is controlled with the help of sensor and actuator over the TrueTime network. The sensor, actuator and controller are implemented as TrueTime kernels.

It is mentioned earlier that the sensor is implemented on the basis of TT mechanism in TrueTime toolbox. In this example, it is also implemented on the basis of ET mechanisms so that the performance of both mechanisms can be analyzed. This example implements the ET mechanism, according to the condition given in equation (2.8). According to the equation, sensor transmits the data over the network only when the $||e(k)|| = ||\bar{y}(k) - y(k)|| > \sigma ||y(k)||$ is satisfied. It means that the ET mechanism follows "sampling on the demand" approach. It is shown in Figure 2.12 that data is transmitted
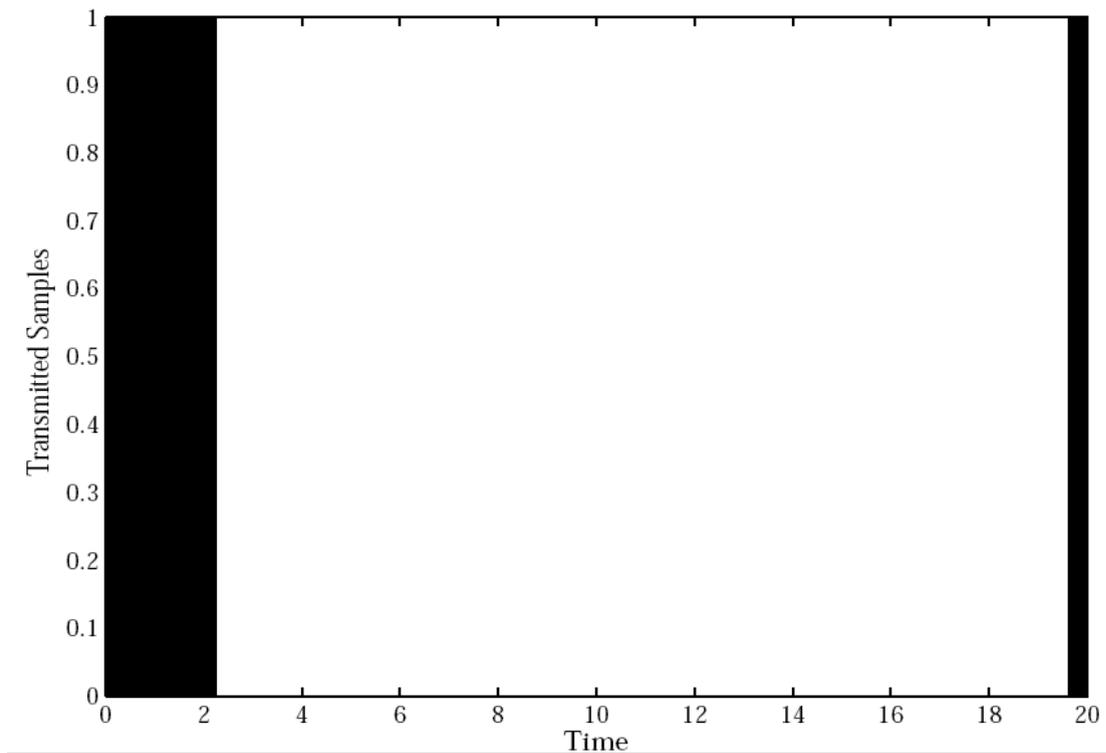
FIGURE 2.12: Number of transmitted samples using ET mechanism

in the start when the difference between $\bar{y}(k)$ and $y(k)$ is large. As the system gets stable and $||e(k)||$ remains in bounds, then no need to transmit further data. However, the error $||e(k)||$ is kept on accumulating and when it satisfies the condition again then the data is transmitted again. It can be evaluated from the figure that it sends only $\simeq 15\%$ of the actual samples (In the figure, shaded area shows the number of transmitted samples). On the other hand, the TT mechanism transmits the data periodically and sends all the samples.

Although, the ET mechanism reduces bandwidth consumption, but there is a tradeoff between the bandwidth consumption and the system performance. It is shown in the Figure 2.13(a) that the system achieves asymptotic stability by using the TT mechanism. The ET mechanism also stabilizes the system but its steady state remains around the origin and does not achieve the asymptotic stability. It is shown in Figure 2.13(b).

In the absence of other interference nodes, the TT mechanism results in fixed delays (latencies) and zero jitter. It is evaluated from 2.14(a) that TT mechanisms produces the fixed delay of 2.5 *msec*. It means that the TT mechanism is quasi-deterministic. It is also concluded in section 2.4. On the other hand, the ET mechanism results in variable delays and jitter. In the Figure 2.14(b), the delays between the samples of sensor and actuator range from 5 *ms* to 30 *ms* that result in an accumulative jitter of 25 *ms*. The

(a) System state using TT mechanism

(b) System state using ET mechanism
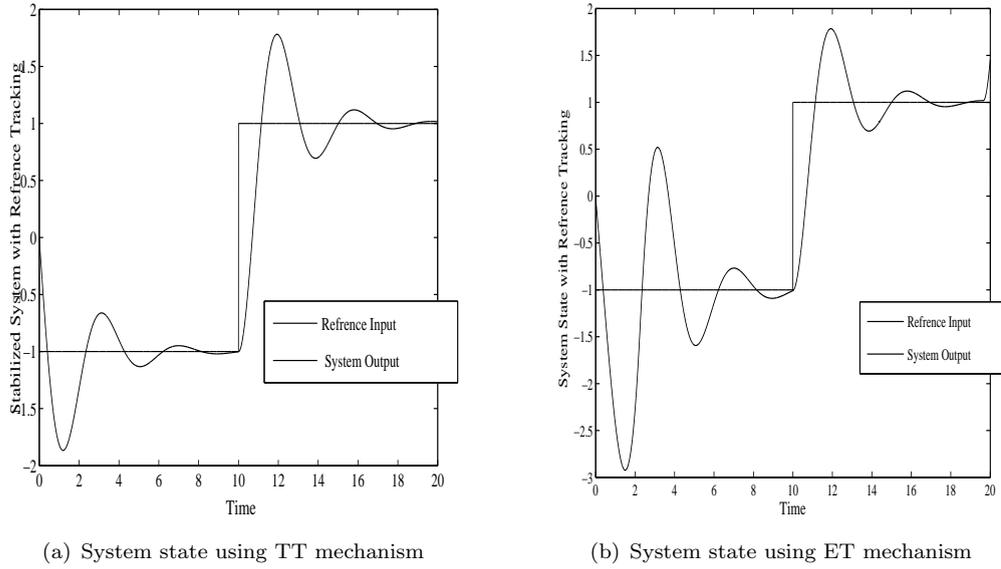
FIGURE 2.13: System states

jitter is calculated by following iterating equation:

$$J = J + |D(i - 1, i)| \tag{2.45}$$

J is the jitter and D is the difference between delays between two samples. It is worth mentioning that the results are according to the discussion of the section 2.4.1.2.

Note: It is evaluated from different simulations that the TT mechanism also results in variable delays in the presence of other interference nodes.

(a) Latency and jitter in TT mechanism

(b) Latency and jitter in ET mechanism
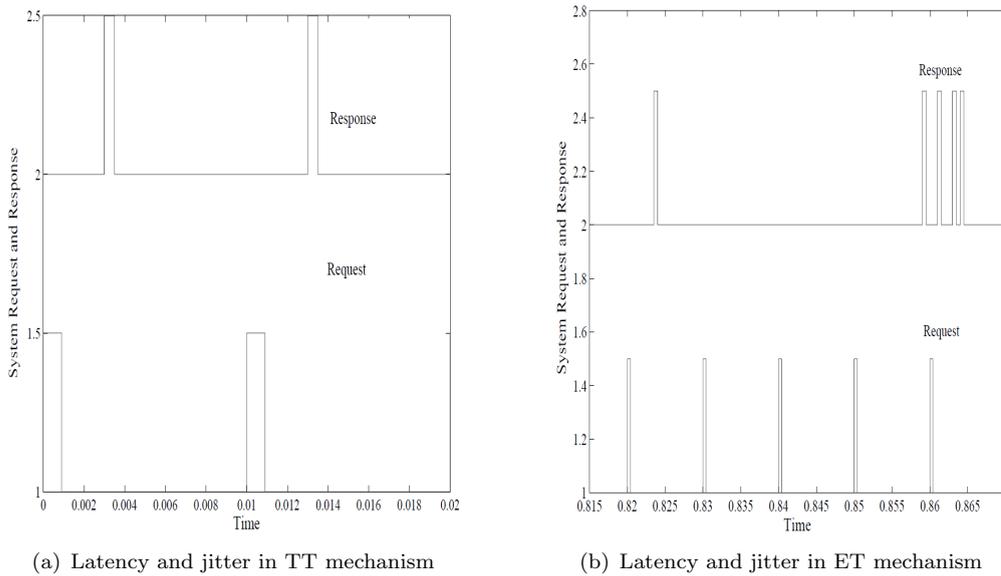
FIGURE 2.14: Latencies and jitters

2.5 Conclusions

This chapter is a literature survey on the TT and ET mechanisms in the context of the NCSs. Firstly, the basic concepts of both sampling mechanisms are discussed. For the ET mechanism, various conditions for generating an event are provided. After this, a detailed literature survey on the NCSs is conducted and various constraints such as time delays, packet dropouts, limited bandwidth and quantization errors are identified. A brief overview of the stability techniques of the NCSs is also provided. The effect of the TT and the ET mechanisms on the NCSs constraints such as time delays and bandwidth are analyzed qualitatively and by simulations. The simulations show that both mechanisms stabilize the system. However, the ET mechanism transmits smaller number of samples, hence reduces bandwidth consumption. On the other hand, TT mechanism results in better control performance but transmits all the samples. It is evaluated that the TT and ET mechanisms result in fixed and time varying delays, respectively. However, it is possible that the TT mechanism may also result in time varying and random delays. It is due to the random nature of network and other interfacing nodes. It is concluded that the delay-dependent control laws are indispensable for the NCSs. It is also evaluated that the identified constraints should be properly modelled and incorporated in the design before providing the stability criteria and control designs.

Chapter 3

Robust $\mathcal{H}_\infty$ State Feedback Control of NCSs with Poisson Noise and Successive Packet Dropouts

This chapter examines various constraints of networked control systems (NCSs) such as network-induced random delays, successive packet dropouts and Poisson noise. The time delays are represented as the modes of a Markov chain and the successive packet dropouts are modelled using the Poisson probability distribution. For each delay-mode, a different Poisson distribution is used with the help of an indicator function. The Poisson noise is incorporated in the design to cater for sudden network link failures. After modelling the constraints, a stability criterion is proposed by using a detailed Lyapunov-Krasovskii(L-K) functional. On the basis of the stability criterion, sufficient conditions for the existence of a robust $\mathcal{H}_\infty$ state feedback controller are given in terms of bilinear matrix inequalities (BMIs). Later, BMIs are converted into quasi-convex linear matrix inequalities (LMIs) and are solved by using a cone complementarity linearization algorithm. The effectiveness of the proposed design is elaborated with the help of two simulation examples. Moreover, the effects of successive packet dropouts and the Poisson noise, on $\mathcal{H}_\infty$ performance, are analyzed [101].

3.1   Introduction

It is a well known fact that in the NCSs the components are spatially distributed. Therefore, the assumption of the prefect information flow between them is not realistic.

It is due to various network constraints such as: (1) time delays due to the network congestion [120], (2) packet dropouts due to the overflow in buffers and queues at the network nodes [30], (3) sudden network failures due to removal of any node or power shutdown, and (4) variable sampling/transmission intervals due to the multiple nodes. Most of the constraints are stochastic in nature and different probabilistic methods are used to model them. In the available literature, time delays are mostly modelled using the Markov chain [125, 128] and the packet dropouts are modelled using the Bernoulli random distribution [30, 129]. The time delays and the packet dropouts may occur on both sides of a control loop i.e., from sensor to controller and from controller to actuator. In [130], the random time delays that exist on both sides are modelled separately by using two Markov chains. Similarly in [129] the packet dropouts are modelled by using two mutually independent random variables following the Bernoulli distributed white sequence. However, the literature on the successive packet dropout sequences that occur frequently in the networks is almost nonexistent. The successive packet dropout sequences can not be modelled using a single Bernoulli distribution due to its discrete nature. Under the Bernoulli, the probability $'0'$ represents a packet dropout event, and $'1'$ denotes the packet delivery. The Bernoulli is not capable of distinguishing between the number of successive dropout random sequences. However, the Poisson distribution is capable of model successive packet dropout sequences precisely. Although the Poisson distribution has infinite expectation, however the probability of an infinite number of the packet dropouts is very small and can be considered zero without loss of the generality. In this case, the previous information stored in the controller buffer will be used. However, if the packets keep on dropping, then the system will become unstable after a maximum interval [132].

In the real world dynamic systems the noise is modelled either as a Wiener or a Poisson process. The Wiener noise adds up continuous fluctuations in the system dynamics while the Poisson noise results in the random discontinuities. Therefore the Poisson noise is expected in any system where there is a possibility of any sudden fluctuations such as the link failure or the power shutdown of any network component in the NCSs. The phenomenon of the Poisson noise can be seen in various other fields e.g., machine breakage in the manufacturing [133], excitatory potential pulses in the neural systems [134], and arrival of new customers in the inventory systems [135]. Therefore the Poisson noise, due to its random pulses, behaves quite differently from the Wiener and the White Gaussian noises. It introduces the random discontinuities in the closed-loop system dynamics and is difficult to model.

The robust $\mathcal{H}_\infty$ control is an efficient control design to minimize the effect of external disturbance in the presence of the system uncertainties [87, 126, 136]. It is worth evaluating $\mathcal{H}_\infty$ performance in the presence of the Poisson noise. Similarly, analyzing the

effect of the random sequences of the successive packet dropouts on the $\mathcal{H}_\infty$ performance is a problem of great significance.

In this design a robust $\mathcal{H}_\infty$ state feedback controller is proposed to compensate for the network-induced random delays, the successive packet dropout sequences and the Poisson noise. Each delay is represented through a mode of the Markov chain. Therefore the system under consideration can be considered as a class of Markovian Jump Systems (MJSs). The successive packet dropout sequences are modelled by using the Poisson distribution. It is worth mentioning that the use of a single Poisson distribution for all the Markov modes is quite conservative. Therefore, an indicator function is proposed to select the separate Poisson probabilities for each mode of the Markov chain. A similar approach is used by [131] where the missing measurement or dropouts from the multiple sensors are compensated for by using a random matrix function for each mode of MJSs separately. In addition to this the sudden network link failure is represented as the Poisson noise jumps. Moreover in the simulations the $\mathcal{H}_\infty$ performance is analyzed under the presence of the Poisson noise and the successive packet dropouts. To the best of authors' knowledge, the problem of designing a state feedback controller with the successive packet dropouts modelling, the Poisson noise and random delays has not been fully investigated. The main contributions of the chapter are listed as follows:

- The Poisson noise is incorporated in the design of a robust $\mathcal{H}_\infty$ state feedback controller to cater for sudden link/node failure for the NCSs.

- The Poisson random distribution is used to model the random sequences of the successive packet dropouts for the first time in the NCSs.

- The stability criteria and the controller design is proposed for the MJSs where adaptive Poisson probability distributions are used for the Markov modes using an indicator function.

- The $\mathcal{H}_\infty$ performance is analyzed under the presence of the Poisson noise and successive packet dropouts.

The rest of this chapter is organized as follows. Section 3.2 discusses the system description with the incorporation of the Poisson noise, modelling of the random delays and the successive packet dropouts. The necessary lemma and problem formulation are also given in this section. In Section 3.3, main results for the stability analysis and the synthesis of a robust $\mathcal{H}_\infty$ state feedback controller are presented in terms of the BMIs. A cone complementarity algorithm is employed to convert these BMIs into the quasi-convex LMIs. Section 3.4 consists of two simulation results to validate the effectiveness of the design. Moreover the impact of the Poisson noise and the packet dropout

sequences on the $\mathcal{H}_\infty$ performance is analyzed. Finally, the conclusions are given in Section 3.5.

3.2   System Description and Definitions

A class of the discrete-time NCSs, as shown in Figure 3.1, is described by the following model:

$$
\begin{aligned}
x(k+1) &= [A + \Delta A(k)]x(k) + [B_1 + \Delta B_1(k)]w(k) + [B_2 + \Delta B_2(k)]u(k) \quad x(0) = 0 \\
z(k) &= [C_1 + \Delta C_1(k)]x(k) + [D_{11} + \Delta D_{11}(k)]w(k) + [D_{12} + \Delta D_{12}(k)]u(k) \quad (3.1)
\end{aligned}
$$

where $x(k) \in \Re^n, u(k) \in \Re^m$ and $z(k) \in \Re^{m_1}$ are the systems states, input and controlled output, respectively. $w(k) \in \Re^{m_3}$ is the disturbance that belongs to $\mathcal{L}_2[0, \infty)$, the space of square summable vector sequence over $[0, \infty)$. The matrices A, B_1, B_2, C_1, D_{11} and D_{12} are of the known matrices with the appropriate dimensions. The matrix functions $\Delta A(k)$, $\Delta B_1(k)$, $\Delta B_2(k)$, $\Delta C_1(k)$, $\Delta D_{11}(k)$ and $\Delta D_{12}(k)$ represent the time-varying uncertainties in the system which satisfies the following assumption:
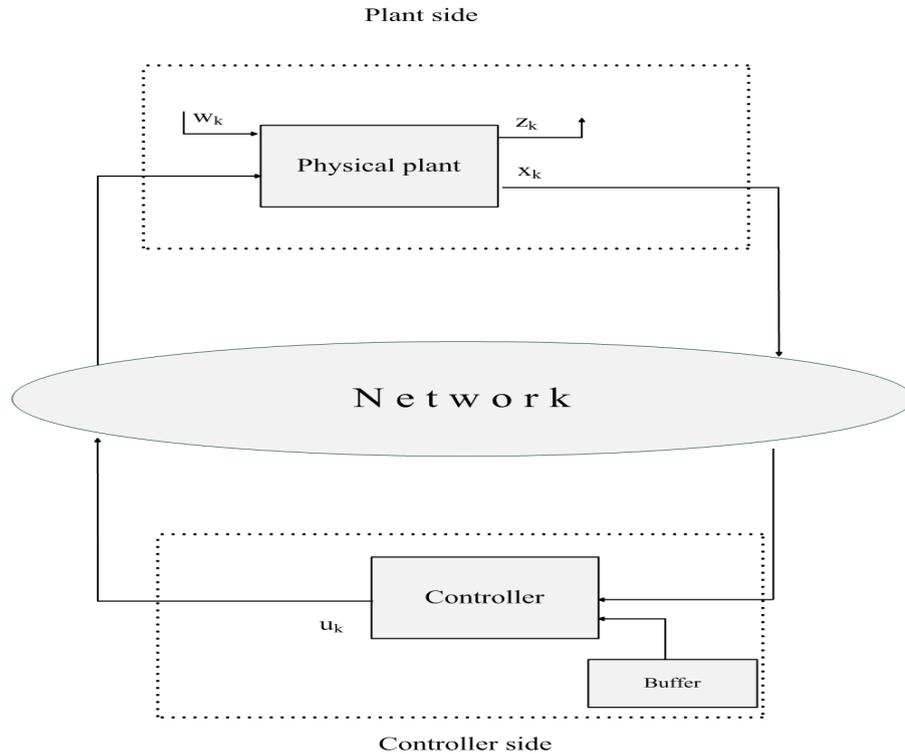
FIGURE 3.1: Networked control systems

Assumption 3.2.1.

$$\begin{bmatrix} \Delta A(k) & \Delta B_1(k) & \Delta B_2(k) \\ \Delta C_1(k) & \Delta D_{11}(k) & \Delta D_{12}(k) \end{bmatrix} = \begin{bmatrix} E_1 \\ E_2 \end{bmatrix} F(k) \begin{bmatrix} H_1 & H_2 & H_3 \end{bmatrix}$$

where E_1, E_2, H_1, H_2, and H_3 are the known matrices which characterize the structure of the uncertainties. Furthermore, there exists a positive-definite matrix $\mathcal{W}$ such that the following inequality holds:

$$F^T(k)\mathcal{W}F(k) \leq \mathcal{W}$$

In the real world dynamical systems, the noise can be either a Wiener or a Poisson process. In the case of the NCSs, noise is mostly a Wiener process, but if the communication link fails or is rusty then it results in discontinuous random fluctuations. This type of noise is a Poisson process in nature.

3.2.1 The Poisson Noise in LTI Discrete Systems

Consider a discontinuous random fluctuation in the states of an LTI discrete system on a given instant k:

$$\sum_\Theta \tau(\theta)x(k)N(\theta,k) \tag{3.2}$$

where

$$
\begin{aligned}
\Theta &= \text{Poisson mark space} \\
\theta \in \Theta &= \text{Random variable that shows the characteristics of the Poisson noise} \\
&\quad \text{(e.g., size shape age etc)} \\
N(\theta,k) &= \text{Poisson noise with values either 0 or 1} \\
\mu(\theta,k) &= E\{N(\theta,k)\} \\
\tau(\theta) &= \text{Amplitude of the Poisson jump} \tag{3.3}
\end{aligned}
$$

By adding (3.2) in the system (3.1):

$$
\begin{aligned}
x(k+1) &= [A + \Delta A(k)]x(k) + [B_1 + \Delta B_1(k)]w(k) + [B_2 + \Delta B_2(k)]u(k) + \\
&\quad \sum_\Theta \tau(\theta)x(k)N(\theta,k) \quad x(0) = 0 \\
z(k) &= [C_1 + \Delta C_1(k)]x(k) + [D_{11} + \Delta D_{11}(k)]w(k) + [D_{12} + \Delta D_{12}(k)]u(k)
\end{aligned}
\tag{3.4}
$$

where $\sum_\Theta \tau(\theta)x(k)N(\theta,k)$ is the Poisson noise. Moreover if there is only one mark in space Θ then $\sum_\Theta \tau(\theta)x(k)N(\theta,k)$ becomes $\tau x(k)N(k)$.

Let $\{r_k,k\}$ be a discrete homogeneous Markov chain taking values in a finite set $\mathcal{S} = \{1,2,\cdots,s\}$ with the following transition probability from the mode i at a time k to the mode j at a time $k+1$:

$$p_{ij} := \mathbf{Prob}\{r_{k+1}=j|r_k=i\}$$

where $i,j \in \mathcal{S}$, $0 \le p_{ij} \le 1$ and $\sum_{j=1}^s p_{ij} = 1$. In this chapter, the random delay τ_k is modelled as a finite state Markov process: $\tau_k = \tau(r_k)$ with $0 \le \tau(1) < \tau(2) < \cdots < \tau(s) \le \infty$. It is assumed that the controller will always use the most recent data i.e., if there is no new information coming at step $k+1$ (data could be lost or there is a longer delay), then $x(k-\tau_k)$ will be used for the feedback. Thus the delay τ_k can only increase at most by 1 at each step, and is constrained:

$$\mathbf{Prob}\{\tau_{k+1} > \tau_k + 1\} = 0$$

Hence, the structured transition probability matrix [84] is

$$P_\tau = \begin{bmatrix} p_{11} & p_{12} & 0 & 0 & \ldots & 0 \\ p_{21} & p_{22} & p_{23} & 0 & \ldots & 0 \\ \vdots & \vdots & \vdots & \vdots & \ddots & \vdots \\ \vdots & \vdots & \vdots & \vdots & \vdots & p_{(s-1)s} \\ p_{s1} & p_{s2} & p_{s3} & p_{s4} & \ldots & p_{ss} \end{bmatrix} \tag{3.5}$$

with $0 \le p_{ij} \le 1$ and $\sum_{j=1}^{i+1} p_{ij} = 1$.

A delay-mode dependent state feedback controller of the following form is proposed:

$$u(k) \;=\; K(r_k)x(k-\tau(r_k)) \tag{3.6}$$

where $K(rk)$ are gains of delay mode-dependent state feedback controller.

3.2.2 Packet Dropouts

It is well known that the packet dropouts result in the performance degradation and the system instability. Therefore they should be appropriately compensated in the NCSs design. The packet dropouts can be modelled using the various probability distributions or their combinations such as Bernoulli, Uniform and Poisson. The Bernoulli and the Uniform distributions have finite expectations while the Poisson distribution has an infinite

expectation. There can be a single or successive packet dropout sequences in a network, existing between the plant and the controller. In the case of a single packet dropout sequence, the Bernoulli random distribution is very effective and popular among the researchers. On the other hand the random sequences of the successive packet dropouts which occur commonly in the real time networks, get much less intension from the researchers. The Bernoulli and the Uniform distribution are not capable of modelling the random sequences of successive packet dropouts. In this section the random sequences of the successive packet dropouts are modelled using the Poisson distribution.

Packet Dropouts Analysis

A series of experiments have been preformed using *OPNET IT Guru* to analyze the packet dropouts in a shared medium. The simulation is run for 1000 seconds in a given experiment and the packet dropouts are calculated for the network. The probability of the successive packet dropout sequences, following the Poisson distribution, is obtained as shown in Table 3.1. The number of the packet dropout sequences, for the given

TABLE 3.1: Successive packet dropouts probabilities

Packet Dropout Sequences κ_d	0	1	2	3	4
p_d	0.4444	0.37037	0.137	0.037	.01054

simulation, are shown in Figure 3.2 with mean, $\lambda = 1.8$. It is worth emphasizing that both the Bernoulli and the Poisson distribution can be combined together to model the successive packet dropout sequences. The Bernoulli can be used to find out if any packet dropout sequence has occurred or not. If the packets are dropped, then the Poisson distribution can be used to find the probability of random sequences of the packet dropouts. Moreover the Poisson distribution itself is capable of modelling the successive packet dropout sequences and this approach is used in this chapter to model the successive packet dropout sequences.

Packet Dropouts Modelling

As mentioned above, the Poisson distribution is used to model the successive packet dropouts. Lets denote the number of packet dropouts by a random variable $\sigma(k)$ following a Poisson distribution. Suppose $\sigma(k)$ is with any n number of the possible values $\kappa_0, \kappa_1 \cdots \kappa_m$. The probability of each outcome κ_d will follow the Poisson distribution as follows:

$$p_d = Prob\{\sigma(k) = \kappa_d\} = \frac{\lambda^{\kappa_d} e^{-\lambda}}{\kappa_d!} \quad d = 0, 1 \cdots m$$
$$Mean = E\{\sigma(k)\} = \lambda$$

$$(3.7)$$
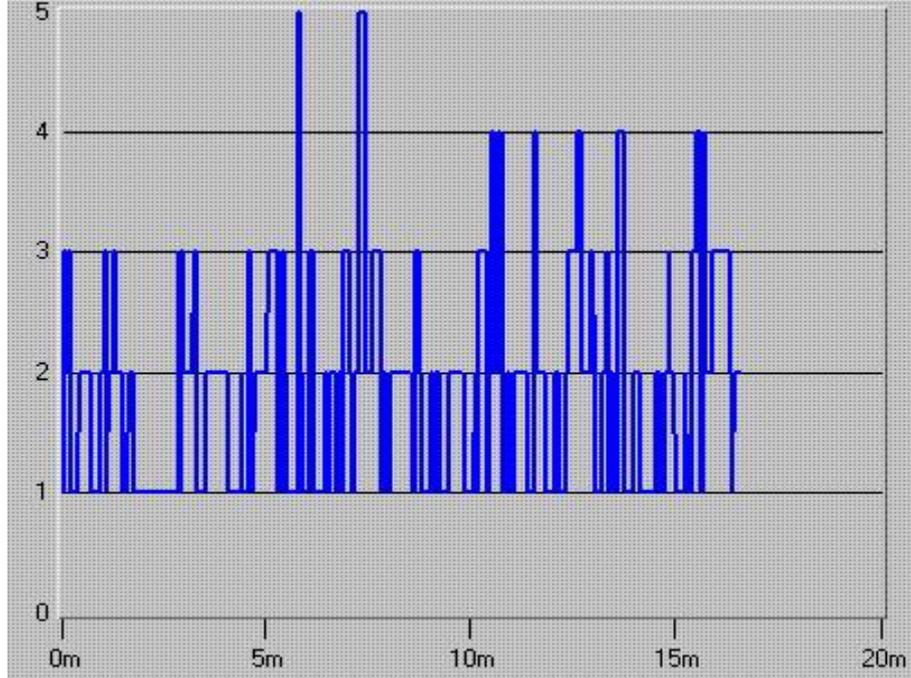
FIGURE 3.2: Communication between sensor nodes and controller using OPNET IT Guru

where m are maximum packet dropouts.

The Poisson distribution has an infinite expectation, therefore the interval of any random sequence of the packet dropouts can range from 0 to ∞. The interval with ∞ value may occur when $m \to \infty$ and always has a very low probability. Therefore this low probability can be considered as 0 without loss of the generality. In this case the current data will be used as the feedback.

Remark 3.2.1. As discussed earlier, the random delays are modelled using the Markov chain. These types of systems are one of the class of the Markovian jump systems (MJSs) in which each Markov mode represents a random delay. On the other hand, the packet dropout sequences are probabilistic in nature and are modelled by the Poisson random distribution. The use of the same Poisson distribution for each delay-mode results in a conservative design. Therefore different Poisson distributions are used for each mode using an indicator function $\chi(i)$:

$$\chi(i) = \begin{cases} 1, & \text{if } r_k = i \\ 0, & \text{if } r_k \neq i \end{cases} \tag{3.8}$$

After modelling the constraints from (3.2)-(3.8), a state feedback controller is proposed as:

$$u(k) \;=\; K(r_k)\left\{ \sum_{\kappa_d(r_k)=0}^{\kappa_m(r_k)} \chi(i)p_d(r_k)x(k-\tau(r_k)-\kappa_d(r_k)) \right\} \tag{3.9}$$

where $K(r_k)$ is delay-mode dependent controller gain, κ_d are the packet dropout sequences, κ_m is the sequence of the maximum dropouts, $\chi(i)$ is the indicator function, p_d are the Poisson probabilities, and $\tau(r_k)$ are the random delays. For the simplicity, the $p_d(r_k)$ will be notated as p_{di}, $\kappa_d(r_k)$ as κ_{di}, $\kappa_m(r_k)$ as κ_{mi}, $\tau(r_k)$ as $\tau(i)$ and $\chi(i)$ as χ_i.

By applying (3.9) on (3.4), following system is obtained:

$$
\begin{aligned}
x(k+1) \;=\;& [A+\Delta A(k)]x(k) + [B_1+\Delta B_1(k)]w(k) + [B_2+\Delta B_2(k)]K(i) \\
& \left\{ \sum_{\kappa_{d_i}=0}^{\kappa_{m_i}} \chi_i p_{di} x(k-\tau(i)-\kappa_{di}) \right\} + \sum_\Theta \tau(\theta)x(k)N(\theta,k) \\
z(k) \;=\;& [C_1+\Delta C_1(k)]x(k) + [D_{11}+\Delta D_{11}(k)]w(k) + [D_{12}+\Delta D_{12}(k)]K(i) \\
& \left\{ \sum_{\kappa_{d_i}=0}^{\kappa_{m_i}} \chi_i p_{di} x(k-\tau(i)-\kappa_{di}) \right\}
\end{aligned}
\tag{3.10}
$$

The problem under study is formulated as follows.

3.2.3 Problem Formulation:

Given a prescribed $\gamma > 0$, design a state feedback controller of the form (3.9) such that

1. the system (3.4) with (3.9) and $w(k) = 0$ is stochastically stable, i.e, there exists a constant $0 < \alpha < \infty$ such that

$$E\left\{ \sum_{\ell=0}^{\infty} x^T(\ell)x(\ell) \right\} < \alpha \tag{3.11}$$

   for all $x(0), r_0$.

2. Under the zero-initial condition, the controlled output $z(k)$ satisfies

$$E\left\{ \sum_{k=0}^{\infty} z^T(k)z(k)|r_0 \right\} < \gamma \sum_{k=0}^{\infty} w^T(k)w(k) \tag{3.12}$$

   for all nonzero $w(k)$.

Before ending this section we introduce the following lemma that will play a vital role in deriving our main results.

Lemma 3.2.1. *Let $y(k) = x(k+1) - x(k)$ and $\tilde{x}(k) = \Big[x^T(k) \ x^T(k-\tau_i) \ x^T(k-\tau_i - \kappa_{1i}) \ \cdots \ x^T(k-\tau_i-\kappa_{mi}) \ w^T(k) \ x^T(k)H_1^T F^T(k) \ x^T(k-\tau_i)K^T(i)H_3^T F^T(k) \ x^T(k-\tau_i - \kappa_{1i})K^T(i)H_3^T F^T(k) \cdots x^T(k-\tau_i-\kappa_{mi})K^T(i)H_3^T F^T(k) \ w^T(k)H_2^T F^T(k) \ x^T(k)N^T(\theta,k)\Big]^T \in \Re^l$, then for any matrices $R \in \Re^{n \times n}$, $M \in \Re^{n \times l}$ and $Z \in \Re^{l \times l}$, satisfying*

$$\begin{bmatrix} R & M \\ M^T & Z \end{bmatrix} \geq 0 \qquad (3.13)$$

the following inequality holds:

$$-\sum_{\kappa_{d_i}=0}^{\kappa_{m_i}} \sum_{i=k-\tau(i)-\kappa_{di}}^{k-1} y^T(i)Ry(i) \leq \tilde{x}^T(k)\Big\{\Upsilon_1 + \Upsilon_1^T + (\tau(i) + \kappa_{m_i} + 1)Z\Big\}\tilde{x}(k) \qquad (3.14)$$

where $\Upsilon_1 = M^T[I \ -I \ -I \ \cdots \ -I \ 0 \ 0 \ 0 \ 0 \ \cdots \ 0 \ 0 \ 0]$.

Proof: The proof is given in appendix 10. $\nabla\nabla\nabla$

3.3 Stability Analysis and Controller Synthesis of NCSs with Poisson Noise and Successive Packet Dropouts

Stability criteria for uncertain discrete-time linear systems with successive packet dropouts and Poisson noise is given in the following theorem.

Theorem 3.3.1. *For given controller gains $K(i)$; $\gamma > 0$, $\mu_\theta > 0$ and $\alpha > 0$ where $i = 1, \cdots, i+1$, if there exist sets of positive-definite matrices $P(i)$, $R_1(i)$, R_1, $R_2(i)$, R_2, $W_1(i)$, $W_2(i)$, $W_3(i)$, Q, $Z(i)$ and matrices $M(i)$ satisfying the following inequalities:*

$$R_1 > R_1(i), R_2 > R_2(i) \qquad (3.15)$$

$$\begin{bmatrix} (1-p_{i(i+1)})R_1(i) + R_2(i) & M(i) \\ * & Z(i) \end{bmatrix} \geq 0 \qquad (3.16)$$

$$\Lambda(i) + \Gamma_1^T(i)\tilde{P}(i)\Gamma_1(i) + \Gamma_2^T[(\tilde{\tau}(i) + \tilde{\kappa}_{di})R_1 + (\tau(s) + \kappa_m)R_2]\Gamma_2(i) +$$
$$\Upsilon_1(i) + \Upsilon_1^T(i) + (\tau(i) + \kappa_{m_i} + 1)Z(i) + \Xi^T(i)\Xi(i) < 0 \qquad (3.17)$$

where

$$
\begin{aligned}
\tilde{P}(i) &= \textstyle\sum_{j=1}^{i+1} p_{ij}P(j) \\
\tilde{\tau}(i) &= \textstyle\sum_{j=1}^{i+1} p_{ij}\tau(j) \\
\tilde{\kappa}_{di} &= \textstyle\sum_{\kappa_{d_i}=0}^{\kappa_{m_i}} \chi_i p_{di}\kappa_{di} \\
\Lambda(i) &= diag\Big\{\Big(-P(i) + (\tau(s) - \tau(1) + \kappa_m + 1)Q + H_1^T(i)F_k^T W_1(i)F_k H_1(i) + \\
&\quad \mu_\theta^T \mu_\theta\Big), \Big(\chi_i p_{0i}K^T(i)H_3^T W_2(i)H_3 K(i) - Q\Big), \cdots \Big(\chi_i p_{mi}K^T(i)H_3^T W_2(i) \\
&\quad H_3 K(i) - Q\Big), \Big(H_2^T W_3(i)H_2 - \gamma I\Big), -W_1(i), -W_2(i), \cdots, -W_2(i), -W_3(i), -I\Big\} \\
\Gamma_1(i) &= \begin{bmatrix} A & \chi_i p_{0i}B_2 K_i & \cdots & \chi_i p_{mi}B_2 K_i & B_1 & E_1 & \chi_i p_{0i}E_1 & \cdots \chi_i p_{mi}E_1 & E_1 & \sum_\Theta \tau_\theta \end{bmatrix} \\
\Xi(i) &= \begin{bmatrix} C_1 & \chi_i p_{0i}D_{12}K_i & \cdots & \chi_i p_{mi}D_{12}K_i & D_{11} & E_2 & \chi_i p_{0i}E_2 & \cdots \chi_i p_{mi}E_2 & E_2 & 0 \end{bmatrix} \\
\Gamma_2(i) &= \begin{bmatrix} A-I & \chi_i p_{0i}B_2 K_i & \cdots & \chi_i p_{mi}B_2 K_i & B_1 & E_1 & \chi_i p_{0i}E_1 & \cdots \chi_i p_{mi}E_1 & E_1 & \sum_\Theta \tau_\theta \end{bmatrix}
\end{aligned}
$$

Then the closed-loop system is stochastically stable with the prescribed $\mathcal{H}_\infty$ performance.

Proof:

Proof is given in Appendix 10.

Theorem 3.3.2. *For a given $\gamma > 0$, $\mu_\theta > 0$ and $\alpha > 0$ and for $i = 1, 2, \cdots, s$, if there exist sets of positive-definite matrices $X(i)$, $\tilde{R}_1(i)$, $\tilde{R}_1$, $\tilde{R}_2(i)$, $\tilde{R}_2$, $W_1(i)$, $W_2(i)$, $W_3(i)$, Q, $\tilde{Q}$, $\tilde{W}_1(i)$, $\tilde{W}_2(i)$, N_1, N_2, $\tilde{S}(i,j)$, $J(i)$ $\tilde{Z}(i)$ and matrices $\tilde{M}(i)$ and $Y(i)$ satisfying the inequalities*

$$
\tilde{R}_1 > \tilde{R}_1(i), \quad \tilde{R}_2 > \tilde{R}_2(i) \tag{3.18}
$$

$$
\begin{bmatrix} (1 - p_{i(i+1)})\tilde{R}_1(i) + \tilde{R}_2(i) & \tilde{M}(i) \\ * & \tilde{Z}(i) \end{bmatrix} \geq 0 \tag{3.19}
$$

$$
\begin{bmatrix} \Pi(i) & \tilde{\Gamma}_1^T(i) & \tilde{\Gamma}_2^T(i) & \tilde{\Xi}^T(i) & \tilde{\Gamma}_3^T(i) & \tilde{\mathcal{H}}_1^T(i) & \tilde{\mu}^T(i) \\ * & \tilde{S}(i) - J^T(i) - J(i) & 0 & 0 & 0 & 0 & 0 \\ * & * & -\mathcal{R} & 0 & 0 & 0 & 0 \\ * & * & * & -I & 0 & 0 & 0 \\ * & * & * & * & -\tilde{Q} & 0 & 0 \\ * & * & * & * & * & -\mathcal{W}(i) & 0 \\ * & * & * & * & * & * & -I \end{bmatrix} < 0 \tag{3.20}
$$

$$
\begin{bmatrix} S(i,j) & J^T(i) \\ * & X(j) \end{bmatrix} > 0 \tag{3.21}
$$

$$
N_1\tilde{R}_1 = I, \; N_2\tilde{R}_2 = I, \tilde{W}_1(i)W_1(i) = I, \; \tilde{W}_2(i)W_2(i) = I \, and \; \tilde{Q}Q = I \tag{3.22}
$$

where

$$\tilde{S}(i) = \sum_{j=1}^{i+1} p_{ij} S(i,j), \quad \mathcal{R} = diag\left\{N_1, N_2\right\}$$

$$\mathcal{W}(i) = diag\left\{\tilde{W}_1(i), \tilde{W}_2(i), \cdots, \tilde{W}_2\right\}$$

$$\Pi(i) = \tilde{\Lambda}(i) + \tilde{\Upsilon}_1(i) + \tilde{\Upsilon}_1^T(i) + (\tau_i + \kappa_{m_i+1})\tilde{Z}(i)$$

$$\tilde{\Gamma}_1(i) = \left[AX_i \ \ \chi_i p_{0i} B_2 Y_i \ \ \cdots \ \ \chi_i p_{mi} B_2 Y_i \ \ B_1 \ \ E_1 \ \ \chi_i p_{0i} E_1 \ \ \cdots \chi_i p_{mi} E_1 \ \ E_1 \ \ \sum_\Theta \tau_\theta \right]$$

$$\tilde{\Xi}(i) = \left[C_1 X_i \ \ \chi_i p_{0i} D_{12} Y_i \ \ \cdots \ \ \chi_i p_{mi} D_{12} Y_i \ \ D_{11} \ \ E_2 \ \ \chi_i p_{0i} E_2 \ \ \cdots \chi_i p_{mi} E_2 \ \ E_2 \ \ 0 \right]$$

$$\tilde{\mathcal{H}}_1(i) = \begin{bmatrix} H_1 X(i) & 0 & \cdots & 0 & 0 & 0 & 0 & \cdots & 0 & 0 & 0 \\ 0 & \chi_i p_{0i} H_3 Y(i) & \cdots & 0 & 0 & 0 & 0 & \cdots & 0 & 0 & 0 \\ \vdots & \vdots & \ddots & \vdots & \vdots & \vdots & \vdots & \ddots & \vdots & \vdots & \vdots \\ 0 & 0 & \cdots & \chi_i p_{mi} H_3 Y(i) & 0 & 0 & 0 & \cdots & 0 & 0 & 0 \end{bmatrix}$$

$$\tilde{\mu}(i) = \left[\mu_\theta X(i) \ \ 0 \ \ \cdots \ \ 0 \ \ 0 \ \ 0 \ \ 0 \ \ \cdots \ \ 0 \ \ 0 \ \ 0 \right]$$

$$\tilde{\Gamma}_2(i) = \begin{bmatrix} \sqrt{\tilde{\tau}(i) + \tilde{\kappa}_{di}} \\ \sqrt{(\tau(s) + \kappa_m)} \end{bmatrix} \Big[(A-I)X(i) \ \ \chi_i p_{0i} B_2 Y(i) \ \ \cdots \ \ \chi_i p_{mi} B_2 Y(i) \ \ B_1$$

$$E_1 \ \ \chi_i p_{0i} E_1 \ \ \cdots \chi_i p_{mi} E_1 \ \ E_1 \ \ \sum_\Theta \tau_\theta \Big]$$

$$\tilde{\Gamma}_3(i) = \left(\sqrt{\tau_s - \tau_1 + \kappa_m + 1}\right)\Big[X(i) \ \ 0 \ \ \cdots \ \ 0 \ \ 0 \ \ 0 \ \ 0 \ \ \cdots \ \ 0 \ \ 0 \ \ 0 \Big]$$

$$\tilde{\Lambda}(i) = diag\Big\{ -X(i), \left(-X^T(i) - X(i) + \tilde{Q} \right), \cdots, \left(-X^T(i) - X(i) + \tilde{Q} \right),$$

$$\left(H_2^T W_3(i) H_2 - \gamma I \right), -W_1(i), -W_2(i), \cdots, -W_2(i), -W_3(i), -I \Big\}$$

$$\tilde{\Upsilon}_1(i) = \tilde{M}^T(i)[I \ \ -I \ \ -I \ \ \cdots \ \ -I \ \ 0 \ \ 0 \ \ 0 \ \ 0 \ \ \cdots \ \ 0 \ \ 0 \ \ 0]. \tag{3.23}$$

Then the closed-loop system is stochastically stable with the prescribed $\mathcal{H}_\infty$ performance. Furthermore, the controller gains are given as follows:

$$K(i) = Y(i)X^{-1}(i) \tag{3.24}$$

Proof: Proof is given in Appendix 10.

It can be seen from Equation 3.22 that obtained sufficient conditions for the existence of the above given controller are BMIs. These BMIs are converted into quasi convex LMIs on the same lines as given in Chapter 6. Using the cone complementary algorithm [127], the feasibility problem formulated by (3.18)-(3.22) that is not a convex problem and can be converted into the following nonlinear minimization problem:

Chapter 3. *Robust $\mathcal{H}_\infty$ State Feedback Control of NCSs with Poisson Noise and Successive Packet Dropouts*

54

Minimize $Tr\left(N_1\tilde{R}_1 + N_2\tilde{R}_2 + \tilde{W}_1(i)W_1(i) + \tilde{W}_2(i)W_2(i) + \tilde{Q}Q\right)$

subject to (3.18)-(3.21) and

$$
\begin{bmatrix} N_1 & I \\ I & \tilde{R}_1 \end{bmatrix} \geq 0, \quad \begin{bmatrix} N_2 & I \\ I & \tilde{R}_2 \end{bmatrix} \geq 0, \quad \begin{bmatrix} \tilde{W}_1(i) & I \\ I & W_1(i) \end{bmatrix} \geq 0,
$$

$$
\begin{bmatrix} \tilde{W}_2(i) & I \\ I & W_2(i) \end{bmatrix} \geq 0 \quad \begin{bmatrix} \tilde{Q} & I \\ I & Q \end{bmatrix} \geq 0 \tag{3.25}
$$

To solve this optimization problem, the following algorithm can be used:

Algorithm :

Step 1: Set $\jmath = 0$ and solve (3.18)-(3.19) and (3.25) to obtain the initial conditions:

$$
\begin{bmatrix} X(i), \tilde{S}(i), J(i), \tilde{R}_1(i), \tilde{R}_1, \tilde{R}_2(i), \tilde{R}_2, W_1(i), W_2(i), W_3(i), \\ \tilde{W}_1(i), \tilde{W}_2(i), \tilde{Q}, N_1, N_2, \tilde{Z}(i), Y(i) \end{bmatrix}^0
$$

Step 2: Solve the LMI problem

Minimize $Tr\left(N_1^\jmath\tilde{R}_1 + N_1\tilde{R}_1^\jmath + N_2^\jmath\tilde{R} + N_2\tilde{R}_2^\jmath + \tilde{W}_1(i)^\jmath W_1(i) + \tilde{W}_1(i)W_1(i)^\jmath + \tilde{W}_2(i)^\jmath W_2(i) + \tilde{W}_2(i)W_2(i)^\jmath\right)$

subject to (3.18)-(3.21) and (3.22)

The obtained solutions are denoted as:

$$
\begin{bmatrix} X(i), \tilde{S}(i), J(i), \tilde{R}_1(i), \tilde{R}_1, \tilde{R}_2(i), \tilde{R}_2, W_1(i), W_2(i), W_3(i), \\ \tilde{W}_1(i), \tilde{W}_2(i), \tilde{Q}, N_1, N_2, \tilde{Z}(i), Y(i) \end{bmatrix}^{\jmath+1}
$$

Step 3: Solve Theorem 3.1 with $K(i)^{\jmath+1} = Y^{\jmath+1}(i)X^{-1}(i)^{\jmath+1}$, if there exist solutions, then $K(i)^{\jmath+1}$ are the desired controller gains and EXIT. Otherwise, if $Tr\left(N_1^\jmath\tilde{R}_1 + N_1\tilde{R}_1^\jmath + N_2^\jmath\tilde{R} + N_2\tilde{R}_2^\jmath + \tilde{W}_1(i)^\jmath W_1(i) + \tilde{W}_1(i)W_1(i)^\jmath + \tilde{W}_2(i)^\jmath W_2(i) + \tilde{W}_2(i)W_2(i)^\jmath\right) > \epsilon$, set $\jmath = \jmath + 1$ and return to Step 2 where ϵ is tolerant else EXIT and no solution will be possible.

3.4   Simulation Examples

3.4.1   Example 1

Consider the following continuous-time plant [137]:

$$T(s) = \frac{e^{-.34s}}{s+1}$$

This plant is discretized using zero order hold with a sampling rate of 1 second with the following state space representation:

$$
\begin{aligned}
x(k+1) &= 1.0152x(k) + 0.1w(k) + 0.1052u(k-\tau(i)) + \tau(\theta)x(k)N(\theta = 0.5, k), \quad x(0) = 0 \\
z(k) &= 0.2x(k) + 0.15w(k) + 0.04u(k-\tau(i))
\end{aligned}
$$

It is assumed that the system uncertainties are norm bounded and are characterized by the following matrices:

$$
\begin{aligned}
E_1 &= 0.01, & E_2 &= 0.005, \\
H_1 &= .05, & H_2 &= 0.12, & H_3 &= 0.07.
\end{aligned}
$$

In this simulation example, the following configurations are used. It is assumed that the network-induced delays are characterized by a Markov chain taking values in a finite set $\mathcal{S} = \{1, 2, 3\}$, which corresponds to delays of 2, 3 and 4 second, respectively. The transitions of the Markov modes follow a probability matrix that is obtained by performing the experiments on a cellular network:

$$
P_\tau =
\begin{bmatrix}
0.4136 & 0.5864 & 0 \\
0.3702 & 0.6157 & 0.0141 \\
0.3702 & 0.6157 & 0.0141
\end{bmatrix}
$$

The Poisson noise $N(\theta = 0.5, k)$, with the Poisson jump rate $\mu = \mathcal{E}\{\tau(\theta)\} = 0.5$ jumps/sec, is considered to cater for the sudden communication link failure or breakage. θ is a random variable that shows the characteristics of the Poisson noise as described in (3.3). Furthermore the successive packet dropout sequences are catered for by using the Poisson distribution with the probabilities given in Table 3.1. Without loss of the generality, it is assumed that the previous data will be used if the successive dropouts are more than 2. The prescribed $\mathcal{H}_\infty$ performance index is $\gamma = 0.5$. Using Theorem 3.3.2, the following set of K values are obtained.

$$K(1) = -3.4158; \ K(2) = -3.4230; \ K(3) = -3.4321.$$

The stabilized system state, in the presence of random delays, is shown in Figure 3.3(a) and Figure 3.3(b) shows the random network-induced delays used in the simulations.

(a) System state   (b) Random delays
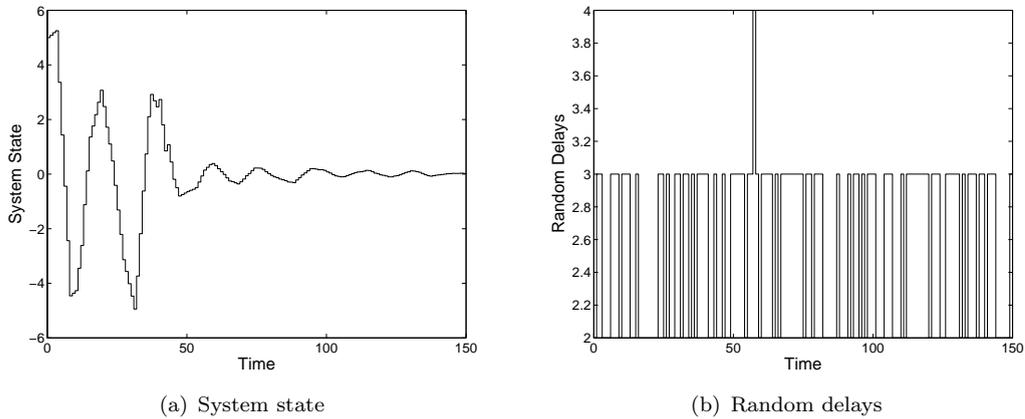
FIGURE 3.3: Stabilized system state and random delays

It can be seen in Figure 3.4(a) that the Poisson noise has random pulses and results in the discontinuities in the state dynamics. It is different from the other noises such as the Gaussian and the Wiener that have continuous diffusion and are comparatively easy to handle. Figure 3.4(b) shows how different θ values effect the $\mathcal{H}_\infty$ performance. As mentioned before, θ is the random variable that shows the characteristics of the Poisson noise such as the amplitude, the shape and the age. The packet dropout sequences are shown in Figure 3.4(c). Furthermore it is observed that the increase in the successive packet dropouts results in the degradation of the system performance. It is worth to comment that if the random sequences have more than four successive dropouts, then the system becomes unstable. The effect of the packet dropout sequences on the $\mathcal{H}_\infty$ performance can be seen in Figure 3.4(d). If the dropouts are more than two, then the prescribed $\mathcal{H}_\infty$ performance index ($\gamma = 0.5$) can not be achieved. The minimized γ for different number of the packet dropouts is achieved by the simulations and is given in Table 3.2.

TABLE 3.2: Minimized gamma for sequences of different dropouts

Packet Dropouts	Minimized γ
2	0.4337
1	0.4048
no dropout	0.3910

(a) Poisson noise discontinuous pulses

(b) Effect of poisson noise on $\mathcal{H}_\infty$ performance

(c) Successive packet dropouts

(d) Effect of packet dropouts on $\mathcal{H}_\infty$ performance
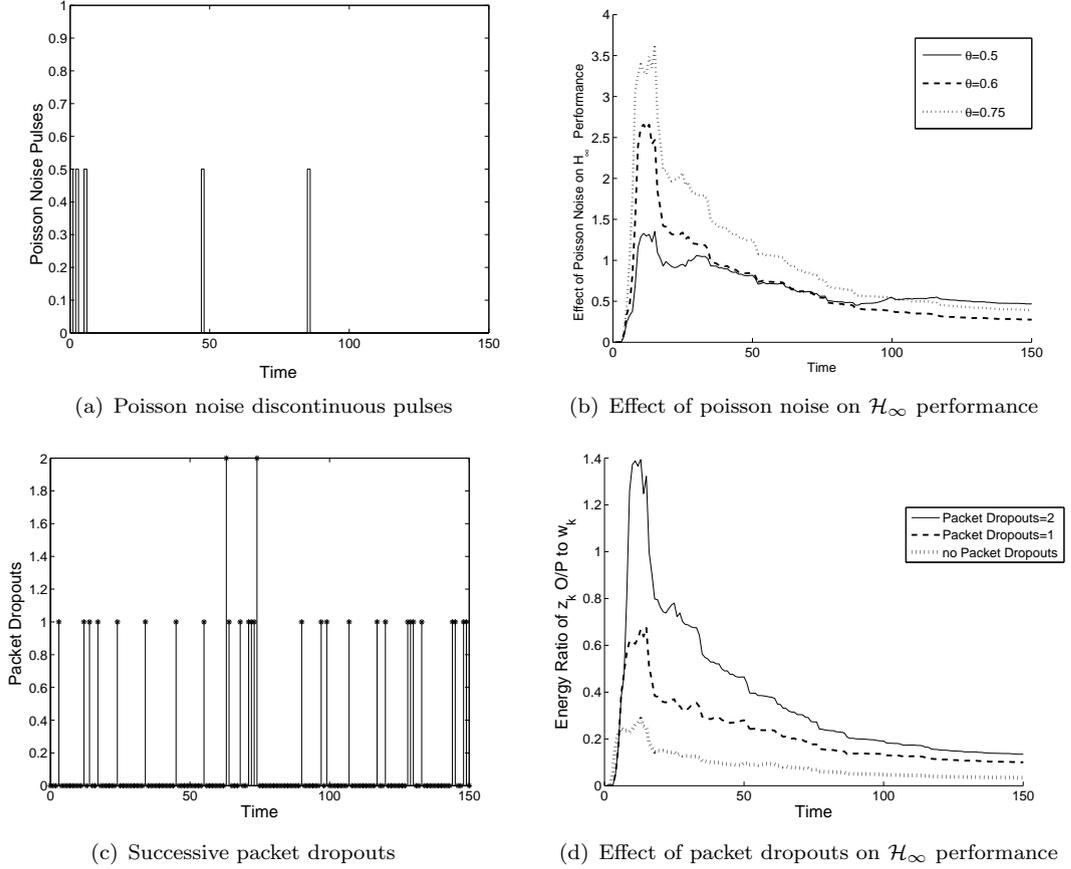
FIGURE 3.4: NCSs constraints and their effects on $\mathcal{H}_\infty$ performance

3.4.2 Example 2

Consider the system (3.1) with the following state space matrices:

$$
A = \begin{bmatrix} 0 & 1 \\ 0.8 & -0.3 \end{bmatrix}, B_1 = \begin{bmatrix} 0.51 \\ 0 \end{bmatrix}, B_2 = \begin{bmatrix} 0.05 \\ 0.01 \end{bmatrix}, C_1 = \begin{bmatrix} 0 & 0.1 \end{bmatrix},
$$

$$
E_1 = \begin{bmatrix} 0.01 \\ 0.05 \end{bmatrix}, E_2 = 0.06, H_1 = \begin{bmatrix} 0.13 & 0 \end{bmatrix}, H_2 = 0.02, H_3 = 0.3. \quad (3.26)
$$

In this example, the random delays are 2, 3, 4 seconds and are modelled by a Markov chain with the transition probabilities given in Example 1. The packet dropout sequences are two in this example, while the Poisson noise parameter $\theta = 0.15$ is used. Using Theorem 3.3.2 with given $\gamma = 0.7$, the following set of the controller gains are obtained:

$$
K(1) = \begin{bmatrix} 2.2323 & -3.4724 \end{bmatrix}, K(2) = \begin{bmatrix} 2.2683 & -3.4997 \end{bmatrix},
$$

$$
K(3) = \begin{bmatrix} 1.8487 & -2.9704 \end{bmatrix}. \quad (3.27)
$$

The stabilized system states are shown in Figure 3.5. It is worth repeating that the closed-loop system bears the multiple NCSs constraints such as the random delays, the successive packet dropouts and the Poisson noise together and the controller is still capable of stabilizing the unstable plan given in Equation 3.26. The minimized γ under different packet dropouts are given in Table 3.3.

(a) $StateX_1$

(b) $StateX_2$
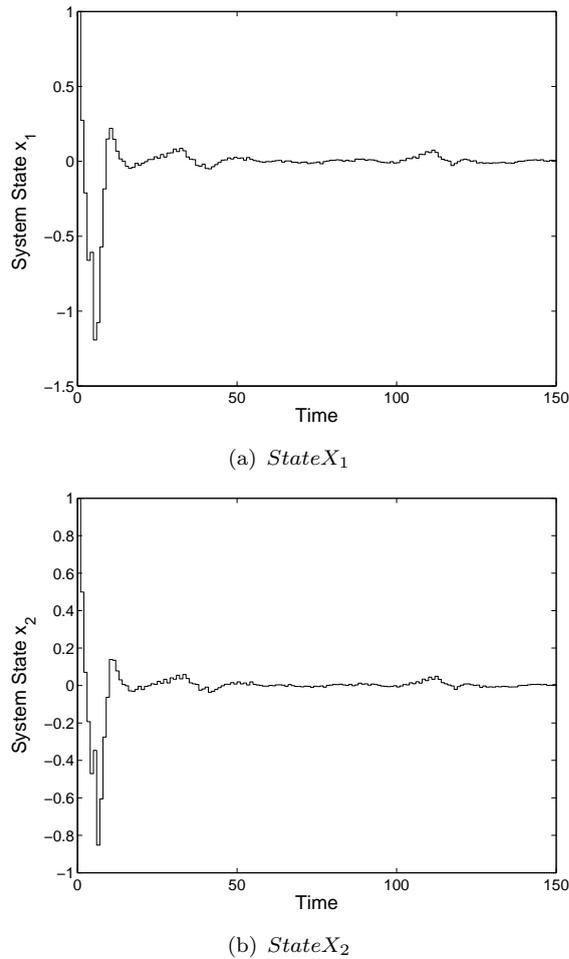
FIGURE 3.5: Stabilized system state

TABLE 3.3: Minimized gamma for different dropouts

Packet Dropouts	Minimized γ
2	0.0691
1	0.0672
no dropout	0.0612

Figure 3.6(a) shows the Poisson noise $N(\theta = 0.15, k)$ with the Poisson jump rate $\mu = \mathcal{E}\{\tau(\theta)\} = 0.5$ jumps/sec. The effect of the Poisson noise with different values of $\theta = \{0.15, 0.25, 0.30\}$ on the $\mathcal{H}_\infty$ performance is elaborated with Figure 3.6(b). The sequences with successive packet dropouts are shown in Figure 3.6(c). Similar to the

previous example, it is assumed that the previous data will be used if the successive dropouts are more than two in a sequence. It can be observed from Figure 3.6(d) that increase in dropouts degrades the system performance.

(a) Poisson noise discontinuous pulses

(b) Effect of poisson noise on $\mathcal{H}_\infty$ performance

(c) Successive packet dropouts

(d) Effect of packet dropouts on $\mathcal{H}_\infty$ performance
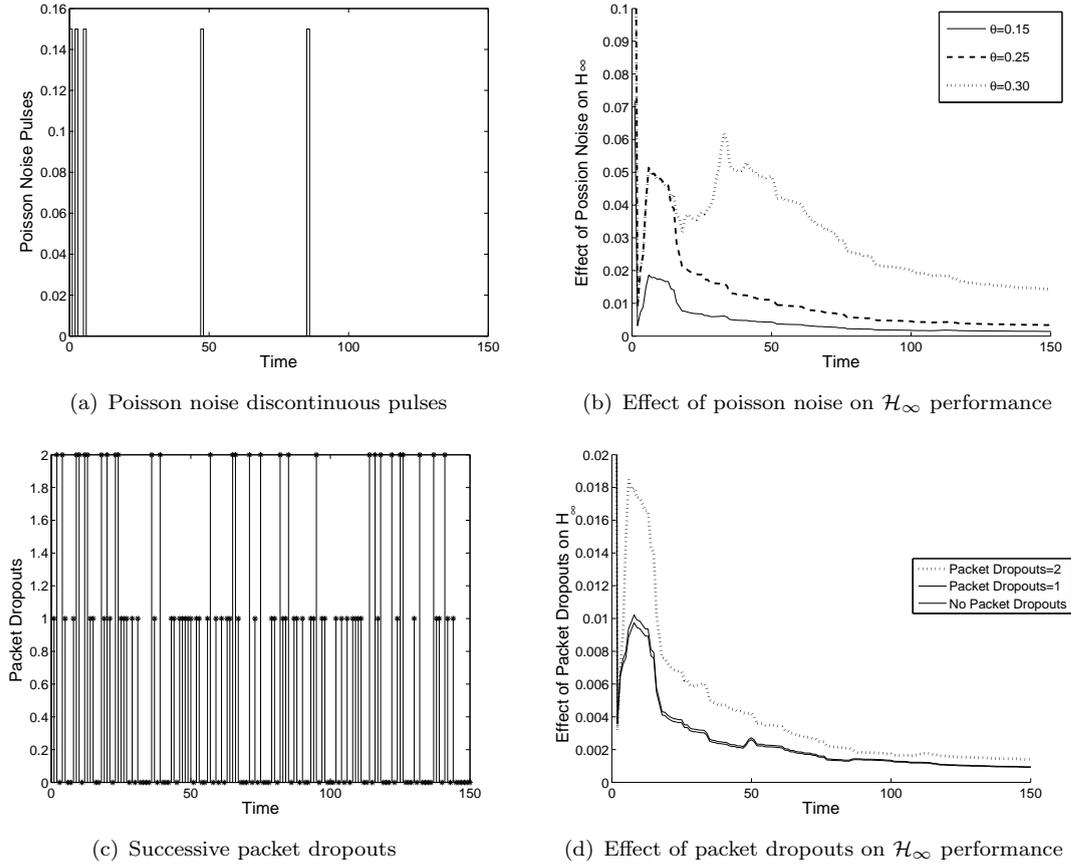
FIGURE 3.6: NCSs constraints and their effects on $\mathcal{H}_\infty$ performance

3.5 Conclusions

In the proposed control design, the various constraints of the NCSs are catered and their effects on the system performance are studied. The network-induced delays are modelled as the modes of the Markov chain that takes the values from a transition probability matrix. The successive packet dropout sequences are modelled using the Poisson distribution. A new indictor function is introduced that helps to select the separate Poisson distributions for each mode of the delays. In addition to this, the Poisson noise is incorporated in the design to represent the network node failure phenomenon. The stability criterion is developed using a L-K functional approach. On the basis of the stability criteria, a delay-mode dependent state feedback controller is obtained. The controller LMIs are implemented using the MATLAB LMI toolbox. The resultant controller gains are

applied on the two different plants and the impact of the NCSs constraints is observed. The simulation examples validated the proposed design and stabilized system states are obtained. The impact of successive packet dropouts are observed on the system stability and the $\mathcal{H}_\infty$ performance. It is observed that the system becomes unstable if packet dropouts are equal to or more than four. Similarly the $\mathcal{H}_\infty$ performance is degraded with the increase in the packet dropouts. It is also detected that the Poisson pulses also degrades the system performance in the sense of $\mathcal{H}_\infty$ and system stability.

Chapter 4

Robust $\mathcal{H}_\infty$ State Feedback Control of NCSs with Congestion Control

This chapter examines the problem of robust $\mathcal{H}_\infty$ state feedback control of Networked Control Systems (NCSs) with a simple congestion control scheme. This simple congestion control scheme is based on comparing current measurements with the last transmitted measurements. If their difference is less than a prescribed percentage of the current measurements then no measurement is transmitted to the controller. The controller always uses the last transmitted measurements to control the system. With this simple congestion control scheme, a robust $\mathcal{H}_\infty$ state feedback controller design methodology is developed based on the Lyapunov-Krasovskii functional approach. Sufficient conditions for the existence of delay mode dependent controllers are given in terms of bilinear matrix inequalities (BMIs). These BMIs are converted into quasi-convex linear matrix inequalities (LMIs) and are solved by using the cone complementarity linearization algorithm. The effectiveness of the simple congestion control scheme, in terms of reducing network bandwidth consumption, is elaborated using simulation examples [103].

4.1   Introduction

The recent advancements in communication networks have resulted in NCSs in which components are connected over the network. The remote supervision and control, the automatic control in hazard environment, the power control in the wireless networks, the medical treatments from a distance and the laboratories for the remote area students are some of the applications of the NCSs. Similarly, Internet-based NCSs result in

the cost minimization due to the already available network infrastructure. However, the insertion of the networks in the control loops introduces various design constraints such as the time delays due to network congestion [120], the packet dropouts due to overflow in buffers and queues in network nodes [30], the quantization error due to limited bandwidth channels [138], the variable sampling/transmission intervals due to multiple nodes; and network security due to the shared communication medium [51, 52]. All these constraints not only degrade the system performance but can also cause system instability.

A lot of the research has been done on the stability analysis and the controller designs of the NCSs over the last decade (see [139] and references therein). In general, the NCSs can be divided into continuous-time and discrete-time systems. In [140] and [141], a descriptor system approach is adopted to model the continuous NCSs with the constant and the time-varying sampling intervals, respectively. Furthermore, the stability criteria of the time-delayed continuous-time NCSs are developed on the basis of L-K functional approach. However, the above techniques are inefficient for the stability analysis of the digital NCSs due to a zero order hold problem (see [142] for details). Same papers propose a less conservative stability criterion with the robust parametric modelling of the time delays. It is worth mentioning that most of the research in the NCSs is done in the discrete-time domain where the continuous-time plants are discretized exactly on a given sampling interval (see [143] and reference therein).

In the discrete-time domain substantial literature is available in which different authors assumed different constraints together in their analysis and designs [86, 144]. The NCSs constraints such as the time delays, the packet dropouts and the variable transmission intervals can be catered for either (1) by considering their upper bounds or (2) by modelling them stochastically using different probability distribution methods. The first technique is adopted by [51, 139, 147] to analyze the effects of the variable transmission intervals, the time delays and the packet dropouts on NCSs performance. In the second approach, the time delays and the packet dropouts are treated as the stochastic processes and are modelled by the Bernoulli random distribution and the Markov chain [96, 145, 146]. In this chapter the latter approach is adopted and the network-induced random delays are modelled by using a Markov chain that follows a transition probability matrix. The quantization error is another control design constraint that can degrade the system performance and can cause instability. In the earlier days research was done to mitigate the effect of the quantization error [70, 148]. However, modern research shows that the quantizers are beneficial in the NCSs because they can be used as the information coders in the digital networks and can provide the rate control in the bandwidth limited channels [72, 138, 144].

The network congestion is another network-induced constraint that can cause delays and packet dropouts and adversely affect the system performance. The transmission control protocol (TCP) provides the congestion control mechanism, however it is not suitable for the real time data transfer due to connection establishment and packet retransmission. Therefore it is suggested by [17] and [149] that the user data-gram protocol (UDP) is a practical solution when the general purpose and the shared networks are used in NCSs implementation. On the other hand, UDP doesn't provide any congestion control. However, this issue can be resolved by providing the congestion control mechanism on the upper (Application) layer. In other words, the congestion control can be incorporated in the control design. In this chapter a simple congestion control mechanism is implemented by analyzing the difference between the current signal and the previously transmitted signal. This approach suggests that there is no need to send the updated information until the difference between the two signals is greater than a prescribed percentage of the current signal. Hence, the signal transmission is controlled to reduce the bandwidth consumption. The main contributions of the chapter are summarized as follows:

- A congestion control technique has been proposed for NCSs

- A state feedback controller design is proposed to ensure stability of the networked control system with random delays and congestion control.

The rest of the chapter is organized as follows. Section 4.2 provides system description, modelling of delays, congestion control technique and problem formulation. In Section 4.3, main results for stability analysis and synthesis of a robust $\mathcal{H}_\infty$ state feedback controller design are formulated in terms of BMIs. A cone complementarity algorithm is employed to convert these BMIs into quasi-convex LMIs. Section 4.4 comprises of two examples to demonstrate the effectiveness of the simple congestion control in terms of reducing network bandwidth. Finally, conclusions are drawn in Section 4.5.

4.2   System Description and Definitions

A NCS framework, with congestion control mechanism, is shown in Figure 4.1.

The class of uncertain discrete-time linear networked systems under consideration is described by the following model:

$$
\begin{aligned}
x(k+1) &= [A + \Delta A(k)]x(k) + [B_1 + \Delta B_1(k)]w(k) + [B_2 + \Delta B_2(k)]u(k), \quad x(0) = 0 \\
z(k) &= [C_1 + \Delta C_1(k)]x(k) + [D_{11} + \Delta D_{11}(k)]w(k) + [D_{12} + \Delta D_{12}(k)]u(k)
\end{aligned}
$$

$$(4.1)$$
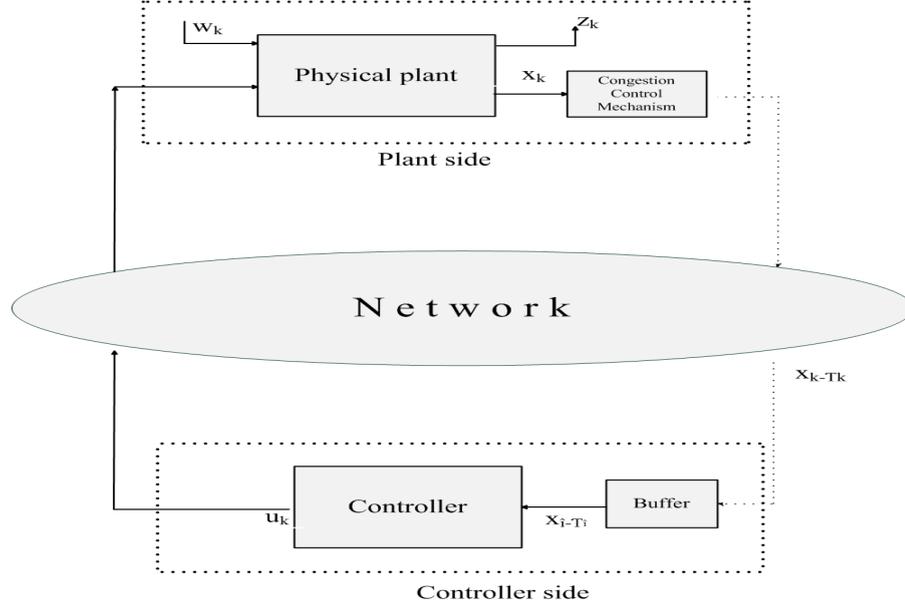
FIGURE 4.1: Layout of the networked control systems

where $x(k) \in \Re^n, u(k) \in \Re^m, z(k) \in \Re^{m_1}$ are the state, input and controlled output, respectively. $w(k) \in \Re^{m_3}$ is the disturbance that belongs to $\mathcal{L}_2[0, \infty)$, the space of square summable vector sequence over $[0, \infty)$. The matrices A, B_1, B_2, C_1, D_{11} and D_{12} are known matrices with appropriate dimensions. The matrix functions $\Delta A(k)$, $\Delta B_1(k)$, $\Delta B_2(k)$, $\Delta C_1(k)$, $\Delta D_{11}(k)$ and $\Delta D_{12}(k)$ represent the time-varying uncertainties in the system that are norm bounded and satisfy conditions given in the assumption 3.2.1.

Let $\{r_k, k\}$ be a discrete homogeneous Markov chain taking values in a finite set $\mathcal{S} = \{1, 2, \cdots, s\}$, with the following transition probability from mode i at time k to mode j at time $k + 1$:

$$p_{ij} := \mathbf{Prob}\{r_{k+1} = j | r_k = i\}$$

where $i, j \in \mathcal{S}$, $0 \le p_{ij} \le 1$ and $\sum_{j=1}^{s} p_{ij} = 1$. In this chapter, the random delay τ_k is modelled as a finite state Markov process as discussed in Chapter 3.

Congestion Control Scheme:

To reduce network congestion a simple congestion control scheme using difference between the signals is proposed. If the difference between the current measurement and the last transmitted measurement is less than a prescribed percentage of the current measurement, then the current measurement will not be transmitted. Mathematically,

if the following condition is valid:

$$
\begin{aligned}
|x(\iota) - x(k)| &\leq \delta |x(k)| \\
|x(\iota)| &\leq |x(k)| + \delta |x(k)|
\end{aligned}
\tag{4.2}
$$

then the current measurement will not be transmitted and the previously transmitted information, available in the controller buffer, will be used as feedback. Here $x(k)$ is the current measurement, $x(\iota)$ is the last measurement which is transmitted on time ι and δ is the congestion control parameter. It can be seen from Figure 4.1, when the condition 4.2 will be violated, then data will be transmitted over the network and previously transmitted information will be updated. Otherwise previous information will be used for the controller. Based on this configuration the following state feedback controller is proposed:

$$
u(k) = K(r_k) x(\iota - \tau_{r_\iota})
\tag{4.3}
$$

where $K(r_k)$ is the controller gain and τ_{r_ι} is the network-induced delay tolerated by the last transmitted information $x(\iota)$. This 'control on demand' can be used in the control systems environment especially when an unstable system is already stabilized and is in steady state or we have a stable system with no disturbance acting on it. In this paper, this privilege is used for the NCSs to control network congestion.

Substituting (4.3) into (4.1), the following closed-loop system is obtained:

$$
\begin{aligned}
x(k+1) &= [A + \Delta A(k)]x(k) + [B_1 + \Delta B_1(k)]w(k) + [B_2 + \Delta B_2(k)]K(r_k)x(\iota - \tau_{r_\iota}) \\
z(k) &= [C_1 + \Delta C_1(k)]x(k) + [D_{11} + \Delta D_{11}(k)]w(k) + [D_{12} + \Delta D_{12}(k)]K(r_k) \\
&\quad x(\iota - \tau_{r_\iota})
\end{aligned}
\tag{4.4}
$$

The problem under study can be formulated as follows.

Problem Formulation:

Given a prescribed $\gamma > 0$, design a state feedback controller of the form (4.3) such that

1. The system (4.1) with (4.3) and $w(k) = 0$ is stochastically stable.

2. Under the zero-initial condition, the controlled output $z(k)$ satisfies $\mathcal{H}_\infty$ performance as described in Chapter 3.

Before ending this section we introduce the following lemma that will play a vital role in deriving our main results.

Lemma 4.2.1. *Let $y(k) = x(k+1) - x(k)$ and $\tilde{x}(k) = \begin{bmatrix} x^T(k) & x^T(k-\tau_{r_k}) & w^T(k) & x^T(k) \end{bmatrix}$*
$H_1^T F^T(k) x^T(k - \tau_{r_k}) K^T(r_k) H_3^T F^T(k) \; (x(\iota - \tau_{r_\iota}) - x(k - \tau_{r_k}))^T K^T(r_k) \; (x(\iota - \tau_{r_\iota}) - $
$x(k - \tau_{r_k}))^T K^T(r_k) H_3^T F_k^T \; w^T(k) H_2^T F^T(k) \Big]^T \in \Re^l,$ *then for any matrices $R \in \Re^{n\times n}$,*
$M \in \Re^{n\times l}$ and $Z \in \Re^{l\times l}$, satisfying

$$\begin{bmatrix} R & M \\ M^T & Z \end{bmatrix} \geq 0 \tag{4.5}$$

the following inequality holds:

$$- \sum_{i=k-\tau(r_k)}^{k-1} y^T(i) R y(i) \leq \tilde{x}^T(k) \Big\{ \Upsilon_1 + \Upsilon_1^T + \tau(r_k) Z \Big\} \tilde{x}(k) \tag{4.6}$$

where $\Upsilon_1 = M^T[I \quad -I \; 0 \; 0 \; 0 \; 0 \; 0 \; 0].$

Proof: The lemma can be proven along the same lines as given in Chapter 3 and is omitted here.

4.3 Stability Analysis and Controller Synthesis of NCSs with Congestion Control

The following theorem proposes stability criteria for uncertain discrete-time systems (4.1) with random communication delays and the simple congestion control mechanism.

Theorem 4.3.1. *For given controller gains $K(i)$, $\delta > 0$ and $\gamma > 0$, $i = 1, 2, \cdots, s$, if there exist positive-definite matrices $P(i)$, $R_1(i)$, R_1, $R_2(i)$, R_2, $W_1(i)$, $W_2(i)$, $W_3(i)$, $W_4(i)$, $W_5(i)$, Q, $Z(i)$ and matrices $M(i)$ satisfying the following inequalities*

$$R_1 > R_1(i), \quad R_2 > R_2(i) \tag{4.7}$$

$$\Lambda(i) + \Gamma_1^T(i)\tilde{P}(i)\Gamma_1(i) + \Gamma_2^T(i)\left[\tilde{\tau}(i)R_1 + \tau(s)R_2\right]\Gamma_2(i) + \Upsilon_1(i) + \Upsilon_1^T(i) + \tau_i Z(i) + \Xi^T(i)\Xi(i) < 0 \tag{4.8}$$

and

$$\begin{bmatrix} (1 - p_{is})R_1(i) + R_2(i) & M(i) \\ M^T(i) & Z(i) \end{bmatrix} \geq 0 \tag{4.9}$$

where

$$
\begin{aligned}
\tilde{P}(i) &= \sum_{j=1}^{s} p_{ij}P(j) \\
\tilde{\tau}(i) &= \sum_{j=1}^{s} p_{ij}\tau(j) \\
\Gamma_1(i) &= \begin{bmatrix} A & B_2K(i) & B_1 & E_1 & E_1 & B_2 & E_1 & E_1 \end{bmatrix} \\
\Xi(i) &= \begin{bmatrix} C_1 & D_{12}K(i) & D_{11} & E_2 & E_2 & D_{12} & E_2 & E_2 \end{bmatrix} \\
\Gamma_2(i) &= \begin{bmatrix} A-I & B_2K(i) & B_1 & E_1 & E_1 & B_2 & E_1 & E_1 \end{bmatrix}
\end{aligned}
$$

$$
\begin{aligned}
\Lambda(i) &= diag\Big\{ \big((\tau(s)-\tau(1)+1)Q + H_1^T W_1(i) H_1 - P(i) \big), \big(K^T(i) H_3^T W_2(i) H_3 K(i) \\
&\quad + \delta^2 K^T(i) W_4 K(i) + \delta^2 K^T(i) H_3^T W_5(i) H_3 K(i) - Q \big), \big(H_2^T W_3(i) H_2 - \gamma I \big), \\
&\quad -W_1(i), -W_2(i), -W_4(i), -W_5(i), -W_3(i) \Big\} \\
\Upsilon_1(i) &= M^T(i)[I \quad -I \ 0 \ 0 \ 0 \ 0 \ 0 \ 0]. \tag{4.10}
\end{aligned}
$$

Then the system (4.1) with (4.3) is stochastically stable with the prescribed $\mathcal{H}_\infty$ performance.

Proof:

The proof is provided in Appendix 11.

Remark 4.3.1. The slack variables R_1 and R_2 are added to LMIs given in Theorem 4.3.1 because of the special structure of the transition probability matrix (3.5). These new slack variables R_1 and R_2 relax the stability criterions. When $R_1 = 0$, $R_2 = 0$ and there is no congestion control, the LMIs are no longer a function of $\tilde{\tau}(i)$ and our result will reduce to the results given by [153]-[156] which are independent on delay's modes. Also notice that the negative terms $-\sum_{\ell=k-\tau(r_k)}^{k-1} y_\ell^T \big[(1-p_{r_k(r_k+1)})R_1 + R_2\big] y_\ell$ obtained from (11.4) are kept whereas in [153]-[156] these negative terms are neglected. Using Lemma 4.2.1 on these negative terms, we introduce more new slack matrices $R_1, R_1(i), R_2, R_2(i), M(i)$ and $Z(i)$ into LMIs. These slack matrices provide additional degrees of freedom that are very important for deriving LMIs solutions in general. Therefore the result given here is much less conservative than the results given by [153]-[156].

The following theorem provides sufficient conditions for the existence of delay mode dependent robust $\mathcal{H}_\infty$ controllers.

Theorem 4.3.2. *For a given $\gamma > 0$ and $\delta > 0$ and $i = 1, 2, \cdots, s$, if there exist positive-definite matrices $X(i)$, $\tilde{R}_1$, $\tilde{R}_2$, $\tilde{R}_1(i)$, $\tilde{R}_2(i)$, $\mathcal{R}_1$ $\mathcal{R}_2(i)$, $W_1(i)$, $W_2(i)$, $W_3(i)$, $W_4(i)$, $W_5(i)$, Q, $\tilde{Q}$, $\tilde{W}_1(i)$, $\tilde{W}_2(i)$, $\tilde{W}_4(i)$, $\tilde{W}_5(i)$, $N(i)$, $S(i,j)$, $\tilde{Z}(i)$ and matrices $\tilde{M}(i)$, $J(i)$ and $Y(i)$ satisfying:*

$$
\tilde{R}_1 > \tilde{R}_1(i), \quad \tilde{R}_2 > \tilde{R}_2(i) \tag{4.11}
$$

$$
\begin{bmatrix} (1-p_{is})\tilde{R}_1(i) + \tilde{R}_2(i) & \tilde{M}(i) \\ * & \tilde{Z}(i) \end{bmatrix} \geq 0 \tag{4.12}
$$

$$
\begin{bmatrix}
\Pi(i) & \tilde{\Gamma}_1^T(i) & \tilde{\Gamma}_2^T(i) & \tilde{\Xi}^T(i) & \tilde{\Gamma}_3^T(i) & \mathcal{H}_1^T(i) & \mathcal{H}_2^T(i) \\
* & \tilde{S}(i) - J^T(i) - J(i) & 0 & 0 & 0 & 0 & 0 \\
* & * & -\mathcal{R} & 0 & 0 & 0 & 0 \\
* & * & * & -I & 0 & 0 & 0 \\
* & * & * & * & -\tilde{Q} & 0 & 0 \\
* & * & * & * & * & -\mathcal{W}_1 & 0 \\
* & * & * & * & * & * & -\mathcal{W}_2
\end{bmatrix} < 0 \qquad (4.13)
$$

$$
\begin{bmatrix}
S(i,j) & J^T(i) \\
* & X(j)
\end{bmatrix} > 0 \qquad (4.14)
$$

$$
\mathcal{R}_1 \tilde{R}_1 = I, \ \mathcal{R}_2 \tilde{R}_2 = I, \ \tilde{W}_1(i) W_1(i) = I, \ \tilde{W}_2(i) W_2(i) = I, \tilde{W}_4(i) W_4(i) = I
$$
$$
\tilde{W}_5(i) W_5(i) = I, \ \tilde{Q} Q = I \qquad (4.15)
$$

where

$$
\tilde{S}(i) = \sum_{j=1}^{s} p_{ij} S(i,j), \mathcal{R} = diag\{\mathcal{R}_1, \mathcal{R}_2\}, \ \mathcal{W}_1 = diag\{\tilde{W}_1(i), \tilde{W}_2(i)\},
$$
$$
\mathcal{W}_2 = diag\{\tilde{W}_4(i), \tilde{W}_5(i)\} \qquad (4.16)
$$

and

$$
\Pi(i) = \tilde{\Lambda}(i) + \tilde{\Upsilon}_1(i) + \tilde{\Upsilon}_1^T(i) + \tau(i)\tilde{Z}(i)
$$
$$
\tilde{\Gamma}_1(i) = \begin{bmatrix} AX(i) & B_2 Y(i) & B_1 & E_1 & E_1 & B_2 & E_1 & E_1 \end{bmatrix}
$$
$$
\tilde{\Xi}(i) = \begin{bmatrix} C_1 X(i) & D_{12} Y(i) & D_{11} & E_2 & E_2 & D_{12} & E_2 & E_2 \end{bmatrix}
$$
$$
\mathcal{H}_1(i) = \begin{bmatrix} H_1 X(i) & 0 & 0 & 0 & 0 & 0 & 0 & 0 \\ 0 & H_3 Y(i) & 0 & 0 & 0 & 0 & 0 & 0 \end{bmatrix}
$$
$$
\mathcal{H}_2(i) = \begin{bmatrix} 0 & \delta Y(i) & 0 & 0 & 0 & 0 & 0 & 0 \\ 0 & \delta H_3 Y(i) & 0 & 0 & 0 & 0 & 0 & 0 \end{bmatrix}
$$

$$
\begin{aligned}
\tilde{\Gamma}_2(i) &= \left[\begin{array}{c} \sqrt{\sum_{j=1}^{s} p_{ij}\tau(j)} \\ \sqrt{\tau(s)} \end{array} \right] \left[AX(i) - X(i)\ \ B_2 Y(i)\ \ B_1\ \ E_1\ \ E_1\ \ B_2\ \ E_1\ \ E_1 \right] \\
\tilde{\Gamma}_3(i) &= \left(\sqrt{\tau_s - \tau_1 + 1} \right) \left[X(i)\ \ 0\ \ 0\ \ 0\ \ 0\ \ 0\ \ 0\ \ 0 \right] \\
\tilde{\Lambda}(i) &= diag\Big\{ -X(i), -X^T(i) - X(i) + \tilde{Q}, \left(H_2^T W_3(i) H_2 - \gamma I \right), \\
&\qquad\qquad -W_1(i), -W_2(i), -W_4(i), -W_5(i), -W_3(i) \Big\} \\
\tilde{\Upsilon}_1(i) &= \tilde{M}^T(i)[I\ \ -I\ \ 0\ \ 0\ \ 0\ \ 0\ \ 0\ \ 0].
\end{aligned}
\tag{4.17}
$$

Then the system (4.1) with (4.3) is stochastically stable with the prescribed $\mathcal{H}_\infty$ perfor-
mance. Furthermore the controller gains are given as follows:

$$
K(i) = Y(i)X^{-1}(i)
\tag{4.18}
$$

Proof: Proof is given in Appendix 11.

4.4　Simulation Examples

4.4.1　Example 1:

Consider the following unstable continuous-time plant given in [137]:

$$
T(s) = \frac{e^{-0.34s}}{s + 1}
\tag{4.19}
$$

This plant is discretized with a sampling rate of 0.1 second and its state space represen-
tation is

$$
\begin{aligned}
x(k+1) &= 1.0152x(k) + 0.1w(k) + 0.1052u(k), \quad x(0) = 0 \\
z(k) &= 0.2x(k) + 0.15w(k) + 0.04u(k)
\end{aligned}
\tag{4.20}
$$

Assume that the system uncertainties are norm bounded and are characterized by the
following matrices:

$$
\begin{aligned}
E_1 &= 0.01, \quad E_2 = 0.005, \\
H_1 &= .05, \quad H_2 = 0.004, \quad H_3 = 0.007.
\end{aligned}
\tag{4.21}
$$

The congestion control parameter δ in the example is set as 0.3. It is assumed that the
network-induced delays are characterized by a Markov chain taking values in a finite
set $\mathcal{S} = \{1, 2, 3\}$, which corresponds to 2, 3 and 4 second delays, respectively. The

transitions in Markov chain modes follow the probability matrix given as

$$P_\tau = \begin{bmatrix} 0.3575 & 0.5864 & 0.0561 \\ 0.3702 & 0.6157 & 0.0141 \\ 0.3702 & 0.6157 & 0.0141 \end{bmatrix} \qquad (4.22)$$

To obtain the transition probability matrix, a series of experiments are performed on a cellular network. The plant data are sent across the cellular channel, using a modem manufactured by MultiTech Systems. This special modem uses AT commands to communicate and capable of the transmission time logging. The data are sent to a remote logging device using Microsoft Visual Studio 2008 and a third party toolkit. The data are periodically sent for a specific time and several experiments are carried out to obtain the multiple distributions of the delays. At the end of the experiment phase a set of data that contains one week's worth of measurements is used to obtain the probabilities.

Figure 4.2 shows the random network-induced delays used in the simulation. Using Theorem 4.3.2, the following set of $K(i)$ values are obtained:

$$K(1) = -1.8321; \ K(2) = -2.1224; \ K(3) = -1.6992. \qquad (4.23)$$

The bandwidth utilization depends upon unstable poles of the plant and can be calculated as

$$B \geq 2 \sum_{i=1}^{n} \log_2 |\lambda_i(A)| \qquad (4.24)$$

where B is bandwidth, λ_i are unstable poles of the plant with system matrix A. In the following discussion, it is assumed that the bandwidth utilized using (4.24)is 100% and its utilization changes with the change in congestion control parameter δ. By using the proposed technique of the congestion control, the reduced data transmission can be seen in Figure 4.3. The transmitted data samples are represented as 1 and the samples that are not sent are represented as 2. It can be seen that the data samples are transmitted frequently in the transient state. However, when the system approaches the steady state then there is a significant reduction in the transmission. The figure shows that as the error increases from the prescribed percentage $\delta x(k)$, then the feedback information is sent to stabilize the system. In Figure 4.4, the system 4.20 is run uncontrolled for the first 50 seconds and has gone unstable. After 50 seconds, the proposed controller is applied which stabilized the system efficiently.

The effect of δ on the channel bandwidth and the system performance is analyzed through a series of simulations. The impact of different values of δ on the bandwidth consumption is summarized in the Table 4.1. It can been seen that the bandwidth
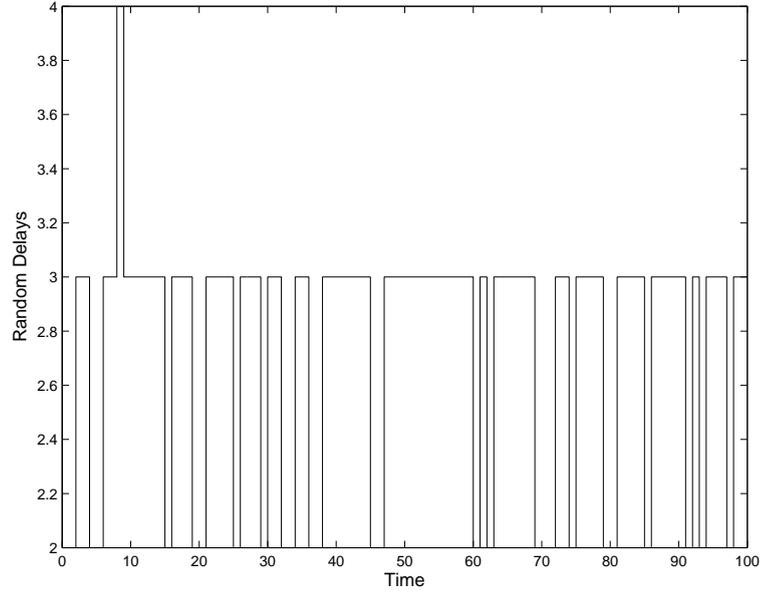
FIGURE 4.2: Random delays

utilization is reduced as δ is increased. However with $\delta > 0.95$, the system becomes unstable. It shows that there is always a trade off between the system performance and the bandwidth utilization. This can be verified by analyzing the $\mathcal{H}_\infty$ performance with different values of the δ. It is shown in Figure 4.5 that by increasing δ, the magnitude of $T_{zw}(k)$ is increasing, which stands for the degradation in the $\mathcal{H}_\infty$ performance.

TABLE 4.1: Effect of δ on bandwidth utilization

δ	Bandwidth utilization
0	100%
0.3	35.6%
0.5	33.66 %
0.8	31.68%
> 0.95	Unstable
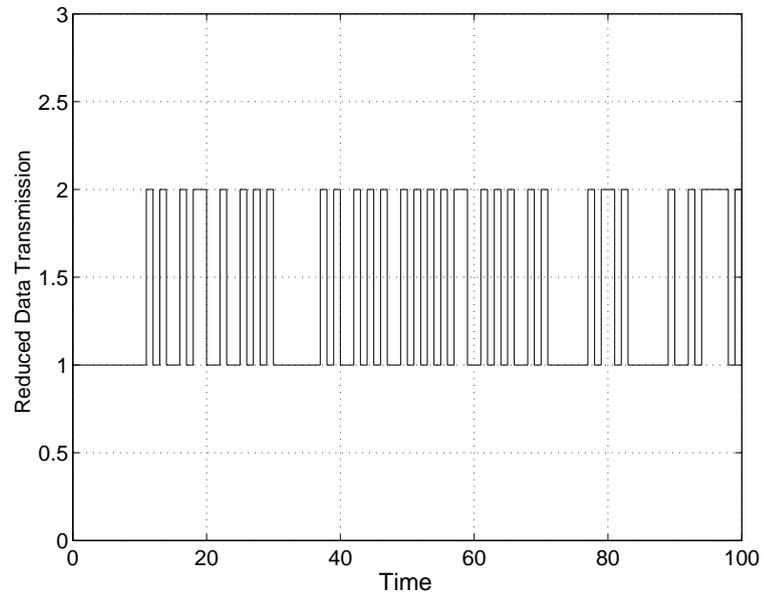
FIGURE 4.3: Reduced data transmission
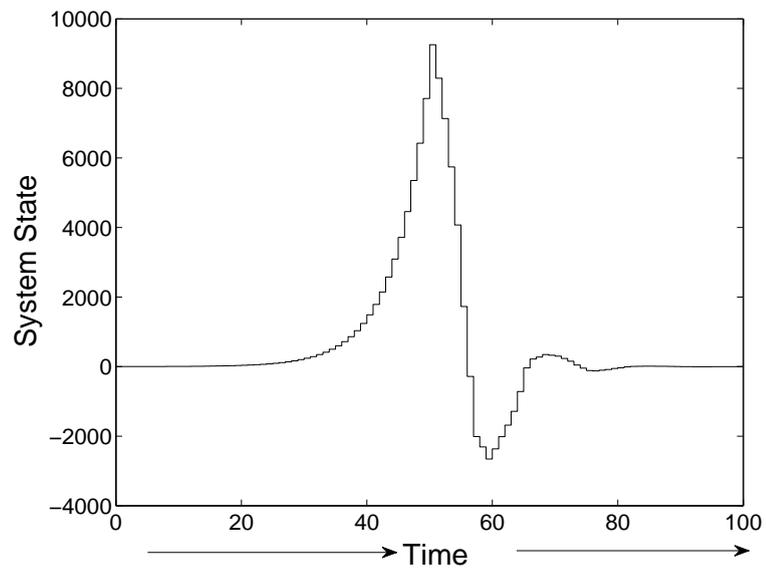
FIGURE 4.4: System state
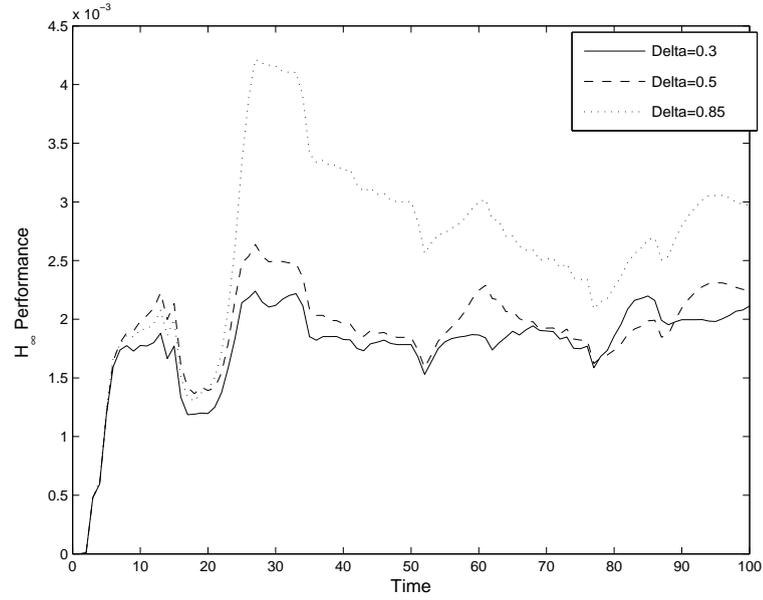
FIGURE 4.5: Energy ratio of output to disturbance

4.4.2 Example 2:

Consider the system (4.1) with the following matrices:

$$
A = \begin{bmatrix} 0.8 & -0.25 & 0 & 1 \\ 1 & 0 & 0 & 0 \\ -.8 & 0.5 & 0.2 & -1.03 \\ 0 & 0 & .5792 & 0 \end{bmatrix}, B_1 = \begin{bmatrix} 0 \\ 0.1000 \\ 0 \\ 0.0500 \end{bmatrix}, B_2 = \begin{bmatrix} 0.1000 \\ 0.0300 \\ 0.0400 \\ 0.1000 \end{bmatrix}
$$

$$
C_1 = \begin{bmatrix} 0 & 0.1000 & 0 & 0 \end{bmatrix}, E_1 = \begin{bmatrix} 0.01 \\ 0.09 \\ 0.02 \\ 0.04 \end{bmatrix}, E_2 = 0.01,
$$

$$
H_1 = \begin{bmatrix} 0.05 & 0.02 & .03 & .04 \end{bmatrix}, H_2 = \begin{bmatrix} 0.07 & 0.04 \end{bmatrix}, H_3 = 0.04
$$

Assume that the same Markov chain is used to model the random delays. Each value of the Markov chain corresponds to 1, 1.5 and 2 second delays, respectively. The same transition probability matrix is assumed as in Example 1. The congestion control parameter δ in this example is set as 0.1. Using Theorem 4.3.2, the following set of gain values are obtained.
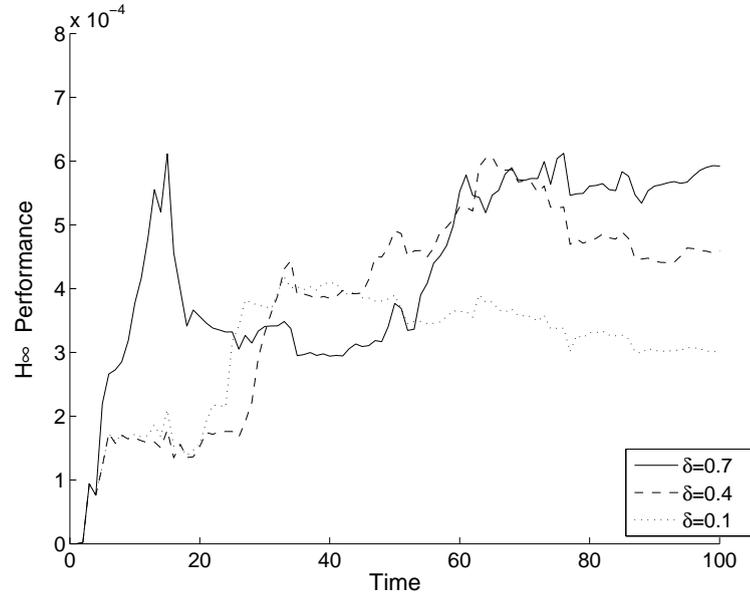
FIGURE 4.6: Energy ratio of output to disturbance

$$K(1) = \begin{bmatrix} -0.0245 & -0.0091 & -0.5614 & -0.2580 \end{bmatrix}$$
$$K(2) = \begin{bmatrix} -0.0166 & -0.0036 & -0.5675 & -0.2489 \end{bmatrix}$$
$$K(3) = \begin{bmatrix} -0.0423 & 0.0081 & -0.4889 & -0.2452 \end{bmatrix} \tag{4.25}$$

TABLE 4.2: Effect of δ on bandwidth utilization

δ	Bandwidth Consumption
0	100%
0.10	81.95%
0.40	69.26%
0.70	55.26%
> 0.90	Unstable

Figure 4.7 shows the closed-loop system response. It can be seen that the proposed design stabilized the system efficiently. Similar to Example 1, the effect of different values of the δ on the bandwidth utilization is analyzed . It can be seen from Table 4.2 that increasing δ results in decreasing the bandwidth utilization. However, the system becomes unstable as $\delta > 0.90$. Furthermore, the effect of δ on the $\mathcal{H}_\infty$ performance is also analyzed and plotted in Figure 4.6.

(a) System state (x_1)

(b) System state (x_2)

(c) System state (x_3)
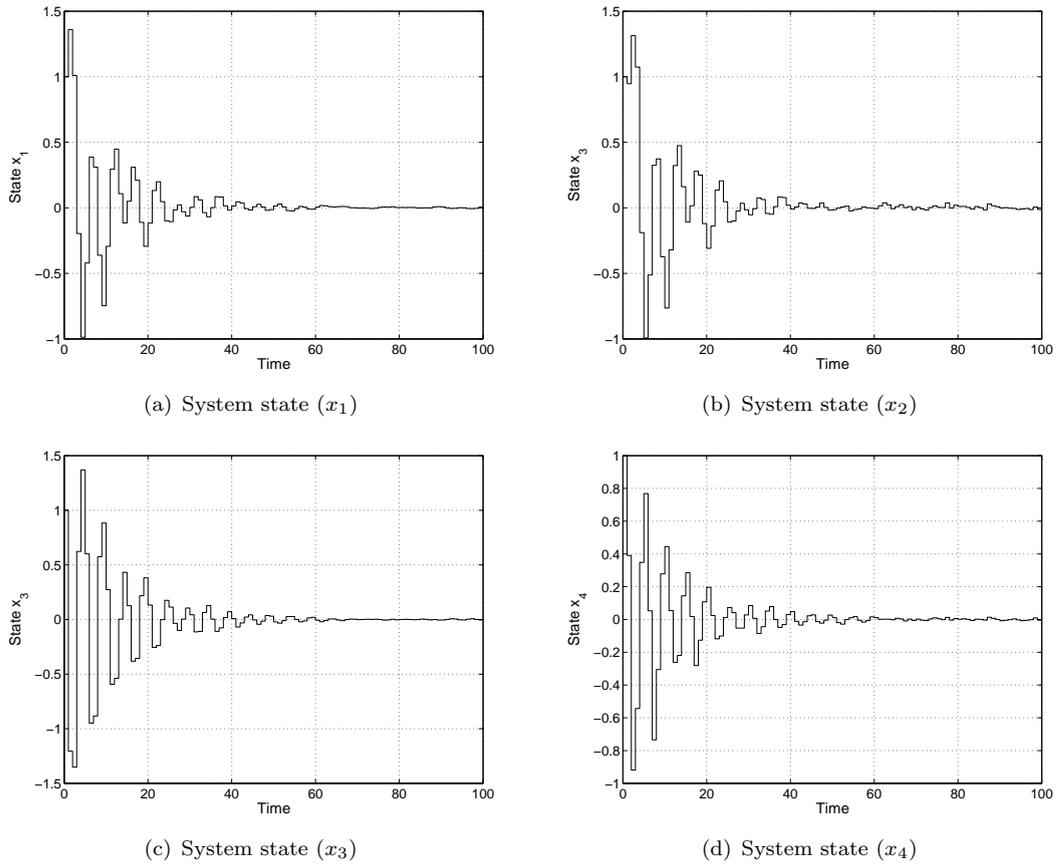
(d) System state (x_4)

FIGURE 4.7: System states

4.5   Conclusions

A congestion control technique is proposed for the NCSs that compares current and last transmitted measurements before sending them over the network. With this simple congestion control scheme the stability criteria for the NCSs are obtained. By applying the Schur's complement and the congruence transformation on the stability criteria, the sufficient conditions for the existence of a delay mode-dependent robust $\mathcal{H}_\infty$ state feedback controller are obtained. The obtained conditions are in BMIs, therefore a cone complementarity algorithm is proposed to convert this non-convex problem into a quasi-convex optimization problem. The controller matrices are obtained effectively by the available mathematical tools e.g., the YALMIP toolbox of the MATLAB. The effectiveness of the proposed technique in terms of the bandwidth utilization and the $\mathcal{H}_\infty$ performance is demonstrated using the simulation examples. It is observed that the bandwidth utilization can be reduced to half without much effect on the system performance. However, the system becomes unstable when congestion control parameter $\delta = 0.90$. It is also noted that the congestion control conditions are violated when the

system is unstable and data is always transmitted. However, as the system moves towards the stability regions then the number of data transmissions reduces gradually.

Chapter 5

Robust $\mathcal{H}_\infty$ Dynamic Output Feedback Control of NCSs with Congestion Control

This chapter investigates a robust $\mathcal{H}_\infty$ dynamic output feedback controller for networked control systems (NCSs) with a simple congestion control scheme. This scheme enables the NCSs design to enjoy the advantages of both time-triggered and event-triggered systems. The proposed scheme compares the current measurement with the last transmitted measurement. If the difference between them is less than a prescribed percentage of the current measurements then no measurement is transmitted to the controller and the controller always uses the last transmitted measurements to calculate the feedback gains. Moreover this technique is applied to the controller output as well. The stability criteria for the closed-loop system is formulated using the Lyapunov-Krasovskii (L-K) functional approach. The sufficient conditions for the controller are given in terms of solvability of bilinear matrix inequalities (BMIs). These BMIs are converted into quasi-convex linear matrix inequalities (LMIs) that are solved using the cone complementarity linearization algorithm. A simulation example is used to evaluate how effective the simple congestion control scheme is in reducing network bandwidth [105].

5.1   Introduction

In the NCSs the control loops are closed over the networks and the control components are distributed over a wide geographical area. The purpose of the network in the NCSs is not only to act as a communication medium for the signal transmission but each system component should also be an active network participant [157]. In the NCSs, it

is no longer feasible to assume the perfect information flow between the plant and the controller [158]. The various network constraints such as packet dropouts and disordering due to different routing paths, time delays due to buffering and queuing in the routers, variable transmission rates due to the bus contention, and quantization errors due to the limited channel capacity make the NCS analysis, design and real time implementation very challenging [51, 138, 150]. On the other hand, the NCSs have wide application in the fields such as power distribution through the smart grids, power control in the communication systems, queue management in the routers, unmanned aerial vehicle (drones) control, and in the manufacturing industry. Therefor researches in the NCSs are very popular in the control systems research community.

In the NCSs literature two techniques have been investigated for the signal sampling between the distributed system components: 1) The time-triggered or periodic sampling 2) The event-triggered sampling. In the first approach the data is sampled and transmitted at the regular time intervals (TDMA, time division multiple access) [30, 86, 96]. This assumption reduces the analysis and the design complexity due to the fact that it is synchronous and quasi-deterministic. These features make the time-triggered technique more fault tolerant and modular [39] than the event-triggered technique. However, it is less efficient for the real-time implementation due to sampling jitter, strict scheduling requirements and the network-induced time delays which can cause performance degradation and the instability. Furthermore, it does not consider the efficient usage of the limited communication resources such as channel bandwidth or capacity. In the event triggered technique, sampling is done on the occurrence of an event, for example the level crossing-based sampling, the Lebesgue sampling [159], or the dead band sampling [165]. The event-triggered technique is more suitable for the real-time NCS implementation due to its ability to react quickly to asynchronous external events, lower CPU usage and efficient network resource utilization [157, 158]. In general, whether a time-triggered or an event-triggered technique is selected, it depends entirely on the application. Recently, some researchers adopted a hybrid approach that benefited both time-triggered and event-triggered sampling [166].

In the NCSs the main issue with the time-triggered sampling approach is that it only considers the plant dynamics and completely ignores the communication constraints such as finite bandwidth and the network congestion. In this chapter this issue is resolved by using a simple technique that considers the difference between current and the previously transmitted signals. In this technique sensor will only transmit the next measurement to the controller when the difference between the two signals exceeds a given value. On the other side, the controller continues to use the previous information until the signal value is updated. This technique results in more efficient utilization of bandwidth and in the congestion control. Hence, this approach has the advantages of both time-triggered and

the event-triggered techniques. Furthermore this congestion control technique is also applied on the controller output. The main contributions of the chapter are summarized as follows:

- A simple congestion control, both on the system input and output, has been proposed for the NCSs.

- An observer-based, dynamic output feedback controller is proposed to ensure the stability of the NCSs with therandom delays.

- The effect of the congestion control on the system is observed in sense of the $\mathcal{H}_\infty$ performance.

The rest of the chapter is organized as follows. Section 5.2 provides the system description, the modelling of the delays, the congestion control technique and the problem formulation. In Section 5.3, the main results for the stability analysis and the synthesis of a robust $\mathcal{H}_\infty$ output feedback controller are given in terms of the BMIs. A cone complementarity algorithm is employed to convert the BMIs into the quasi-convex LMIs. Section 5.4 comprises of an example to demonstrate the effectiveness of the simple congestion control in terms of reducing the network's bandwidth. Finally, the conclusions are drawn in Section 5.5.

5.2 System Description and Definitions

Consider the system framework shown in Figure 5.1. A class of the uncertain discrete-time linear systems under consideration is described by the following model:

$$
\begin{aligned}
x(k+1) &= [A + \Delta A(k)]x(k) + [B_1 + \Delta B_1(k)]w(k) + [B_2 + \Delta B_2(k)]u(k), \quad x(0) = 0 \\
z(k) &= [C_1 + \Delta C_1(k)]x(k) + [D_{11} + \Delta D_{11}(k)]w(k) + [D_{12} + \Delta D_{12}(k)]u(k) \\
y(k) &= C_2 x(k)
\end{aligned}
$$

(5.1)

where $x(k) \in \Re^n, u(k) \in \Re^m, z(k) \in \Re^{m_1}, y(k) \in \Re^{m_2}$ are the state, input, controlled output and measured output, respectively. $w(k) \in \Re^{m_3}$ is the disturbance that belongs to $\mathcal{L}_2[0, \infty)$, the space of square summable vector sequence over $[0, \infty)$. The matrices A, B_1, B_2, C_1, D_{11}, D_{12} and C_2 are of the known matrices with appropriate dimensions. The matrix functions $\Delta A(k)$, $\Delta B_1(k)$, $\Delta B_2(k)$, $\Delta C_1(k)$, $\Delta D_{11}(k)$ and $\Delta D_{12}(k)$ represent the norm bounded time-varying uncertainties in the system which satisfy the conditions given in the assumption 3.2.1.
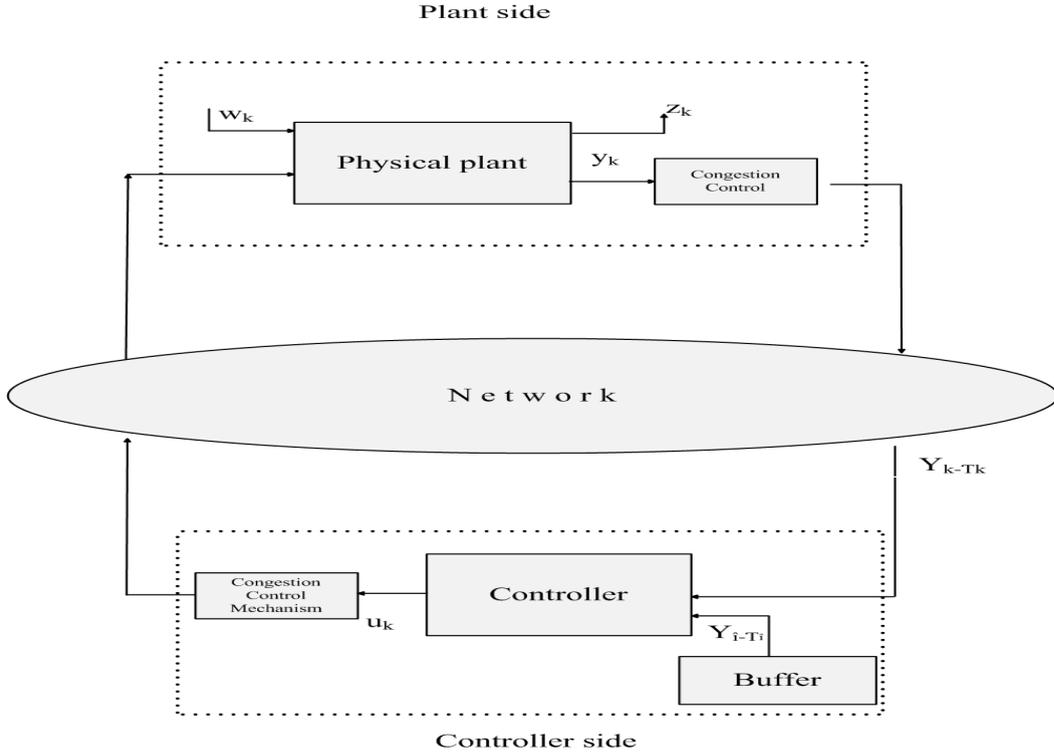
FIGURE 5.1: NCSs with sensor-to-controller delay

Let $\{r_k, k\}$ be a discrete homogeneous Markov chain taking values in a finite set $\mathcal{S} = \{1, 2, \cdots, s\}$, with the following transition probability from the mode i at a time k to the mode j at a time $k+1$:

$$p_{ij} := \mathbf{Prob}\{r_{k+1} = j | r_k = i\}$$

where $i, j \in \mathcal{S}$, $0 \leq p_{ij} \leq 1$ and $\sum_{j=1}^{s} p_{ij} = 1$. In this chapter, the random delay τ_k is modelled by a finite state Markov process as $\tau_k = \tau(r_k)$.

5.2.1 Congestion Control Scheme

To reduce the network congestion, a new technique using the difference between the signals is proposed. If the difference between the current measurement and the previously transmitted measurement is less than a prescribed percentage of the current measurement, then the current measurement will not be transmitted. i.e., if:

$$|y(v) - y(k)| \leq \delta_1 |y(k)| \tag{5.2}$$

then $y(k)$ is not transmitted. Otherwise, $y(k)$ will be transmitted and value stored in the controller buffer will be updated i.e., $y(\upsilon) = y(k)$, where $y(k)$ is the current measurement, $y(\upsilon)$ is the last transmitted measurement and is stored in in buffer, δ_1 is the congestion control parameter on the plant output.

On the controller side, the transmitted signal $y(\upsilon)$, after the network-induced delay τ_{r_υ}, will be used as the feedback information. It will be either currently updated i.e., $y(\upsilon - \tau_{r_\upsilon}) = y(k - \tau_{r_k})$ or previously stored information i.e., $y(\upsilon - \tau_{r_\upsilon})$. A dynamic observer based output feedback controller is proposed:

$$
\begin{aligned}
\hat{x}(k+1) &= A_c(r_k)\hat{x}(k) + B_c(r_k)y(\upsilon - \tau_{r_\upsilon}) \\
u(k) &= C_c(r_k)\hat{x}(k)
\end{aligned}
\tag{5.3}
$$

where $\hat{x}(k)$ is the controller state, $A_c(i), B_c(i)$ and $C_c(i)$ are the controller matrices. The similar congestion control technique is applied to controller output:

$$
|u(\vartheta) - u(k)| \leq \delta_2 |u(k)|
\tag{5.4}
$$

where $u(\vartheta)$ is the previously transmitted controller output, $u(k)$ is the currently calculated controller output and δ_2 is the congestion control parameter for the controller output.

By using (5.1), (5.2), (5.3) and (5.4), the following closed-loop system is obtained:

$$
\begin{aligned}
\zeta(k+1) &= [A_{cl}(r_k) + \bar{E}_1 F(k)\bar{H}_1(r_k)]\zeta(k) + [\bar{B}_2 + \bar{E}_1 F(k)H_3]C_{cl}(r_k)\{\zeta(\vartheta) - \zeta(k)\} + \\
&\quad B_{cl}(r_k)\bar{C}_2\zeta(\upsilon - \tau_{r_\upsilon}) + [\bar{B}_1 + \bar{E}_1 F(k)H_2]w(k) \\
z(k) &= [\bar{C}_1(r_k) + E_2 F(k)\bar{H}_1(r_k)]\zeta(k) + [D_{12} + E_2 F(k)H_3]C_{cl}(r_k)\{\zeta(\vartheta) - \zeta(k)\} \\
&\quad + [D_{11} + E_2 F(k)H_2]w(k).
\end{aligned}
\tag{5.5}
$$

where $\zeta(k) = [x(k) \ \hat{x}(k)]^T$,

$$
\begin{aligned}
A_{cl}(r_k) &= \begin{bmatrix} A & B_2 C_c(r_k) \\ 0 & A_c(r_k) \end{bmatrix}, B_{cl}(r_k) = \begin{bmatrix} 0 \\ B_c(r_k) \end{bmatrix}, \bar{B}_1 = \begin{bmatrix} B_1 \\ 0 \end{bmatrix} \\
\bar{B}_2 &= \begin{bmatrix} B_2 \\ 0 \end{bmatrix}, \bar{C}_2 = \begin{bmatrix} C_2 & 0 \end{bmatrix}, \bar{E}_1 = \begin{bmatrix} E_1 \\ 0 \end{bmatrix}, \bar{H}_1(r_k) = \begin{bmatrix} H_1 & H_3 C_c(r_k) \end{bmatrix} \\
C_{cl}(r_k) &= \begin{bmatrix} 0 & C_c(r_k) \end{bmatrix}, \bar{C}_1(r_k) = \begin{bmatrix} C_1 & D_{12} C_c(r_k) \end{bmatrix}.
\end{aligned}
$$

The problem under our study is formulated as follows.

Problem Formulation:

Given a prescribed $\gamma > 0$, design a dynamic output feedback controller of the form (5.3) such that

1. The system (5.1) with (5.5) and $w(k) = 0$ is stochastically stable, i.e, there exists a constant $0 < \alpha < \infty$ such that

$$E\left\{\sum_{\ell=0}^{\infty} \zeta^T(\ell)\zeta(\ell)\right\} < \alpha \tag{5.6}$$

   for all $\zeta(0), r_0$.

2. Under the zero-initial condition, the controlled output $z(k)$ satisfies

$$E\left\{\sum_{k=0}^{\infty} z^T(k)z(k)|r_0\right\} < \gamma^2 \sum_{k=0}^{\infty} w^T(k)w(k) \tag{5.7}$$

   for all nonzero $w(k)$.

Before ending this section, we introduce the following lemma, which will play a vital role in deriving our main results.

Lemma 5.2.1. *Let $\bar{x}(k) = x(k+1) - x(k)$ and $\tilde{\zeta}(k) = \Big[\zeta^T(k) \ \zeta^T(k - \tau(k)) \ w^T(k)$ $\zeta^T(k)\bar{H}_1^T(r_k)F^T(k)w^T(k)H_2^T F^T(k) \ (\zeta^T(v - \tau_{r_v}) - \zeta^T(k - \tau_{r_k})) \ (\zeta^T(\vartheta) - \zeta^T(k))C_{cl}^T(r_k)$ $(\zeta^T(\vartheta) - \zeta^T(k))C_{cl}^T(r_k)H_3^T F^T(k)\Big]^T \in \Re^l$, then for any matrices $R \in \Re^{n \times n}$, $M \in \Re^{n \times l}$ and $Z \in \Re^{l \times l}$, satisfying*

$$\begin{bmatrix} R & M \\ M^T & Z \end{bmatrix} \geq 0 \tag{5.8}$$

the following inequality holds:

$$\sum_{i=k-\tau(r_k)}^{k-1} \bar{x}^T(i)R\bar{x}(i) \leq \tilde{\zeta}^T(k)\Big\{\Upsilon_1 + \Upsilon_1^T + \tau(r_k)Z\Big\}\tilde{\zeta}(k) \tag{5.9}$$

where $\Upsilon_1 = M^T[diag\{I, 0\} \ \ diag\{-I, 0\} \ \ 0 \ \ 0 \ \ 0 \ \ 0 \ \ 0].$

Proof:

The lemma can be proved along the same lines as given in 3.2.1.

5.3 Stability Analysis and Controller Synthesis of NCSs with Congestion Control

The following theorem proposes stability criteria for uncertain discrete-time systems (5.1) with random communication delays and congestion control on both system input and output.

Theorem 5.3.1. *For given controller matrices $A_c(i)$, $B_c(i)$ and $C_c(i)$ where $i = 1, \cdots, s$, $\delta_1 > 0$, $\delta_2 > 0$ and $\gamma > 0$, if there exist sets of positive-definite matrices $P(i)$, $R_1(i)$, R_1, $R_2(i)$, R_2, $W_1(i)$, $W_2(i)$, $W_3(i)$, Q, $Z(i)$, and matrices $M(i)$ satisfying the following inequalities:*

$$R_1 > R_1(i), \quad R_2 > R_2(i) \tag{5.10}$$

$$\begin{bmatrix} (1 - p_{i(i+1)})R_1(i) + R_2(i) & M(i) \\ * & Z(i) \end{bmatrix} \geq 0 \tag{5.11}$$

$$\Lambda(i) + \Gamma_1^T(i)\tilde{P}(i)\Gamma_1(i) + \Gamma_2^T(i)\left[\tilde{\tau}_i R_1 + \tau_s R_2\right]\Gamma_2(i) + \Upsilon_1(i) + \Upsilon_1^T(i) + \tau(i)Z_i + \Gamma_3^T(i)\Gamma_3(i) < 0 \tag{5.12}$$

where

$$
\begin{aligned}
\Gamma_1(i) &= \begin{bmatrix} A_{cl}(i) & B_{cl}(i)\bar{C}_2 & \bar{B}_1 & \bar{E}_1 & \bar{E}_1 & B_{cl}(i)\bar{C}_2 & \bar{B}_2 & \bar{E}_1 \end{bmatrix} \\
\Gamma_2(i) &= \begin{bmatrix} \bar{A}(i) & 0 & \bar{B}_1 & \bar{E}_1 & \bar{E}_1 & 0 & \bar{B}_2 & \bar{E}_1 \end{bmatrix} \\
\Gamma_3(i) &= \begin{bmatrix} C_1(i) & 0 & D_{11} & E_2 & E_2 & 0 & D_{12} & E_2 \end{bmatrix} \\
\Lambda(i) &= diag\Big\{ \big((\tau(s) - \tau(1) + 1)Q + \delta_2^2 C_{cl}^T(i)C_{cl}(i) + \delta_2^2 C_{cl}^T(i)H_3(i)^T W_3(i)H_3 C_{cl}(i) \\
&\quad + \bar{H}_1^T(i)W_1(i)\bar{H}_1(i) - P(i)\big), (\delta_1^2 I - Q), \big(H_2^T W_2(i)H_2 - \gamma^2 I\big), -W_1(i), \\
&\quad -W_2(i), -I, -I, -W_3(i)\Big\} \\
\tilde{P}(i) &= \sum_{j=1}^{i+1} p_{ij}P(j) \\
\tilde{\tau}(i) &= \sum_{j=1}^{i+1} p_{ij}\tau(j) \\
\Upsilon_1(i) &= M^T(i)[diag\{I, 0\} \quad diag\{-I, 0\} \quad 0 \ 0 \ 0 \ 0 \ 0 \ 0] \\
\bar{A}(i) &= \begin{bmatrix} A - I & B_2 C_c(i) \\ 0 & 0 \end{bmatrix}.
\end{aligned} \tag{5.13}
$$

Then the system (5.5) with (5.3) is stochastically stable with the prescribed $\mathcal{H}_\infty$ performance.

Proof: Theorem is proved in Appendix 12

The following theorem provides sufficient conditions for the existence of delay mode dependent robust $\mathcal{H}_\infty$ controller.

Theorem 5.3.2. *For given $\gamma > 0$, $\delta_1 > 0$ and $\delta_2 > 0$, if there exist positive symmetric matrices $X(i) > 0$, $Y(i) > 0$, $\mathcal{Y}(i) > 0$, $W_1(i)$, $\mathcal{W}_1(i)$, $W_2(i)$, $W_3(i)$, $\mathcal{W}_3(i)$, $\mathcal{Q}$, Q, $N(i)$, $\mathcal{N}(i)$, R_1, $\mathcal{R}_1$, $R_1(i)$, R_2, $\mathcal{R}_2$, $R_2(i)$, $S(i,j)$, $\bar{Z}(i)$, and matrices $\mathcal{A}(i)$, $\mathcal{B}(i)$, $\mathcal{C}(i)$, $J(i)$, $\bar{M}(i)$ satisfying the following inequalities for all $i, j \in \mathcal{S}$:*

$$R_1 > R_1(i), \quad R_2 > R_2(i) \tag{5.14}$$

$$\begin{bmatrix} N(i) & \bar{M}(i) \\ * & \bar{Z}(i) \end{bmatrix} \geq 0 \tag{5.15}$$

$$\begin{bmatrix} \Pi(i) & \bar{\Gamma}_1^T(i) & \bar{\Gamma}_2^T(i) & \bar{\Gamma}_3^T(i) & \bar{\Gamma}_4^T(i) & \bar{\Gamma}_5^T(i) & \bar{\Gamma}_6^T(i) \\ * & -\tilde{\Xi}(i) & 0 & 0 & 0 & 0 & 0 \\ * & * & -\mathcal{R} & 0 & 0 & 0 & 0 \\ * & * & * & -I & 0 & 0 & 0 \\ * & * & * & * & -\mathcal{Q} & 0 & 0 \\ * & * & * & * & * & -\mathcal{W}_1(i) & 0 \\ * & * & * & * & * & * & -\mathcal{W}(i) \end{bmatrix} < 0 \tag{5.16}$$

$$\begin{bmatrix} S(i,j) & J^T(i) \\ & Y(j) \end{bmatrix} > 0 \tag{5.17}$$

$$\begin{bmatrix} (1 - p_{i(i+1)})R_1(i) + R_2(i) & \mathcal{T}^T(i) \\ * & \mathcal{N}(i) \end{bmatrix} > 0 \tag{5.18}$$

$$\mathcal{N}(i)N(i) = I, \; \mathcal{R}_1 R_1 = I, \; \mathcal{R}_2 R_2 = I, \; \mathcal{Q}Q = I, \tag{5.19}$$

$$\mathcal{Y}(i)Y(i) = I, \; \mathcal{W}_1(i)W_1(i) = I, \; \mathcal{W}_3(i)W_3(i) = I, \tag{5.20}$$

where

$$
\begin{aligned}
Pi(i) &= \bar{\Lambda}(i) + \bar{\Upsilon}_1(i) + \bar{\Upsilon}_1^T(i) + \tau(i)\bar{Z}(i) \\
\bar{\Lambda}(i) &= diag\left\{ -\begin{bmatrix} Y(i) & I \\ I & X(i) \end{bmatrix}, -Q, \left(H_2^T W_2(i)H_2 - \gamma^2 I\right), -W_1(i), -W_2(i), \right. \\
&\qquad \left. -I, -I, -W_3(i) \right\} \\
\bar{\Upsilon}(i) &= \bar{M}^T(i)[diag\{I,0\} \;\; diag\{-I,0\} \;\; 0 \;\; 0 \;\; 0 \;\; 0 \;\; 0 \;\; 0] \\
\bar{\Gamma}_1(i) &= \begin{bmatrix} \check{A}_{cl}(i) & \check{B}_{cl}(i)\bar{C}_2 & \check{B}_1 & \check{E}_1 & \check{E}_1 & \check{B}_{cl}(i)\bar{C}_2 & \check{B}_2 & \check{E}_1 \end{bmatrix} \\
\bar{\Gamma}_2(i) &= \begin{bmatrix} \sqrt{\tilde{\tau}(i)}I & \sqrt{\tau(s)}I \end{bmatrix}^T \begin{bmatrix} \check{A}(i) & 0 & \bar{B}_1 & \bar{E}_1 & \bar{E}_1 & 0 & \bar{B}_2 & \bar{E}_1 \end{bmatrix} \\
\bar{\Gamma}_3(i) &= \begin{bmatrix} \check{C}_1(i) & 0 & D_{11} & E_2 & E_2 & 0 & D_{12} & E_2 \end{bmatrix} \\
\bar{\Gamma}_4(i) &= \begin{bmatrix} \sqrt{(\tau(s) - \tau(1) + 1)}T(i) & 0 & 0 & 0 & 0 & 0 & 0 & 0 \end{bmatrix} \\
\bar{\Gamma}_5(i) &= \begin{bmatrix} \check{H}_1(i) & 0 & 0 & 0 & 0 & 0 & 0 & 0 \end{bmatrix} \\
\bar{\Gamma}_6(i) &= \begin{bmatrix} 0 & \delta_1 I & 0 & 0 & 0 & 0 & 0 & 0 \\ \delta_2\check{C}_{cl} & 0 & 0 & 0 & 0 & 0 & 0 & 0 \\ \delta_2 H_3\check{C}_{cl} & 0 & 0 & 0 & 0 & 0 & 0 & 0 \end{bmatrix}
\end{aligned}
$$

$$
\begin{aligned}
\mathcal{W}(i) &= diag\left\{I, I, \mathcal{W}_3(i)\right\}, \quad \mathcal{R} = diag\left\{\mathcal{R}_1, \mathcal{R}_2\right\} \\
\tilde{\Xi}(i) &= \begin{bmatrix} -(\tilde{S}(i) - J(i) - J^T(i)) & I \\ I & \tilde{X}(i) \end{bmatrix}, \tilde{X}(i) = \sum_{j=1}^{i+1} p_{ij}X(j), \tilde{S}(i) = \sum_{j=1}^{i+1} p_{ij}S(i,j), \\
\check{A}_{cl}(i) &= \begin{bmatrix} AY(i) + B_2\mathcal{C}(i) & A \\ \mathcal{A}(i) & \tilde{X}(i)A \end{bmatrix}, \check{B}_{cl}(i) = \begin{bmatrix} 0 \\ \mathcal{B}(i) \end{bmatrix}, \check{B}_1(i) = \begin{bmatrix} B_1 \\ \tilde{X}(i)B_1 \end{bmatrix}, \\
\check{E}_1(i) &= \begin{bmatrix} E_1 \\ \tilde{X}(i)E_1 \end{bmatrix}, \check{A}(i) = \begin{bmatrix} (A-I)Y(i) & B_2\mathcal{C} \\ 0 & 0 \end{bmatrix}, \check{C}_{cl}(i) = [\mathcal{C}(i) \;\; 0], \\
\check{C}_1(i) &= [C_1Y(i) + D_{12}\mathcal{C}(i) \;\; C_1], \check{B}_2(i) = \begin{bmatrix} B_2 \\ \tilde{X}(i)B_2 \end{bmatrix}, \check{H}_1(i) = [H_1Y(i) + H_3\mathcal{C} \;\; H_1], \\
T(i) &= \begin{bmatrix} Y(i) & I \\ Y(i) & 0 \end{bmatrix} \; and \; \mathcal{T}(i) = \begin{bmatrix} 0 & \mathcal{Y}(i) \\ I & -I \end{bmatrix}.
\end{aligned}
$$

Then the closed-loop system is stochastically stable with the prescribed $\mathcal{H}_\infty$ performance. Furthermore, a suitable controller is given as follows

$$
\begin{aligned}
A_c(i) &= \left(\sum_{j=1}^{i+1} p_{ij}Y^{-1}(j) - \tilde{X}(i)\right)^{-1}\left(\mathcal{A}(i) - \tilde{X}(i)(AY(i) + B_2\mathcal{C}(i))\right)Y^{-1}(i) \\
B_c(i) &= \left(\sum_{j=1}^{i+1} p_{ij}Y^{-1}(j) - \tilde{X}(i)\right)^{-1}\mathcal{B}(i) \\
C_c(i) &= \mathcal{C}(i)Y^{-1}(i).
\end{aligned}
$$

$$(5.21)$$

Proof: Theorem is proved in Appendix 12.

5.4   Simulation Example

Consider the uncertain discrete system with the following parameters:

$$
A = \begin{bmatrix} 0.8 & -0.25 & 0 & 1 \\ 1 & 0 & 0 & 0 \\ -.8 & 0.5 & 0.2 & -1.03 \\ 0 & 0 & 0.5793 & 0 \end{bmatrix}, B_1 = \begin{bmatrix} 0 \\ 0.1000 \\ 0 \\ 0.0500 \end{bmatrix}, B_2 = \begin{bmatrix} 0.1000 \\ 0.0300 \\ 0.0400 \\ 0.1000 \end{bmatrix}
$$

$$
C_1 = \begin{bmatrix} 0 & 0.1000 & 0 & 0 \end{bmatrix}, E_1 = \begin{bmatrix} 0.01 \\ 0.09 \\ 0.02 \\ 0.04 \end{bmatrix}, E_2 = 0.01,
$$

$$
H_1 = \begin{bmatrix} 0.05 & 0.02 & .03 & .04 \end{bmatrix}, H_2 = \begin{bmatrix} 0.07 & 0.04 \end{bmatrix}, H_3 = 0.04
$$

In the following simulation it is assumed that the $F(k) = sin(k)$, and it can be seen that $F^T(k)\mathcal{W}F(k) \leq \mathcal{W}$. It is also assumed that the network-induced delays are characterized by a Markov chain taking values in a finite set $\mathcal{S} = \{1, 2, 3\}$, that corresponds to the delays of 2, 3 and 4 seconds, respectively. The transitions in the Markov chain modes are under the following probability matrix which is obtained by performing the experiments on Vodafone cellular network:

$$
P_\tau = \begin{bmatrix} 0.4175 & 0.5825 & 0 \\ 0.3702 & 0.6157 & 0.0141 \\ 0.3702 & 0.6157 & 0.0141 \end{bmatrix} \tag{5.22}
$$

Figure 5.2 shows the random network-induced delays used in the example. The congestion control parameters δ_1 and δ_2 are set as 0.5 for the simulation. Using Theorem 5.3.2, the following set of the controller matrices are obtained.
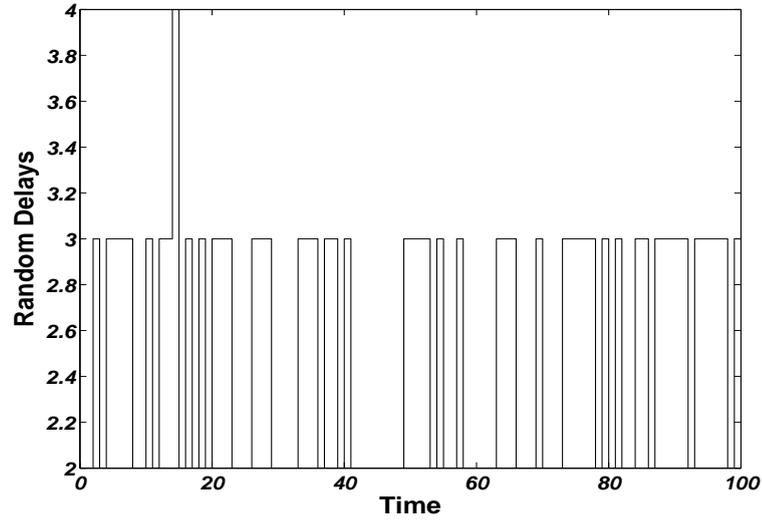
FIGURE 5.2: Random delays

$$
A_c(1) = \begin{bmatrix} -0.3522 & -0.0693 & 0.2142 & -0.1467 \\ 1.0003 & -0.0003 & -0.0001 & 0.0003 \\ -0.8006 & 0.5005 & 0.2001 & -1.0304 \\ -0.0002 & 0.0002 & 0.5792 & -0.0002 \end{bmatrix}, \ B_c(1) = \begin{bmatrix} -0.0027 \\ -0.0020 \\ 0.0035 \\ 0.0015 \end{bmatrix}
$$

$$
C_c(1) = \begin{bmatrix} -1.1527 & 0.1811 & 0.2144 & -1.1470 \end{bmatrix}.
$$

$$
A_c(2) = \begin{bmatrix} -0.3828 & -0.0659 & 0.2318 & -0.1380 \\ 1.0003 & -0.0003 & -0.0001 & 0.0003 \\ -0.8005 & 0.5005 & 0.2001 & -1.0304 \\ -0.0002 & 0.0002 & 0.5792 & -0.0002 \end{bmatrix}, \ B_c(2) = \begin{bmatrix} -0.0027 \\ -0.0020 \\ 0.0035 \\ 0.0015 \end{bmatrix}
$$

$$
C_c(2) = \begin{bmatrix} -1.1833 & 0.1844 & 0.2319 & -1.1383 \end{bmatrix}.
$$

$$
A_c(3) = \begin{bmatrix} -0.1994 & 0.0855 & 0.0716 & 7-0.3468 \\ 1.0004 & -0.0005 & -0.0001 & 0.0004 \\ -0.8008 & 0.5006 & 0.2002 & -1.0306 \\ -0.0003 & 0.0003 & 0.5792 & -0.0003 \end{bmatrix}, \ B_c(3) = \begin{bmatrix} -0.0028 \\ -0.0021 \\ 0.0036 \\ 0.0015 \end{bmatrix}
$$

$$
C_c(3) = \begin{bmatrix} -1.0000 & 0.3360 & 0.0718 & -1.3472 \end{bmatrix}.
$$

The stabilized system states, in the presence of the time delays and the congestion control mechanism, are shown in the Figure 5.3.

The effect of δ_1 and δ_2 on the channel bandwidth consumption and the system performance is analyzed through a series of the simulations. It is summarized in the Table 5.1, where it can been seen that the bandwidth consumption is reduced as δ_1 and δ_2

(a) System state x_1

(b) System state x_2

(c) System state x_3
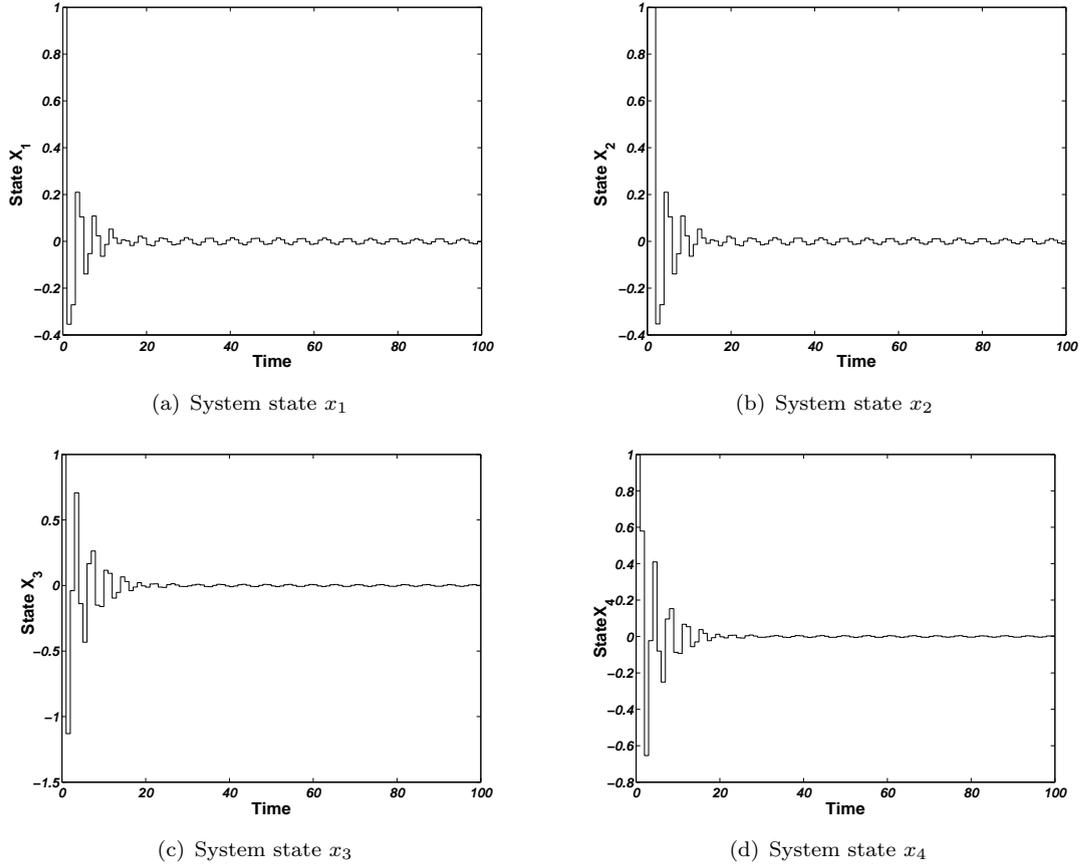
(d) System state x_4

FIGURE 5.3: System states

TABLE 5.1: Effect of δ_1 and δ_2 on bandwidth consumption

δ_1	δ_2	Aggregated Bandwidth Consumption	Minimized γ
0.1	0.1	75.00%	0.6302
0.5	0.5	73.00 %	0.6380
0.9	0.8	70.00 %	0.6576
> 1	> 1	undesired response	∞

are increased. However, the bandwidth consumption can not be reduced to less than 70%, because with either $\delta_1 > 1$ or $\delta_2 > 1$, the system becomes oscillatory. It shows that there is always a trade off between the system performance and the bandwidth consumption. The minimized γ, the $\mathcal{H}_\infty$ performance parameter, for different values of δ_1 or δ_2 is obtained and is plotted in the Figure 5.4. It is observed that the lower bound on the γ is increased with the increase in the congestion control parameters. It supports the argument that there is a trade off between the system performance and the reduced bandwidth.

Finally, for the prescribed value of the $\gamma = 0.5$ the effect of changing δ_1 and δ_2 on the $\mathcal{H}_\infty$ performance is analyzed. It is elaborated in the Figure 5.5 that by increasing the
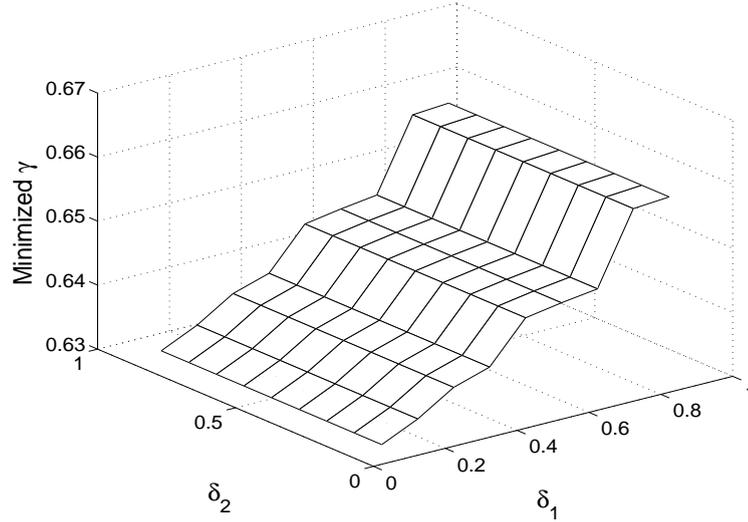
FIGURE 5.4: Minimized γ for different values of δ_1 and δ_2
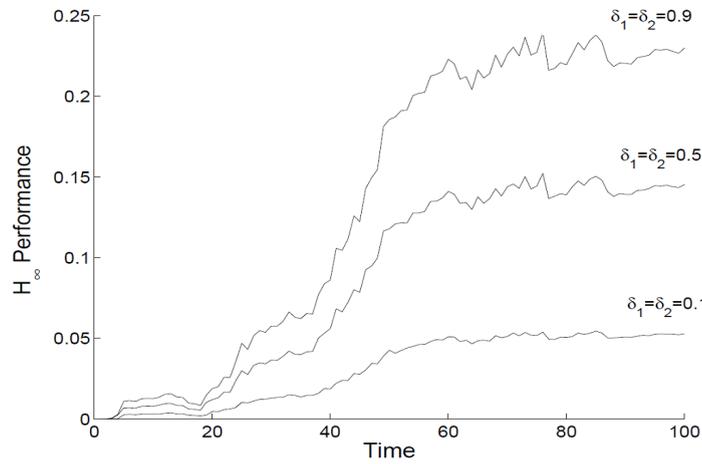
FIGURE 5.5: Effect of δ_1 and δ_2 on $\mathcal{H}_\infty$ performance

δ_1 and δ_2, the magnitude of $T_{zw}(k)$ i.e., the transfer function between the disturbance and the output is increasing which shows the degradation in the $\mathcal{H}_\infty$ performance.

Remark 5.4.1. The proposed design enjoys the advantages of both time triggered and event triggered systems.The proposed theory uses comparatively mature and well developed methods to present the stability criteria and controller synthesize as it considers the closed -loop system as time triggered system. On the other hand it uses the reduced communication resources such as channel bandwidth and the transmission power (Wireless LANs),that is the key feature of the event triggered systems. However, the design does not help in the computational efficiency at the controller side and requires same computational cycles as the time triggered systems.

5.5   Conclusions

A simple but the efficient network resource utilization and the congestion control scheme has been provided in Chapter 4 for the NCSs. This technique compares the current and the last transmitted measurements before sending them over the network. In this chapter, the proposed scheme is applied both on the system inputs and outputs. The scheme takes the advantage of both time triggered and event triggered sampling mechanisms. With this congestion control scheme the stability conditions and a robust delay mode-dependent output feedback controller are proposed. The closed-loop system stability is obtained by using a L-K functional approach. On the basis of the stability conditions sufficient conditions for the controller matrices have been obtained in terms of the BMIs. Since BMIs are non-convex in nature, a cone complimentarity algorithm is used to convert the non-convex problem into a quasi-convex optimization problem that are easily solved by the available mathematical tools, for example, the YALMIP and the LMI toolboxes of the MATLAB. The effectiveness of the developed technique in terms of the bandwidth utilization and the $\mathcal{H}_\infty$ performance is demonstrated using a simulation example. It is observed that there is always tradeoff between the bandwidth utilization and the $\mathcal{H}_\infty$ performance.

Chapter 6

Robust $\mathcal{H}_\infty$ Dynamic Output Feedback Control of NCSs with Multiple Quantizers

This chapter talks about stability and stabilizability problems of networked control systems(NCSs) with multiple quantizers. More precisely, the system and controller outputs are quantized at different quantization levels and experiencing different network-induced delays. This configuration is more natural in NCSs. Network-induced delays are modelled by a Markov chain. Quantization errors are bounded by a sector bound approach and represented as convex poly-topic uncertainties. Lyapunove-Krasovskii(L-K) functional approach is used to develop stability criteria for NCSs with multiple quantizers. On the basis of the stability criteria, a quantized robust $\mathcal{H}_\infty$ output feedback control law is proposed in terms of bilinear matrix inequalities (BMIs). Furthermore an iterative cone complementarity algorithm is used to convert these BOIS into a quasi-convex optimization problem which can be solved easily. A simulation example is provided to demonstrate the effectiveness of proposed theorems [107].

6.1   Introduction

The distributed control system in which control loops are closed over real time networks are called NCSs. The rapid development in the communication systems and advancement in the control designs greatly enhanced the system modularity, flexibility and reduced processing cost in the NCSs making them highly popular in the industry. However incorporation of the network in the control loops results in the various constraints such as (1) time delays and packet dropouts due to limited bandwidth; (2) quantization

errors caused by hybrid nature of NCSs; (3) variable sampling/transmission intervals due to multiple nodes; and (4) network security due to shared communication networks [51, 52, 86]. The quality of control (QOC) in the NCSs can be improved either by developing network scheduling algorithms or by designing modified control strategies that can cater for network constraints.

The time delays are inevitable in the NCSs due to remote location of the controllers and the network congestion. Therefore, the NCSs are considered as a sub class of time-delayed systems (TDSs) [53]. In NCSs, most of the research has been carried out on time varying delays because the network-induced delays are always time varying in nature. The time varying delays are treated with two approaches (1) deterministic methods and (2) stochastic methods [57]. In the first method the delays are bounded while in the second method delays follow certain probability distributions such as Markov chains and Bernoulli random sequences [64–66, 68]. In this chapter the time varying delays are modelled as random modes of a Markov chain.

In the recent years the problem of quantized feedback control has seen a growing research interest due to the evolution of computer based control and NCSs. The quantization effects can be investigated in two aspects: (1) mitigation of the quantization effects to achieve the system performance and stability and (2) considering quantizers as information coders. In the first approach, stability analysis and controller synthesis are done in the presence of a quantizer by [69, 70]. The second approach investigates how much information from a quantizer is enough to achieve the system stability and certain performance level. It is proved by [72] that the minimum quantization information required for the system stability depends on the unstable poles of plant. The logarithmic quantizers can give minimum or coarsest quantization densities [75]. The similar research to use optimal quantizers and coarsest quantization densities is carried out by [76], while sustaining the system stability for Markovian jump systems (MJSs).

The quantized feedback control problem can be classified as: (1) the quantized feedback with static quantizers and (2) the quantized feedback with dynamic quantizers. The former approach assumes that the quantization value at any time instant k does not depend on the previous quantization values [72, 75]. The latter approach considers dynamic quantizers with an internal state. It helps to enlarge the region of attraction and reduces limit cycles [69, 77]. A static quantizer can be used as a dynamic quantizer with help of dynamic scaling. In this case the input signal for the quantization is pre-scaled and this scaling can be done online [78].

A lot of research has been done on the NCSs with a single quantizer on one side of communication network such as from sensor to controller end [80]. However, the quantizers are required on both controller input and output in real time NCSs. This scenario is

discussed by [81] in which a quantized state feedback is proposed with a single quantizer each on system inputs and outputs. On the other hand, the data on different sensor nodes is available on different times that requires a separate quantizer for each node. This consideration results in a less conservative design due to different timing parameters of the sensor nodes. It is more natural in the NCSs because a single quantizer for the multiple sensors requires a centralized decoder. This fact motivated the author to propose a robust $\mathcal{H}_\infty$ output feedback controller for the NCSs with multiple quantizers. As each node with a separate quantizer acquires communication channels at different times, therefore each quantized-signal experiences different network-induced delays. The random delays are modelled by a Markov chain. The logarithmic quantizers are deployed both on the sensors and the controller outputs. The quantization errors, bounded by sectors, are represented as the convex poly-topic uncertainties. L-K functional approach is used to develop the stability criterion for the NCSs. On the basis of the stability criterion sufficient conditions for the existence of a quantized $\mathcal{H}_\infty$ robust output feedback controller are given in terms of bilinear matrix inequalities (BMIs). An iterative algorithm is suggested to convert the BMIs into quasi-convex LMIs that can be solved easily by MATLAB LMI ToolBox. An example is presented to illustrate the effectiveness of the proposed design. Following are the main contributions of Chapter 3:

- The system and controller outputs are quantized at different quantization levels and experience different network-induced delays. To the best of authors' knowledge, this has not been formally investigated before

- The quantization errors are bounded by a sector bound approach and are represented as poly-topic parametric uncertainties. The multiple quantizers are assumed on both sensors and controller outputs.

This chapter is organized into five sections. In Section 6.2, system description, time delay and quantization error modelling, the problem formulation and necessary lemmas are given. Main results are provided in Section 6.3. Section 6.4 comprises a simulation example to demonstrate the validity of proposed design. The conclusions are given in Section 6.5.

6.2 System Description and Definitions

A networked control system, with input and output quantization, is shown in Figure 6.1.
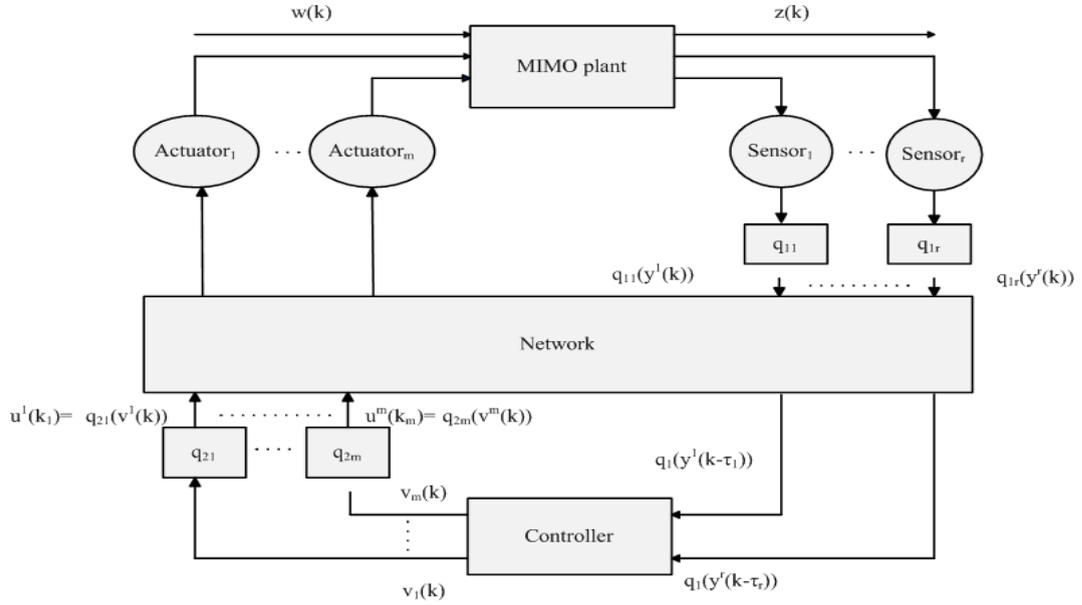
FIGURE 6.1: Layout of a networked control system with multiple quantizers

The class of uncertain discrete-time linear plants is described by the following model:

$$
\begin{aligned}
x(k+1) &= [A + \Delta A(k)]x(k) + [B_1 + \Delta B_1(k)]w(k) + [B_2 + \Delta B_2(k)]u(k), \quad x(0) = 0 \\
z(k) &= [C_1 + \Delta C_1(k)]x(k) + [D_{11} + \Delta D_{11}(k)]w(k) + [D_{12} + \Delta D_{12}(k)]u(k) \\
y(k) &= C_2 x(k)
\end{aligned}
\tag{6.1}
$$

where $x(k) \in \Re^n, u(k) \in \Re^m, z(k) \in \Re^p, y(k) \in \Re^r$ are the state, input, controlled output and measured output, respectively. $w(k) \in \Re^{m_1}$ is the disturbance that belongs to $\mathcal{L}_2[0, \infty)$, the space of square summable vector sequence over $[0, \infty]$. The matrices A, B_1, B_2, C_1, D_{11}, D_{12} and C_2 are of known dimensions. The matrix functions $\Delta A(k)$, $\Delta B_1(k)$, $\Delta B_2(k)$, $\Delta C_1(k)$, $\Delta D_{11}(k)$ and $\Delta D_{12}(k)$ represent time-varying uncertainties and satisfy conditions given in the assumption 3.2.1.

In NCSs, there exist various type of delays such as sensor to controller delay $\tau_{sc}(k)$; controller to actuator delay $\tau_{ca}(k)$; and processing delay $\tau_c(k)$. However, all the delays can be lumped together as [83]:

$$
\tau(k) = \tau_{sc}(k) + \tau_{ca}(k) + \tau_c(k)
$$

Remark 6.2.1. Despite of the fact that if there is a same communication network between sensor to controller and controller to actuator, it is true that $\tau_{sc}(k)$, $\tau_c(k)$ and $\tau_{ca}(k)$ can be different in size and nature and in other properties. Therefore all the delays should be treated separately and the use of a separate Markov chains to model these

delays is better. However in this work, one Markov chain is used to model closed-loop lumped delays for the sack of simplicity. Separate Markov chains for different delays can be considered in the future to reduce the conservatism of the design. It is worth mentioning that transition probability matrix for the Markov chain is obtained by performing a series of experiments on a wireless network for closed-loop delays.

All measured outputs will be quantized separately as shown in Figure 6.1. That's why each output $y^r(k)$ will bear different network-induced delay $\tau^r(k)$:

$$y(k - \tau(k)) = \begin{bmatrix} C_2^1 x(k - \tau^1(k)) \\ C_2^2 x(k - \tau^2(k)) \\ \cdots \\ C_2^r x(k - \tau^r(k)) \end{bmatrix} = \sum_{l=1}^{r} G^l x(k - \tau^l(k)) \tag{6.2}$$

where l^{th} line of $G^l \in \Re^{r \times n}$ is C_2^l and all other lines will be zeros. Consider a quantized dynamic output feedback controller:

$$\begin{aligned} \hat{x}(k+1) &= A_c(i)\hat{x}(k) + B_c(i)q_1(y(k - \tau(k))) \\ v(k) &= C_c(i)\hat{x}(k) \\ u(k) &= q_2(v(k)) \end{aligned} \tag{6.3}$$

where $\hat{x}(k)$ is controller state; $A_c(i), B_c(i)$ and $C_c(i)$ are controller matrices and

$$q_1(.) = \begin{bmatrix} q_{11}(.) & q_{12}(.) & \cdots & q_{1r}(.) \end{bmatrix}^T$$

$$q_2(.) = \begin{bmatrix} q_{21}(.) & q_{22}(.) & \cdots & q_{1m}(.) \end{bmatrix}^T$$

Quantizer Description:

Quantization process can be accomplished using uniform and logarithmic quantizers. Here, it is worth mentioning that in logarithmic quantizers the number of quantization levels, although infinite, grow logarithmically in radial direction, rather than linearly. It means that logarithmic quantizers result in coarser quantization densities than uniform quantizers. In fact they result in coarsest quantization densities [72]. This fact motivated the author to use logarithmic quantizers, described as follows:

$$q_{ij}(\nu) = \begin{cases} \rho_{ij}^n & \text{if } \frac{1}{1+\delta_{ij}}\rho_{ij}^n < \nu \leq \frac{1}{1-\delta_{ij}}\rho_{ij}^n, \ \nu > 0 \ n = 0, \pm 1, \pm 2, \cdots \\ 0, & \text{if } \nu = 0 \\ -q_{ij}(-\nu) & \text{if } \nu < 0 \end{cases} \tag{6.4}$$

where $0 < \rho_{ij} < 1$ is the quantization density of $q_{ij}(\cdot)$, and δ_{ij} is related to ρ_{ij} by:

$$\delta_{ij} = \frac{1 - \rho_{ij}}{1 + \rho_{ij}} \tag{6.5}$$

The associated quantized set $\mathcal{U}$ is given by:

$$\mathcal{U} = \left\{ \pm \rho_{ij}^n, n = 0, \pm 1, \pm 2, \cdots \right\} \bigcup \{0\}. \tag{6.6}$$

Now define the quantization error as:

$$e_{ij}(k) = q_{ij}(v(k)) - v(k) = \Delta_{qij}(k)v(k), \tag{6.7}$$

It has been shown by [75] that quantization error can be bounded by sector bound approach and $\Delta_{qij}(k) \in [-\delta_{ij}, \delta_{ij}]$.

Time delay Modelling:

Let $\{r_k, k\}$ be a discrete homogeneous Markov chain taking values in a finite set $\mathcal{S} = \{1, 2, \cdots, s\}$, transition probability from mode i at k to mode j at time $k+1$ is given as

$$p_{ij} := \mathbf{Prob}\{r_{k+1} = j | r_k = i\}$$

where $i, j \in \mathcal{S}$.

The random delay $\tau(r_k)$ is modelled by a finite state Markov process as $\tau^r(i) = \tau^r(r_k)$ with $0 \le \tau^r(1) < \tau^r(2) < \cdots < \tau^r(s) \le \infty$. We assume that the controller will always use the most recent data, i.e., if there is no new information coming at step $k + 1$, to compensate longer delays, then $q(y(k - \tau(r_k)))$ will be used for feedback. Thus the delay $\tau(r_k)$ can only increase at most by 1 at each step, and we constrain:

$$\mathbf{Prob}\{\tau^r(r_{k+1}) > \tau^r(r_k) + 1\} = 0$$

With this assumption, we define the transition probability matrix as:

$$P_\tau = \begin{bmatrix} p_{11} & p_{12} & 0 & 0 & \ldots & 0 \\ p_{21} & p_{22} & p_{23} & 0 & \ldots & 0 \\ \vdots & \vdots & \vdots & \vdots & \ddots & \vdots \\ \vdots & \vdots & \vdots & \vdots & \vdots & p_{(s-1)s} \\ p_{s1} & p_{s2} & p_{s3} & p_{s4} & \cdots & p_{ss} \end{bmatrix} \tag{6.8}$$

with $0 \leq p_{ij} \leq 1$ and $\sum_{j=1}^{i+1} p_{ij} = 1$.

Using (6.3), (6.4) and (6.7) , a quantized output feedback controller is proposed:

$$
\begin{aligned}
\hat{x}(k+1) &= A_c(i)\hat{x}(k) + B_c(i)(I + \Delta_1(k)) \sum_{l=1}^{r} G^l x(k - \tau^l(i)) \\
v(k) &= C_c(i)\hat{x}(k) \\
u(k) &= q_2(v(k)) = (I + \Delta_2(k))C_c(i)\hat{x}(k)
\end{aligned}
\tag{6.9}
$$

where $\Delta_1(k)$, $\Delta_2(k)$ are quantization errors:

$$
\begin{aligned}
\Delta_1(k) &= \operatorname{diag}\Big\{\Delta_{11}(k), \Delta_{12}(k), \cdots \Delta_{1r}(k)\Big\} \\
\Delta_2(k) &= \operatorname{diag}\Big\{\Delta_{21}(k), \Delta_{22}(k), \cdots \Delta_{2m}(k)\Big\}
\end{aligned}
$$

$\Delta_1(k)$ and $\Delta_2(k)$ can be represented as [79]:

$$
\begin{aligned}
\Delta_1(k) &= \sum_{g=1}^{2^r} \lambda_{1g}(k)\delta_1^g, \quad \sum_{g=1}^{2^r} \lambda_{1g}(k) = 1, \quad \lambda_{1g}(k) \geq 0 \\
\Delta_2(k) &= \sum_{h=1}^{2^m} \lambda_{2h}(k)\delta_2^h, \quad \sum_{h=1}^{2^m} \lambda_{2h}(k) = 1, \quad \lambda_{2h}(k) \geq 0
\end{aligned}
\tag{6.10}
$$

where r and m are number of sensors and actuators respectively and $\delta_1^{(g)}$, $\delta_2^{(h)}$ are diagonal matrices of appropriate dimensions. Each matrix comprises of values either $-\delta$ or δ, that is the sector bound for quantization error.

Using (6.10), the closed-loop system of (6.1) with (6.9) is given as follows:

$$
\begin{aligned}
\zeta(k+1) &= \sum_{g=1}^{2^r} \lambda_{1g}(k) \sum_{h=1}^{2^m} \lambda_{2h}(k)\Big([A_{cl}^h(i) + \bar{E}_1 F(k)\bar{H}_1^h(i)]\zeta(k) + B_{cl}(i)(I + \delta_1^g)\sum_{l=1}^{r} \bar{G}^l \\
&\quad \zeta(k - \tau^l(i)) + [\bar{B}_1 + \bar{E}_1 F(k)H_2]w(k)\Big) \\
z(k) &= \sum_{g=1}^{2^r} \lambda_{1g}(k) \sum_{h=1}^{2^m} \lambda_{2h}(k)\Big([C_{cl}^h(i) + E_2 F(k)\bar{H}_1^h(i)]\zeta(k) + [D_{11} + E_2 F(k)H_2]w(k)\Big)
\end{aligned}
\tag{6.11}
$$

where $\zeta(k) = [x(k) \ \hat{x}(k)]^T$,

$$
\begin{aligned}
A_{cl}^h(i) &= \begin{bmatrix} A & B_2(I + \delta_2^h)C_c(i) \\ 0 & A_c(i) \end{bmatrix}, B_{cl}(i) = \begin{bmatrix} 0 \\ B_c(i) \end{bmatrix} \\
\bar{B}_1 &= \begin{bmatrix} B_1 \\ 0 \end{bmatrix}, \bar{G}^l = \begin{bmatrix} G^l & 0 \end{bmatrix}, \bar{E}_1 = \begin{bmatrix} E_1 \\ 0 \end{bmatrix} \\
\bar{H}_1^h(i) &= \begin{bmatrix} H_1 & H_3(I + \delta_2^h)C_c(i) \end{bmatrix} \\
C_{cl}^h(i) &= \begin{bmatrix} C_1 & D_{12}(I + \delta_2^h)C_c(i) \end{bmatrix}.
\end{aligned}
$$

The problem under our study is formulated as follows.

Problem Formulation:

Given a prescribed $\gamma > 0$, design a dynamic output feedback controller such that

1. the closed-loop system with $w(k) = 0$ is stochastically stable, i.e, there exists a constant $0 < \alpha < \infty$ such that

$$
E\left\{ \sum_{\ell=0}^{\infty} \zeta^T(\ell)\zeta(\ell) \right\} < \alpha \tag{6.12}
$$

for all $\zeta(0), r_0$.

2. Under the zero-initial condition, the controlled output $z(k)$ satisfies

$$
E\left\{ \sum_{k=0}^{\infty} z^T(k)z(k) | r_0 \right\} < \gamma^2 \sum_{k=0}^{\infty} w^T(k)w(k) \tag{6.13}
$$

for all nonzero $w(k)$.

The following lemmas play important roles in the derivation of the main results.

Lemma 6.2.1. *Let $\bar{x}(k) = x(k+1) - x(k)$ and $\tilde{\zeta}(k) = \left[\zeta^T(k) \ \zeta^T(k - \tau^1(r_k)) \cdots \ \zeta^T(k - \tau^r(r_k)) \ w^T(k) \ \zeta^T(k)(\bar{H}_1^h)^T(i)F^T(k) \ w^T(k)H_2^T F^T(k) \right]^T \in \Re^l$, then for any matrices $R \in \Re^{n \times n}$, $M \in \Re^{n \times t}$ and $Z \in \Re^{t \times t}$ satisfying*

$$
\begin{bmatrix} R & M \\ M^T & Z \end{bmatrix} \geq 0 \tag{6.14}
$$

the following inequality holds:

$$
-\sum_{l=1}^{r} \sum_{i=k-\tau^l(r_k)}^{k-1} \bar{x}^T(i)R\bar{x}(i) \leq \tilde{\zeta}^T(k)\left\{ \Upsilon_1 + \Upsilon_1^T + \sum_{l=1}^{r} \tau^l(r_k)Z \right\}\tilde{\zeta}(k)
$$

where $\Upsilon_1 = M^T[diag\{I, 0\} \ diag^1\{-I, 0\} \cdots \ diag^r\{-I, 0\} \ 0 \ 0 \ 0]$.

Proof: Proof follows the same line of Lemma 3.2.1. $\nabla\nabla\nabla$

Lemma 6.2.2. *[87]:*

If $P > 0$ then

$$A_i^T P A_j + A_j^T P A_i \leq A_i^T P A_i + A_j^T P A_j$$

6.3 Stability Analysis and Controller Synthesis of NCSs with Multiple Quantizers

Stability criterion for uncertain discrete-time systems with random communication delays and multiple quantizers are given in the following theorem.

Theorem 6.3.1. *For given $\gamma > 0$ and controller matrices $A_c(i)$, $B_c(i)$ and $C_c(i)$ where $i = 1, \cdots, s$, if there exist sets of positive-definite matrices $P(i)$, $R_1(i)$, R_1, $R_2(i)$, R_2, $W_1(i)$, $W_2(i)$, $Q^1, \cdots, Q^r$, $Z(i)$, and matrices $M(i)$ satisfying the following inequalities and (6.17):*

$$R_1 > R_1(i), \quad R_2 > R_2(i) \tag{6.15}$$

$$\begin{bmatrix} (1 - p_{i(i+1)})R_1(i) + R_2(i) & M(i) \\ * & Z(i) \end{bmatrix} \geq 0 \tag{6.16}$$

$$\begin{bmatrix} \Lambda^{g,h}(i) + \left(\Gamma_1^{g,h}(i) + \Gamma_1^{h,g}(i)\right)^T \tilde{P}(i)\left(\Gamma_1^{g,h}(i) + \Gamma_1^{h,g}(i)\right) + \\ \left(\Gamma_2^g(i) + \Gamma_2^h(i)\right)^T \sum_{l=1}^r \left[\tilde{\tau}^l(i)R_1 + \tau^l(s)R_2\right]\left(\Gamma_2^g(i) + \Gamma_2^h(i)\right) \\ + \left(\Gamma_3^g(i) + \Gamma_3^h(i)\right)^T \left(\Gamma_3^g(i) + \Gamma_3^h(i)\right) + 4\Upsilon_1(i) + 4\Upsilon_1^T(i) + 4\sum_{l=1}^r \tau^l(i)Z(i) \end{bmatrix} < 0 \tag{6.17}$$

for all $g = 1 \cdots 2^r$ and $h = 1 \cdots 2^m$

where

$$\Gamma_1^{g,h}(i) = \left[\begin{array}{cccccc} A_{cl}^h(i) & B_{cl}(i)(I+\delta_1^g)\bar{G}^1 \cdots B_{cl}(i)(I+\delta_1^g)\bar{G}^r & \bar{B}_1 & \bar{E}_1 & \bar{E}_1 \end{array}\right]$$

$$\Gamma_2^h(i) = \left[\begin{array}{ccccc} \bar{A}^h(i) & 0 & \bar{B}_1 & \bar{E}_1 & \bar{E}_1 \end{array}\right]$$

$$\Gamma_3^h(i) = \left[\begin{array}{ccccc} C_{cl}^h(i) & 0 & D_{11} & E_2 & E_2 \end{array}\right]$$

$$\Lambda^{g,h}(i) = diag\Bigg\{\left(4\sum_{l=1}^r(\tau^l(s)-\tau^l(1)+1)Q^l + \left(\bar{H}_1^g(i)+\bar{H}_1^h(i)\right)^T W_1(i)\left(\bar{H}_1^g(i)+\bar{H}_1^h(i)\right)\right.$$
$$\left. -4P(i)\right), -4Q^1, \cdots, -4Q^r, 4\left(H_2^T W_2(i)H_2 - \gamma^2 I\right), -4W_1(i), -4W_2(i)\Bigg\}$$

$$\tilde{P}(i) = \sum_{j=1}^{i+1} p_{ij}P(j)$$

$$\tilde{\tau}^1(i) = \sum_{j=1}^{i+1} p_{ij}\tau^1(j)$$

$$\vdots$$

$$\tilde{\tau}^r(i) = \sum_{j=1}^{i+1} p_{ij}\tau^r(j)$$

$$\Upsilon_1(i) = M^T(i)\left[\begin{array}{cccccc} diag\{I,0\} & diag^1\{-I,0\} & \cdots diag^r\{-I,0\} & 0 & 0 & 0 \end{array}\right]$$

$$\bar{A}^h(i) = \left[\begin{array}{cc} A-I & B_2(I+\delta_2^h)C_c(i) \\ 0 & 0 \end{array}\right]$$

$$\delta_1^g = diag\left\{\delta_{11}^g, \delta_{12}^g, \cdots \delta_{1r}^g\right\}$$

$$\delta_2^h = diag\left\{\delta_{21}^h, \delta_{22}^h, \cdots \delta_{2m}^h\right\} \tag{6.18}$$

Then the closed-loop system is stochastically stable with the prescribed $\mathcal{H}_\infty$ performance.

Proof: See Appendix 13. $\nabla\nabla\nabla$

The following theorem provides procedure for designing an $\mathcal{H}_\infty$ quantized output feedback controller.

Theorem 6.3.2. *For a given $\gamma > 0$, if there exist positive symmetric matrices $X(i) > 0$, $Y(i) > 0$, $\mathcal{Y}(i) > 0$, $W_1(i)$, $\mathcal{W}_1(i)$, $W_2(i)$, $\mathcal{Q}^1 \cdots \mathcal{Q}^r$, $Q^1 \cdots Q^r$, , $\mathcal{D}^l, N(i)$, $\mathcal{N}(i)$, R_1, $\mathcal{R}_1$, $R_1(i)$, R_2, $\mathcal{R}_2$, $R_2(i)$, $S(i,j)$, $\bar{Z}(i)$ and matrices $\mathcal{A}(i)$, $\mathcal{B}(i)$, $\mathcal{C}(i)$, $J(i)$, $\tilde{J}$, $\bar{M}(i)$ satisfying the following inequalities, and (6.21) for all $i, j \in \mathcal{S}$:*

$$R_1 > R_1(i), \quad R_2 > R_2(i) \tag{6.19}$$

$$\left[\begin{array}{cc} N(i) & \bar{M}(i) \\ * & \bar{Z}(i) \end{array}\right] \geq 0 \tag{6.20}$$

$$
\begin{bmatrix}
\tilde{\Lambda}(i) & \left(\bar{\Gamma}_1^{g,h}(i)+\bar{\Gamma}_1^{h,g}(i)\right)^T & \left(\bar{\Gamma}_2^{g}(i)+\bar{\Gamma}_2^{h}(i)\right)^T & \left(\bar{\Gamma}_3^{g}(i)+\bar{\Gamma}_3^{h}(i)\right)^T & \bar{\Gamma}_4^{T}(i) & \left(\bar{\Gamma}_5^{g,h}(i)\right)^T \\
* & \tilde{\Xi}(i) & 0 & 0 & 0 & 0 \\
* & * & -\mathcal{R} & 0 & 0 & 0 \\
* & * & * & -I & 0 & 0 \\
* & * & * & * & 4(\tilde{\mathcal{D}}-\tilde{J}^T-\tilde{J}) & 0 \\
* & * & * & * & * & -\mathcal{W}_1(i)
\end{bmatrix} < 0
\tag{6.21}
$$

for all $g = 1\cdots 2^r$ and $h = 1\cdots 2^m$

$$
\begin{bmatrix}
S(i,j) & J^T(i) \\
* & Y(j)
\end{bmatrix} > 0
\tag{6.22}
$$

$$
\begin{bmatrix}
\mathcal{D}^l & \tilde{J}^T \\
* & \mathcal{Q}^l
\end{bmatrix} > 0
\tag{6.23}
$$

$$
\begin{bmatrix}
(1-p_{i(i+1)})R_1(i)+R_2(i) & \mathcal{T}^T \\
* & \mathcal{N}(i)
\end{bmatrix} > 0
\tag{6.24}
$$

$$
\mathcal{N}(i)N(i) = I,\; \mathcal{R}_1 R_1 = I,\; \mathcal{Q}^l Q^l = I, \mathcal{R}_2 R_2 = I,\; \mathcal{Y}(i)Y(i) = I,\; \mathcal{W}_1(i)W_1(i) = I
\tag{6.25}
$$

where

$$\tilde{\Lambda}(i) = 4\Big(\bar{\Lambda}(i) + \bar{\Upsilon}_1(i) + \bar{\Upsilon}_1^T(i) + \sum_{l=1}^{r}\tau^l(i)\bar{Z}(i)\Big)$$

$$\bar{\Lambda}(i) = diag\Big\{ -\begin{bmatrix} Y(i) & I \\ I & X(i) \end{bmatrix}, -Q^1, \cdots, -Q^r, \big(H_2^T W_2(i)H_2 - \gamma^2 I\big),$$

$$-W_1(i), -W_2(i)\Big\}$$

$$\bar{\Upsilon}(i) = \bar{M}^T(i)[diag\{I,0\} \ \ diag^1\{-I,0\} \cdots diag^r\{-I,0\} \ \ 0 \ \ 0 \ \ 0]$$

$$\bar{\Gamma}_1^{g,h}(i) = \begin{bmatrix} \check{A}_{cl}^h(i) & \check{B}_{cl}(i)(I+\delta^g)\bar{G}^1 & \cdots\check{B}_{cl}(i)(I+\delta^g)\bar{G}^r & \check{B}_1 & \check{E}_1 & \check{E}_1 \end{bmatrix}$$

$$\bar{\Gamma}_2^h(i) = \begin{bmatrix} \sqrt{\sum_{l=1}^{r}\tilde{\tau}^l(i)}I & \sqrt{\sum_{l=1}^{r}\tau^l(s)}I \end{bmatrix}^T \begin{bmatrix} \check{A}^h(i) & 0 & \bar{B}_1 & \bar{E}_1 & \bar{E}_1 \end{bmatrix}$$

$$\mathcal{R} = diag\Big\{\mathcal{R}_1, \mathcal{R}_2\Big\}$$

$$\bar{\Gamma}_3^h(i) = \begin{bmatrix} \check{C}_{cl}^h(i) & 0 & \bar{D}_{11} & \bar{E}_2 & \bar{E}_2 \end{bmatrix}$$

$$\bar{\Gamma}_4(i) = \begin{bmatrix} T(i) & 0 & 0 & 0 & 0 \end{bmatrix}$$

$$\bar{\Gamma}_5^{g,h}(i) = \begin{bmatrix} \check{H}_1^g(i) + \check{H}_1^h(i) & 0 & 0 & 0 & 0 \end{bmatrix}$$

$$\tilde{\mathcal{D}} = \sum_{l=1}^{r}(\tau^l(s) - \tau^l(1) + 1)\mathcal{D}^l$$

$$\tilde{\Xi}(i) = \begin{bmatrix} \tilde{S}(i) - J(i) - J^T(i) & I \\ I & -\tilde{X}(i) \end{bmatrix}$$

$$\tilde{X}(i) = \sum_{j=1}^{i+1}p_{ij}X(j), \tilde{S}(i) = \sum_{j=1}^{i+1}p_{ij}S(i,j)$$

$$\check{A}_{cl}^h(i) = \begin{bmatrix} AY(i) + B_2(I+\delta_2^{(h)})\mathcal{C}(i) & A \\ \mathcal{A}(i) & \tilde{X}(i)A \end{bmatrix}$$

$$\check{B}_1(i) = \begin{bmatrix} B_1 \\ \tilde{X}(i)B_1 \end{bmatrix}$$

$$\check{E}_1(i) = \begin{bmatrix} E_1 \\ \tilde{X}(i)E_1 \end{bmatrix}$$

$$\check{C}_{cl}^h(i) = \begin{bmatrix} C_1Y(i) + D_{12}(I+\delta_2^{(h)})\mathcal{C}(i) & C_1 \end{bmatrix}$$

$$\check{H}_1^h(i) = \begin{bmatrix} H_1Y(i) + H_3(I+\delta_2^{(h)})\mathcal{C}(i) & H_1 \end{bmatrix}$$

$$T(i) = \begin{bmatrix} Y(i) & I \\ Y(i) & 0 \end{bmatrix} \ and \ \mathcal{T}(i) = \begin{bmatrix} 0 & \mathcal{Y}(i) \\ I & -I \end{bmatrix} \tag{6.26}$$

Then the closed-loop system is stochastically stable with the prescribed $\mathcal{H}_\infty$ performance. Furthermore, a suitable controller is given as follows

$$
\begin{aligned}
A_c(i) &= \left(\sum_{j=1}^{i+1} p_{ij} Y^{-1}(j) - \tilde{X}(i) \right)^{-1} \left(\mathcal{A}(i) - \tilde{X}(i)(AY(i) + B_2(I + \delta_2^{(h)})\mathcal{C}(i)) \right) Y^{-1}(i) \\
B_c(i) &= \left(\sum_{j=1}^{i+1} p_{ij} Y^{-1}(j) - \tilde{X}(i) \right)^{-1} \mathcal{B}(i) \\
C_c(i) &= \mathcal{C}(i) Y^{-1}(i).
\end{aligned}
$$

$$(6.27)$$

Proof: The proof is given in the appendix 13. $\nabla\nabla\nabla$

6.4   Simulation Example

This example is demonstrated using MATLAB and Simulink-based TrueTime Simulator. This toolbox is developed to simulate real time and networked control systems and facilitates co-simulation of controller task execution in the real-time kernels and network transmissions. The plant and controller communicate with each other over CSMA/AMP (control area network) using the TrueTime functional blocks. The plant sends data using *ttSendMsg* and *ttGetMsg* blocks. The controller is implemented using *TrueTime Kernel* that is not only capable to transceive the analog data but can also communicate with other nodes over the network. The TrueTime kernel supports the multi-task execution and their scheduling on the basis of priorities and deadlines.

The following state space representation of a discrete time LTI system with the parametric uncertainties is considered:

$$
A = \begin{bmatrix} 0.8 & -0.25 & 0 & 1 \\ 1 & 0 & 0 & 0 \\ -.8 & 0.5 & 0.2 & -1.03 \\ 0 & 0 & 1 & 0 \end{bmatrix}, B_1 = \begin{bmatrix} 0.5 \\ 0 \\ 0 \\ 0 \end{bmatrix}, B_2 = \begin{bmatrix} 0.1 & 0.1 \\ 0.5 & 0 \\ 0.6 & 0.7 \\ 0 & 0.3 \end{bmatrix}
$$

$$
C_1 = \begin{bmatrix} 0.8875 & -0.1404 \end{bmatrix}, C_2 = \begin{bmatrix} 4.5 & -4.5 & 0 & 2 \\ 4.5 & -4.5 & 0 & 2 \end{bmatrix}, D_{11} = 0.4
$$

$$
D_{12} = \begin{bmatrix} 0.4 & 0.5 \end{bmatrix}, E_1 = \begin{bmatrix} 0.01 \\ 0.09 \\ 0.02 \\ 0.04 \end{bmatrix}, E_2 = 0.01, H_1 = \begin{bmatrix} 0.05 & 0.02 & .03 & .04 \end{bmatrix}
$$

$$
H_2 = \begin{bmatrix} 0.07 & 0.04 \end{bmatrix}, H_3 = 0.04.
$$
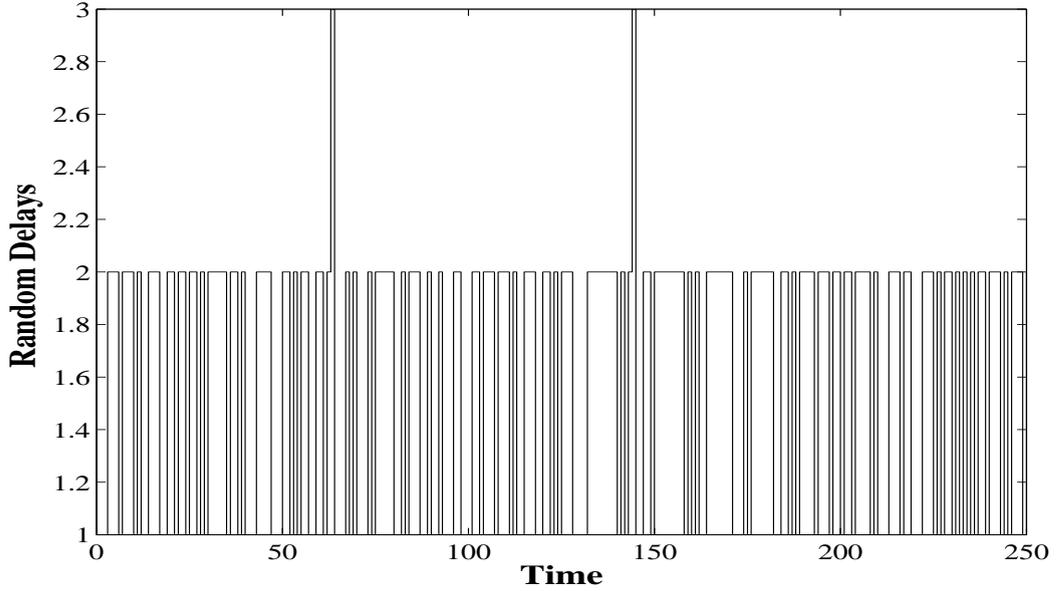
FIGURE 6.2: Random modes

The TrueTime simulator only supports local area networked control systems (LANCSs) and ignores time delays, therefore the time delay block is introduced separately. A Markov chain, that takes values from a finite set $\mathcal{S} = \{1, 2, 3\}$, is used to model the random delays. Each value of the Markov chain corresponds to 1, 2 and 3 second delays, respectively. It is shown in Figure 6.2. The transition probability matrix governing the modes of Markov chain is obtained through various experiments performed on a wireless network:

$$P_\tau = \begin{bmatrix} 0.4206 & 0.5794 & 0 \\ 0.4206 & 0.5705 & 0.0089 \\ 0.4206 & 0.5705 & 0.0089 \end{bmatrix}$$

In this example, individual quantizers are used to quantize each control input and system output. The quantization densities are set using equations (6.5) and (6.10) as:

$$\rho_1 = \begin{bmatrix} 0.9019 & 0 \\ 0 & 0.8981 \end{bmatrix}, \; \rho_2 = \begin{bmatrix} 0.8705 & 0 \\ 0 & 0.8508 \end{bmatrix}$$

where ρ_1 and ρ_2 are the quantization densities at the system outputs and the control inputs, respectively. The $\mathcal{H}_\infty$ performance objective γ, against non-parametric uncertainties, is set 0.5. For the closed-loop system, controller matrices are obtained using MATLAB LMI Control Toolbox and the cone complementary algorithm, outlined in the

previous section:

$$A_c(1) = \begin{bmatrix} 0.0384 & 0.4677 & -0.0631 & 0.7252 \\ 0.2325 & 0.2524 & 0.5041 & 0.3259 \\ 0.1614 & -0.6649 & -0.3427 & -0.2896 \\ 0.3370 & -0.1594 & 0.5081 & -0.0591 \end{bmatrix}, B_c(1) = \begin{bmatrix} -47.1536 & 47.314 \\ 7.1768 & -7.0820 \\ -4.8139 & 4.6236 \\ -20.3464 & 20.3152 \end{bmatrix}$$

$$C_c(1) = \begin{bmatrix} -0.6050 & -0.3737 & 0.9579 & 0.9986 \\ 0.5994 & -0.0367 & -1.5576 & -0.3952 \end{bmatrix}$$

$$A_c(2) = \begin{bmatrix} 0.0384 & 0.4675 & -0.0638 & 0.7154 \\ 0.2416 & 0.2223 & 0.7115 & 0.2277 \\ 0.2601 & -0.6241 & -0.3428 & -0.2906 \\ 0.3391 & -0.1504 & 0.5077 & -0.0501 \end{bmatrix}, B_c(2) = \begin{bmatrix} -43.1521 & 47.0001 \\ 11.0768 & -5.0210 \\ -7.0149 & 5.1246 \\ -19.1422 & 19.0111 \end{bmatrix}$$

$$C_c(2) = \begin{bmatrix} -0.6051 & -0.3123 & 0.9435 & 0.9666 \\ 0.5004 & -0.0361 & -1.1271 & -0.3763 \end{bmatrix}$$

$$A_c(3) = \begin{bmatrix} 0.0380 & 0.4670 & -0.0638 & 0.7258 \\ 0.2322 & 0.2523 & 0.5045 & 0.3257 \\ 0.1613 & -0.6549 & -0.5627 & -0.2566 \\ 0.3670 & -0.1584 & 0.5061 & -0.0891 \end{bmatrix}, B_c(3) = \begin{bmatrix} -47.1536 & 47.314 \\ 7.1568 & -7.0824 \\ -4.8339 & 6.6216 \\ -20.3454 & 22.3152 \end{bmatrix}$$

$$C_c(3) = \begin{bmatrix} -0.6095 & -0.3734 & 0.9999 & 0.9965 \\ 0.5966 & -0.0364 & -1.5506 & -0.3987 \end{bmatrix}$$

The proposed control design efficiently stabilizes the system states, as shown in Figure 6.3. The disturbance matrix B_1 introduces uncertainty in the state x_1 that acquires stochastic stability. It is shown in Figure 6.3(a). All other system states are not affected by the disturbance and achieve asymptotic stability. The obtained $\mathcal{H}_\infty$ performance is 0.008, as shown in Figure 6.4 that is much less than prescribed value of γ.

Remark 6.4.1. Single quantizer is a special case of multiple quantizers that combines multiple outputs together in a packet, and then quantizes. However, it is not feasible in the NCSs environment, because each sensor/actuator is considered as a separate node, hence requires a separate quantizer. Secondly, it is already proven that the infimum quantization density for the multiple quantizers is the same as for the single quantizer [88]. Similarly, NCSs are meant for the scenarios where it is infeasible to deploy a controller near the plant location and the same is the case for a centralized decoder. Therefore the essence of the NCSs lies in the fact that every output should be quantized and transmitted separately without a centralized decoder. Moreover, the multiple

(a) State x_1

(b) State x_2

(c) State x_3

(d) State x_4
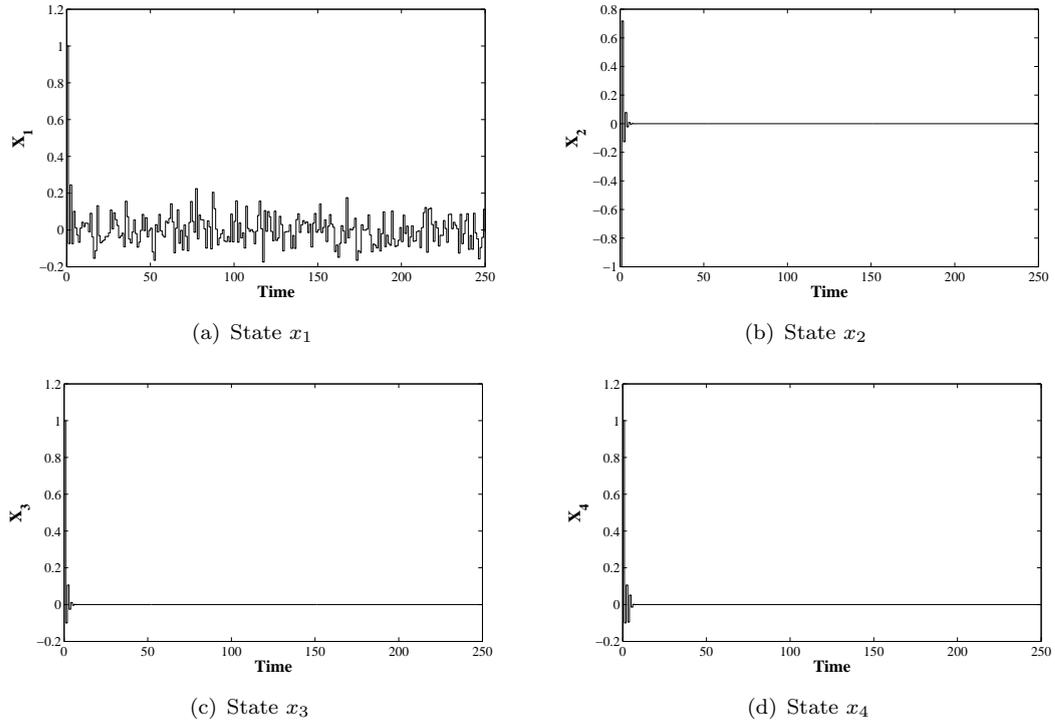
FIGURE 6.3: System states
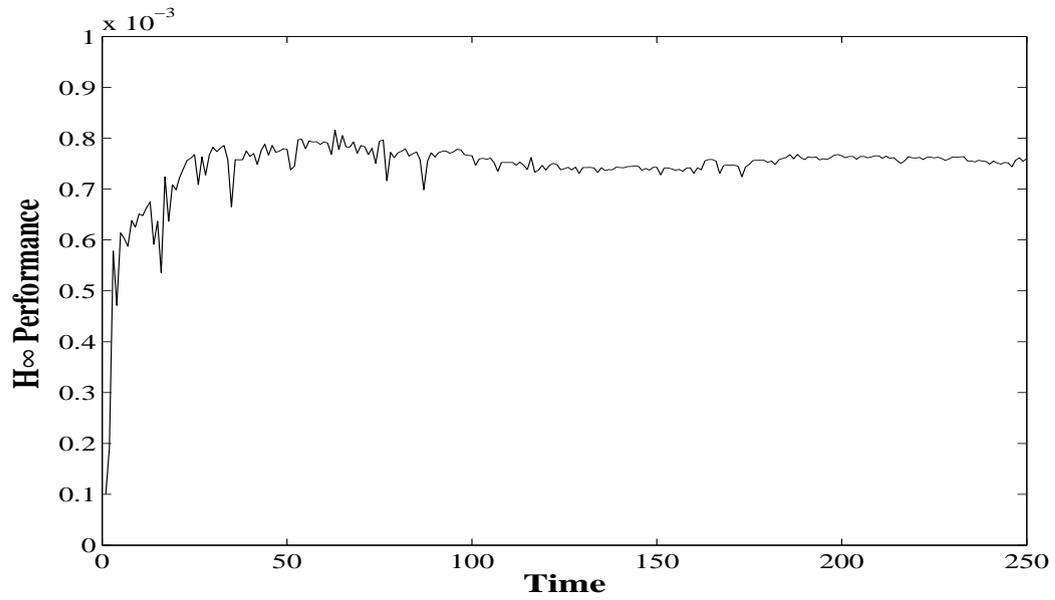
FIGURE 6.4: $\mathcal{H}_\infty$ performance of output feedback controller with multiple quantizers

quantizers give leverage to use different quantization densities for different outputs with respect to network congestion.

6.5   Conclusions

In this chapter, the stability analysis and the controller design for the NCSs with the multiple quantizers, deployed on both plant and controller outputs, are proposed. The quantizers access the network at different times, consequently each quantized signal experiences a different network-induced delay. A finite state Markov chain is used to model these delays. The quantization errors are bounded by a sector bound approach and are characterized by the convex poly-topic uncertainties. A new L-K functional approach is proposed to develop the stability condition. After applying the Schur's complement and the congruence transformation on the stability conditions, a dynamic output feedback controller is achieved in terms of the BMIs. The BMIs are converted into the quasi-convex optimization problem by an iterative algorithm that is solved by the MATLAB LMI toolbox. An example is provided to illustrate the effectiveness of the proposed method by using the SIMULINK based TrueTime toolbox of the MATLAB. It is observed that the proposed design effectively stabilizes the system with multiple quantizers. It is remarked that the essence of the NCSs design lies in the use of a separate quantizer for each signal. By doing this, the quantization densities can be varied according to network load conditions and performance requirements.

Chapter 7

Robust $\mathcal{H}_\infty$ Dynamic Output Feedback Control of NCSs with Limited Information

Quantization effects are inevitable in networked control systems (NCSs). These quantization effects can be reduced by increasing the number of quantization levels. However, increasing the number of quantization levels may lead to network congestion, (i.e., the network needs to transfer more information). In this chapter I investigate the problem of designing a robust $\mathcal{H}_\infty$ output feedback controller for discrete-time networked systems with an adaptive quantization density or limited information. More precisely, the quantization density is designed to be a function of the network load condition that is modelled by a Markov process. A stability criterion is developed by using Lyapunov-Krasovskii(L-K) functional and sufficient conditions for the existence of a dynamic quantized output feedback controller are given in terms of Bilinear Matrix Inequalities(BMIs). An iterative algorithm is suggested to obtain quasi-convex Linear Matrix Inequalities (LMIs) from BMIs. An example is presented to illustrate the effectiveness of the proposed design [109].

7.1   Introduction

With emerging technologies such as shared digital wired and wireless networks, new research areas are opened in the field of NCSs. The NCSs are distributed systems in which the plant, sensors, controller and actuators are spatially distributed and interconnected through the communication networks. This development has greatly improved the modularity, the system flexibility and reduced the processing cost. However, the NCSs also

bring many new challenges for the control system design such as network-induced delays, packet dropouts, quantization errors, variable transmission intervals, network security and other communication constraints.

The issues of network induced time delays and packet dropouts have been considered by many researchers [1, 86, 94, 96, 117–119, 124]. Most of them used the Markov processes to model the randomness of the network-induced delays [1, 96, 118, 119, 124]. The Markov chain takes values in a finite set based on the known transition probabilities. However, the main drawback of the aforementioned papers is that the real communication networks are not able to send the data with infinite precision. In the communication networks the length of each data packet is finite, therefore in order to improve the performance of the NCSs the effect of data quantization must be incorporated into any controller design. In most studies the quantization error is treated as an uncertainty in the stability analysis and robust controllers are designed [121–123]. The size of the uncertainty depends on the quantization density. For a logarithm quantizer, the size of uncertainty can be bounded by a sector bound approach [75].

In [72] it is mentioned that the quantization process is useful in the NCSs . The quantizers with the coarser quantization densities help in reducing the network congestion. Consequently the network-induced delays can be reduced because less information is transmitted. However, the coarser the quantization density the larger the quantization error. Hence, this is a tradeoff between the quantization error and the network congestion or the network-induced delay. In this chapter the quantization density is designed to be a function of the network load condition that is modelled by a Markov process. More precisely, when the network load is heavy a coarser quantization density is used so that less information should be transmitted. While in the lighter network load case a finer quantization density is selected. In doing so the network load condition can be maintained. Based on the Lyapunov-Krasovskii functional approach stability criterion and the design procedures for an output feedback with an adaptive quantization density are given in terms of the BMIs which are then converted into the quasi-convex LMIs to be solved by using an iterative cone complementarity algorithm [127]. The simulation example is provided to verify the proposed design.

The main contributions of the chapter can be summarized as follows:

- To ease the network congestion, the quantization density is designed to be a function of the network load which is modelled by a Markov process. To the best of the authors' knowledge, this issue has never been investigated previously

- The controllers are parameterized by the BMIs. Its dimensions depend upon the dimension of the state variable of the open loop system and it is independent of

the number of the modes on the Markov chain. This decreases the computational burden and it has not been formally investigated in the NCSs.

This chapter is organized into five sections. In Section 7.2, system description, quantization error modelling, packet dropouts and problem formulation are presented. Main results for the stability criterion and the controller synthesis are given in Section 7.3. Section 7.4 contains simulation results to prove the validity of the proposed theorems. Conclusions are given in Section 7.5.

7.2   System Description and Definitions

A simple networked control system is shown in Figure 7.1.   The class of uncertain
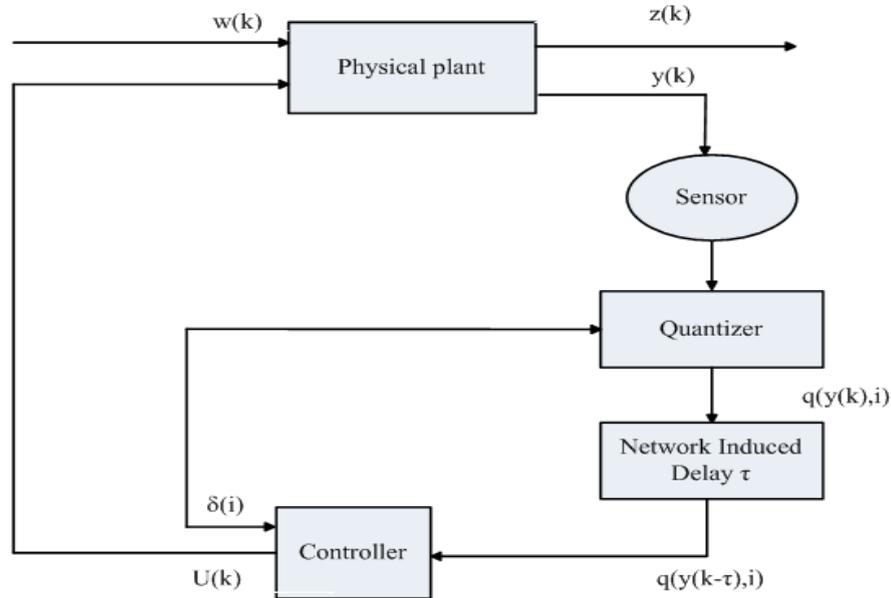
FIGURE 7.1: Layout of networked control systems with an adaptive quantizer

discrete-time linear systems under consideration is described by the following model:

$$
\begin{aligned}
x(k+1) &= [A + \Delta A(k)]x(k) + [B_1 + \Delta B_1(k)]w(k) + [B_2 + \Delta B_2(k)]u(k), \quad x(0) = 0 \\
z(k) &= [C_1 + \Delta C_1(k)]x(k) + [D_{11} + \Delta D_{11}(k)]w(k) + [D_{12} + \Delta D_{12}(k)]u(k) \\
y(k) &= C_2 x(k)
\end{aligned}
\tag{7.1}
$$

where $x(k) \in \Re^n, u(k) \in \Re^m, z(k) \in \Re^{m_1}, y(k) \in \Re^{m_2}$ are the state, input, controlled output and measured output, respectively. $w(k) \in \Re^{m_3}$ is the disturbance that belongs to $\mathcal{L}_2[0, \infty)$, the space of square summable vector sequence over $[0, \infty)$. The matrices A, B_1, B_2, C_1, D_{11}, D_{12} and C_2 are known matrices with the appropriate dimensions. The

matrix functions $\Delta A(k)$, $\Delta B_1(k)$, $\Delta B_2(k)$, $\Delta C_1(k)$, $\Delta D_{11}(k)$ and $\Delta D_{12}(k)$ represent the time-varying uncertainties and satisfy conditions given in the assumption 3.2.1.

Quantizer Modelling and Description:

The quantization process is useful in NCSs design. Network congestion and network-induced time delay can be reduced by using a coarser quantizer. Hence, by adjusting the quantization density, the network load capacity can be sustained. In this chapter, the quantization density is designed to be a function of the network load condition.

Let $\{r_k, k\}$ be a discrete homogeneous Markov chain taking values in a finite set $\mathcal{S} = \{1, 2, \cdots, s\}$, with the following transition probability from mode i at k to mode j at time $k + 1$

$$p_{ij} := \mathbf{Prob}\{r_{k+1} = j | r_k = i\}$$

where $i, j \in \mathcal{S}$.

The quantization density, δ, is described as a finite state Markov process as $\delta = \delta(r_k)$. On the basis of this technique, a network load dependent quantizer is proposed as follows:

$$q(\nu, i) = \begin{cases} \rho^h(i) & \text{if } \frac{1}{1+\delta(i)}\rho^h(i) < \nu \le \frac{1}{1-\delta(i)}\rho^h(i), \ \ \nu > 0, h = 0, \pm1, \pm2, \cdots \\ 0, & \text{if } \nu = 0 \\ -q(-\nu, i) & \text{if } \nu < 0 \end{cases} \tag{7.2}$$

where $0 < \rho(i) < 1$ is the quantization density of $q(\cdot, \cdot)$, and $\delta(i)$ is related to $\rho(i)$ by

$$\delta(i) = \frac{1 - \rho(i)}{1 + \rho(i)} \tag{7.3}$$

The associated quantized set $\mathcal{U}$ is given by

$$\mathcal{U} = \left\{ \pm\rho^h(i), h = 0, \pm1, \pm2, \cdots \right\} \bigcup \{0\}. \tag{7.4}$$

Now defines the quantization error as

$$e(k, i) = q(v(k), i) - v(k) = \Delta_q(k, i)v(k), \tag{7.5}$$

where $v(k)$ is signal to be quantized, $q(v(k), i)$ is the quantized signal. It has been shown by [75] that $\Delta_q(k, i) \in [-\delta(i), \delta(i)]$.

Packet Dropouts Modelling:

The measured output $y(k)$, that is used as feedback information for the controller, may not be available all the time due to packet dropouts. To compensate these packet dropouts a stochastic variable following Bernoulli sequence is used. We are interested in the following mode dependent dynamic output feedback control law:

$$
\begin{aligned}
\hat{x}(k+1) &= \alpha(k)\{A_c(i)\hat{x}(k) + B_c(i)q(y(k-\tau(k)),i)\} + (1-\alpha(k))A_{cf}(i)\hat{x}(k) \\
u(k) &= C_c(i)\hat{x}(k)
\end{aligned}
\tag{7.6}
$$

where $A_c(i)$, $A_{cf}(i)$, $B_c(i)$, $C_c(i)$ are controller matrices. $\alpha(k) \in \Re$ is random variable following Bernoulli random distribution:

$$
\alpha(k) = \begin{cases} 1, & \text{if feedback information is available} \\ 0, & \text{Without feedback signal} \end{cases}
$$

Assume that $\alpha(k)$ has probability:

$$
Prob\{\alpha(k) = 1\} = E\{\alpha(k)\} = \alpha, Prob\{\alpha(k) = 0\} = 1 - \alpha
$$

where $0 \leq \alpha \leq 1$ is a constant and

$$
E\{\alpha(k) - \alpha\} = 0, \beta^2 \equiv E\{(\alpha(k) - \alpha)^2\} = \alpha(1 - \alpha)
$$

where $E(\cdot)$ is the expectation operator and β^2 is the variance. $\tau(k)$ is the time varying delay satisfying:

$$
0 < \underline{\tau} \leq \tau(k) \leq \bar{\tau}
$$

where $\underline{\tau}$ and $\bar{\tau}$ are known constants. It is worth mentioning that in NCSs there exist various types of delays such as sensor to controller delays $\tau_{sc}(k)$; controller to actuator delays $\tau_{ca}(k)$ and processing delays $\tau_c(k)$. However, these delays can all be lumped together [83]:

$$
\tau(k) = \tau_{sc}(k) + \tau_{ca}(k) + \tau_c(k)
$$

Using (7.5), the closed-loop system of (7.1) with (7.6) is given as follows:

$$
\begin{aligned}
\zeta(k+1) &= [A_{cl1}(i) + \alpha(k)A_{cl2}(i) + (1-\alpha(k))A_{cl3}(i) + \bar{E}_1 F(k)\bar{H}_1(i)]\zeta(k) + [\bar{B}_1 + \\
&\quad \bar{E}_1 F(k)H_2]w(k) + \alpha(k)B_{cl}(i)(1 + \Delta_q(k,i))\bar{C}_2\zeta(k-\tau(k)) \\
z(k) &= [C_{cl}(i) + E_2 F(k)\bar{H}_1(i)]\zeta(k) + [D_{11} + E_2 F(k)H_2]w(k).
\end{aligned}
\tag{7.7}
$$

where $\zeta(k) = [x(k) \ \hat{x}(k)]^T$ and

$$A_{cl1}(i) = \begin{bmatrix} A & B_2 C_c(i) \\ 0 & 0 \end{bmatrix}, A_{cl2}(i) = \begin{bmatrix} 0 & 0 \\ 0 & A_c(i) \end{bmatrix}$$

$$A_{cl3}(i) = \begin{bmatrix} 0 & 0 \\ 0 & A_{cf}(i) \end{bmatrix}, B_{cl}(i) = \begin{bmatrix} 0 \\ B_c(i) \end{bmatrix}$$

$$\bar{B}_1 = \begin{bmatrix} B_1 \\ 0 \end{bmatrix}, \bar{C}_2 = \begin{bmatrix} C_2 & 0 \end{bmatrix}, \bar{E}_1 = \begin{bmatrix} E_1 \\ 0 \end{bmatrix}$$

$$\bar{H}_1(i) = \begin{bmatrix} H_1 & H_3 C_c(i) \end{bmatrix}, C_{cl}(i) = \begin{bmatrix} C_1 & D_{12} C_c(i) \end{bmatrix}$$

Equation (7.7) can be simplified as:

$$
\begin{aligned}
\zeta(k+1) &= [A_{cl}(i) + \bar{E}_1 F(k) \bar{H}_1(i)]\zeta(k) + [\bar{B}_1 + \bar{E}_1 F(k) H_2]w(k) + \alpha B_{cl}(i)(1 + \Delta_q(k,i)) \\
&\quad \bar{C}_2\zeta(k - \tau(k)) + (\alpha(k) - \alpha)\{(A_{cl2}(i)\zeta(k) - A_{cl3}(i)\zeta(k) + \\
&\quad B_{cl}(i)(1 + \Delta_q(k,i))\zeta(k - \tau(k))\} \\
z(k) &= [C_{cl}(i) + E_2 F(k)\bar{H}_1(i)]\zeta(k) + [D_{11} + E_2 F(k)H_2]w(k).
\end{aligned}
\tag{7.8}
$$

where

$$A_{cl}(i) = A_{cl1}(i) + \alpha A_{cl2}(i) + (1 - \alpha)A_{cl3}(i)$$

The problem under study is formulated as follows:

Problem Formulation:

Given a prescribed $\gamma > 0$ and quantization densities $\rho(i)$, design a dynamic output feedback controller of the form (7.6) such that:

1. The system , given in (7.7) with (7.6) and $w(k) = 0$ is stochastically stable , i.e, there exists a constant $0 < \alpha < \infty$ such that

$$E\left\{\sum_{\ell=0}^{\infty} \zeta^T(\ell)\zeta(\ell)\right\} < \alpha_1 \tag{7.9}$$

for all $\zeta(0)$ and r_0.

2. Under the zero-initial condition, the controlled output $z(k)$ satisfies $\mathcal{H}_\infty$ performance.

$$E\left\{\sum_{k=0}^{\infty} z^T(k)z(k)|r_0\right\} < \gamma^2 \sum_{k=0}^{\infty} w^T(k)w(k) \tag{7.10}$$

for all nonzero $w(k)$.

The following lemma plays an important role in the derivation of the main results.

Lemma 7.2.1. *Let $\bar{x}(k) = x(k+1) - x(k)$ and $\tilde{\zeta}(k) = \Big[\zeta^T(k) \ \ \zeta^T(k-\tau(k)) \ \ w^T(k)$*

$\zeta^T(k)\bar{H}_1^T(i)F^T(k)\zeta^T(k-\tau(k))\bar{C}_2^T\Delta q^T(k) \ \ w^T(k)H_2^TF^T(k)\Big]^T \in \Re^l$, then for any matrices
$R \in \Re^{n\times n}$, $M \in \Re^{n\times l}$ and $Z \in \Re^{l\times l}$, satisfying

$$\begin{bmatrix} R & M \\ M^T & Z \end{bmatrix} \geq 0 \tag{7.11}$$

the following inequality holds:

$$\sum_{i=k-\bar{\tau}}^{k-1} \bar{x}^T(i)R\bar{x}(i) \leq \tilde{\zeta}^T(k)\Big\{\Upsilon_1 + \Upsilon_1^T + \bar{\tau}Z\Big\}\tilde{\zeta}(k) \tag{7.12}$$

where $\Upsilon_1 = M^T[diag\{I,0\} \ \ diag\{-I,0\} \ \ 0 \ \ 0 \ \ 0 \ \ 0]$.

Proof follows the same line of Lemma 3.2.1. ▽▽▽

7.3 Stability Analysis and Controller Synthesis of NCSs with Limited Information

Stability criterion for uncertain discrete-time systems with adaptive quantization densities are given in the following theorem.

Theorem 7.3.1. *For given controller matrices $A_c(i)$, $A_{cf}(i)$, $B_c(i)$ and $C_c(i)$ and quantization densities $\rho(i)$ where $i = 1,\cdots,s$, $\gamma > 0$, if there exist sets of positive-definite matrices $P(i)$, $R_1(i)$, R_1, $W_1(i)$, $W_2(i)$,$W_3(i)$,Q, $Z(i)$, and matrices $M(i)$ satisfying the following inequalities:*

$$R_1 > R_1(i) \tag{7.13}$$

$$\begin{bmatrix} R_1(i) & M(i) \\ * & Z(i) \end{bmatrix} \geq 0 \tag{7.14}$$

$$\Lambda(i) + \Gamma_1^T(i)\tilde{P}(i)\Gamma_1(i) + \Gamma_2^T(i)\bar{\tau}R_1\Gamma_2(i) + \Upsilon_1(i) + \Upsilon_1^T(i) + \bar{\tau}Z(i) + \Xi^T(i)\Xi(i) < 0 \tag{7.15}$$

where

$$
\begin{aligned}
\Gamma_1(i) &= \left[\begin{array}{cccccc} \bar{A}_{cl}(i) & \bar{B}_{cl}(i)\bar{C}_2 & \bar{B}_1 & \bar{E}_1 & \bar{B}_{cl}(i) & \bar{E}_1 \end{array}\right] \\
\Gamma_2(i) &= \left[\begin{array}{cccccc} \bar{A} & 0 & \bar{B}_1 & \bar{E}_1 & 0 & \bar{E}_1 \end{array}\right] \\
\Xi(i) &= \left[\begin{array}{cccccc} C_{cl}(i) & 0 & D_{11} & E_2 & 0 & E_2 \end{array}\right] \\
\Lambda(i) &= diag\Big\{\big((\bar{\tau} - \underline{\tau} + 1)Q + \bar{H}_1^T(i)W_1(i)\bar{H}_1(i) - P(i)\big), (\delta^2(i)\bar{C}_2^T W_2(i)\bar{C}_2 - Q), \\
&\qquad \big(H_2^T W_3(i)H_2 - \gamma^2 I\big), -W_1(i), -W_2(i), -W_3(i)\Big\} \\
\tilde{P}(i) &= \textstyle\sum_{j=1}^s p_{ij}P(j) \\
\Upsilon_1(i) &= M^T(i)[diag\{I,0\} \quad diag\{-I,0\} \quad 0 \quad 0 \quad 0 \quad 0] \\
\bar{A} &= \left[\begin{array}{cc} A - I & B_2 C_c(i) \\ 0 & 0 \end{array}\right] \\
\bar{A}_{cl}(i) &= A_{cl}(i) + \beta\{A_{cl2}(i) - A_{cl3}(i)\}, \\
\bar{B}_{cl}(i) &= (\alpha + \beta)B_{cl}(i).
\end{aligned}
$$

$$(7.16)$$

Then the closed-loop system is stochastically stable with the prescribed $\mathcal{H}_\infty$ performance.

Proof: See Appendix 14.

The following theorem provides procedures for designing a quantized output feedback controller.

Theorem 7.3.2. *For given $\gamma > 0$ and quantization densities $\rho(i)$, if there exist positive symmetric matrices $X(i) > 0$, $Y(i) > 0$, $\mathcal{Y}(i) > 0$, $W_1(i)$, $\mathcal{W}_1(i)$, $\mathcal{W}_2(i)$, $W_2(i)$, $W_3(i)$, $\mathcal{Q}$, Q, $N(i)$, $\mathcal{N}(i)$, R_1, $\mathcal{R}_1$, $R_1(i)$, $S(i,j)$, $\bar{Z}(i)$, and matrices $\mathcal{A}(i)$, $\mathcal{A}_f(i)$, $\mathcal{B}(i)$, $\mathcal{C}(i)$, $J(i)$, $\bar{M}(i)$ satisfying the following inequalities for all $i, j \in \mathcal{S}$:*

$$R_1 > R_1(i) \tag{7.17}$$

$$\left[\begin{array}{cc} N(i) & \bar{M}(i) \\ * & \bar{Z}(i) \end{array}\right] \geq 0 \tag{7.18}$$

$$
\left[\begin{array}{ccccccc}
\bar{\Lambda}(i) + \bar{\Upsilon}_1(i) + \bar{\Upsilon}_1^T(i) + \bar{\tau}\bar{Z}(i) & \bar{\Gamma}_1^T(i) & \bar{\Gamma}_2^T(i) & \bar{\Gamma}_3^T(i) & \bar{\Gamma}_4^T(i) & \bar{\Gamma}_5^T(i) & \bar{\Gamma}_6^T(i) \\
* & -\tilde{\Xi}(i) & 0 & 0 & 0 & 0 & 0 \\
* & * & -\mathcal{R}_1 & 0 & 0 & 0 & 0 \\
* & * & * & -I & 0 & 0 & 0 \\
* & * & * & * & -\mathcal{Q} & 0 & 0 \\
* & * & * & * & * & -\tilde{W}_1(i) & 0 \\
* & * & * & * & * & * & -\tilde{W}_2(i)
\end{array}\right] < 0
$$

$$(7.19)$$

$$\left[\begin{array}{cc} S(i,j) & J^T(i) \\ * & Y(j) \end{array}\right] > 0 \tag{7.20}$$

$$\begin{bmatrix} R_1(i) & \mathcal{T}^T(i) \\ * & \mathcal{N}(i) \end{bmatrix} > 0 \tag{7.21}$$

$$\mathcal{Y}(i)Y(i) = I, \ \mathcal{Q}Q = I, \ \mathcal{N}(i)N(i) = I, \ \mathcal{R}_1 R_1 = I. \tag{7.22}$$

$$\tilde{W}_1(i)W_1(i) = I, \tilde{W}_2(i)W_2(i) = I, \tag{7.23}$$

where

$$\bar{\Lambda}(i) = diag\left[-\begin{bmatrix} Y(i) & I \\ I & X(i) \end{bmatrix}, -Q, \left(H_2^T W_3(i)H_2 - \gamma^2 I\right), -W_1(i), -W_2(i), -W_3(i) \right]$$

$$\bar{\Upsilon}(i) = \bar{M}^T(i)[diag\{I,0\} \ \ diag\{-I,0\} \ \ 0 \ \ 0 \ \ 0 \ \ 0]$$

$$\bar{\Gamma}_1(i) = \begin{bmatrix} \check{A}_{cl}(i) & \check{B}_{cl}(i)\bar{C}_2 & \check{B}_1 & \check{E}_1 & \check{B}_{cl}(i) & \check{E}_1 \end{bmatrix}$$

$$\bar{\Gamma}_2(i) = \sqrt{\bar{\tau}}\begin{bmatrix} \check{A}(i) & 0 & \bar{B}_1 & \bar{E}_1 & 0 & \bar{E}_1 \end{bmatrix},$$

$$\bar{\Gamma}_3(i) = \begin{bmatrix} \check{C}_{cl}(i) & 0 & D_{11} & \bar{E}_2 & 0 & \bar{E}_2 \end{bmatrix}$$

$$\bar{\Gamma}_4(i) = \begin{bmatrix} (\sqrt{\bar{\tau} - \underline{\tau} + 1})T(i) & 0 & 0 & 0 & 0 & 0 \end{bmatrix}$$

$$\bar{\Gamma}_5(i) = \begin{bmatrix} \check{H}_1(i) & 0 & 0 & 0 & 0 & 0 \end{bmatrix}$$

$$\bar{\Gamma}_6(i) = \begin{bmatrix} 0 & \delta(i)\bar{C}_2 & 0 & 0 & 0 & 0 \end{bmatrix}$$

$$\tilde{\Xi}(i) = \begin{bmatrix} -(\tilde{S}(i) - J(i) - J^T(i)) & I \\ I & \tilde{X}(i) \end{bmatrix}, \tilde{X}(i) = \sum_{j=1}^{s} p_{ij}X(j), \tilde{S}(i) = \sum_{j=1}^{s} p_{ij}S(i,j),$$

$$\check{A}_{cl} = \begin{bmatrix} AY(i) + B_2\mathcal{C}(i) & A \\ (\alpha + \beta)\mathcal{A}(i) + (1 - \alpha - \beta)\mathcal{A}_f(i) & \tilde{X}(i)A \end{bmatrix}, \check{B}_{cl} = \begin{bmatrix} 0 \\ (\alpha + \beta)\mathcal{B}(i) \end{bmatrix},$$

$$\check{B}_1 = \begin{bmatrix} B_1 \\ \tilde{X}(i)B_1 \end{bmatrix}, \check{E}_1 = \begin{bmatrix} E_1 \\ \tilde{X}(i)E_1 \end{bmatrix}, \check{A} = \begin{bmatrix} (A - I)Y(i) + B_2\mathcal{C} & A - I \\ 0 & 0 \end{bmatrix},$$

$$\check{C}_{cl}(i) = [C_1Y(i) + D_{12}\mathcal{C}(i) \ \ C_1] \check{H}_1(i) = [H_1Y(i) + H_3\mathcal{C} \ \ H_1],$$

$$T(i) = \begin{bmatrix} Y(i) & I \\ Y(i) & 0 \end{bmatrix} \ and \ \mathcal{T}(i) = \begin{bmatrix} 0 & \mathcal{Y}(i) \\ I & -I \end{bmatrix}$$

Then the closed-loop system is stochastically stable with the prescribed $\mathcal{H}_\infty$ performance. Furthermore, a suitable controller is given as follows

$$
\begin{aligned}
A_c(i) &= \left(\sum_{j=1}^{s} p_{ij} Y^{-1}(j) - \tilde{X}(i) \right)^{-1} \left(\mathcal{A}(i) - \tilde{X}(i)(AY(i) + B_2 \mathcal{C}(i)) \right) Y^{-1}(i) \\
A_{cf}(i) &= \left(\sum_{j=1}^{s} p_{ij} Y^{-1}(j) - \tilde{X}(i) \right)^{-1} \mathcal{A}_f(i) Y^{-1}(i) \\
B_c(i) &= \left(\sum_{j=1}^{s} p_{ij} Y^{-1}(j) - \tilde{X}(i) \right)^{-1} \mathcal{B}(i) \\
C_c(i) &= \mathcal{C}(i) Y^{-1}(i).
\end{aligned}
$$

$$(7.24)$$

Proof: See Appendix 14.

7.4   Simulation Example

Consider the following state space representation of a discrete time LTI system with the parametric uncertainties:

$$
A = \begin{bmatrix} 0.8 & -.25 & 0 & 1 \\ 1 & 0 & 0 & 0 \\ -.8 & 0.5 & 0.2 & -1.03 \\ 0 & 0 & 0.5792 & 0 \end{bmatrix}, \; B_1 = \begin{bmatrix} 0 \\ 0.1 \\ 0 \\ 0.05 \end{bmatrix}, \; B_2 = \begin{bmatrix} 1 \\ 0 \\ 0 \\ 0 \end{bmatrix}
$$

$$
C_1 = \begin{bmatrix} 0 & 0.1 & 0 & 0 \end{bmatrix}, \; C_2 = \begin{bmatrix} 4.5 & -4.5 & 0 & 2 \end{bmatrix},
$$

$$
D_{11} = 0.03, \; D_{12} = 0.05, \; E_1 = \begin{bmatrix} 0.01 \\ 0.05 \\ 0 \\ 0 \end{bmatrix}, \; E_2 = 0.06,
$$

$$
H_1 = \begin{bmatrix} 0.013 & 0.027 & 0 & 0 \end{bmatrix}, \; H_2 = 0.02, \; H_3 = 0.03.
$$

The network load is assumed to be modelled by a Markov chain that takes values from a finite set $\mathcal{S} = \{1, 2, 3\}$ and the transition probability matrix is taken as:

$$
P_\delta = \begin{bmatrix} 0.4205 & 0.5791 & 0.0004 \\ 0.4206 & 0.5705 & 0.0089 \\ 0.4206 & 0.5705 & 0.0089 \end{bmatrix}
$$

The modes 1, 2 and 3 correspond to the light load ($1 \leq \tau(k) \leq 2$), medium load ($2 < \tau(k) \leq 3$) and heavy load ($3 < \tau(k) \leq 4$), respectively. The quantization density for each mode is assumed as $\delta(1) = 0.2$, $\delta(2) = 0.3$ and $\delta(3) = 0.4$. The disturbance

attenuation level $\gamma = 0.9$ is chosen for the design. The Bernoulli stochastic variable α is set as 0.95. By using the MATLAB LMI Control toolbox and the cone complementary algorithm outlined in the previous section, the controller matrices are obtained as follows:

$$A_c(1) = \begin{bmatrix} 0.6800 & -0.0256 & -0.1380 & 0.0738 \\ 1.0000 & -0.00001 & -0.00003 & 0.00002 \\ -0.8000 & 0.5000 & 0.2000 & -1.0300 \\ -0.00001 & 0.00003 & 0.5792 & -0.00009 \end{bmatrix}$$

$$A_{cf}(1) = \begin{bmatrix} 0.2300 & -0.0231 & -0.0382 & 0.0136 \\ 1.0003 & -0.00001 & -0.00003 & 0.00122 \\ -0.7800 & 0.3001 & 0.2000 & -1.0300 \\ -0.00011 & 0.00013 & 0.5792 & -0.00004 \end{bmatrix}$$

$$B_c(1) = 1.0e-004 \times \begin{bmatrix} 0.3073 \\ 0.166 \\ -0.3960 \\ -0.1275 \end{bmatrix}$$

$$C_c(1) = \begin{bmatrix} -0.1200 & 0.2244 & -0.1380 & -0.9262 \end{bmatrix}.$$

$$A_c(2) = \begin{bmatrix} 0.7375 & -0.0232 & -0.1104 & 0.0560 \\ 1.00001 & -0.00004 & -0.00003 & 0.0000 \\ -0.80002 & 0.50003 & 0.20002 & -1.0300 \\ -0.00003 & 0.00002 & 0.5792 & -0.0000 \end{bmatrix}$$

$$A_{cf}(2) = \begin{bmatrix} 0.735 & -0.0212 & -0.1104 & 0.050 \\ 1.002 & -0.0000 & -0.00001 & 0.0100 \\ -0.1800 & 0.5000 & 0.20001 & -1.1300 \\ -0.0210 & 0.0400 & 0.7902 & -0.10000 \end{bmatrix}$$

$$B_c(2) = 1.0e-004 \times \begin{bmatrix} -0.1572 \\ -0.1295 \\ 0.1927 \\ 0.0463 \end{bmatrix}$$

$$C_c(2) = \begin{bmatrix} -0.0625 & 0.2268 & -0.1104 & -0.9440 \end{bmatrix}.$$
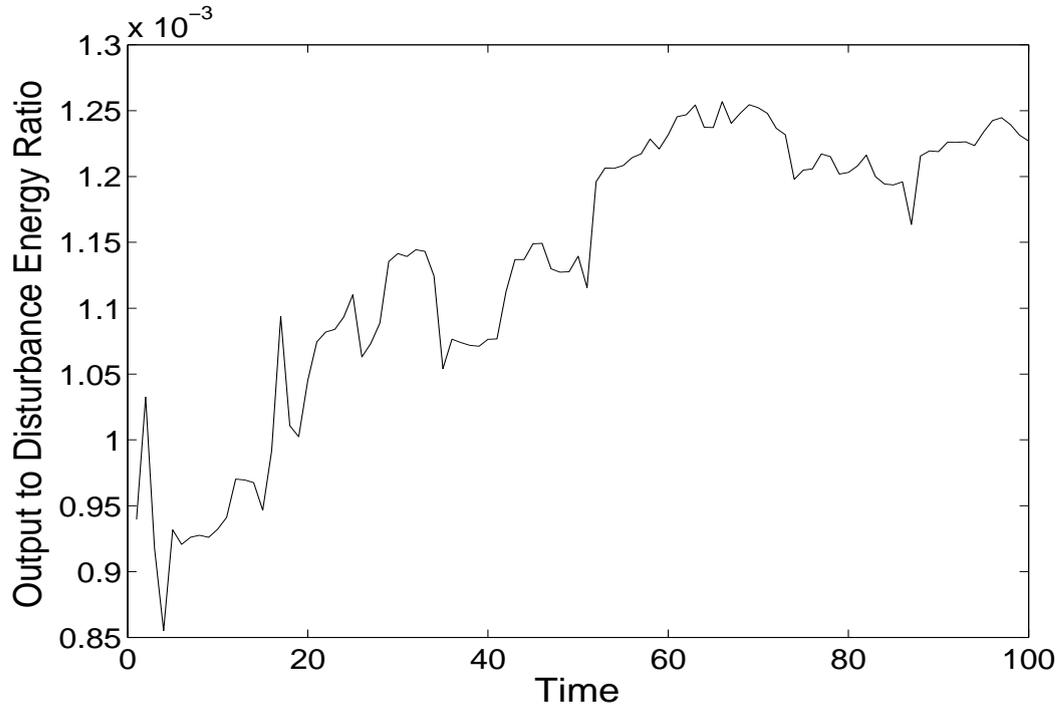
FIGURE 7.2: Energy ratio of regulated output to disturbance

$$
A_c(3) \;=\; \begin{bmatrix}
0.8699 & -0.0231 & -0.0763 & 0.0488 \\
1.0001 & -0.0021 & -0.0000 & 0.00009 \\
-0.8001 & 0.5000 & 0.2000 & -1.03007 \\
-0.0001 & 0.0007 & 0.5792 & -0.00080
\end{bmatrix}
$$

$$
A_{cf}(3) \;=\; \begin{bmatrix}
0.8691 & -0.0211 & -0.0703 & 0.0488 \\
1.0002 & -0.0003 & -0.0000 & 0.0000 \\
-0.8004 & 0.5002 & 0.2000 & -1.0300 \\
-0.0005 & 0.0001 & 0.212 & -0.0000
\end{bmatrix}
$$

$$
B_c(3) \;=\; 1.0e-004 \times \begin{bmatrix}
-0.1794 \\
-0.1105 \\
0.2231 \\
0.0433
\end{bmatrix}
$$

$$
C_c(3) \;=\; \begin{bmatrix} 0.0699 & 0.2269 & -0.0763 & -0.9512 \end{bmatrix}.
$$

Remark 7.4.1. The controller matrices are obtained after five iterations. Figure 7.2 shows the ratio of the regulated output energy to the disturbance input noise energy. It can be seen that the ratio of the regulated output energy to the disturbance input noise energy is about 1.25×10^{-3} that is less than the prescribed level 0.9. Figure 7.3 shows the change of modes in the Markov chain. The mode transition is governed by the
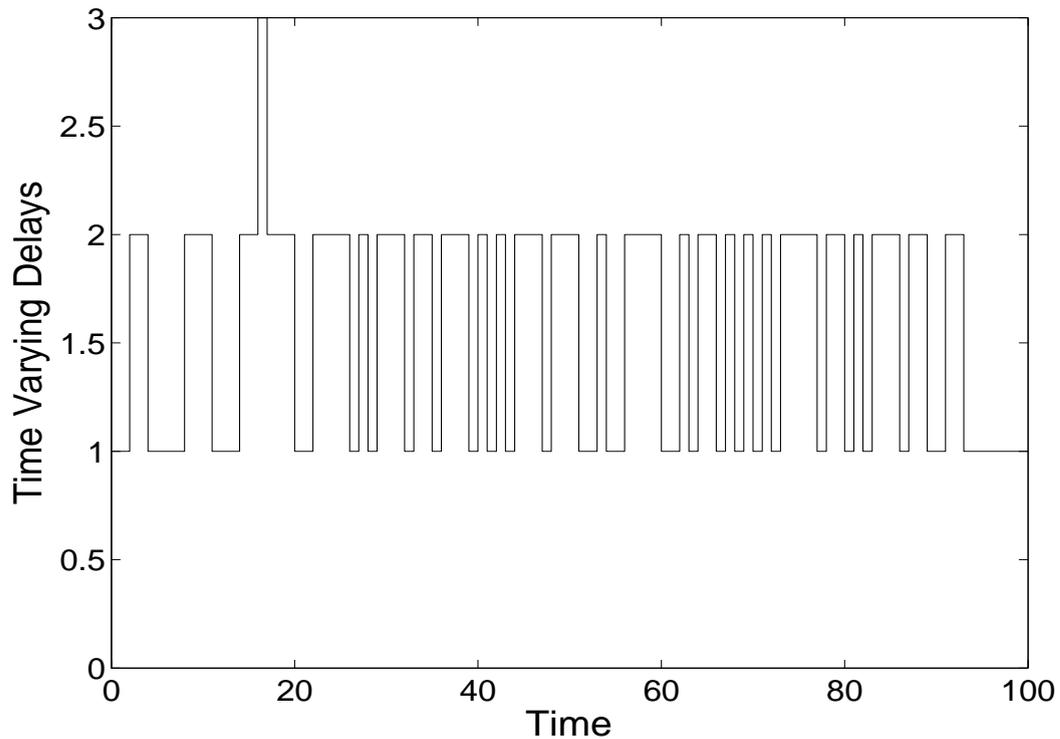
FIGURE 7.3: Random modes

transition probability matrix P_δ. The system states are shown in Figure 7.4. If a design for a fixed quantization density is intended, then the quantization density should be $\delta = 0.4$ that corresponds to the quantization density used in the heavy load conditions. It means that if the quantization density is fixed and the network loads are ignored then the design will be for the worst network load conditions. Moreover, no solution can be found using Theorem 7.3.2 with a fixed quantization density. This concludes that the proposed design is less conservative.

7.5 Conclusions

A novel method for designing a robust $\mathcal{H}_\infty$ output feedback control for the discrete-time NCSs with an adaptive quantization density or the limited information is developed. The quantization density is designed to be a function of the network load condition which is modelled by a Markov chain. The Bernoulli random distribution is used to model the packet dropouts in the network. After incorporating all the constraints appropriately, the robust stability criterion and the controller design are provided. The resultant controller gains were adaptive due to the adaptive quantization densities. The design procedures for a robust $\mathcal{H}_\infty$ quantized observer based output feedback controller are given in terms

(a) State (x_1)

(b) State (x_2)

(c) State (x_3)

(d) State (x_4)
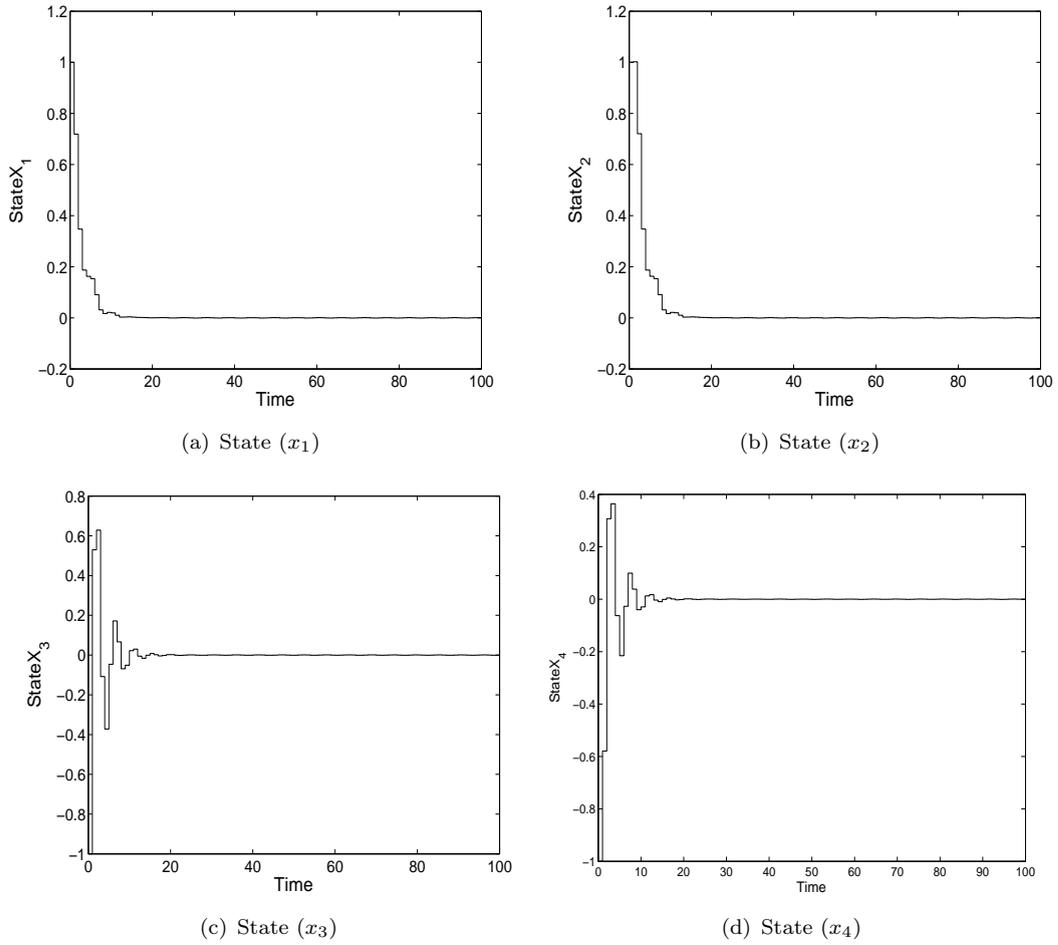
FIGURE 7.4: System states

of the BMIs. A cone complementarity algorithm is suggested for achieving the quasi-convex LMIs from the BMIs. The simulation example to stabilize a discrete LTI system with the help of the proposed design, is presented at the end. The simulation results show that by changing the quantization densities, an upper bound on the network load or the time delays is achieved.

Chapter 8

Stability Analysis of Distributed Event Triggered NCSs with Packet Dropouts

This chapter provides the stability criteria, with $\mathcal{H}_\infty$ performance, for discrete-time networked control systems with decentralized event-triggered mechanism on both system inputs and outputs. The conditions for minimum inter-event time are also provided. A novel event generation criterion is provided which states that an event will be generated when the difference between the current value and previously transmitted value increased from weighted current value, accumulated error and an additional positive threshold. Impulsive system description is used to represent discrete LTI systems as event triggered systems. Furthermore the system incorporates modeling of random packet dropouts. The proposed design is verified by a simulation example that considers various cases such as validation of stability criteria, effects of disturbance, ET parameters and packet dropouts on system stability and $\mathcal{H}_\infty$ performance.

8.1   Introduction

Stability analysis and controller synthesis of the control systems with equidistant or time-triggered (TT) sampling is comparatively easy due to well developed techniques, available in the literature [3]-[12]. However, this approach is a waste of communication resources when the system is stable around its equilibrium point and is not affected by any disturbance. To cater for this issue, a state of the art sampling technique called event-triggered (ET) sampling, can be deployed to execute a task on need basis instead of elapse of a given time. Therefore this technique is called 'sampling on demand'.

Although advantages of the ET sampling mechanism are obvious, however few formal design methods are proposed so far. One of the approaches is an impulsive control action performed on the first order stochastic systems to reset state when it exceeds a minimum threshold [159, 160]. Another approach is used in an open-loop system with prediction of states. Control input is applied to the system if states deviate from a given threshold [161, 161, 162]. An emulation based approach is proposed in [164] where controller and ET mechanisms are designed separately. Few ET mechanisms used to generate events are: 1) when plant state is larger than a given threshold, 2) when the difference between plant current state and previously transmitted state crosses a prescribed threshold, and 3) absolute difference between plant current state and previously transmitted state crosses a threshold.

Two types of the ET mechanisms are: 1) centralized, and 2) distributed. In the first type, conditions to generate events require information from all the systems inputs and outputs on the same time. It is not a feasible approach in NCSs framework, where inputs and outputs are considered network nodes and are spatially apart from each other. In the distributed ET mechanism events are generated on the basis of local information only, and are suitable for NCSs. Stability analysis of an output feedback case is proposed for continuous system with $\mathcal{L}_\infty$ gain and distributed ET mechanism in [44]. A lower bound on minimum inter-event time and upper bound on the number of events are also provided. The results of [44] are extended to discrete-time NCSs in this design. A distributed ET mechanism is proposed for discrete-time NCSs with packet dropouts. Novel and more flexible ET conditions are proposed for the first time. In the proposed mechanism the next event is generated when the norm of error (difference between current and previously transmitted data) violates a particular value. This value depends on norm of current states, a prescribed constant and previously accumulative error. Packet dropouts are incorporated in forward and backward links. Two mutually independent Bernoulli distributions are used to model the dropouts. Stability analysis is performed for ET distributed NCSs, represented as impulsive systems. Main contributions of the chapter are summarised as follows:

- A distributed ET based control is proposed for discrete-time systems with $\mathcal{H}_\infty$ performance

- A new and more flexible event generation mechanism is proposed for the first time

- An impulsive system representation is proposed for ET based distributed NCSs

- Packet Dropouts are modelled and compensated in the proposed design

- Stability analysis is performed and presented in terms of LMIs

- A lower bound on minimum inter-event instance is calculated

- Effect of the packet dropouts is analyzed in terms of $\mathcal{H}_\infty$ performance.

8.2 System Description and Definitions

A class of discrete-time linear systems is described by the following model:

$$
\begin{aligned}
x(k+1) &= Ax(k) + B_1 w(k) + B_2 \bar{u}(k), \quad x(0) = 0 \\
z(k) &= C_1 x(k) + D_{11} w(k) \\
y(k) &= C_2 x(k)
\end{aligned}
\tag{8.1}
$$

where $x(k) \in \Re^n, \bar{u}(k) \in \Re^m, z(k) \in \Re^{m_1}, y(k) \in \Re^{m_2}$ are the state, event-based input, controlled output and measured output, respectively. $w(k) \in \Re^{m_3}$ is disturbance that belongs to $\mathcal{L}_2[0, \infty)$, the space of square summable vector sequence over $[0, \infty]$. The matrices A, B_1, B_2, C_1, D_{11}, D_{12} and C_2 are of known dimensions.

A dynamic output feedback controller of the following form is proposed:

$$
\begin{aligned}
\hat{x}(k+1) &= A_c \hat{x}(k) + B_c \bar{y}(k) \\
u(k) &= C_c \hat{x}(k)
\end{aligned}
\tag{8.2}
$$

where $\hat{x}(k) \in \Re^n$ are the controller states, $\bar{y}(k) \in \Re^{m_2}$ is event-based feedback, and A_c, B_c, C_c are the controller matrices.

In the equidistant sampling, $\bar{u}(k) = u(k)$ and $\bar{y}(k) = y(k)$. In the ET mechanism, $\bar{u}(k)$, $\bar{y}(k)$ are the system input and output, sent over the communication channel after the occurrence of an event. In a distributed control system, inputs and outputs can be gathered as a bunch of nodes N. Each node, $i \in \{1, 2, \cdots, N\}$, transmits its respective information on event-generation instance, $k_{t_i}^i$, with $t_i \in \mathbb{N}$ to update their corresponding values i.e., $\bar{u}(k)$ and $\bar{y}(k)$. This way of data communication can be expressed as:

$$
\bar{d}(k_{t_i+1}^i) = \Omega_i d(k_{t_i}^i) + (I - \Omega_i)\bar{d}(k_{t_i}^i)
\tag{8.3}
$$

where $\bar{d}(k_{t_i}^i) = [\bar{y}(k_{t_i}^i) \quad \bar{u}(k_{t_i}^i)]$, $d(k_{t_i}^i) = [y(k_{t_i}^i) \quad u(k_{t_i}^i)]$, and $\Omega_i = \text{diag}\{\delta_i^1, \cdots, \delta_i^{m+m2}\}$.

For $i = 1, \cdots, N$, and $j = 1, \cdots, m_2$, if the system output $y_j(k)$ is not shared among different nodes, then $\delta_i^j = 1$ at node i and 0 elsewhere in the distributed ET based control. In other words, if an event is generated at node i, then its corresponding value $\bar{d}(k_{t_i}^i)$ will be updated only, and all other values will remain as they are. In addition to this, $1 \geq \sum_{i=1}^N \delta_i^j > 0$, which means that each sensor and actuator should be at least in one node. Without loss of generality, it is assumed that $\bar{d}(0) = d(0)$, and

data can be transmitted among multiple nodes simultaneously. It is also assumed that previous information will be used and rate of change will be zero in between events. Mathematically:

$$\Delta \bar{d}(k_{t_i}^i) = 0 \text{ for all} \quad k \in \Re_+ \setminus \left[\bigcup_{i=1}^{n} \{k_{t_i}^i | t_i \in \mathbb{N}\} \right] \tag{8.4}$$

On the other hand, sampled data mechanism send data at equidistant instances i.e., $k_{t_i+1}^i = k_{t_i}^i + \hbar$, with $\hbar > 0$ and is fixed.

The transmitted signal, $\bar{d}(k_{t_i}^i)$, may be missed due to packet dropouts. To compensate the packet dropouts on both system inputs and outputs, stochastic and mutually independent variables $\alpha_1(k)$ and $\alpha_2(k)$ are proposed. Both variables follow separate Bernoulli random distribution. Consider $\alpha(k) = \text{diag}\{\alpha_2(k), \alpha_1(k)\}$ with following statistical properties:

$$\alpha(k) = \begin{cases} 1, & \text{if data is transmitted over the network} \\ 0, & \text{if data is dropped over the network} \end{cases} \tag{8.5}$$

Assume that $\alpha(k)$ has probability:

$$Prob\{\alpha(k) = 1\} = E\{\alpha(k)\} = \alpha, Prob\{\alpha(k) = 0\} = 1 - \alpha$$

where $0 \leq \alpha \leq 1$ is a constant and

$$E\{\alpha(k) - \alpha\} = 0, \beta^2 \equiv E\{(\alpha(k) - \alpha)^2\} = \alpha(1 - \alpha)$$

where $E(\cdot)$ is the expectation operator and β^2 is the variance.

By applying (8.5) on the (8.2), following dynamic output feedback controller is obtained:

$$\begin{aligned} \hat{x}(k+1) &= A_c \hat{x}(k) + \alpha_1(k) B_c \bar{y}(k) + (1 - \alpha_1(k)) B_c \bar{y}(k-1) \\ u(k) &= C_c \hat{x}(k) \end{aligned} \tag{8.6}$$

In the case of packet dropout, previous value of $\bar{y}(k)$, stored in the controller buffer, will be used.

On the controller to actuator transmission link, the stochastic variable $\alpha_2(k)$ is used to model packet dropouts. After incorporating packet dropout compensation, (8.1) can be

rewritten as:

$$
\begin{aligned}
x(k+1) &= Ax(k) + B_1 w(k) + \alpha_2(k) B_2 \bar{u}(k) + (1 - \alpha_2(k)) B_2 \bar{u}(k-1), \quad x(0) = 0 \\
z(k) &= C_1 x(k) + D_{11} w(k) \\
y(k) &= C_2 x(k)
\end{aligned}
\tag{8.7}
$$

In [44], ET conditions are depended on the norm of the current value and a constant. However, in our design more flexible conditions are provided. The proposed conditions not only depend on the current value and constant but previously accumulated error as well. Mathematically, proposed ET mechanism is represented as follows:

$$
k^i_{t_i+1} = \inf\{ k > k_{t_i} | \quad ||e_{\jmath_i}(k)||^2 = \sigma_i ||d_{\jmath_i}(k)||^2 + \rho_i ||e_{\jmath_i}(k-1)||^2 + \epsilon_i \}
\tag{8.8}
$$

where $k^i_0 = 0$, $\sigma_i > 0$, $\rho_i > 0$ and $\epsilon_i > 0$. $e_{\jmath_i}(k)$ and $d_{\jmath_i}(k)$ represent vectors, consist of the elements from $e(k)$ and $d(k)$ that are in set $\jmath = \{ j \in \{1, \cdots, m + m_2\} | \delta^j_i = 1 \}$. $e(k)$ is the error induced by ET mechanism:

$$
e(k) = \bar{d}(k) - d(k)
\tag{8.9}
$$

It can be seen from (8.3) and (8.8) that when $||e_{\jmath_i}(k)||^2 \geq \sigma_i ||d_{\jmath_i}(k)||^2 + \rho_i ||e_{\jmath_i}(k-1)||^2 + \epsilon_i$, then data will be transmitted and the corresponding values will be updated. It results in $e_{\jmath_i}(k_{t_i+1}) = 0$ and $e(k_{t_i+1}) = (I - \Omega_i)e(k^i_{t_i})$. The main objective of this work is to find appropriate σ_i, ρ_i and ϵ_i to stabilized system.

In the following we are going to represent discrete-time NCSs as impulsive systems. Impulsive systems can be seen as the combination of discrete-time systems with ET mechanism.

8.2.1   An Impulsive System Representation

An impulsive closed-loop system, with packet dropouts, is described as follows:

$$
\begin{aligned}
x_{cl}(k+1) &= A_{cl} x_{cl}(k) + B_{cl} x_{cl}(k-1) + \tilde{B}_w w(k) \\
z(k) &= C_{cl} x_{cl}(k) + D_{cl} w(k) \quad when \quad \tilde{x} \in \mathcal{D} \tag{8.10} \\
x_{cl}(k^i_{t_i+1}) &= G_{cl_i} \tilde{x}(k^i_{t_i}) \quad\quad when \quad x_{cl}(k) \in \mathcal{I}_i, \quad i \in \{1, ..., N\} \tag{8.11}
\end{aligned}
$$

where $x_{cl}(k) \in \mathcal{X} \subseteq \Re^{nx}$ represents impulsive system states, $w(k) \in \Re^{m_3}$ is the disturbance. The flow and jump dynamics of the system are represented as set $\mathcal{D} \subseteq \Re^{n_x}$, set $\mathcal{I}_i, \subseteq \Re^{n_x}$, where $i \in \{1, ..., N\}$, $\mathcal{X} = \mathcal{D}(\cup^N_{i=1} \mathcal{I}_i)$, and $k^i_{t_i}$ is jump time of the impulsive system. In the following, problem is formulated:

- Flow dynamics of the impulsive system is:

$$
\begin{aligned}
x_{cl}(k+1) &= A_{cl}x_{cl}(k) + B_{cl}x_{cl}(k-1) + \tilde{B}_w w(k) \\
z(k) &= C_{cl}x_{cl}(k) + D_{cl}w(k)
\end{aligned}
\tag{8.12}
$$

where

$$
\begin{aligned}
x_{cl}(k) &\in \Re^{n_x} \\
n_x &= n + n + m_2 + m \\
x_{cl}(k) &= [\tilde{x}^T(k) \quad e^T(k)]^T \\
\tilde{x}(k) &= [x^T(k) \quad \hat{x}^T(k)]^T \\
e(k) &= [\{\bar{y}^T(k_{t_i}) - y^T(k_{t_i})\} \quad \{\bar{u}^T(k_{t_i}) - u^T(k_{t_i})\}]^T
\end{aligned}
$$

$$
\begin{aligned}
A_{cl} &= \begin{bmatrix} \tilde{A} + \tilde{B}_\alpha \tilde{C} & \tilde{B}_\alpha \\ -\tilde{C}\tilde{A} - \tilde{C}\tilde{B}_\alpha\tilde{C} & -\tilde{C}\tilde{B}_\alpha \end{bmatrix}, B_{cl} = \begin{bmatrix} \tilde{B}_{1-\alpha}\tilde{C} & \tilde{B}_{1-\alpha} \\ -\tilde{C}\tilde{B}_{1-\alpha}\tilde{C} & -\tilde{C}\tilde{B}_{1-\alpha} \end{bmatrix}, \\
\tilde{B}_w &= \begin{bmatrix} \tilde{E} \\ -\tilde{C}\tilde{E} \end{bmatrix}, C_{cl} = \begin{bmatrix} C_1 & 0 \end{bmatrix}, D_{cl} = D_{11}
\end{aligned}
$$

and

$$
\begin{aligned}
\tilde{A} &= \begin{bmatrix} A & 0 \\ 0 & A_c \end{bmatrix}, \tilde{B}_\alpha = \begin{bmatrix} 0 & \alpha_2(k)B_2 \\ \alpha_1(k)B_c & 0 \end{bmatrix}, \\
\tilde{B}_{1-\alpha} &= \begin{bmatrix} 0 & (1-\alpha_2(k))B_2 \\ (1-\alpha_1(k))B_c & 0 \end{bmatrix}, \tilde{C} = \begin{bmatrix} C_2 & 0 \\ 0 & C_c \end{bmatrix}, \tilde{E} = \begin{bmatrix} B_1 \\ 0 \end{bmatrix}.
\end{aligned}
$$

- System flow will continue until the following conditions are true:

$$
||e_i(k)||^2 \leq \sigma_i||d_i(k)||^2 + \rho_i||e_i(k-1)||^2 + \epsilon_i
\tag{8.13}
$$

In other words:

$$
\mathcal{D} = \{x_{cl}(k) \in \Re^{n_x} | \{x_{cl}^T(k)Q_i x_{cl}(k) + x_{cl}^T(k-1)R_i x_{cl}(k-1)\} < \epsilon_i \quad \forall i \in 1, \cdots, N\}
\tag{8.14}
$$

where

$$Q_i = \begin{bmatrix} -\sigma_i \tilde{C}^T \Omega_i \tilde{C} & 0 \\ 0 & \Omega_i \end{bmatrix}$$

$$R_i = \begin{bmatrix} 0 & 0 \\ 0 & -\rho_i \Omega_i \end{bmatrix}$$

- In the case of an event node i transmits data and error becomes reset. In ET based distributed control any input or output can be in multiple nodes. Therefore error will be reset according to (8.3) as $e(k_{t_i+1}) = (I - \Omega_i)e(k_{t_i}^i)$, and:

$$\mathcal{I}_i = \{x_{cl}(k_{t_i}^i) \in \Re^{n_x} | \{x_{cl}^T(k_{t_i}^i)Q_i x_{cl}(k_{t_i}^i) + x_{cl}^T(k_{t_i}^i - 1)R_i x_{cl}(k_{t_i}^i - 1)\} \geq \epsilon_i\} \tag{8.15}$$

It is equivalent to

$$x_{cl}(k_{t_i+1}^i) = G_{cl_i} x_{cl}(k_{t_i}^i) \tag{8.16}$$

where

$$G_{cl_i} = \begin{bmatrix} I & 0 \\ 0 & I - \Omega_i \end{bmatrix}$$

It can be revealed from (8.16), that system states remains the same while system inputs and outputs will be reset.

In this chapter ET based NCS is modelled as an impulsive system. Therefore review of some basic stability and $\mathcal{H}_\infty$ results for the impulsive systems are mandatory for the derivation of main results.

Definition 8.2.1. [167] For the impulsive system (8.10) with $w(k) = 0$, suppose there is a compact set $\mathcal{E} \subset \mathcal{X}$:

- $\mathcal{E}$ is stable for the impulsive system, if for each $\infty > \epsilon > 0$ there is $\infty > \varepsilon > 0$, such that $\min_{x^* \in \mathcal{E}} \{||x_{cl}(0) - x^*||\} < \varepsilon$ infers that

$$\min_{x^* \in \mathcal{E}} \{||x_{cl}(k) - x^*||\} < \epsilon \tag{8.17}$$

for $w(k) = 0$

- With $w(k) = 0$, $\mathcal{E}$ is stochastically stable, i.e., there exists a constant $0 < \Pi < \infty$, such that:

$$\min{}_{x^* \in \mathcal{E}} E \left\{ \sum_{\ell=0}^{\infty} x^T(\ell)x(\ell) \right\} - ||x^*|| < \Pi \qquad (8.18)$$

for all $x(0)$

Definition 8.2.2. [23] For the given impulsive system with no disturbance and the compact set $\mathcal{E}$, a function $\mathcal{F} : \mathcal{X} \to \Re$ is Lyapunov candidate function:

- If function $\mathcal{F}$ is positive definite on $(\mathcal{D}(\cup_{i=1}^{N}\mathcal{I}_i)\backslash\mathcal{E} \subset \mathcal{X})$

- If function $\mathcal{F}$ is locally Lipschitz on an open set $\mathcal{O}$ with $(\mathcal{D}\backslash\mathcal{E} \subset \mathcal{O} \subset \mathcal{X})$

- $\lim_{x_{cl} \to \mathcal{E}, x_{cl} \in \mathcal{X}} \mathcal{F}(x_{cl}) = 0$

- Subsets of $\mathcal{F}$ are compact on $\mathcal{X}$. By definition, $\{x_{cl} \in \mathcal{X} | \mathcal{F}(x_{cl}) \le c_{\mathcal{F}}\}$ for all $c_{\mathcal{F}} > 0$

To prove the stochastic stability of the set $\mathcal{E}$ of system given in (8.10) following lemma is used.

Lemma 8.2.1. *Consider the system (8.10) with $w(k) = 0$ and the compact set $\mathcal{E} \subset \mathcal{X}$ satisfying $G_i x_{cl}(k_{t_i}^i) \in \mathcal{E}$ $\forall x_{cl}(k_{t_i}^i) \in \mathcal{I}_i \cap \mathcal{E}$ $\forall i = \{1, 2, \cdots, N\}$. Lets assume that minimum inter-event time is one discrete sample time, i.e., $k_{t_i+1}^i = k_{t_i}^i + 1 - k_{t_i}^i$, and the Lyapunov function $\mathcal{F}$ with $w(k) = 0$ exist, such that:*

$$\begin{aligned}
\mathcal{F}(x_{k+1}, k+1) - \mathcal{F}(x_k, k) &< 0 \quad \text{for almost all} \quad x_{cl} \in \mathcal{D} \backslash \mathcal{E} \\
\mathcal{F}(G_i x_{cl}(k_{t_i}^i)) - \mathcal{F}(x_{cl}(k_{t_i}^i)) &\le 0 \text{ for all} \quad x_{cl} \in \mathcal{I}_i \backslash \mathcal{E} \quad \text{for all} \quad i = \{1, 2, \cdots, N\}
\end{aligned}$$

$$(8.19)$$

Then $\mathcal{E}$ will be stochastically stable.

Proof:

The proof is similar to Theorem 20 of [167] that is for hybrid systems. As $x_{cl}(k_{t_i+1}^i) = G_{cl_i} x_{cl}(k_{t_i}^i)$ for all the $x_{cl}(k_{t_i}^i) \in \mathcal{I}_i$, $i \in \{1, ..., N\}$, therefore the second condition, i.e., $\mathcal{F}(g) - \mathcal{F}(x_{cl}(k_{t_i}^i)) < 0$ for all $x_{cl}(k_{t_i}^i) \in \mathcal{I}_i \backslash \mathcal{E}$ and $g \in \{G_{cl_i} x_{cl}(k_{t_i}^i) | x_{cl}(k_{t_i}^i) \in \mathcal{I}_i\}$ can be inferred if the following holds:

$$\mathcal{F}(G_i x_{cl}(k_{t_i}^i)) - \mathcal{F}(x_{cl}(k_{t_i}^i)) < 0 \text{ for all} \quad x_{cl} \in \mathcal{I}_i \backslash \mathcal{E} \quad \text{for all} \quad i = \{1, 2, \cdots, N\} \quad (8.20)$$

As the system is discrete in nature, the positive minimum inter-event time exists, and the system does not show 'zeno behavior'. It renders the equation (8.20) to (8.19) because Lyapunov function $\mathcal{F}$ is decreasing until the equilibrium set $\mathcal{E}$ is reached.

Definition 8.2.3. Under non-zero disturbance and zero initial conditions i.e, $w(k) \neq 0, x_{cl}(0) = 0$, $\mathcal{H}_\infty$ performance parameter can be defined as:

$$\gamma = \inf\{\gamma^2 \in \Re_+ \text{ such that } E\{\sum_{k=0}^\infty ||z(k)||\} \leq \gamma^2 \sum_{k=0}^\infty ||w(k)||\} \qquad (8.21)$$

8.3 Stability Analysis of an Impulsive Control System

In this section stochastic stability criterion is given for the compact set $\mathcal{E}$ of the impulsive system (8.10). In the case of disturbance $w(k)$, $\mathcal{H}_\infty$ performance is obtained with zero initial conditions.

Theorem 8.3.1. *Consider the ET based NCSs given in (8.1) with its representation as an impulsive system (8.10). It is assumed that with all $\tilde{x}(0) \in \mathcal{X}$ and $w(k) \in \mathcal{L}_2[0, \infty)$, if there exists a minimum inter-event time equal to one discrete sample. Consider there exist positive definite matrices $P, S \in \Re^{(n+n) \times (n+n)}$, positive semi-definite matrices U_1 and $U_2 \in \Re^{(n_x) \times (n_x)}$ and scalers $\mu_i, \Pi, \eta, \gamma > 0$ satisfying:*

$$\Gamma_1^T(k)P_{cl}(k)\Gamma_1(k) + \Lambda(k) + \Gamma_2^T(k)\Gamma_2(k) \leq 0 \quad for \ x_{cl} \in \mathcal{D} \ (8.22)$$

$$\tilde{G}_{cl_i}^T P_{cl} \tilde{G}_{cl_i} + diag\{S_{cl} - P_{cl} + \mu_i Q_i, -S_{cl} + \mu_i R_i, 0\} \leq 0 \quad for \ x_{cl} \in \mathcal{I} \ (8.23)$$

where

$$\begin{aligned}
\Gamma_1(k) &= [A_{cl}(k) \quad B_{cl}(k) \quad \tilde{B}_w(k)] \\
\Gamma_2(k) &= [C_{cl}(k) \quad 0 \quad D_{cl}(k)] \\
\Lambda(k) &= diag\Big\{S_{cl} + (\eta - 1)P_{cl} - \sum_{i=1}^N \mu_i Q_i, \ (\eta - 1)S_{cl} - \sum_{i=1}^N \mu_i R_i, -\gamma\Big\} \\
\tilde{G}_{cl_i} &= [G_{cl_i} \quad 0 \quad 0] \\
P_{cl} &= diag\{P, 0\} + U_1, \quad S_{cl} = diag\{S, 0\} + U_2 \qquad (8.24)
\end{aligned}$$

Then

$$\mathcal{E} = \Big\{x_{cl} \in D \cup \Big(\cup_{i=1}^N \mathcal{I}_i\Big) | x_{cl}^T P_{cl} x_{cl} + x_{cl}^T(k-1)S_{cl}x_{cl}(k-1) \leq \sum_{i=1}^N \frac{\mu_i \epsilon_i}{\eta}\Big\} \qquad (8.25)$$

is stochastically stable set for the system given as (8.10) with no disturbance. $\mathcal{H}_\infty$ performance, described in Definition (8.2.3), will be obtained in the case of non-zero disturbance $w(k)$.

Proof:

For $x_{cl} \in \mathcal{D}$:

The system (8.10) can be written as:

$$
\begin{aligned}
x_{cl}(k+1) &= \Gamma_1 \tilde{x}_{cl}(k) \\
z_{cl}(k) &= \Gamma_2 \tilde{x}_{cl}(k)
\end{aligned}
\tag{8.26}
$$

where

$$
\tilde{x}_{cl}(k) = [x_{cl}^T(k) \quad x_{cl}^T(k-1) \quad w^T(k)]^T
$$

Let us consider the following Lyapunov function:

$$
V(x_{cl}(k)) = x_{cl}^T(k) P_{cl} x_{cl}(k) + x_{cl}^T(k-1) S_{cl} x_{cl}(k-1)
\tag{8.27}
$$

First forward difference of $V(x_{cl}(k))$ is given as follows:

$$
\begin{aligned}
V(x_{cl}(k+1)) - V(x_{cl}(k)) &\leq x_{cl}^T(k+1) P_{cl} x_{cl}(k+1) + x_{cl}^T(k) S_{cl} x_{cl}(k) - \\
&\quad x_{cl}^T(k) P_{cl} x_{cl}(k) - x_{cl}^T(k-1) S_{cl} x_{cl}(k-1) \\
\Delta V(x_{cl}(k)) &\leq \tilde{x}_{cl}^T(k) \Gamma_1^T P_{cl}(r_k) \Gamma_1 \tilde{x}_{cl}(k) + x_{cl}^T(k) S_{cl} x_{cl}(k) - \\
&\quad x_{cl}^T(k) P_{cl}(r_k) x_{cl}(k) - x_{cl}^T(k-1) S_{cl} x_{cl}(k-1) \tag{8.28}
\end{aligned}
$$

By adding $\eta V(x_{cl}(k)) - x_{cl}^T(k) \sum_{i=1}^N \mu_i Q_i x_{cl}(k) - x_{cl}^T(k-1) \sum_{i=1}^N \mu_i R_i x_{cl}(k-1)$ on the R.H.S of the equation (8.28), we get:

$$
\Delta V(x_{cl}(k)) \leq \tilde{x}_{cl}^T(k) \{\Gamma_1^T(k) P_{cl}(k) \Gamma_1(k) + \tilde{\Lambda}(k)\} \tilde{x}_{cl}(k)
\tag{8.29}
$$

where $\Gamma_1(k)$ is given in (8.24) and

$$
\tilde{\Lambda}(k) = \operatorname{diag}\left\{ S_{cl} + (\eta - 1)P - \sum_{i=1}^N \mu_i Q_i, \ (\eta - 1)S - \sum_{i=1}^N \mu_i R_i, 0 \right\}
$$

By adding and subtracting $z_k^T z_k$, $\gamma^2 w_k^T w_k$ in the equation (8.29):

$$
\Delta V(x_{cl}(k)) \leq \Gamma_1^T(k) P_{cl}(k) \Gamma_1(k) + \Lambda(k) + \Gamma_2^T(k) \Gamma_2(k) - z_k^T z_k + \gamma^2 w_k^T w_k
\tag{8.30}
$$

where $\Gamma_2(k)$ and $\Lambda(k)$ are given in (8.24).

Using (8.22), we have

$$\Delta V(x_{cl}(k)) \leq -z_k^T z_k + \gamma^2 w_k^T w_k \tag{8.31}$$

Taking expectation and sum from 0 to ∞ on both sides of (8.31) yields

$$E\{V(x_{cl}(\infty))\} - E\{V(x_{cl}(0))\} \leq -E\Big\{\sum_{k=0}^{\infty} z_k^T z_k\Big\} + \gamma^2 \sum_{k=0}^{\infty} w_k^T w_k \tag{8.32}$$

Under zero initial condition, $V(x_{cl}(0)) = 0$, we have

$$E\Big\{\sum_{k=0}^{\infty} z_k^T z_k\Big\} \leq \gamma^2 \sum_{k=0}^{\infty} w_k^T w_k \tag{8.33}$$

That is, Definition (8.2.3) satisfies.

Next, under no disturbance, we need to show that the closed-loop system is stochastically stable. Using condition $w(k) = 0, \forall k \geq 0$ in (8.22), we learn that

$$V(x_{cl}(k+1)) - V(x_{cl}(k)) \leq -\beta \tilde{x}_{cl}^T(k)\tilde{x}_{cl}(k) \tag{8.34}$$

where $\beta = \inf\{\lambda_{\min}[-\mathcal{M}]\}$ with

$$\mathcal{M} = \Gamma_1^T(k)P_{cl}(k)\Gamma_1(k) + \Lambda(k) + \Gamma_2^T(k)\Gamma_2(k) \tag{8.35}$$

Taking expectation and sum from 0 to ∞ on both sides of (8.34) yields

$$
\begin{aligned}
E\{V(x_{cl}(\infty))\} - E\{V(x_{cl}(0))\} &\leq -\beta E\Big\{\sum_{k=0}^{\infty} \tilde{x}_k^T \tilde{x}_{cl}(k)\Big\} \\
&\leq -\beta E\Big\{\sum_{k=0}^{\infty} x_{cl}(k)^T x_{cl}(k)\Big\}
\end{aligned}
\tag{8.36}
$$

Rearranging (8.36), we get

$$
\begin{aligned}
E\Big\{\sum_{k=0}^{\infty} x_{cl}^T(k)x_{cl}(k)\Big\} &\leq \frac{1}{\beta}E\{V(x_{cl}(0))\} - \frac{1}{\beta}E\{V(x_{cl}(\infty))\} \\
E\Big\{\sum_{k=0}^{\infty} x_{cl}^T(k)x_{cl}(k)\Big\} &\leq \frac{1}{\beta}E\{V(x_{cl}(0))\} \\
E\Big\{\sum_{k=0}^{\infty} x_{cl}^T(k)x_{cl}(k)\Big\} - ||x^*|| &\leq \frac{1}{\beta}E\{V(x_{cl}(0))\} \\
&\leq \Pi
\end{aligned}
\tag{8.37}
$$

where $\Pi = \frac{1}{\beta} E\{V(x_{cl}(0))\} < \infty$ and $x^* \in \mathcal{E}$. Hence, we can conclude that the closed-loop system is stochastically stable.

For $x_{cl} \in \mathcal{I}$:

$$x_{cl}(k+1) = G_{cli}x_{cl}(k) \tag{8.38}$$

By using Lyapunov function given in (8.27), we obtain

$$\Delta V(x_{cl}(k)) = \tilde{G}_{cl_i}^T P_{cl} \tilde{G}_{cl_i} + \text{diag}\{S_{cl} - P_{cl}, -S, 0\} \tag{8.39}$$

By adding $\mu_i x_{cl}^T(k)_i Q_i x_{cl}(k) + \mu_i x_{cl}^T(k-1) R_i x_{cl}(k-1)$ on the R.H.S of the equation (8.39), we get (8.23).

Remark 8.3.1. Our proof of Theorem (8.3.1) based on the assumption that, with $w(k) = 0$, the sufficient conditions (8.22) and (8.23) should reduce to a particular Lyapunov candidate function that satisfies Definition (8.2.2). It is proved as follows:

The condition given in (8.22) reduces to:

$$
\begin{aligned}
V(x_{cl}(k+1)) - V(x_{cl}(k)) &\leq -\eta V(x_{cl}(k)) + x_{cl}^T(k) \sum_{i=1}^{N} \mu_i Q_i x_{cl}(k) \\
&\quad + x_{cl}^T(k-1) \sum_{i=1}^{N} \mu_i R_i x_{cl}(k-1) + \gamma \|w(k)\| \\
\Delta V(x_{cl}(k)) &\leq -\eta V(x_{cl}(k)) + \mu_i \sum_{i=1}^{N} \left\{ x_{cl}^T(k) Q_i x_{cl}(k) \right. \\
&\quad \left. + x_{cl}^T(k-1) R_i x_{cl}(k-1) - \epsilon_i \right\} + \sum_{i=1}^{N} \mu_i \epsilon_i + \gamma \|w(k)\|
\end{aligned}
\tag{8.40}
$$

Form (8.14), it can be seen $\left\{ x_{cl}^T(k) Q_i x_{cl}(k) + x_{cl}^T(k-1) R_i x_{cl}(k-1) - \epsilon_i \right\} < 0$, hence:

$$
\begin{aligned}
\Delta V(x_{cl}(k)) &\leq -\eta V(x_{cl}(k)) + \sum_{i=1}^{N} \mu_i \epsilon_i + \gamma \|w(k)\| \\
\Delta V(x_{cl}(k)) &\leq -V(x_{cl}(k)) + \sum_{i=1}^{N} \frac{\mu_i \epsilon_i}{\eta} + \frac{\gamma \|w(k)\|}{\eta}
\end{aligned}
\tag{8.41}
$$

With $w(k) = 0$, (8.41) reduces to

$$\Delta V(x_{cl}(k)) \leq -V(x_{cl}(k)) + \sum_{i=1}^{N} \frac{\mu_i \epsilon_i}{\eta}$$

Similarly, (8.23) reduces to

$$V(G_{cli}x_{cl}(k)) - V(x_{cl}) \leq -v_i\{Q_i x_{cl}(k) + x_{cl}^T(k-1)R_i x_{cl}(k-1) - \epsilon\} - v_i \epsilon \tag{8.42}$$

By using (8.15):

$$\begin{aligned} V(G_{cli}x_{cl}(k)) - V(x_{cl}) &\leq -v_i \epsilon_i \\ V(G_{cli}x_{cl}(k)) - V(x_{cl}) &\leq 0 \end{aligned}$$

$$\tag{8.43}$$

It can be seen that the equations (8.41) and (8.43) results in a Lyapunov function of the following form:

$$\mathcal{F}(x_{cl}) = max\{V(x_{cl}) - \sum_{i=1}^{N} \frac{\mu_i \epsilon_i}{\eta}, 0\} \tag{8.44}$$

$\mathcal{F}(x_{cl})$ is a proper Lyapunov candidate because it satisfies (8.2.2) as:

1. $\mathcal{F}(x_{cl}) = max\{V(x_{cl}) - \sum_{i=1}^{N} \frac{\mu_i \epsilon_i}{\eta}, 0\}$ is positive semi definite on $x_{cl} \in (\mathcal{D}(\cup_{i=1}^{N}\mathcal{I}_i)\backslash\mathcal{E}$, due to (8.22) and (8.23). Hence, $\mathcal{F}(x_{cl})$ is continuous and non-negative $(\mathcal{D}(\cup_{i=1}^{N}\mathcal{I}_i)\backslash\mathcal{E}$.

2. $\mathcal{F}(x_{cl})$ is locally Lipschitz, for all open sets $\mathcal{O}$ with $(\mathcal{D}\backslash\mathcal{E} \subset \mathcal{O} \subset \mathcal{X})$.

3. $\mathcal{F}(x_{cl})$ is zero for all $x_{cl} \in \mathcal{E}$.

4. If all subsets of $\mathcal{F}(x_{cl})$ are compact then all the conditions of Definition (8.2.2) will be fulfilled. To prove the last condition, consider $\mathcal{F}(x_{cl}) \leq \mathcal{C}_\mathcal{F}$ for $\mathcal{C}_\mathcal{F} \geq 0$. In other words:

$$\begin{aligned} \mathcal{F}(x_{cl}) &\leq \mathcal{C}_\mathcal{F} \\ x_k^T P_{cl} x_k + x_{k-1}^T S_{cl} x_{k-1} &\leq \mathcal{C}_\mathcal{F} \\ x_k^T P x_k + x_{cl}^T U_1 x_{cl} + x_{k-1}^T S x_{k-1} + x_{cl}(k-1)^T U_2 x_{cl}(k-1) &\leq \mathcal{C}_\mathcal{F} + \sum_{i=1}^{N} \frac{\mu_i \epsilon_i}{\eta} \\ x_k^T P x_k &\leq \mathcal{C}_\mathcal{F} + \sum_{i=1}^{N} \frac{\mu_i \epsilon_i}{\eta} \end{aligned}$$

$$\tag{8.45}$$

It implies that

$$||x||^2 \leq \mathcal{C}_x \tag{8.46}$$

where $\mathcal{C}_x = (1/\lambda_{min}(P))(\mathcal{C}_\mathcal{F} + \sum_{i=1}^{N} \frac{\mu_i \epsilon_i}{\eta})$.

Considering (8.8), it can be revealed that

$$\begin{aligned} ||e_{\mathcal{J}_i}(k)||^2 &\leq \sigma_i ||d_{\mathcal{J}_i}(k)||^2 + \epsilon_i \\ ||e_{\mathcal{J}_i}(k)||^2 &\leq \sigma_i ||C||^2 \mathcal{C}_x + \epsilon_i \end{aligned} \tag{8.47}$$

Similarly:

$$\begin{aligned} ||x_{cl}||^2 &= ||x||^2 + ||e||^2 \\ ||x_{cl}||^2 &\leq ||x||^2 + \sum_{i=1}^{N} ||e_{\mathcal{J}_i}(k)||^2 \\ ||x_{cl}||^2 &\leq \mathcal{C}_{x_{cl}} \end{aligned} \tag{8.48}$$

where $\mathcal{C}_{x_{cl}} = \mathcal{C}_x + \sum_{i=1}^{N} \sigma_i ||C||^2 \mathcal{C}_x + \epsilon_i$. Equations (8.46-8.48) show that all the subsets of $\mathcal{F}(x_{cl})$ are compact in $\mathcal{X}$.

Since all the conditions are proved, therefore $\mathcal{F}(x_{cl})$ is Lyapunov candidate function and stochastic stability of $\mathcal{E}$ can be guaranteed by satisfying the conditions of Lemma (8.2.1). For all $x_{cl} \in (\mathcal{D}(\cup_{i=1}^{N} \mathcal{I}_i) \backslash \mathcal{E}$, it holds that $x_{cl} > \sum_{i=1}^{N} \frac{\mu_i \epsilon_i}{\eta}$, hence $\mathcal{F}(x_{cl}) = V(x_{cl}) - \sum_{i=1}^{N} \frac{\mu_i \epsilon_i}{\eta}$. Therefore, it can be seen that both conditions of (8.19) are implied by (8.29) and (8.22), respectively. Similarly, $G_{cl} x_{cl} \in \mathcal{E}$ holds for all $x_{cl} \in \mathcal{I}_i \cap \mathcal{E}$ by (8.19).

Remark 8.3.2. It is worth mentioning that feasibility of LMIs (8.22-8.23) depends upon on α, β σ_i and μ_i. On the other hand, ϵ_i has no impact on the feasibility of LMIs, however it determines the size of set $\mathcal{E}$ along with other variables. It can be revealed from the equation (8.13) that ϵ_i controls the size of $\mathcal{E}$, hence controls the number of events. By increasing ϵ_i, set $\mathcal{E}$ expands and results in a lower number of events and vice versa. In our configuration, if ϵ_i reduces to zero then it will result in $\mathcal{E} = \{0\}$, hence asymptotic stability can be achieved in the absence of $w(k)$ and packet dropouts.

8.3.1 Lower Bound on the Inter-event Time

In discrete-time systems, sampling interval $\hbar$ is always a lower bound on inter-event time and no need for mathematical computation, as performed in [44] for continuous case. Therefore, discrete-time systems have advantages over continuous-time systems in ET

based control, however the actual lower bound can be larger than $\hbar$. In the following exact lower bound is calculated for discrete-time ET based NCSs. Consider the impulsive system (8.10), with current state $\tilde{x} = \tilde{x}(k_{t_i}^i)$, where $k_{t_i}^i$ is the time on which the event occurs and state updates. Next state will be updated on $k_{t_i+1}^i = k_{t_i}^i + \hbar k(\tilde{x})$, where

$$k(\tilde{x}) := inf\left\{s \in \mathbf{N}\backslash\{0\}|\tilde{x}^T(k)(A_{cl}^{s-1}G_{cl_i})^T Q(A_{cl}^{s-1}G_{cl_i})\tilde{x}(k) + \tilde{x}^T(k-1)(B_{cl}^{s-1}G_{cl_i})^T R \right.$$
$$\left. (B_{cl}^{s-1}G_{cl_i})\tilde{x}(k-1) \geq \epsilon\right\} \tag{8.49}$$

It states that signal will be updated as $\tilde{x}^T(k_{t_i+1}^i)Q\tilde{x}(k_{t_i+1}^i) + \tilde{x}^T(k_{t_i+1}^i - 1)R\tilde{x}(k_{t_i+1}^i - 1) \geq \epsilon$. However, error will keep on accumulating as $\tilde{x}^T(k_{t_i}^i + 1) = A_{cl}^{s-1}G_{cl_i}\tilde{x}^T(k_{t_i}^i) + B_{cl}^{s-1}G_{cl_i}\tilde{x}^T(k_{t_i}^i)$ provided that control signal is not updated. Consider a minimum inter-event time $k_{min,h}^i = \hbar k_{min,h}^* \geq \hbar$, where

$$k_{min,h}^* := inf\{k(\tilde{x})|\tilde{x} \in \mathbf{R}^n \tilde{x}\} \tag{8.50}$$

It can be calculated as

$$k_{min,h}^* = inf\{s \in \mathbf{N}\backslash\{0\}|\lambda_{max}[(A_{cl}^{s-1}G_{cl_i})^T Q(A_{cl}^{s-1}G_{cl_i}) +$$
$$(B_{cl}^{s-1}G_{cl_i})^T R(B_{cl}^{s-1}G_{cl_i})] > 0\} \tag{8.51}$$

8.4 Simulation Example

In this section, a well known example of batch reactor control [51] is considered to validate the proposed design. A discrete-time version of the linearised continuous batch reactor is obtained by using a zero-order-hold discretization method, with a sampling interval $\hbar = 1$ second. State space representation of the discrete-time plant:

$$A = \begin{bmatrix} 7.2060 & 1.5290 & 5.1940 & -2.4050 \\ -0.7112 & 0.0058 & -0.4827 & 0.3574 \\ 0.2188 & 0.8881 & 0.3241 & 0.6066 \\ -0.5146 & 0.7423 & -0.2028 & 0.8597 \end{bmatrix}, B_2 = \begin{bmatrix} 3.7150 & -6.6490 \\ 1.5780 & 0.5289 \\ 4.9800 & -1.1450 \\ 4.6490 & -0.1119 \end{bmatrix},$$

$$B_1 = \begin{bmatrix} 0.15000.020000 \end{bmatrix}, C_2 = \begin{bmatrix} 1 & 0 & 1 & -1 \\ 0 & 1 & 0 & 0 \end{bmatrix},$$

$$C_1 = \begin{bmatrix} 0.15000.052000 \end{bmatrix}, D11 = .0023.$$

The eigen values of the open-loop unstable system are: [7.3237 1.0654 0.0002 0.0064]. In this example, an emulation based approach is used and a stabilising discrete-time

controller of the form (8.2) is obtained using YALMIP toolbox:

$$
A_c = \begin{bmatrix}
-6.8964 & -1.2357 & -6.9149 & 6.9413 \\
0.8628 & -0.1807 & 0.7651 & -0.9108 \\
-0.5079 & -0.8906 & -0.4473 & 0.3452 \\
0.6170 & -0.7329 & 0.5518 & -0.5300
\end{bmatrix}, B_2 = \begin{bmatrix}
6.9703 & 1.2278 \\
-0.6788 & 0.0301 \\
0.2580 & 0.8682 \\
-0.4489 & 0.7670
\end{bmatrix}
$$

$$
C_c = \begin{bmatrix}
0.1750 & -0.1488 & 0.0856 & -0.2139 \\
1.1703 & 0.1481 & 0.8208 & -0.4766
\end{bmatrix}
$$

Each system input and output are considered in sperate nodes i.e., $\delta_1^1 = \delta_2^2 = \delta_3^3 = \delta_4^4 = 1$, and is zero everywhere else. In this example, we perform simulations for different cases, to analyse the effect of different parameters on system stability and performance:

Case 1: System Stability with ET mechanism

In this case, effect of ET mechanism on the system stability is analyzed in the absence of disturbance i.e., $w(k) = 0$. Parameters of the decentralized ET mechanism (8.8) are considered as: $\sigma_1 = \sigma_3 = \sigma_3 = \sigma_4 \leq 1e^{-3}$, $\rho_1 = \rho_2 = \rho_3 = \rho_4 \leq 1e^{-3}$, and $\epsilon_1 = \epsilon_2 = \epsilon_3 = \epsilon_4 \leq 1e^{-4}$. The controller gains are applied on (8.22) and (8.23) to validate the system stability conditions. The obtained system states, for the initial conditions: $x_{cl}(0) = [10 \quad 10 \quad -10 \quad -10 \quad 10 \quad 10 \quad -10 \quad -10 \quad 0 \quad 0 \quad 0 \quad 0]^T$, are shown in Figure 8.1.

TABLE 8.1: Effect of packet dropouts on number of events

$\alpha_1 \& \alpha_2$	Number of packet dropouts	Number of events
0.99	5	219
0.98	6	227
0.97	8	234
0.96	9	242

By implementing the ET mechanisms on both system inputs and outputs, resource compensation is reduced significantly. It is shown in Figure 8.2 that at one of the system outputs (y_1), 167 events are generated to sent over the communication link for feedback. In the absence of ET mechanism, number of transmissions would be 250. It shows that 33% resource are saved by using the proposed mechanism. It is also concluded from the figure that minimum inter-event time is 1 second, that is equal to one sample time. This value is also equal to exact minimum inter-event time ($k_{min,h}^* = 1$), calculated by using equation (8.51).

(a) State (x_1)

(b) State (x_2)

(c) State (x_3)

(d) State (x_4)
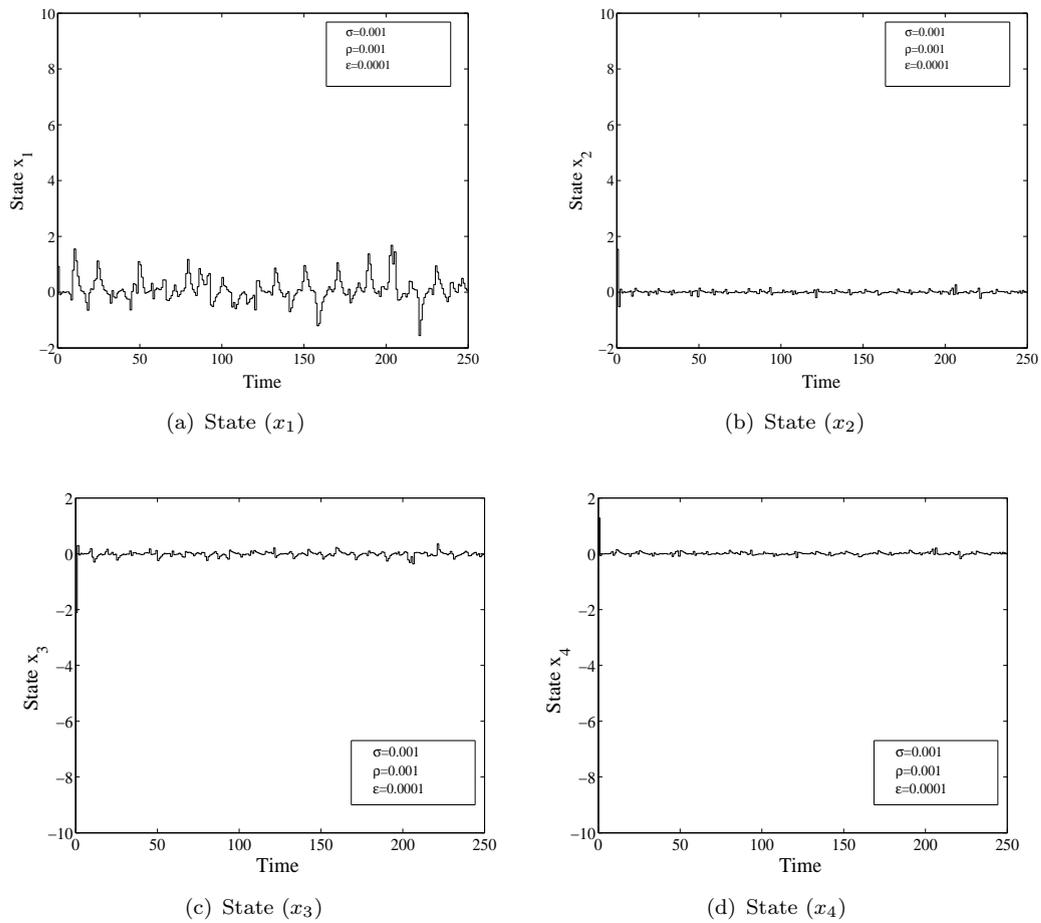
FIGURE 8.1: System states

Effect of packet dropouts are also analyzed on number of events. It can be determined from Table (8.1) that number of packet dropouts results in the increase of number of the events that must be transmitted, as a feedback, for the system stability.

Case 2: Effect of ϵ on stability region (set $\mathcal{E}$)

By equation (8.13), it can be determined that ϵ determines the size of the set $\mathcal{E}$. In this case, effect of the ϵ on the stability region is determined by using simulations. It is shown in Figure 8.3 that size of the set $\mathcal{E}$ increases with increase in the ϵ.

Case 3: Effect of noise on number of events

Response of the system is simulated with zero initial conditions, no packet dropouts and a disturbance $w(k)$ acting on the system. It can be observed from Figure 8.4 that number of events will be almost equal to zero when the system is stable and no noise is acting on the system (see time steps $k \in \{0, 150\}$, no events are generated). Outputs of the plant and controller only have to be transmitted when disturbances are acting on
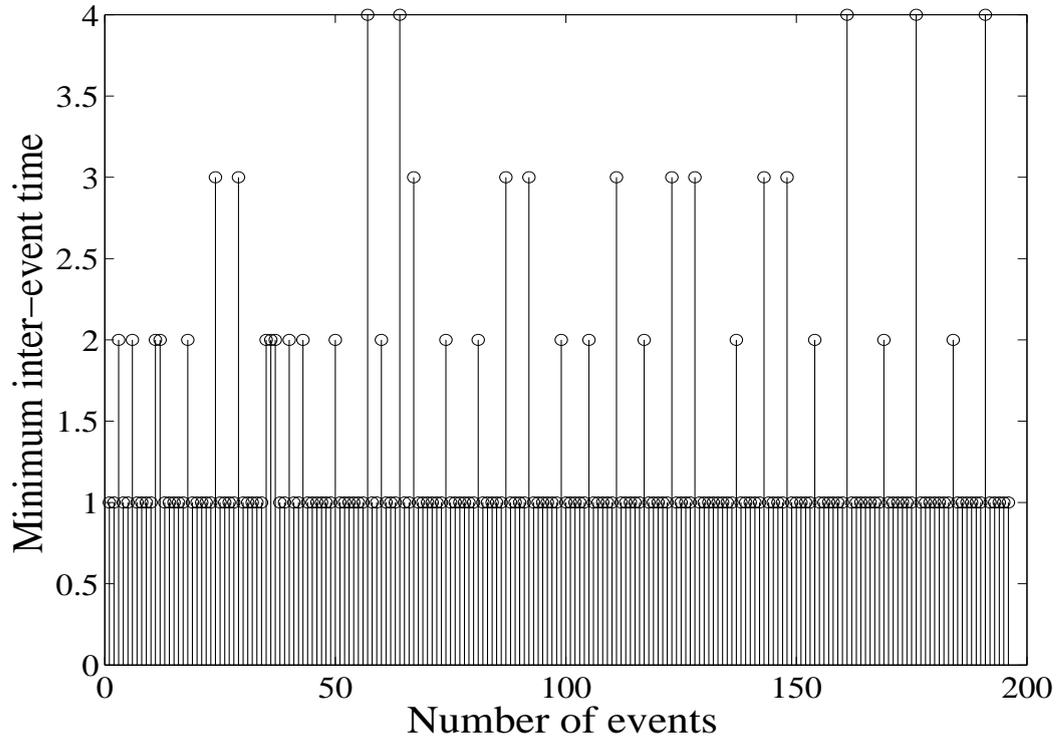
FIGURE 8.2: Number of events with minimum inter-event time

(a) State (x_1)

(b) State (x_2)
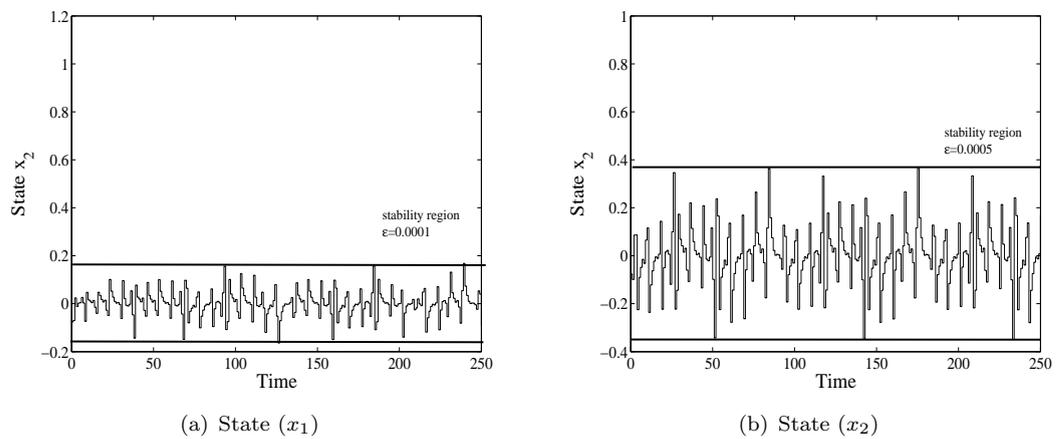
FIGURE 8.3: Effect of ϵ on stability region (set $\mathcal{E}$)

the system (see time steps $k \in \{150, 250\}$, number of events are generated). It can be said that ET control only acts when it is required for stability or performance. It can also be called 'control on demand', and a useful feature that makes the ET mechanism based control of high interest. Control systems with periodic transmissions do not have this property.
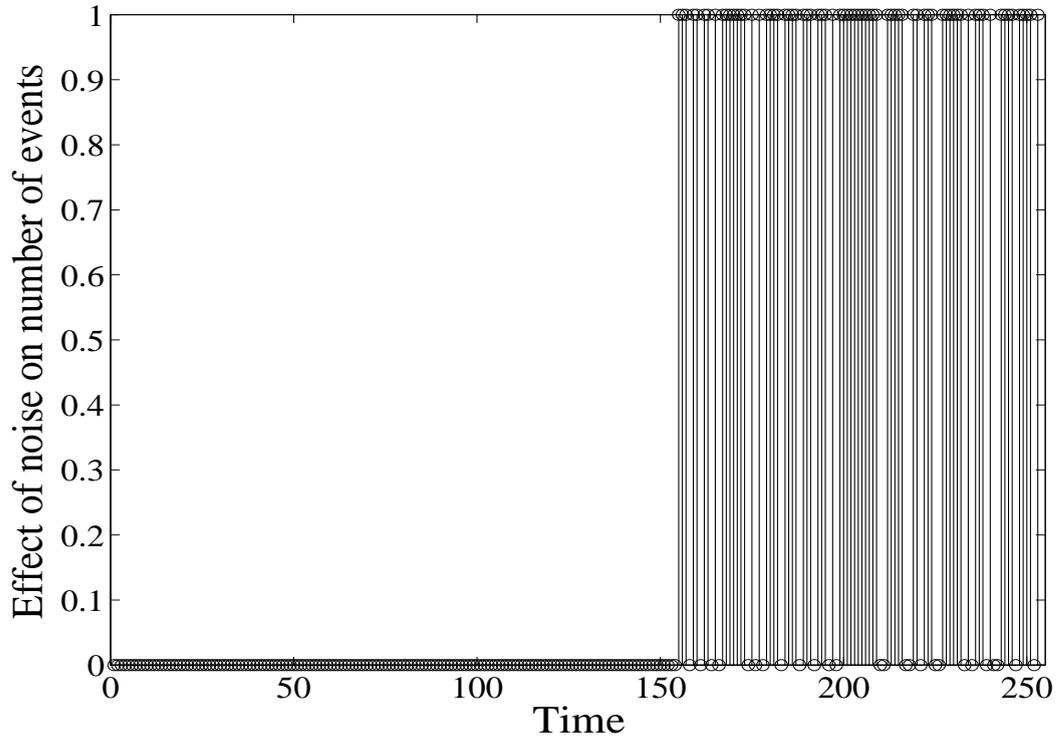
FIGURE 8.4: Effect of Noise on number of events

8.5   Conclusions

This chapter presentes stability analysis of distributed ET mechanism based NCSs with packet dropouts. The proposed design obtains $\mathcal{H}_\infty$ control performance objective as well. In this design, discrete-time ET mechanism based NCSs are represented as impulsive systems. For these hybrid systems, the satiability conditions are given in terms of LMIs and an upper bound on the stability set is provided. After this, a lower bound on minimum inter-event time is also presented. Stability conditions are satisfied with the help of simulation examples. The simulation results show that system stability is achieved with less number of transmission. A plot for transmitted events with minimum inter-event time is presented. It is observed that number of the packet dropouts increases number of the required events for the system stability. By analyzing the simulation result, it is presented that ϵ controls the width of stability set $\mathcal{E}$. Effect of noise $w(k)$ on number of the events is also presented. It is evaluated that the ET mechanism based control can be called 'control on demand' that reduces the use of communication, computational and power resources.

Chapter 9

Conclusions and Future Work

9.1 Conclusions

This thesis comprises novel design techniques for Networked Control Systems (NCSs), a dynamic research area with wide applications. These control techniques talk about stability analysis and controller synthesis for various NCSs frameworks. The NCSs are the control systems in which loops are closed over networks. Insertion of networks provides many advantages such as flexibility, modularity and reduced wiring cost etc. However, networks also introduce challenging constraints in the NCSs design. In this work the network-induced constraints have been identified through a literature survey presented in Chapter 2. Time delay, packet dropout, quantization error and limited bandwidth have been recognized as potential NCSs constraints. Furthermore, time-triggered (TT) and event-triggered (ET) sampling mechanisms have been compared through qualitative analysis and simulations. The effect of the mechanisms has been analyzed on the network-induced constraints as well.

Since time delay is a major NCSs constraint, the NCSs have been considered as a special class of time-delayed systems (TDSs). The delays occur due to bandwidth sharing in networks and remote locations of system components. It is commonly known that networks are random in nature, therefore the time delays have been considered as stochastic processes and have been modelled by the Markov chain in Chapters 3-7. In TDSs, the stability criteria are defined with the help of Lyapunov-Krasovskii (L-K) functional and Lyapunov-Razumikhin (L-R) function. New and sufficient conditions for the NCS stability have been proposed on the basis of L-K functional approach. By applying the Schur's complement and congruence transformation on the stability conditions, novel feedback controllers have been achieved in terms of bilinear matrix inequalities (BMIs). The BMIs have been converted into quasi-convex linear matrix inequalities (LMIs) by

an iterative algorithm. Controller gains have been obtained by solving the LMIs using LMI and YALMIP toolboxes of MATLAB. The obtained gains have been applied on different discrete-time plants in the presence of prescribed constraints. By performing simulations, all the proposed designs have been verified in terms of system stability, robustness and $\mathcal{H}_\infty$ performance. Simulation results, presented in Chapters 3-7, showed that the network-induced delays can cause instability in an already stable system if they are not properly incorporated in the system design.

Packet dropout between system components is another NCSs constraint. It occurs due to overflows in buffers and queues of network nodes. Successive and single packet dropouts have been modelled using Poisson distributions in Chapter 3, and Bernoulli in Chapter 7. Chapter 3 discussed that the Bernoulli distribution is capable of modelling the single packet dropout, however the successive packet dropouts require either Poisson or its combination with the Bernoulli distribution. In Chapter 3, solely Poisson distribution is used to model the successive packet dropouts. It is worth mentioning that multiple Bernoulli distributions can be used in the modelling of successive packet dropouts, however the detailed investigation is beyond the scope of this thesis. Simulation results presented in Chapter 3, showed that an increase in the successive packet dropouts results in the degradation of the system performance. The system can even become unstable if the successive packet dropouts are increased up to 4.

The quantization process is required in the NCSs due to the digital nature of networks and controllers. The quantization process helps in the adjustment of bandwidth utilization. However, it also results in the quantization error. Both aspects of the quantization process have been explored in Chapter 6 and 7. The quantization errors have been bounded by a sector bound approach in Chapter 6. Multiple quantizers have been considered and their errors have been characterized by the convex poly-topic uncertainties. On the other hand, the use of quantizers as information coders have been explored in Chapter 7. In this chapter, adaptive quantization densities have been considered and modelled with the help of Markov chain. By doing that, data rate has been adjusted according to the network load conditions. This technique helped me to propose a design of NCSs with limited bandwidth.

The last constraint considered in this thesis is limited bandwidth. It is indispensable in networks due to bandwidth sharing and scheduling. To cater for this constraint, various mechanisms such as congestion control and ET sampling have been investigated in Chapters 4, 5 and 8. Simulation results showed that the system stability can be achieved with less samples. It is also concluded that there is always a tradeoff between the system performance and limited bandwidth.

9.2   Future Work

Energy efficient and novel control designs enhance the usage of the NCSs in real-time applications. In future, different NCSs constraints will be identified and new horizons in the NCSs will be explored. My future research plans include:

- **Stability Analysis and Controller Design of NCSs using Event Triggered and Self Triggered Mechanisms**

  The event-triggered (ET) and Self Triggered (ST) controls reduce the use of communication and computational resources. Literature on the ET and ST control systems have seen a considerable growth in the last decade. However, this field is still in its early stages. The system theories for the ET and ST control are not as mature as time-triggered(TT) control system theories, thus require further investigation. By developing the novel co-design theories, the use of ET and ST control can be enhanced in practical applications. Recent simulation and experimental results show that the ET and ST control systems outperform the TT control systems in terms of the number of samples with satisfactory control performance [39, 42–44]. However, detailed qualitative, quantitative theories and simulation analysis are still required. Along with this the real-time implementations of ET and ST controls can result in further research issues.

  The ET and ST based control paradigms with networks in system loop are new research trends in the NCSs and will be the focus of my future research. Stability analysis of ET based distributed control systems,with packet dropouts, are discussed in the current work. Another potential research gap includes time delays, that will be considered in the future research.

- **Numerical Computing Techniques for Stability and Stabilization of the NCSs:**

  It is a well known fact that the NCSs are new frontiers in control systems. The research in the NCSs includes the concepts of applied mathematics, engineering and computer science. The use of numerical computing techniques in the linear control theory is an interesting topic that not only solves several control problems such as pole placement, stabilization and $\mathcal{H}_\infty$ control but can also be used to develop control toolboxes. The use of the numerical techniques in the control theory should take a number of considerations into account. Firstly, a problem formulation should reflect the physical properties of the system in a maximal way. Secondly, the control problems should be formulated mathematically in such a way that 'sensitivity to perturbations' should be less. Thirdly, a well formulated control

problem should not result in the drastic solution due to intermediate ill-conditioned numerical steps. Lastly, novel and improved numerical techniques should be developed for the large scale control problems such as control systems with time delays. As a future research interest, novel problem formulations and stabilization methods for the NCSs will be investigated using numerical techniques. It is also intended to formulate the NCSs problem as a well conditioned mathematical problem. Furthermore, numerical solutions to minimize the condition numbers and to avoid unnecessary errors will be investigated .

- **Design for the Polynomial NCSs using Sums of Squares Approach:**

Stability analysis and design of nonlinear systems is a challenging task. Most of the past research works utilized the conventional control approaches such as fuzzy systems, Lyapunov, control Lyapunov and storage functions [55, 168–170]. However, these techniques are computationally expensive and complex. The computational complexities are relaxed with the help of a newly emerged technique of the sum of squares (SOS) [171], and its solution using semi-definite programming (SDP) [172]. It is worth mentioning that the SOS approach can only be used for a specific class of nonlinear systems, called polynomial systems. A considerable research has been done on the stability analysis and controller design of polynomial systems using the SOS approach (see [173, 174] and references therein).

According to the authors' knowledge, the SOS approach is not deeply investigated for the nonlinear NCSs. Therefore the stability analysis and controller design of nonlinear NCSs with the SOS approach is a potential research field for the future work.

- **Design and Implementation of Direct and Hierarchical Structure NCSs:**

In direct structure NCSs, the system components are connected over either wireline or wireless network. For wireless NCSs, multiple communication standard have been proposed such as $WirelessHART(2007)$ and $ISA100.11a(2009)$. However, the design and implementation of test bed for wireless NCSs is quite expensive and difficult to implement. Therefore, co-simulation frameworks have been proposed in the literature. For example, a framework based on TrueTime toolbox and OMNET++ based wireless network simulator is proposed in [175]. This type of frameworks are quite useful to demonstrate the accurate features of network and devices. Various NCSs designs can be verified with this framework. This type of framework are also useful to analyze the control performance of dedicated communication standards e.g. $WirelessHART$.

For a physical NCSs test bed, a suitable integration of control systems, real-time operating system, and network communication systems is important. A basic

DC motor based NCSs test-bed consist of following parts: 1) a DC motor and associated sensor; 2) communication network; 3) remote controller; and 4) actuator as shown in Figure 9.1. In real time setup, difficulties exist on each of these four levels: 1) transmission of suitable data from sensors to controller over the network, 2) generation of real time network traffic and different constraint phenomena to analyze the controller performance and network security issues, 3) selection of real-time environment to impalement controllers, and 4) transmission of suitable data from controller to actuator over the network. The proposed designs will be verified after the implementation of NCSs test bed in the future.
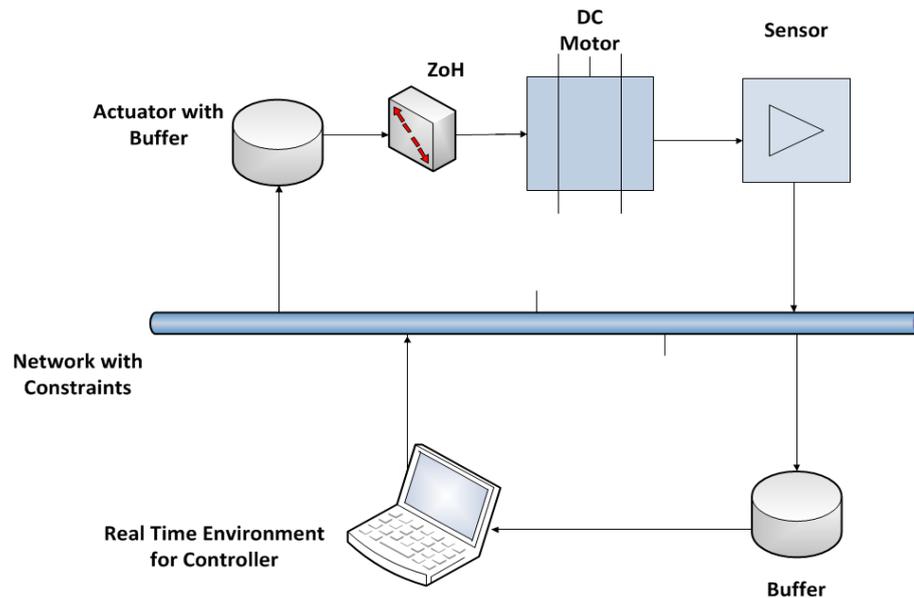
FIGURE 9.1: A direct structured NCS testbed: Dc motor setup

In the hierarchical NCSs, local controllers perform the control tasks according to the settings provided by the remote controller. One of the classic examples of this type of the NCSs is remote lab. A remote lab helps in distant engineering education. I have already developed and tested a prototype, however the real time design requires further investigation. The block diagram of the remote lab prototype is shown in the Figure 9.2. In this design a plant is controlled with the help of XPC target machine. The machine acts as a controller in a local closed-loop. It is further connected with a remote controller over the Internet, with the help XPC host. The host also acts as a web and monitoring server. The remote controllers can be distant learners who provide set-values for the control tasks. A web camera is also attached with the host so that the remote controllers can check the performance of the local close-loop.
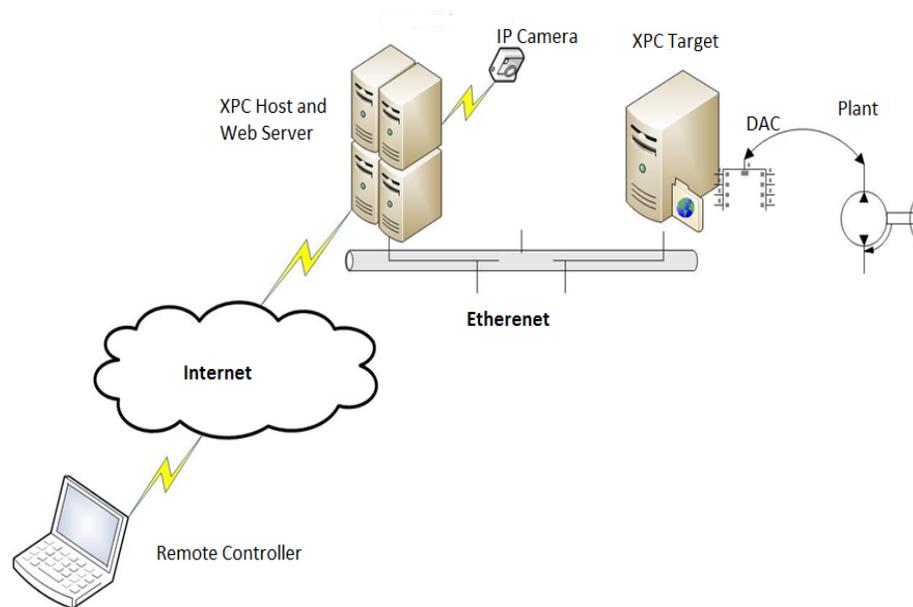
FIGURE 9.2: A hierarchical structured NCS: The remote lab

Chapter 10

Appendix

Proof of Lemma 3.2.1:

From (3.13), we learn that

$$\sum_{\kappa_{d_i}=0}^{\kappa_{m_i}} \sum_{i=k-\tau(i)-\kappa_{di}}^{k-1} \begin{bmatrix} y(i) \\ \tilde{x}(k) \end{bmatrix}^T \begin{bmatrix} R & M \\ M^T & Z \end{bmatrix} \begin{bmatrix} y(i) \\ \tilde{x}(k) \end{bmatrix} \geq 0 \qquad (10.1)$$

$$\sum_{\kappa_{d_i}=0}^{\kappa_{m_i}} \sum_{i=k-\tau(i)-\kappa_{di}}^{k-1} \left[y^T(i)Ry(i) + \tilde{x}^T(k)M^T y(i) + y^T(i)M\tilde{x}(k) + \tilde{x}^T(k)Z\tilde{x}(k) \right] \geq 0$$

$$\sum_{\kappa_{d_i}=0}^{\kappa_{m_i}} \sum_{i=k-\tau(i)-\kappa_{di}}^{k-1} y^T(i)Ry(i) + \sum_{\kappa_{d_i}=0}^{\kappa_{m_i}} \sum_{i=k-\tau(i)-\kappa_{di}}^{k-1} \tilde{x}^T(k)M^T y(i) +$$
$$\sum_{\kappa_{d_i}=0}^{\kappa_{m_i}} \sum_{i=k-\tau(i)-\kappa_{di}}^{k-1} y^T(i)M\tilde{x}(k) + \sum_{\kappa_{d_i}=0}^{\kappa_{m_i}} \sum_{i=k-\tau(i)-\kappa_{di}}^{k-1} \tilde{x}^T(k)Z\tilde{x}(k) \geq 0$$

$$\sum_{\kappa_{d_i}=0}^{\kappa_{m_i}} \sum_{i=k-\tau(i)-\kappa_{di}}^{k-1} \tilde{x}^T(k)M^T y(i) + \sum_{\kappa_{d_i}=0}^{\kappa_{m_i}} \sum_{i=k-\tau(i)-\kappa_{di}}^{k-1} y^T(i)M\tilde{x}(k) +$$
$$\sum_{\kappa_{d_i}=0}^{\kappa_{m_i}} \sum_{i=k-\tau(i)-\kappa_{di}}^{k-1} \tilde{x}^T(k)Z\tilde{x}(k) \geq -\sum_{\kappa_{d_i}=0}^{\kappa_{m_i}} \sum_{i=k-\tau(i)-\kappa_{di}}^{k-1} y^T(i)Ry(i)$$

$$\sum_{\kappa_{d_i}=0}^{\kappa_{m_i}} \tilde{x}^T(k)M^T\{x(k) - x(k-\tau(i)-\kappa_{di})\} + \sum_{\kappa_{d_i}=0}^{\kappa_{m_i}} \{x(k) - x(k-\tau(i)-\kappa_{di})\}^T M\tilde{x}(k) +$$
$$(\tau(i) + \kappa_{m_i} + 1)\tilde{x}^T(k)Z\tilde{x}(k) \geq -\sum_{\kappa_{d_i}=0}^{\kappa_{m_i}} \sum_{i=k-\tau(i)-\kappa_{di}}^{k-1} y^T(i)Ry(i)$$

as

$$\sum_{\kappa_{d_i}=0}^{\kappa_{m_i}} x(k) - x(k-\tau(i)-\kappa_{di}) = \begin{bmatrix} I & -I & -I & \cdots & -I & 0 & 0 & 0 & 0 & \cdots & 0 & 0 & 0 \end{bmatrix} \tilde{x}(k)$$

so

$$
\begin{bmatrix}
\tilde{x}^T(k)M^T \begin{bmatrix} I & -I & -I & \cdots & -I & 0 & 0 & 0 & 0 & \cdots & 0 & 0 & 0 \end{bmatrix} \tilde{x}(k) \\
+ \\
\tilde{x}(k)^T \begin{bmatrix} I & -I & -I & \cdots & -I & 0 & 0 & 0 & 0 & \cdots & 0 & 0 & 0 \end{bmatrix}^T M\tilde{x}(k) \\
+ \\
(\tau(i) + \kappa_{m_i} + 1)\tilde{x}^T(k)Z\tilde{x}(k)
\end{bmatrix}
$$
$$
\geq - \sum_{\kappa_{d_i}=0}^{\kappa_{m_i}} \sum_{i=k-\tau(i)-\kappa_{di}}^{k-1} y^T(i)Ry(i)
$$

putting $\Upsilon_1 = M^T[I \quad -I \quad -I \quad \cdots \quad -I \ 0 \ 0 \ 0 \ 0 \ \cdots \ 0 \ 0 \ 0]$ in above equation gives (3.14).

Proof of Theorem 3.3.1: The system (3.10) can be written as:

$$
\begin{aligned}
x_{k+1} &= \Gamma_1(i)\tilde{x}_k \\
z_k &= \Xi(i)\tilde{x}_k
\end{aligned} \tag{10.2}
$$

where $x(k+1) = x_{k+1}$, $z(k) = z_k$, $\Gamma_1(i)$ and $\Xi(i)$ are given in (3.18) and $\tilde{x}_k$ is defined in Lemma 3.2.1.

An improved L-K candidate functional for the closed loop system with time delays and multiple packet dropouts is selected as:

$$
V(x_k, i) = V_1(x_k, i) + V_2(x_k, i) + V_3(x_k, i) \tag{10.3}
$$

with

$$
V_1(x_k, i) = x_k^T P(i) x_k \tag{10.4}
$$

$$
V_2(x_k, i) = \sum_{\kappa_{d_i}=0}^{\kappa_{m_i}} \left[\sum_{\ell=-\tau(i)-\kappa_{di}}^{-1} \sum_{j=k+\ell}^{k-1} y_j^T R_1 y_j + \sum_{\ell=-\tau(s)-\kappa_m}^{-1} \sum_{j=k+\ell}^{k-1} y_j^T R_2 y_j \right] \tag{10.5}
$$

$$
V_3(x_k, i) = \sum_{\kappa_{d_i}=0}^{\kappa_{m_i}} \left[\sum_{\ell=k-\tau(i)-\kappa_{di}}^{k-1} x_\ell^T Q x_\ell + \sum_{\ell=-\tau(s)-\kappa_m+2}^{-\tau(1)+1} \sum_{j=k+\ell-1}^{k-1} x_j^T Q x_j \right] \tag{10.6}
$$

where κ_m are maximum number of packet dropouts of all Markov modes. In other words, $\kappa_{m_i} \leq \kappa_m$.

First forward difference of $V(x_k, i)$ is given as follows:

$$
\Delta V(x_k, i) = \Delta V_1(x_k, i) + \Delta V_2(x_k, i) + \Delta V_3(x_k, i) \tag{10.7}
$$

where

$$
\begin{aligned}
\Delta V_1(x_k, i) &= x_{k+1}^T \tilde{P}(i) x_{k+1} - x_k^T P(i) x_k \\
&= \tilde{x}_k^T \Gamma_1^T \tilde{P}(i) \Gamma_1 \tilde{x}_k - x_k^T P(i) x_k
\end{aligned}
\tag{10.8}
$$

$$
\begin{aligned}
\Delta V_2(x_k, i) \leq\ & y_k^T \Big[(\tilde{\tau}(i) + \tilde{\kappa}_{di}) R_1 + (\tau(s) + \kappa_m) R_2 \Big] y_k - \\
& \sum_{\kappa_{d_i}=0}^{\kappa_{m_i}} \sum_{\ell=k-\tau(i)-\kappa_{di}}^{k-1} y_\ell^T \Big[(1 - p_{i(i+1)}) R_1 + R_2 \Big] y_\ell
\end{aligned}
\tag{10.9}
$$

Using Lemma 3.2.1 and $y_k = x_{k+1} - x_k = \Gamma_2(i)\tilde{x}_k$, we have

$$
\begin{aligned}
\Delta V_2(x_k, i) \leq\ & \tilde{x}_k^T \Big\{ \Gamma_2^T \left[(\tilde{\tau}(i) + \tilde{\kappa}_{di}) R_1 + (\tau(s) + \kappa_m) R_2 \right] \Gamma_2 + \Upsilon_1(i) + \Upsilon_1^T(i) + (\tau(i) + \kappa_{m_i} \\
& + 1) Z(i) \Big\} \tilde{x}_k
\end{aligned}
\tag{10.10}
$$

where $\Gamma_2(i)$ is given in (3.18). and

$$
\Delta V_3(x_k, i) \leq (\tau(s) - \tau(1) + \kappa_m + 1) x_k^T Q x_k - \sum_{\kappa_{d_i}=0}^{\kappa_{m_i}} x_{k-\tau(i)-\kappa_{di}}^T Q x_{k-\tau(i)-\kappa_{di}}.
\tag{10.11}
$$

$$
\begin{aligned}
\Delta V_3(x_k, i) \leq\ & (\tau(s) - \tau(1) + \kappa_m + 1) x_k^T Q x_k - x_{k-\tau(i)-\kappa_{0i}}^T Q x_{k-\tau(i)-\kappa_{0i}} - \cdots - \\
& x_{k-\tau(i)-\kappa_{mi}}^T Q x_{k-\tau(i)-\kappa_{mi}}.
\end{aligned}
\tag{10.12}
$$

By combining (10.8-10.12):

$$
\begin{aligned}
\Delta V(x_k, i) \leq\ & -x_k^T \Big(P(i) - (\tau(s) - \tau(1) + \kappa_m + 1) Q \Big) x_k - x_{k-\tau(i)-\kappa_{0i}}^T Q x_{k-\tau(i)-\kappa_{0i}} - \\
& x_{k-\tau(i)-\kappa_{mi}}^T Q x_{k-\tau(i)-\kappa_{mi}} - \tilde{x}_k^T \Big\{ \Gamma_1^T \tilde{P}(i) \Gamma_1 + \Gamma_2^T \Big[(\tilde{\tau}(i) + \tilde{\kappa}_{di}) R_1 + (\tau(s) + \\
& \kappa_m) R_2 \Big] \Gamma_2 + \Upsilon_1(i) + \Upsilon_1^T(i) + (\tau(i) + \kappa_{m_i} + 1) Z(i) \Big\} \tilde{x}_k
\end{aligned}
\tag{10.13}
$$

Using Assumption 3.2.1, and adding and subtracting $x_k^T H_1^T F_k^T W_1(i) F_k H_1 x_k$,
$w_k^T H_2^T F_k^T W_3(i) F_k H_2 w_k$, $z_k^T z_k$, $\gamma w_k^T w_k$ and $x_{(k-\tau_i-\kappa_{0i})}^T \chi_i p_{0i} K^T(i) H_3^T F_k^T W_2(i) F_k H_3 K(i)$
$x_{(k-\tau_i-\kappa_{0i})} \cdots x_{(k-\tau_i-\kappa_{mi})}^T \chi_i p_{mi} K^T(i) H_3^T F_k^T W_2(i) F_k H_3 K(i) x_{(k-\tau_i-\kappa_{mi})}$ to and from (10.13),

we obtain:

$$
\begin{aligned}
\Delta V(x_k, i) \;\leq\; & -x_k^T\Big(P(i) - (\tau(s) - \tau(1) + \kappa_m + 1)Q - H_1^T(i)F_k^T W_1(i)F_k H_1(i) - \\
& \mu_\theta^T \mu_\theta\Big)x_k - x_{k-\tau_i-\kappa_{0i}}^T\Big(Q - \chi_i p_0 i K^T(i)H_3^T W_2(i)H_3 K(i)\Big)x_{k-\tau_i-\kappa_{0i}} \\
& - \cdots - x_{k-\tau_i-\kappa_{mi}}^T\Big(Q - \chi_i p_m i K^T(i)H_3^T W_2(i)H_3 K(i)\Big)x_{k-\tau_i-\kappa_{mi}} + \\
& \tilde{x}_k\Big\{\Gamma_1^T \tilde{P}(i)\Gamma_1 + \Gamma_2^T[(\tilde{\tau}(i) + \tilde{\kappa}_{di})R_1 + (\tau(s) + \kappa_m)R_2]\Gamma_2 + \Upsilon_1(i) + \Upsilon_1^T(i) \\
& + (\tau(i) + \kappa_{m_i} + 1)Z(i) + \Xi^T(i)\Xi(i)\Big\}\tilde{x}_k - z_k^T z_k + \gamma^2 w_k^T w_k - w_k^T\Big(\gamma^2 I - \\
& H_2^T W_3(i)H_2\Big)w_k - x_k^T H_1^T(i)F_k^T W_1(i)F_k H_1(i)x_k - x_{(k-\tau_i-\kappa_{0i})}^T \chi_i p_{0i} \\
& K^T(i)H_3^T F_k^T W_2(i)F_k H_3 K(i)x_{(k-\tau_i-\kappa_{0i})} - \cdots x_{(k-\tau_i-\kappa_{m_i})}^T \chi_i p_{mi} K^T(i) \\
& - H_3^T F_k^T W_2(i)F_k H_3 K(i)x_{(k-\tau_i-\kappa_{mi})} - w_k^T H_2^T F_k^T W_3(i)F_k H_2 w_k \\
& - x^T(k)\mu_\theta^T \mu_\theta x(k)
\end{aligned}
\tag{10.14}
$$

Using (3.18), (10.14) can be rewritten as

$$
\begin{aligned}
\Delta V(x_k, i) \;\leq\; & \tilde{x}_k^T\Big\{\Lambda(i) + \Gamma_1^T \tilde{P}(i)\Gamma_1 + \Gamma_2^T[(\tilde{\tau}(i) + \tilde{\kappa}_{di})R_1 + (\tau(s) + \kappa_m)R_2]\Gamma_2 + \Upsilon_1(i) \\
& + \Upsilon_1^T(i) + (\tau(i) + \kappa_{m_i} + 1)Z(i) + \Xi^T(i)\Xi(i)\Big\}\tilde{x}_k - z_k^T z_k + \gamma^2 w_k^T w_k
\end{aligned}
\tag{10.15}
$$

Using (3.17), we have

$$
\Delta V(x_k, i) \leq -z_k^T z_k + \gamma^2 w_k^T w_k
\tag{10.16}
$$

Taking expectation and sum from 0 to ∞ on both sides of (10.16) yields:

$$
E\{V(x_\infty, i_\infty)\} - E\{V(x_0, i_0)\} \leq -E\Big\{\sum_{\ell=0}^{\infty} z_\ell^T z_\ell\Big\} + \gamma^2 \sum_{\ell=0}^{\infty} w_\ell^T w_\ell.
\tag{10.17}
$$

where $i_0 = r_0$ and $i_\infty = r_\infty$.

As initial conditions, which are given in problem formulation, are considered to be zero, i.e, $V(x_0, i_0) = 0$, we get:

$$
E\Big\{\sum_{\ell=0}^{\infty} z_\ell^T z_\ell\Big\} \leq \gamma^2 \sum_{\ell=0}^{\infty} w_\ell^T w_\ell.
\tag{10.18}
$$

If $w(k) = 0, \forall k \geq 0$ closed-loop system should be stochastically stable. From (10.15) and (3.17), we learn that

$$V(x_{(k+1)}, j) - V(x_k, i) \leq -\beta \tilde{x}_k^T \tilde{x}_k \tag{10.19}$$

where $\beta = \inf\{\Lambda(i)_{\min}[-\mathcal{M}(i)], i \in S\}$ with

$$\begin{aligned}
\mathcal{M} &= \Lambda(i) + \Gamma_1^T(i)\tilde{P}(i)\Gamma_1(i) + \Gamma_2^T[(\tilde{\tau}(i) + \tilde{\kappa}_{di})R_1 + (\tau(s) + \kappa_m)R_2]\Gamma_2 + \\
&\quad \Upsilon_1(i) + \Upsilon_1^T(i) + (\tau(i) + \kappa_{m_i} + 1)Z(i) + \Xi^T(i)\Xi(i) \tag{10.20}
\end{aligned}$$

Summing from 0 to ∞ and by taking expectation on both sides of (10.19) gives

$$\begin{aligned}
E\{V(x_\infty, i_\infty)\} - E\{V(x_0, i_0)\} &\leq -\beta E\Big\{\sum_{k=0}^{\infty} \tilde{x}_\ell^T \tilde{x}_\ell\Big\} \\
&\leq -\beta E\Big\{\sum_{k=0}^{\infty} x_\ell^T x_\ell\Big\} \tag{10.21}
\end{aligned}$$

Re-arranging (10.21), we have

$$\begin{aligned}
E\Big\{\sum_{k=0}^{\infty} x_\ell^T x_\ell\Big\} &\leq \frac{1}{\beta}E\{V(x_0, i_0)\} - \frac{1}{\beta}E\{V(x_\infty, i_\infty)\} \\
&\leq \alpha \tag{10.22}
\end{aligned}$$

where $\alpha = \frac{1}{\beta}E\{V(x_0, i_0)\} < \infty$. This shows that the closed loop system is stable and (3.12) holds. $\nabla\nabla\nabla$

Proof of Theorem 3.3.2:

Rearranging (3.17) as

$$\begin{aligned}
&\tilde{\Lambda}_1(i) + \Upsilon_1(i) + \Upsilon_1^T(i) + (\tau(i) + \kappa_{m_i} + 1)Z(i) + \Gamma_1^T(i)\tilde{P}(i)\Gamma_1(i) + \Xi^T(i)\Xi(i) + \Gamma_2^T(i) \\
&[(\tilde{\tau}(i) + \tilde{\kappa}_{di})R_1 + (\tau(s) + \kappa_m)R_2]\Gamma_2(i) + \text{diag}\Big\{\mu_\theta^T\mu_\theta, 0, \cdots, 0, 0, 0, 0, \cdots, 0, 0, 0\Big\} \\
&+\text{diag}\Big\{H_1^T W_1(i)H_1, \chi_i p_{0i}K^T(i)H_3^T W_2(i)H_3 K(i), \cdots, \chi_i p_{mi}K^T(i)H_3^T W_2(i)H_3 K(i) \\
&, 0, 0, 0, \cdots, 0, 0, 0\Big\} < 0 \tag{10.23}
\end{aligned}$$

where

$$\begin{aligned}
\Lambda(i) &= \tilde{\Lambda}_1(i) + \text{diag}\Big\{\mu_\theta^T\mu_\theta, 0, \cdots, 0, 0, 0, 0, \cdots, 0, 0, 0\Big\} + \\
&\quad \text{diag}\Big\{H_1^T W_1(i)H_1, \chi_i p_{0i}K^T(i)H_3^T W_2(i)H_3 K(i), \cdots, \\
&\quad \chi_i p_{mi}K^T(i)H_3^T W_2(i)H_3 K(i), 0, 0, 0, \cdots, 0, 0, 0\Big\}
\end{aligned}$$

and

$$\tilde{\Lambda}_1(i) = \text{diag}\Big\{(\tau(s) - \tau(1) + \kappa_m + 1)Q - P(i), -Q, \cdots, -Q, H_2^T W_3(i) H_2 - \gamma I, -W_1(i),$$
$$-W_2(i), \cdots, -W_2(i), -W_3(i), -I\Big\}$$

Applying Schur complement on (10.23) we get

$$\begin{bmatrix} \tilde{\Pi}(i) & \Gamma_1^T(i) & \Gamma_2^T(i) & \Xi^T(i) & \mathcal{H}_1^T(i) & \bar{\mu}_\theta^T \\ * & -\tilde{P}^{-1}(i) & 0 & 0 & 0 & 0 \\ * & * & -\mathcal{R}_1 & 0 & 0 & 0 \\ * & * & * & -I & 0 & 0 \\ * & * & * & * & -\tilde{\mathcal{W}}_1 & 0 \\ * & * & * & * & * & -I \end{bmatrix} < 0 \qquad (10.24)$$

where

$$\tilde{\Pi}(i) = \tilde{\Lambda}_1(i) + \Upsilon_1(i) + \Upsilon_1^T(i) + (\tau(i) + \kappa_{m_i} + 1)Z(i)$$

$$\mathcal{H}_1(i) = \begin{bmatrix} H_1 & 0 & \cdots & 0 & 0 & 0 & 0 & \cdots & 0 & 0 & 0 \\ 0 & \chi_i p_{0i} H_3 K(i) & \cdots & 0 & 0 & 0 & 0 & \cdots & 0 & 0 & 0 \\ \vdots & \vdots & \ddots & \vdots & \vdots & \vdots & \vdots & \ddots & \vdots & \vdots & \vdots \\ 0 & 0 & \cdots & \chi_i p_{mi} H_3 K(i) & 0 & 0 & 0 & \cdots & 0 & 0 & 0 \end{bmatrix},$$

$$\bar{\mu}_\theta = \begin{bmatrix} \mu_\theta & 0 & \cdots & 0 & 0 & 0 & 0 & \cdots & 0 & 0 & 0 \end{bmatrix},$$

$$\mathcal{R}_1 = \text{diag}\Big\{(\tilde{\tau}(i) + \tilde{\kappa}_{di})R_1^{-1}, (\tau(s) + \kappa_m)R_2^{-1}\Big\}, \tilde{\mathcal{W}}_1 = \text{diag}\Big\{W_1^{-1}(i), W_2^{-1}(i), \cdots, W_2^{-1}(i)\Big\}.$$

Multiplying (10.24) to the right by the matrix $\text{diag}\Big\{X(i), X(i), \cdots, X(i), I, I, I, \cdots, I, I, I\Big\}$ and the left by its transpose, we obtain (3.3.2) with $\tilde{P}^{-1}(i)$ at the place of $\tilde{S}(i) - J^T(i) - J(i)$.

Applying Schur complement on (3.21) and consequently multiplying these inequalities by p_{ij} and summing up for all $j = \mathcal{S}$, we obtain

$$\begin{aligned} \tilde{S}(i) - J^T(i) - J(i) &= -J^T(i) - J(i) + \sum_{j=1}^{i+1} p_{ij} S(i,j) \\ &\geq -J^T(i) - J(i) + J^T(i)\tilde{P}(i)J(i) \\ &= -\tilde{P}^{-1}(i) + \Big(J(i) - \tilde{P}^{-1}(i)\Big)^T \tilde{P}(i)\Big(J(i) - \tilde{P}^{-1}(i)\Big) \\ &\geq -\tilde{P}^{-1}(i) \qquad (10.25) \end{aligned}$$

which implies that (3.3.2) remains valid if $\tilde{S}(i) - J^T(i) - J(i)$ is replaced by $-\tilde{P}^{-1}(i)$.

Furthermore, the multiplication of $\text{diag}\Big\{X(i), X(i), \cdots, X(i), I, I, I, \cdots, I, I, I\Big\}$ and its

transpose on (10.24) creates two terms $X(i)^T Q X(i)$ and $-X(i)^T Q X(i)$ in $\tilde{\Lambda}$. Using Schur complement on $X(i)^T Q X(i)$ and the identity shown below, (3.3.2) is obtained. Note that:

$$
\begin{aligned}
-\left(X(i) - Q^{-1}\right)^T Q \left(X(i) - Q^{-1}\right) &< 0 \qquad\qquad (10.26) \\
\Rightarrow\quad -X(i)^T Q X(i) + X^T(i) + X(i) - Q^{-1} &< 0 \\
\Rightarrow\quad -X(i)^T Q X(i) &< -X^T(i) - X(i) + Q^{-1}
\end{aligned}
$$

holds true since Q is a positive matrix. Therefore the $-X(i)^T Q X(i)$ term can be replaced with $-X^T(i) - X(i) + Q^{-1}$. where $\tilde{Q} = Q^{-1}$.

This concludes the proof that the closed-loop system is stochastically stable with the prescribed $\mathcal{H}_\infty$ performance. $\nabla\nabla\nabla$

Chapter 11

Appendix

Proof of Theorem 4.3.1: Using (4.10), the closed loop system given in (4.4) can be rewritten as:

$$\begin{aligned} x_{k+1} &= \Gamma_1(r_k)\tilde{x}_k \\ z_k &= \Xi(r_k)\tilde{x}_k \end{aligned} \tag{11.1}$$

where $x_k = x(k)$, $z_k = z(k)$, $\tilde{x}_k = \tilde{x}(k)$. $\Gamma_1(r_k)$ and $\Xi(r_k)$ are given in (4.10), and $\tilde{x}_k$ is defined in Lemma 4.2.1.

Let us consider the following Lyapunov-Krasovskii functional:

$$V(x_k, r_k) = V_1(x_k, r_k) + V_2(x_k, r_k) + V_3(x_k, r_k) \tag{11.2}$$

with

$$V_1(x_k, r_k) = x_k^T P(r_k) x_k \tag{11.3}$$

$$V_2(x_k, r_k) = \sum_{\ell=-\tau(r_k)}^{-1} \sum_{j=k+\ell}^{k-1} y_j^T R_1 y_j + \sum_{\ell=-\tau(s)}^{-1} \sum_{j=k+\ell}^{k-1} y_j^T R_2 y_j \tag{11.4}$$

$$V_3(x_k, r_k) = \sum_{\ell=k-\tau(r_k)}^{k-1} x_\ell^T Q x_\ell + \sum_{\ell=-\tau(s)+2}^{-\tau(1)+1} \sum_{j=k+\ell-1}^{k-1} x_\ell^T Q x_\ell \tag{11.5}$$

Along any trajectory of the closed-loop system, the expectation value of the first forward difference of $V(x_k, r_k)$ is given as follows:

$$\Delta V(x_k, r_k) = \Delta V_1(x_k, r_k) + \Delta V_2(x_k, r_k) + \Delta V_3(x_k, r_k) \tag{11.6}$$

Employing the same technique as [151], (11.6) can be reduced to

$$
\begin{aligned}
\Delta V(x_k, r_k) \quad \leq \quad & -x_k^T \Big(P(r_k) - (\tau(s) - \tau(1) + 1)Q \Big) x_k - x_{k-\tau(r_k)}^T Q x_{k-\tau(r_k)} + \tilde{x}_k^T \Big\{ \Gamma_1^T \tilde{P}(r_k) \\
& \Gamma_1 + \Gamma_2^T \left[\tilde{\tau}(r_k) R_1 + \tau(s) R_2 \right] \Gamma_2 + \Upsilon_1(r_k) + \Upsilon_1^T(r_k) + \tau(r_k) Z(r_k) \Big\} \tilde{x}_k
\end{aligned}
$$
(11.7)

Using Assumption 3.2.1, and adding and subtracting $x_k^T H_1^T F_k^T W_1(r_k) F_k H_1 x_k$,
$w_k^T H_2^T F_k^T W_3(r_k) F_k H_2 w_k$, $z_k^T z_k$, $x_{(k-\tau_{r_k})}^T K^T(r_k) H_3^T F_k^T W_2(r_k) F_k H_3 K(r_k) x_{(k-\tau_{r_k})}$,
$\{x(\iota - \tau_\iota) - x(k - \tau_{r_k})\}^T K^T(r_k) W_4(r_k) K(r_k) \{x(\iota - \tau_\iota) - x(k - \tau_{r_k})\}$,
$\{x(\iota - \tau_\iota) - x(k - \tau_{r_k})\}^T K^T(r_k) H_3^T F_k^T W_5(r_k) F_k H_3 \{x(\iota - \tau_\iota) - x(k - \tau_{r_k})\}$ and $\gamma w_k^T w_k$
to and from (11.7) and using (4.2), we obtain

$$
\begin{aligned}
\Delta V(x_k, r_k) \quad \leq \quad & -x_k^T \Big(P(r_k) - (\tau(s) - \tau(1) + 1)Q - H_1^T W_1(r_k) H_1 \Big) x_k - x_{k-\tau_{r_k}}^T \Big(Q \\
& - K^T(r_k) H_3^T W_2(r_k) H_3 K(r_k) - \delta^2 K^T(r_k) W_4(r_k) K(r_k) - \delta^2 K^T(r_k) H_3^T \\
& W_5(r_k) H_3 K(r_k) \Big) x_{k-\tau_{r_k}} + \tilde{x}_k^T \Big\{ \Gamma_1^T \tilde{P}(r_k) \Gamma_1 + \Gamma_2^T \Big[\tilde{\tau}_k R_1 + \tau(s) R_2 \Big] \Gamma_2 + \\
& \Upsilon_1(r_k) + \Upsilon_1^T(r_k) + \tau_{r_k} Z(r_k) + \Xi^T \Xi \Big\} \tilde{x}_k - z_k^T z_k + \gamma w_k^T w_k - w_k^T \Big(\gamma I - \\
& H_2^T W_3(r_k) H_2 \Big) w_k - x_k^T H_1^T F_k^T W_1(r_k) F_k H_1 x_k - x_{(k-\tau_{r_k})}^T K^T(r_k) H_3^T \\
& F_k^T W_2(r_k) F_k H_3 K(r_k) x_{(k-\tau_{r_k})} - \{x(\iota - \tau_\iota) - x(k - \tau_{r_k})\}^T K^T(r_k) W_4(r_k) \\
& K(r_k) \{x(\iota - \tau_\iota) - x(k - \tau_{r_k})\} - \{x(\iota - \tau_\iota) - x(k - \tau_{r_k})\}^T K^T(r_k) H_3^T \\
& F_k^T W_5(r_k) F_k H_3 K(r_k) \{x(\iota - \tau_\iota) - x(k - \tau_{r_k})\} - \\
& w_k^T H_2^T F_k^T W_3(r_k) F_k H_2 w_k
\end{aligned}
$$
(11.8)

$$
\begin{aligned}
\Delta V(x_k, r_k) \quad \leq \quad & \tilde{x}_k^T \Big\{ \Lambda(r_k) + \Gamma_1^T \tilde{P}(r_k) \Gamma_1 + \Gamma_2^T \left[\tilde{\tau}(r_k) R_1 + \tau(s) R_2 \right] \Gamma_2 + \Upsilon_1(r_k) + \Upsilon_1^T(r_k) \\
& + \tau(r_k) Z(r_k) + \Xi^T \Xi \Big\} \tilde{x}_k - z_k^T z_k + \gamma w_k^T w_k
\end{aligned}
$$
(11.9)

Using (4.8), we have

$$
\Delta V(x_k, r_k) \leq -z_k^T z_k + \gamma w_k^T w_k
$$
(11.10)

Taking expectation and sum from 0 to ∞ on both sides of (11.10) yields

$$
E\{V(x_\infty, r_\infty)\} - E\{V(x_0, r_0)\} \leq -E\Big\{ \sum_{\ell=0}^{\infty} z_\ell^T z_\ell \Big\} + \gamma \sum_{\ell=0}^{\infty} w_\ell^T w_\ell
$$
(11.11)

Under zero initial condition, $V(x_0, r_0) = 0$, we have

$$
E\Big\{ \sum_{\ell=0}^{\infty} z_\ell^T z_\ell \Big\} \leq \gamma \sum_{\ell=0}^{\infty} w_\ell^T w_\ell
$$
(11.12)

That is, $\mathcal{H}_\infty$ performance criteria, given in Chapter 6 as (6.13), is satisfied.

Next, under $w(k) = 0, \forall k \geq 0$ we need to show that the closed-loop system is stochastically stable. From (11.9) and (4.8), we learn that

$$V(x_{k+1}, r_{k+1}) - V(x_k, r_k) \leq -\beta \tilde{x}_k^T \tilde{x}_k \tag{11.13}$$

where $\beta = \inf\{\lambda_{\min}[-\mathcal{M}(i)], i \in S\}$ with

$$
\begin{aligned}
\mathcal{M}(i) &= \Lambda(i) + \Gamma_1^T(i)\tilde{P}(i)\Gamma_1(i) + \Gamma_2^T(i)\left[\tilde{\tau}(i)R_1 + \tau(s)R_2\right]\Gamma_2(i) + \Upsilon_1(i) + \Upsilon_1^T(i) \\
&\quad + \tau(i)Z(i) + \Xi^T(i)\Xi(i)
\end{aligned}
\tag{11.14}
$$

Taking expectation and sum from 0 to ∞ on both sides of (11.13) yields

$$
\begin{aligned}
E\{V(x_\infty, r_\infty)\} - E\{V(x_0, r_0)\} &\leq -\beta E\left\{\sum_{k=0}^{\infty} \tilde{x}_\ell^T \tilde{x}_\ell\right\} \\
&\leq -\beta E\left\{\sum_{k=0}^{\infty} x_\ell^T x_\ell\right\}
\end{aligned}
\tag{11.15}
$$

Re-arranging (11.15), we get

$$
\begin{aligned}
E\left\{\sum_{k=0}^{\infty} x_\ell^T x_\ell\right\} &\leq \frac{1}{\beta}E\{V(x_0, r_0)\} - \frac{1}{\beta}E\{V(x_\infty, r_\infty)\} \\
&\leq \alpha
\end{aligned}
\tag{11.16}
$$

where $\alpha = \frac{1}{\beta}E\{V(x_0, r_0)\} < \infty$. Hence, we can conclude that the closed-loop system is stochastically stable. $\nabla\nabla\nabla$

Proof of Theorem 4.3.2:

Rearranging (4.8) as

$$
\begin{aligned}
&\tilde{\Lambda}_1(i) + \Upsilon_1(i) + \Upsilon_1^T(i) + \tau(i)Z(i) + \Gamma_1^T(i)\tilde{P}(i)\Gamma_1(i) + \Gamma_2^T(i)\left[\tilde{\tau}(i)R_1 + \tau(s)R_2\right]\Gamma_2(i) + \\
&\qquad \Xi^T(i)\Xi(i) + \text{diag}\left\{H_1^T W_1(i)H_1, K^T(i)H_3^T W_2(i)H_3 K(i), 0, 0, 0, 0, 0, 0\right\} \\
&\qquad + \text{diag}\left\{0, \delta^2 K(i)^T W_4(i)K(i) + \delta^2 K^T(i)H_3^T W_2(i)H_3 K(i), 0, 0, 0, 0, 0\right\} < 0
\end{aligned}
\tag{11.17}
$$

where

$$
\begin{aligned}
\Lambda(i) \;=\;& \tilde{\Lambda}_1(i) + \mathrm{diag}\Big\{ H_1^T W_1(i) H_1, K^T(i) H_3^T W_2(i) H_3 K(i), 0, 0, 0, 0, 0, 0 \Big\} \\
& + \mathrm{diag}\Big\{ 0, \delta^2 K(i)^T W_4(i) K(i) + \delta^2 K^T(i) H_3^T W_2(i) H_3 K(i), 0, 0, 0, 0, 0 \Big\}
\end{aligned}
\tag{11.18}
$$

and

$$
\begin{aligned}
\tilde{\Lambda}_1(i) \;=\;& \mathrm{diag}\Big\{ \big((\tau(s) - \tau(1) + 1)Q - P(i) \big), -Q, \big(H_2^T W_3(i) H_2 - \gamma I \big), -W_1(i), -W_2(i), \\
& -W_4(i), -W_5(i), -W_3(i) \Big\}
\end{aligned}
\tag{11.19}
$$

Applying Schur complement on (11.17) we get

$$
\begin{bmatrix}
\tilde{\Lambda}_1(i) + \Upsilon_1(i) + \Upsilon_1^T(i) + \tau(i)Z(i) & \Gamma_1^T(i) & \Gamma_2^T(i) & \Xi^T(i) & \tilde{\mathcal{H}}_1^T(i) & \tilde{\mathcal{H}}_2^T(i) \\
* & -\tilde{P}^{-1}(i) & 0 & 0 & 0 & 0 \\
* & * & -\mathcal{R}_1 & 0 & 0 & 0 \\
* & * & * & -I & 0 & 0 \\
* & * & * & * & -\tilde{\mathcal{W}}_1 & 0 \\
* & * & * & * & * & -\tilde{\mathcal{W}}_2
\end{bmatrix} < 0
\tag{11.20}
$$

where

$$
\begin{aligned}
\tilde{\mathcal{H}}_1^T(i) \;=\;& \begin{bmatrix} H_1 & 0 & 0 & 0 & 0 & 0 & 0 & 0 \\ 0 & H_3 K(i) & 0 & 0 & 0 & 0 & 0 & 0 \end{bmatrix} \\
\tilde{\mathcal{H}}_2^T(i) \;=\;& \begin{bmatrix} 0 & \delta K(i) & 0 & 0 & 0 & 0 & 0 & 0 \\ 0 & \delta H_3 K(i) & 0 & 0 & 0 & 0 & 0 & 0 \end{bmatrix}
\end{aligned}
\tag{11.21}
$$

$$
\mathcal{R}_1 = \mathrm{diag}\Big\{ \tilde{\tau}(i) R_1^{-1}, \tau(s) R_2^{-1} \Big\}, \tilde{\mathcal{W}}_1 = \mathrm{diag}\Big\{ W_1^{-1}(i), W_2^{-1}(i) \Big\}, \tilde{\mathcal{W}}_2 = \mathrm{diag}\Big\{ W_4^{-1}(i), W_5^{-1}(i) \Big\}
$$

Multiplying (11.20) to the right by the matrix $\mathrm{diag}\Big\{ X(i), X(i), I, I, I, I, I, I, I, I, I, I, I \Big\}$ and the left by its transpose, we obtain (4.3.2) with $\tilde{P}^{-1}(i)$ at the place of $\tilde{S}(i) - J^T(i) - J(i)$.

Applying Schur complement on (4.14) and consequently multiplying these inequalities

by p_{ij} and summing up for all $j = S$, we obtain

$$
\begin{aligned}
\tilde{S}(i) - J^T(i) - J(i) &= -J^T(i) - J(i) + \sum_{j=1}^{i+1} p_{ij} S(i,j) \\
&\geq -J^T(i) - J(i) + J^T(i)\tilde{P}(i)J(i) \\
&= -\tilde{P}^{-1}(i) + \left(J(i) - \tilde{P}^{-1}(i)\right)^T \tilde{P}(i)\left(J(i) - \tilde{P}^{-1}(i)\right) \\
&\geq -\tilde{P}^{-1}(i) \tag{11.22}
\end{aligned}
$$

which implies that (4.3.2) remains valid if $\tilde{S}(i) - J^T(i) - J(i)$ is replaced by $-\tilde{P}^{-1}(i)$.

Furthermore, the multiplication of $\text{diag}\left\{X(i), X(i), I, I, I, I, I, I\right\}$ and its transpose on (11.20) creates two terms $X(i)^T Q X(i)$ and $-X(i)^T Q X(i)$ in $\tilde{\Lambda}$. Using Schur complement on $X(i)^T Q X(i)$ and the identity shown below, (4.3.2) is obtained.

Note that

$$
\begin{aligned}
&-\left(X(i) - Q^{-1}\right)^T Q\left(X(i) - Q^{-1}\right) < 0 \tag{11.23} \\
\Rightarrow\quad &-X(i)^T Q X(i) + X^T(i) + X(i) - Q^{-1} < 0 \\
\Rightarrow\quad &-X(i)^T Q X(i) < -X^T(i) - X(i) + Q^{-1}
\end{aligned}
$$

holds true since Q is a positive matrix. Therefore the $-X(i)^T Q X(i)$ term can be replaced with $-X^T(i) - X(i) + Q^{-1}$. Then it is obvious that $\tilde{Q} = Q^{-1}$. This concludes the proof that the closed-loop system is stochastically stable with the prescribed $\mathcal{H}_\infty$ performance. $\nabla\nabla\nabla$

Using cone complementary algorithm, the feasibility problem formulated by (4.11)-(4.12) which is not a convex problem can be converted into the following nonlinear minimization problem subject to LMIs:

Minimize $Tr\left(\mathcal{R}_1\tilde{R}_1 + \mathcal{R}_2\tilde{R}_2 + \tilde{W}_1(i)W_1(i) + \tilde{W}_2(i)W_2(i) + \tilde{W}_4(i)W_4(i) + \tilde{W}_5(i)W_5(i) + \tilde{Q}Q\right)$

subject to (4.11)-(4.12) and

$$
\begin{bmatrix} \mathcal{R}_1 & I \\ I & \tilde{R}_1 \end{bmatrix} \geq 0, \quad
\begin{bmatrix} \mathcal{R}_2 & I \\ I & \tilde{R}_2 \end{bmatrix} \geq 0, \quad
\begin{bmatrix} \tilde{W}_1(i) & I \\ I & W_1(i) \end{bmatrix} \geq 0, \quad
\begin{bmatrix} \tilde{W}_2(i) & I \\ I & W_2(i) \end{bmatrix} \geq 0
$$

$$
\begin{bmatrix} \tilde{W}_4(i) & I \\ I & W_4(i) \end{bmatrix} \geq 0, \quad
\begin{bmatrix} \tilde{W}_5(i) & I \\ I & W_5(i) \end{bmatrix} \geq 0 \quad
\begin{bmatrix} \tilde{Q} & I \\ I & Q \end{bmatrix} \geq 0 \tag{11.24}
$$

To solve this optimization problem, algorithm introduced in 6, is used:

Algorithm :

Step 1: Set $\jmath = 0$ and solve (4.11)-(4.12) and (11.24) to obtain the initial conditions,

$$\begin{bmatrix} X(i), \tilde{S}(i), J(i), \tilde{R}_1(i), \tilde{R}_1, \tilde{R}_2(i), \tilde{R}_2, W_1(i), W_2(i), W_3(i), \\ W_4(i), W_5(i), \tilde{W}_1(i), \tilde{W}_2(i), \tilde{W}_4(i), \tilde{W}_5(i), \tilde{Q}, \mathcal{R}_1, \mathcal{R}_2, \tilde{Z}(i), Y(i) \end{bmatrix}^0$$

Step 2: Solve the LMI problem

Minimize $Tr\Big(\mathcal{R}_1^{\jmath}\tilde{R}_1 + \mathcal{R}_1\tilde{R}_1^{\jmath} + \mathcal{R}_2^{\jmath}\tilde{R} + \mathcal{R}_2\tilde{R}_2^{\jmath} + \tilde{W}_1(i)^{\jmath}W_1(i) + \tilde{W}_1(i)W_1(i)^{\jmath} + \tilde{W}_2(i)^{\jmath}W_2(i) + \tilde{W}_2(i)W_2(i)^{\jmath} + \tilde{W}_4(i)^{\jmath}W_4(i) + \tilde{W}_4(i)W_4(i)^{\jmath} + \tilde{W}_5(i)^{\jmath}W_5(i) + \tilde{W}_5(i)W_5(i)^{\jmath} + Q^{\jmath}\tilde{Q} + Q\tilde{Q}^{\jmath}\Big)$

subject to (4.11)-(4.12) and (11.24)

The obtained solutions are denoted as:

$$\begin{bmatrix} X(i), \tilde{S}(i), J(i), \tilde{R}_1(i), \tilde{R}_1, \tilde{R}_2(i), \tilde{R}_2, W_1(i), W_2(i), W_3(i), W_4(i), \\ W_5(i), \tilde{W}_1(i), \tilde{W}_2(i), \tilde{W}_4(i), \tilde{W}_5(i), \tilde{Q}, \mathcal{R}_1, \mathcal{R}_2, \tilde{Z}(i), Y(i) \end{bmatrix}^{\jmath+1}$$

Step 3: Solve Theorem 3.1 with $K(i)^{\jmath+1} = Y^{\jmath+1}(i)X^{-1}(i)^{\jmath+1}$, if there exist solutions, then $K(i)^{\jmath+1}$ are the desired controller gains and EXIT. Otherwise, if

$Tr\Big(\mathcal{R}_1^{\jmath}\tilde{R}_1 + \mathcal{R}_1\tilde{R}_1^{\jmath} + \mathcal{R}_2^{\jmath}\tilde{R} + \mathcal{R}_2\tilde{R}_2^{\jmath} + \tilde{W}_1(i)^{\jmath}W_1(i) + \tilde{W}_1(i)W_1(i)^{\jmath} + \tilde{W}_2(i)^{\jmath}W_2(i) + \tilde{W}_2(i)W_2(i)^{\jmath} + \tilde{W}_4(i)^{\jmath}W_4(i) + \tilde{W}_4(i)W_4(i)^{\jmath} + \tilde{W}_5(i)^{\jmath}W_5(i) + \tilde{W}_5(i)W_5(i)^{\jmath} + Q^{\jmath}\tilde{Q} + Q\tilde{Q}^{\jmath}\Big) > \epsilon$, set $\jmath = \jmath + 1$ and return to Step 2 where ϵ is tolerant else EXIT and no solution will be possible.

Chapter 12

Appendix

Proof of Theorem 5.3.1:

The system (5.5) can be written as

$$\zeta_{k+1} = \Gamma_1(r_k)\tilde{\zeta}_k$$
$$z_k = \Gamma_3(r_k)\tilde{\zeta}_k$$

where $\zeta(k+1) = \zeta_{k+1}$, $\Gamma_1(r_k)$ and Γ_3 are given in (5.13) and $\tilde{\zeta}_k$ is defined in Lemma 5.2.1.

Select the L-K candidate functional for the closed loop system as:

$$V(\zeta_k, r_k) = V_1(\zeta_k, r_k) + V_2(\zeta_k, r_k) + V_3(\zeta_k, r_k) \tag{12.1}$$

with

$$V_1(\zeta_k, r_k) = \zeta_k^T P(r_k)\zeta_k \tag{12.2}$$

$$V_2(\zeta_k, r_k) = \sum_{\ell=-\tau(r_k)}^{-1} \sum_{j=k+\ell}^{k-1} \bar{x}_j^T R_1 \bar{x}_j + \sum_{\ell=-\tau(s)}^{-1} \sum_{j=k+\ell}^{k-1} \bar{x}_j^T R_2 \bar{x}_j \tag{12.3}$$

$$V_3(\zeta_k, r_k) = \sum_{\ell=k-\tau(r_k)}^{k-1} \zeta_\ell^T Q\zeta_\ell + \sum_{\ell=-\tau(s)+2}^{-\tau(1)+1} \sum_{j=k+\ell-1}^{k-1} \zeta_j^T Q\zeta_j \tag{12.4}$$

Along any trajectory of the closed-loop system, the expectation value of the first forward difference of $V(x_k, r_k)$ is given as follows:

$$\Delta V(\zeta_k, r_k) = \Delta V_1(\zeta_k, r_k) + \Delta V_2(\zeta_k, r_k) + \Delta V_3(\zeta_k, r_k) \tag{12.5}$$

After mathematical manipulation :

$$\begin{aligned}
\Delta V_1(\zeta_k, r_k) &= \zeta_{k+1}^T \tilde{P}(r_k)\zeta_{k+1} - \zeta_k^T P(r_k)\zeta_k \\
&= \tilde{\zeta}_k^T \Gamma_1^T \tilde{P}(r_k)\Gamma_1 \tilde{\zeta}_k - \zeta_k^T P(r_k)\zeta_k
\end{aligned} \tag{12.6}$$

$$\Delta V_2(\zeta_k, r_k) \leq \bar{x}_k^T \Big[\tilde{\tau}(r_k)R_1 + \tau(s)R_2\Big]\bar{x}_k - \sum_{\ell=k-\tau(r_k)}^{k-1} \bar{x}_\ell^T \Big[(1 - p_{r_k(r_k+1)})R_1 + R_2\Big]\bar{x}_\ell \tag{12.7}$$

and

$$\Delta V_3(\zeta_k, r_k) \leq (\tau(s) - \tau(1) + 1)\zeta_k^T Q\zeta_k - \zeta_{k-\tau(r_k)}^T Q\zeta_{k-\tau(r_k)}. \tag{12.8}$$

Using Lemma 5.2.1 and $\bar{x}_k = x_{k+1} - x_k = \Gamma_2(r_k)$, we have

$$\Delta V_2(\zeta_k, r_k) \leq \tilde{\zeta}_k^T \Big\{\Gamma_2^T \left[\tilde{\tau}(r_k)R_1 + \tau(s)R_2\right]\Gamma_2 + \Upsilon_1(r_k) + \Upsilon_1^T(r_k) + \tau(r_k)Z(r_k)\Big\}\tilde{\zeta}_k \tag{12.9}$$

where $\Gamma_2(r_k)$ is given in (5.13).

Putting (12.6-12.8) in (12.5), we obtain

$$\begin{aligned}
\Delta V(\zeta_k, r_k) \leq &-\zeta_k^T \Big(P(r_k) - (\tau(s) - \tau(1) + 1)Q\Big)\zeta_k - \zeta_{k-\tau(r_k)}^T Q\zeta_{k-\tau(r_k)} + \tilde{\zeta}_k^T \Big\{\Gamma_1^T \tilde{P}(r_k) \\
&\Gamma_1 + \Gamma_2^T \left[\tilde{\tau}(r_k)R_1 + \tau(s)R_2\right]\Gamma_2 + \Upsilon_1(r_k) + \Upsilon_1^T(r_k) + \tau(r_k)Z(r_k)\Big\}\tilde{\zeta}_k
\end{aligned} \tag{12.10}$$

Using Assumption 3.2.1 given in Chapter 4, and adding and subtracting $\zeta_k^T \bar{H}_1^T(r_k)F_k^T W_1(rk)F_k\bar{H}_1(r_k)\zeta_k$, $\Big(\zeta_{v-\tau(r_v)} - \zeta_{k-\tau(r_k)}\Big)^T \Big(\zeta_{v-\tau(r_v)} - \zeta_{k-\tau(r_k)}\Big)$, $\Big(\zeta^T(\vartheta) - \zeta^T(k)\Big)C_{cl}^T(r_k)C_{cl}(r_k)\Big(\zeta(\vartheta) - \zeta(k)\Big)$, $w_k^T H_2^T F_k^T W_2(r_k)F_k H_2 w_k$, $\Big(\zeta^T(\vartheta) - \zeta^T(k)\Big)C_{cl}^T(r_k)H_3^T F^T(k)W_3(r_k)F(k)H_3 C_{cl}(r_k)\Big(\zeta(\vartheta) -$

$\zeta(k)\Big)$, $z_k^T z_k$ and $\gamma^2 w_k^T w_k$ to and from (12.10), we obtain

$$
\begin{aligned}
\Delta V(\zeta_k, r_k) \leq & -\zeta_k^T \Big(P(r_k) - (\tau(s) - \tau(1) + 1)Q - \delta_2^2 C_{cl}^T(r_k)C_{cl}(r_k) - \bar{H}_1^T(r_k)F_k^T W_1(r_k) \\
& F_k \bar{H}_1(r_k) - \delta_2^2 C_{cl}^T(r_k)H_3^T W_3(r_k)H_3 C_{cl}(r_k) \Big)\zeta_k - \zeta_{k-\tau(r_k)}^T \delta_1^2 \zeta_{k-\tau(r_k)} + \tilde{\zeta}_k^T \\
& \Big\{ \Gamma_1^T \tilde{P}(r_k)\Gamma_1 + \Gamma_2^T \left[\tilde{\tau}(r_k)R_1 + \tau(s)R_2\right]\Gamma_2 + \Upsilon_1(r_k) + \Upsilon_1^T(r_k) + \tau(r_k)Z(r_k) \\
& + \Gamma_3^T \Gamma_3 \Big\}\tilde{\zeta}_k - z_k^T z_k + \gamma^2 w_k^T w_k - w_k^T \Big(\gamma^2 I - H_2^T W_2(r_k)H_2 \Big)w_k - \Big(\zeta_{\upsilon-\tau(r_\upsilon)} - \\
& \zeta_{k-\tau(r_k)}\Big)^T \Big(\zeta_{\upsilon-\tau(r_\upsilon)} - \zeta_{k-\tau(r_k)}\Big) - \zeta_k^T \bar{H}_1^T(r_k)F_k^T W_1(r_k)F_k \bar{H}_1(r_k)\zeta_k - w_k^T \\
& H_2^T F_k^T W_2(r_k)F_k H_2 w_k - \Big(\zeta^T(\vartheta) - \zeta^T(k)\Big)C_{cl}^T(r_k)C_{cl}(r_k)\Big(\zeta(\vartheta) - \zeta(k)\Big) - \\
& \Big(\zeta^T(\vartheta) - \zeta^T(k)\Big)C_{cl}^T(r_k)H_3^T F^T(k)W_3(r_k)F(k)H_3 C_{cl}(r_k)\Big(\zeta(\vartheta) - \zeta(k)\Big)
\end{aligned}
$$

$$(12.11)$$

Using (5.13), (12.11) can be rewritten as

$$
\begin{aligned}
\Delta V(x_k, r_k) \leq & \ \tilde{\zeta}_k^T \Big\{ \Lambda(r_k) + \Gamma_1^T \tilde{P}(r_k)\Gamma_1 + \Gamma_2^T \left[\tilde{\tau}(r_k)R_1 + \tau(s)R_2\right]\Gamma_2 + \Upsilon_1(r_k) + \Upsilon_1^T(r_k) \\
& + \tau(r_k)Z(r_k) + \Gamma_3^T \Gamma_3 \Big\}\tilde{\zeta}_k - z_k^T z_k + \gamma^2 w_k^T w_k
\end{aligned}
$$

$$(12.12)$$

Using (5.12), we have

$$\Delta V(\zeta_k, r_k) \leq -z_k^T z_k + \gamma^2 w_k^T w_k \tag{12.13}$$

Taking expectation and sum from 0 to ∞ on both sides of (12.13) yields

$$E\{V(\zeta_\infty, r_\infty)\} - E\{V(\zeta_0, r_0)\} \leq -E\Big\{ \sum_{\ell=0}^{\infty} z_\ell^T z_\ell \Big\} + \gamma^2 \sum_{\ell=0}^{\infty} w_\ell^T w_\ell \tag{12.14}$$

As initial condition are considered zero i.e, $V(\zeta_0, r_0) = 0$, so

$$E\Big\{ \sum_{\ell=0}^{\infty} z_\ell^T z_\ell \Big\} \leq \gamma^2 \sum_{\ell=0}^{\infty} w_\ell^T w_\ell \tag{12.15}$$

If $w(k) = 0, \forall k \geq 0$ closed-loop system should be stochastically stable. From (12.12) and (5.12), we learn that

$$V(\zeta_{(k+1)}, r_{(k+1)}) - V(\zeta_k, r_k) \leq -\beta \tilde{\zeta}_k^T \tilde{\zeta}_k \tag{12.16}$$

where $\beta = \inf\{\Lambda(r_k)_{\min}[-\mathcal{M}(r_k)], r_k \in S\}$ with

$$
\begin{aligned}
\mathcal{M} &= \Lambda(r_k) + \Gamma_1^T(r_k)\tilde{P}(r_k)\Gamma_1(r_k) + \Gamma_2^T(r_k)\left[\tilde{\tau}(r_k)R_1 + \tau(s)R_2\right]\Gamma_2(r_k) \\
&+ \Upsilon_1(r_k) + \Upsilon_1^T(r_k) + \tau(r_k)Z(r_k) + \Gamma_3^T(r_k)\Gamma_3(r_k)
\end{aligned}
\tag{12.17}
$$

Summing from 0 to ∞ and by taking expectation on both sides of (12.16) gives

$$
\begin{aligned}
E\{V(\zeta_\infty, r_\infty)\} - E\{V(\zeta_0, r_0)\} &\leq -\beta E\left\{\sum_{k=0}^{\infty} \tilde{\zeta}_\ell^T \tilde{\zeta}_\ell\right\} \\
&\leq -\beta E\left\{\sum_{k=0}^{\infty} \zeta_\ell^T \zeta_\ell\right\}
\end{aligned}
\tag{12.18}
$$

Re-arranging (12.18), we have

$$
\begin{aligned}
E\left\{\sum_{k=0}^{\infty} \zeta_\ell^T \zeta_\ell\right\} &\leq \frac{1}{\beta}E\{V(\zeta_0, r_0)\} - \frac{1}{\beta}E\{V(\zeta_\infty, r_\infty)\} \\
&\leq \alpha
\end{aligned}
\tag{12.19}
$$

where $\alpha = \frac{1}{\beta}E\{V(\zeta_0, r_0)\} < \infty$. This shows that the closed loop system is stable and (5.7) holds. $\qquad \nabla\nabla\nabla$

Proof of Theorem 5.3.2:

Applying Schur complement on (5.12), we have

$$
\begin{bmatrix}
\Pi(i) & \Gamma_1^T(i) & \Gamma_2^T(i) & \Gamma_3^T(i) & \Gamma_4^T(i) & \Gamma_5^T(i) & \Gamma_6^T(i) \\
* & -\tilde{P}^{-1}(i) & 0 & 0 & 0 & 0 & 0 \\
* & * & -R^{-1} & 0 & 0 & 0 & 0 \\
* & * & * & -I & 0 & 0 & 0 \\
* & * & * & * & -Q^{-1} & 0 & 0 \\
* & * & * & * & * & -\tilde{W}_1(i) & 0 \\
* & * & * & * & * & * & \mathcal{W}(i)
\end{bmatrix} < 0
\tag{12.20}
$$

where

$$
\begin{aligned}
\Pi(i) &= \tilde{\Lambda}(i) + \Upsilon_1(i) + \Upsilon_1^T(i) + \tau(i)Z(i) \\
\tilde{\Lambda}(i) &= \mathrm{diag}\left\{ -\tilde{P}(i), -Q, \left(H_2^T W_2(i) H_2 - \gamma^2 I\right), -W_1(i), -W_2(i), -I, -I, -W_3(i) \right\} \\
\Gamma_4(i) &= \left[\begin{array}{cccccccc} \sqrt{(\tau(s) - \tau(1) + 1)}I & 0 & 0 & 0 & 0 & 0 & 0 & 0 \end{array} \right], \\
\Gamma_5(i) &= \left[\begin{array}{cccccccc} \bar{H}_1(i) & 0 & 0 & 0 & 0 & 0 & 0 & 0 \end{array} \right], \\
\Gamma_6(i) &= \left[\begin{array}{cccccccc} 0 & \delta_1 I & 0 & 0 & 0 & 0 & 0 & 0 \\ \delta_2 \bar{C}_2 & 0 & 0 & 0 & 0 & 0 & 0 & 0 \\ \delta_2 H_3 \bar{C}_2 & 0 & 0 & 0 & 0 & 0 & 0 & 0 \end{array} \right]
\end{aligned}
$$

Following from [136], with loss of generality, $P(i)$ and $\tilde{P}(i)$ are, respectively, partitioned as

$$
P(i) = \left[\begin{array}{cc} X(i) & Y^{-1}(i) - X(i) \\ Y^{-1}(i) - X(i) & X(i) - Y^{-1}(i) \end{array} \right] \tag{12.21}
$$

and

$$
\tilde{P}(i) = \left[\begin{array}{cc} \tilde{X}(i) & \sum_{j=1}^{i+1} p_{ij} Y^{-1}(j) - \tilde{X}(i) \\ \sum_{j=1}^{i+1} p_{ij} Y^{-1}(j) - \tilde{X}(i) & \tilde{X}(i) - \sum_{j=1}^{i+1} p_{ij} Y^{-1}(j) \end{array} \right]. \tag{12.22}
$$

Now define

$$
T_2(i) = \left[\begin{array}{cc} I & \tilde{X}(i) \\ 0 & \sum_{j=1}^{i+1} p_{ij} Y^{-1}(j) - \tilde{X}(i) \end{array} \right] \tag{12.23}
$$

Multiplying (12.20) to the right by the matrix $\mathrm{diag}\left\{ \mathrm{diag}\left\{ T(i), I, I, I, I \right\}, T_2(i), I, I, I, I, I \right\}$ and the left by its transpose, we obtain (5.16) with $\left(\sum_{j=1}^{i+1} p_{ij} Y^{-1}(j) \right)^{-1}$ at the place of $\tilde{S}(i) - J(i) - J^T(i)$ in $\tilde{\Xi}(i)$, $\bar{Z}(i) = T^T(i) Z(i) T(i)$, $\bar{M}^T(i) = T^T(i) M^T(i) T(i)$, $\mathcal{R} = \mathrm{diag}\{ R_1^{-1}, R_2^{-1} \}$, $\mathcal{Q} = Q^{-1}$, $\mathcal{W}_1(i) = W_1^{-1}(i)$, $\mathcal{W}_2(i) = W_2^{-1}(i)$, and $\mathcal{A}(i), \mathcal{B}(i)$ and $\mathcal{C}(i)$ are given in Theorem 5.3.2.

Applying the Schur complement on (5.17) and consequently multiplying these inequalities by p_{ij} and summing up for all $j = S$, we obtain

$$
\begin{aligned}
\tilde{S}(i) - J^T(i) - J(i) &= -J^T(i) - J(i) + \sum_{j=1}^{i+1} p_{ij} S(i,j) \\
&\leq -J^T(i) - J(i) + J^T(i)\tilde{Y}^{-1}(i)J(i) \\
&= \Big(\sum_{j=1}^{i+1} p_{ij}Y^{-1}(j)\Big)^{-1} - \Big(J(i) - \Big(\sum_{j=1}^{i+1} p_{ij}Y^{-1}(j)\Big)^{-1}\Big)^T \\
&\quad \Big(\sum_{j=1}^{i+1} p_{ij}Y^{-1}(j)\Big)\Big(J(i) - \Big(\sum_{j=1}^{i+1} p_{ij}Y^{-1}(j)\Big)^{-1}\Big) \\
&\leq -\Big(\sum_{j=1}^{i+1} p_{ij}Y^{-1}(j)\Big)^{-1}
\end{aligned}
\tag{12.24}
$$

which implies that (5.16) remains valid if $\tilde{S}(i) - J^T(i) - J(i)$ is replaced by $\Big(\sum_{j=1}^{i+1} p_{ij}Y^{-1}(j)\Big)^{-1}$.

Multiplying (5.11) to the right by the matrix $\text{diag}\big\{T(i), T(i)\big\}$ and the left by its transpose, we obtain (5.15) with $T^T(i)\big((1 - p_{i(i+1)})R_1(i) + R_2(i)\big)T(i)$ at the place of $N(i)$ where $\bar{Z}(i) = T^T(i)Z(i)T(i)$ and $\bar{M}^T(i) = T^T(i)M^T(i)T(i)$.

Applying the Schur complement on (5.18) and consequently multiplying these inequalities by $T_1(i)$ to the right and its transpose to the left , we obtain

$$
T^T(i)\big((1 - p_{i(i+1)})R_1(i) + R_2(i)\big)T(i) > \mathcal{N}^{-1}(i)
\tag{12.25}
$$

which implies that (5.15) remains valid if $N(i)$ is replaced by $T^T(i)\big((1 - p_{i(i+1)})R_1(i) + R_2(i)\big)T(i)$ where $\mathcal{Y}(i) = Y^{-1}(i)$, $\mathcal{N}^{-1}(i) = N(i)$. This concludes the proof that the closed-loop system is stochastically stable with the prescribed $\mathcal{H}_\infty$ performance. $\nabla\nabla\nabla$

Remark 12.0.1. Theorem 3.2 LMI is not strict LMI due to equality constraints in (5.20). However, the cone complementarity linearization algorithm that suggested in [127] can be used to convert it into nonlinear minimization problem subject to specific LMIs.

Using cone complementary algorithm, the feasibility problem formulated by (5.14)-(5.18) which is not a convex problem can be converted into the following nonlinear minimization problem subject to LMIs:

Minimize $Tr\Big(\mathcal{R}_1 R_1 + \mathcal{R}_2 R_2 + \mathcal{W}_1(i)W_1(i) + \mathcal{W}_3(i)W_3(i) + \mathcal{N}(i)N(i) + \mathcal{Y}(i)Y(i) + \mathcal{Q}Q\Big)$

subject to (5.14)-(5.18) and

$$\begin{bmatrix} \mathcal{R}_1 & I \\ I & R_1 \end{bmatrix} \geq 0, \begin{bmatrix} \mathcal{R}_2 & I \\ I & R_2 \end{bmatrix} \geq 0, \begin{bmatrix} \mathcal{W}_1(i) & I \\ I & W_1(i) \end{bmatrix} \geq 0, \begin{bmatrix} \mathcal{W}_3(i) & I \\ I & W_3(i) \end{bmatrix} \geq 0$$

$$\begin{bmatrix} \mathcal{N}(i) & I \\ I & N(i) \end{bmatrix} \geq 0, \begin{bmatrix} \mathcal{Y}(i) & I \\ I & Y(i) \end{bmatrix} \geq 0 \begin{bmatrix} \mathcal{Q} & I \\ I & Q \end{bmatrix} \geq 0 \qquad (12.26)$$

To solve this optimization problem, the following algorithm can be used:

Algorithm :

Step 1: Set $\jmath = 0$ and solve (5.14)-(5.18) and (12.26) to obtain the initial conditions,

$$\begin{bmatrix} X(i), \tilde{S}(i), J(i), R_1(i), R_1, R_2(i), R_2, W_1(i), W_2(i), W_3(i), \\ \mathcal{W}_1(i), \mathcal{W}_3(i), Q, \tilde{Q}, \mathcal{R}_1, \mathcal{R}_2, \tilde{Z}(i), Y(i), \mathcal{Y}(i), N(i), \mathcal{N}(i) \end{bmatrix}^0$$

Step 2: Solve the LMI problem

Minimize $Tr\Big(\mathcal{R}_1^\jmath R_1 + \mathcal{R}_1 R_1^\jmath + \mathcal{R}_2^\jmath R_2 + \mathcal{R}_2 R_2^\jmath + \mathcal{W}_1(i)^\jmath W_1(i) + \mathcal{W}_1(i)W_1(i)^\jmath + \mathcal{W}_3(i)^\jmath W_3(i) + \mathcal{W}_3(i)W_3(i)^\jmath + Q^\jmath \mathcal{Q} + Q\mathcal{Q}^\jmath + N^\jmath(i)\mathcal{N}(i) + N(i)\mathcal{N}^\jmath(i) + Y^\jmath(i)\mathcal{Y}(i) + Y(i)\mathcal{Y}^\jmath(i)\Big)$

subject to (5.14)-(5.18) and (12.26)

The obtained solutions are denoted as:

$$\begin{bmatrix} X(i), \tilde{S}(i), J(i), R_1(i), R_1, R_2(i), R_2, W_1(i), W_2(i), W_3(i), \\ \mathcal{W}_1(i), \mathcal{W}_3(i), Q, \tilde{Q}, \mathcal{R}_1, \mathcal{R}_2, \tilde{Z}(i), Y(i), \mathcal{Y}(i), N(i), \mathcal{N}(i) \end{bmatrix}^{\jmath+1}$$

Step 3: Solve Theorem 3.1 with $K(i)^{\jmath+1} = Y^{\jmath+1}(i)X^{-1}(i)^{\jmath+1}$, if there exist solutions, then $K(i)^{\jmath+1}$ are the desired controller gains and EXIT. Otherwise, if
$Tr\Big(\mathcal{R}_1^\jmath R_1 + \mathcal{R}_1 R_1^\jmath + \mathcal{R}_2^\jmath R_2 + \mathcal{R}_2 R_2^\jmath + \mathcal{W}_1(i)^\jmath W_1(i) + \mathcal{W}_1(i)W_1(i)^\jmath + \mathcal{W}_3(i)^\jmath W_3(i) + \mathcal{W}_3(i)W_3(i)^\jmath + Q^\jmath \mathcal{Q} + Q\mathcal{Q}^\jmath + N^\jmath(i)\mathcal{N}(i) + N(i)\mathcal{N}^\jmath(i) + Y^\jmath(i)\mathcal{Y}(i) + Y(i)\mathcal{Y}^\jmath(i)\Big) > \epsilon$,
set $\jmath = \jmath + 1$ and return to Step 2 where ϵ is tolerant else EXIT and no solution will be possible.

Chapter 13

Appendix

Proof of Theorem 3.1:

The system (6.11) can be written as

$$
\begin{aligned}
\zeta_{k+1} &= \sum_{g=1}^{2^r} \sum_{h=1}^{2^m} \lambda_{1g}(k)\lambda_{2h}(k)\Big(\Gamma_1^{g,h}(r_k)\tilde{\zeta}_k\Big) \\
z_k &= \sum_{g=1}^{2^r} \sum_{h=1}^{2^m} \lambda_{1g}(k)\lambda_{2h}(k)\Big(\Gamma_3^{h}(r_k)\tilde{\zeta}_k\Big)
\end{aligned}
\tag{13.1}
$$

where $\zeta(k+1) = \zeta_{k+1}$, $\Gamma_1^{g,h}(r_k)$ and $\Gamma_3^{h}(r_k)$ are given in (6.18) and $\tilde{\zeta}_k$ is defined in Lemma 6.2.1.

Select the L-K candidate functional for the closed loop system as:

$$
V(\zeta_k, r_k) = V_1(\zeta_k, r_k) + V_2(\zeta_k, r_k) + V_3(\zeta_k, r_k)
\tag{13.2}
$$

$$
V_1(\zeta_k, r_k) = \zeta_k^T P(r_k)\zeta_k
\tag{13.3}
$$

$$
V_2(\zeta_k, r_k) = \sum_{l=1}^{r} \Big(\sum_{\ell=-\tau^l(r_k)}^{-1} \sum_{j=k+\ell}^{k-1} \bar{x}_j^T R_1 \bar{x}_j + \sum_{\ell=-\tau^l(s)}^{-1} \sum_{j=k+\ell}^{k-1} \bar{x}_j^T R_2 \bar{x}_j \Big)
\tag{13.4}
$$

$$
V_3(\zeta_k, r_k) = \sum_{l=1}^{r} \Big(\sum_{\ell=k-\tau^l(r_k)}^{k-1} \zeta_\ell^T Q^l \zeta_\ell + \sum_{\ell=-\tau^l(s)+2}^{-\tau^l(1)+1} \sum_{j=k+\ell-1}^{k-1} \zeta_j^T Q^l \zeta_j \Big)
\tag{13.5}
$$

First forward difference of $V(\zeta_k, r_k)$ is given as follows:

$$
\Delta V(\zeta_k, r_k) = \Delta V_1(\zeta_k, r_k) + \Delta V_2(\zeta_k, r_k) + \Delta V_3(\zeta_k, r_k)
\tag{13.6}
$$

$$\Delta V_1(\zeta_k, r_k) = \zeta_{k+1}^T \tilde{P}(r_k)\zeta_{k+1} - \zeta_k^T P(r_k)\zeta_k$$

$$= \sum_{g=1}^{2^r}\sum_{h=1}^{2^m}\sum_{u=1}^{2^r}\sum_{v=1}^{2^m} \lambda_{1g}(k)\lambda_{2h}(k)\lambda_{1u}(k)\lambda_{2v}(k)\tilde{\zeta}_k^T \left(\Gamma_1^{g,h}(r_k)\right)^T \tilde{P}(r_k)\Gamma_1^{u,v}(r_k)\tilde{\zeta}_k$$

$$-\zeta_k^T P(r_k)\zeta_k$$

$$= \frac{1}{4}\sum_{g=1}^{2^r}\sum_{h=1}^{2^m}\sum_{u=1}^{2^r}\sum_{v=1}^{2^m} \lambda_{1g}(k)\lambda_{2h}(k)\lambda_{1u}(k)\lambda_{2v}(k)\tilde{\zeta}_k^T \left(\Gamma_1^{g,h}(r_k) + \Gamma_1^{h,g}(r_k)\right)^T \tilde{P}(r_k)$$

$$\left(\Gamma_1^{u,v}(r_k) + \Gamma_1^{v,u}(r_k)\right)\tilde{\zeta}_k - \zeta_k^T P(r_k)\zeta_k \tag{13.7}$$

Using Lemma(6.2.2) and noting (6.10):

$$\sum_{g=1}^{2^r}\sum_{h=1}^{2^m}\sum_{u=1}^{2^r}\sum_{v=1}^{2^m} \lambda_{1g}(k)\lambda_{2h}(k)\lambda_{1u}(k)\lambda_{2v}(k)\tilde{\zeta}_k^T \left(\Gamma_1^{g,h}(r_k) + \Gamma_1^{h,g}(r_k)\right)^T \tilde{P}(r_k)$$

$$\left(\Gamma_1^{u,v}(r_k) + \Gamma_1^{v,u}(r_k)\right)\tilde{\zeta}_k \leq \sum_{g=1}^{2^r}\sum_{h=1}^{2^m} \lambda_{1g}(k)\lambda_{2h}(k)\tilde{\zeta}_k^T \left(\Gamma_1^{g,h}(r_k)\right.$$

$$\left.+\Gamma_1^{h,g}(r_k)\right)^T \tilde{P}(r_k)\left(\Gamma_1^{g,h}(r_k) + \Gamma_1^{h,g}(r_k)\right)\tilde{\zeta}_k$$

It implies that

$$\Delta V_1(\zeta_k, r_k) \leq \frac{1}{4}\sum_{g=1}^{2^r}\sum_{h=1}^{2^m} \lambda_{1g}(k)\lambda_{2h}(k)\tilde{\zeta}_k^T \left(\Gamma_1^{g,h}(r_k) + \Gamma_1^{h,g}(r_k)\right)^T \tilde{P}(r_k)$$

$$\left(\Gamma_1^{g,h}(r_k) + \Gamma_1^{h,g}(r_k)\right)\tilde{\zeta}_k - \zeta_k^T P(r_k)\zeta_k \tag{13.8}$$

$$\Delta V_2(\zeta_k, r_k) = V_2(\zeta_{k+1}, r_{k+1}) - V_2(\zeta_k, r_k)$$

$$= \sum_{l=1}^{r} \Big(\sum_{i=1}^{s} p_{r_k i} \sum_{\ell=-\tau^l(i)}^{-1} \sum_{j=k+1+\ell}^{k} \bar{x}_j^T R_1 \bar{x}_j - \sum_{\ell=-\tau_k^l}^{-1} \sum_{j=k+\ell}^{k-1} \bar{x}_j^T R_1 \bar{x}_j$$

$$+ \sum_{\ell=-\tau^l(s)}^{-1} \sum_{j=k+1+\ell}^{k} \bar{x}_j^T R_2 \bar{x}_j - \sum_{\ell=-\tau^l(s)}^{-1} \sum_{j=k+\ell}^{k-1} \bar{x}_j^T R_2 \bar{x}_j \Big)$$

$$= \sum_{l=1}^{r} \sum_{i=1}^{s} p_{r_k i} \left\{ \sum_{\ell=-\tau^l(i)}^{-1} \bar{x}_k^T R_1 \bar{x}_k + \sum_{\ell=-\tau^l(i)}^{-1} \sum_{j=k+1+\ell}^{k-1} \bar{x}_j^T R_1 \bar{x}_j \right.$$

$$\left. - \sum_{\ell=-\tau_k^l}^{-1} \sum_{j=k+\ell+1}^{k-1} \bar{x}_j^T R_1 \bar{x}_j - \sum_{\ell=-\tau_k^l}^{-1} \bar{x}_{k+\ell}^T R_1 \bar{x}_{k+\ell} \right\} +$$

$$\sum_{l=1}^{r} \sum_{\ell=-\tau^l(s)}^{-1} \left\{ \bar{x}_k^T R_2 \bar{x}_k - \bar{x}_{k+\ell}^T R_2 \bar{x}_{k+\ell} \right\}$$

$$= \sum_{l=1}^{r} \sum_{i=1}^{s} p_{r_k i} \left\{ \sum_{\ell=-\tau^l(i)}^{-1} \sum_{j=k+1+\ell}^{k-1} \bar{x}_j^T R_1 \bar{x}_j - \sum_{\ell=-\tau_k^l}^{-1} \sum_{j=k+\ell+1}^{k-1} \bar{x}_j^T R_1 \bar{x}_j - \right.$$

$$\left. \sum_{j=k-\tau_k^l}^{k-1} \bar{x}_j^T R_1 \bar{x}_j \right\} - \sum_{l=1}^{r} \sum_{j=k-\tau^l(s)}^{k-1} \bar{x}_j^T R_2 \bar{x}_j + \sum_{l=1}^{r} \left(\bar{x}_k^T \left[\tilde{\tau}^l{}_k R_1 + \tau^l(s) R_2 \right] \bar{x}_k \right)$$

$$= \sum_{l=1}^{r} \sum_{i=1}^{s} p_{r_k i} \left\{ \sum_{\ell=-\tau^l(i)}^{-(\tau_k^l+1)} \sum_{j=k+1+\ell}^{k-1} \bar{x}_j^T R_1 \bar{x}_j - \sum_{j=k-\tau_k^l}^{k-1} \bar{x}_j^T R_1 \bar{x}_j \right\}$$

$$- \sum_{l=1}^{r} \sum_{j=k-\tau^l(s)}^{k-1} \bar{x}_j^T R_2 \bar{x}_j + \sum_{l=1}^{r} \left(\bar{x}_k^T \left[\tilde{\tau}^l{}_k R_1 + \tau^l(s) R_2 \right] \bar{x}_k \right) \qquad (13.9)$$

Using the transition probability matrix and the fact $\tau^l(1) \le \tau_{k+1}^l \le \tau_k^l + 1 \le \tau^l(s)$ and $\tau^l(1) \le \tau_k^l \le \tau^l(s)$:

$$\Delta V_2(\zeta_k, r_k) \le \sum_{l=1}^{r} \left(\bar{x}_k^T \left[\tilde{\tau}^l(r_k) R_1 + \tau^l(s) R_2 \right] \bar{x}_k \right) -$$

$$\sum_{l=1}^{r} \left(\sum_{\ell=k-\tau^l(r_k)}^{k-1} \bar{x}_\ell^T \left[(1 - p_{r_k(r_k+1)}) R_1 + R_2 \right] \bar{x}_\ell \right)$$

$$(13.10)$$

Using Lemma 6.2.1 and $\bar{x}_k = x_{k+1} - x_k = \sum_{g=1}^{2^r} \sum_{h=1}^{2^m} \lambda_{1g}(k) \lambda_{2h}(k) \Gamma_2^h(r_k) \tilde{\zeta}_k$, we have:

$$\Delta V_2(\zeta_k, r_k) \le \tilde{\zeta}_k^T \left\{ \sum_{g=1}^{2^r} \sum_{h=1}^{2^m} \sum_{u=1}^{2^r} \sum_{v=1}^{2^m} \lambda_{1g}(k) \lambda_{2h}(k) \lambda_{1u}(k) \lambda_{2v}(k) (\Gamma_2^h)^T \sum_{l=1}^{r} \left[\tilde{\tau}^l(r_k) R_1 \right. \right.$$

$$\left. \left. + \tau^l(s) R_2 \right] \Gamma_2^v + \Upsilon_1(r_k) + \Upsilon_1^T(r_k) + \sum_{l=1}^{r} \tau^l(r_k) Z(r_k) \right\} \tilde{\zeta}_k \qquad (13.11)$$

where $\Gamma_2^h(r_k)$ is given in (6.18).

and

$$\Delta V_3(\zeta_k, r_k) \leq \sum_{l=1}^{r} \left((\tau^l(s) - \tau^l(1) + 1)\zeta_k^T Q^l \zeta_k - \zeta_{k-\tau^l(r_k)}^T Q^l \zeta_{k-\tau^l(r_k)} \right). \qquad (13.12)$$

Therefore, by putting (13.7) to (13.12) in (13.6):

$$\begin{aligned}
\Delta V(\zeta_k, r_k) &\leq -\zeta_k^T \Big(P(r_k) - \sum_{l=1}^{r}(\tau^l(s) - \tau^l(1) + 1)Q^l \Big)\zeta_k - \sum_{l=1}^{r} \zeta_{k-\tau^l(r_k)}^T Q^l \zeta_{k-\tau^l(r_k)} + \\
&\quad \tilde{\zeta}_k^T \Big\{ \frac{1}{4} \sum_{g=1}^{2^r} \sum_{h=1}^{2^m} \sum_{u=1}^{2^r} \sum_{v=1}^{2^m} \lambda_{1g}(k)\lambda_{2h}(k)\lambda_{1u}(k)\lambda_{2v}(k) \Big[\Big(\Gamma_1^{g,h}(r_k) + \Gamma_1^{h,g}(r_k) \Big)^T \\
&\quad \tilde{P}(r_k) \Big(\Gamma_1^{u,v}(r_k) + \Gamma_1^{v,u}(r_k) \Big) + \Big(\Gamma_2^g + \Gamma_2^h \Big)^T \sum_{l=1}^{r} (\tilde{\tau}^l(r_k)R_1 + \tau^l(s)R_2) \\
&\quad \Big(\Gamma_2^u + \Gamma_2^v \Big) \Big] + \Upsilon_1(r_k) + \Upsilon_1^T(r_k) + \sum_{l=1}^{r} \tau^l(r_k)Z(r_k) \Big\} \tilde{\zeta}_k \qquad (13.13)
\end{aligned}$$

Using Assumption 3.2.1 and adding and subtracting $w_k^T H_2^T F_k^T W_2(r_k) F_k H_2 w_k$, $z_k^T z_k$ $\gamma^2 w_k^T w_k$ and $\sum_{g=1}^{2^r} \sum_{h=1}^{2^m} \sum_{u=1}^{2^r} \sum_{v=1}^{2^m} \lambda_{1g}(k)\lambda_{2h}(k)\lambda_{1u}(k)\lambda_{2v}(k)\zeta_k^T (\bar{H}_1^h)^T(r_k) F_k^T W_1(rk)$ $F_k \bar{H}_1^v(r_k)\zeta_k$, to and from (13.13), we obtain:

$$\begin{aligned}
\Delta V(\zeta_k, r_k) &\leq -\zeta_k^T \Big[P(r_k) - \sum_{l=1}^{r}(\tau^l(s) - \tau^l(1) + 1)Q^l - \sum_{g=1}^{2^r} \sum_{h=1}^{2^m} \sum_{u=1}^{2^r} \sum_{v=1}^{2^m} \lambda_{1g}(k)\lambda_{2h}(k) \\
&\quad \lambda_{1u}(k)\lambda_{2v}(k) \Big(\bar{H}_1^h(r_k) \Big)^T F_k^T W_1(r_k) F_k \bar{H}_1^v(r_k) \Big]\zeta_k - \zeta_{k-\tau^1(r_k)}^T Q^1 \zeta_{k-\tau^1(r_k)} \\
&\quad \cdots \zeta_{k-\tau^r(r_k)}^T Q^r \zeta_{k-\tau^r(r_k)} + \frac{1}{4} \tilde{\zeta}_k^T \Big\{ \sum_{g=1}^{2^r} \sum_{h=1}^{2^m} \sum_{u=1}^{2^r} \sum_{v=1}^{2^m} \lambda_{1g}(k)\lambda_{2h}(k)\lambda_{1u}(k)\lambda_{2v}(k) \\
&\quad \Big(\Gamma_1^{g,h}(r_k) + \Gamma_1^{h,g}(r_k) \Big)^T \tilde{P}(r_k) \Big(\Gamma_1^{u,v}(r_k) + \Gamma_1^{v,u}(r_k) \Big) + \Big(\Gamma_2^g + \Gamma_2^h \Big)^T \sum_{l=1}^{r} \\
&\quad (\tilde{\tau}^l(r_k)R_1 + \tau^l(s)R_2) \Big(\Gamma_2^u + \Gamma_2^v \Big) + \Big(\Gamma_3^g + \Gamma_3^h \Big)^T \Big(\Gamma_3^u + \Gamma_3^v \Big) + 4\Upsilon_1(r_k) \\
&\quad + 4\Upsilon_1^T(r_k) + 4 \sum_{l=1}^{r} \tau^l(r_k)Z(r_k) \Big\} \tilde{\zeta}_k - z_k^T z_k + \gamma^2 w_k^T w_k - w_k^T \Big(\gamma^2 I - H_2^T \\
&\quad W_2(r_k)H_2 \Big) w_k - \frac{1}{4} \sum_{g=1}^{2^r} \sum_{h=1}^{2^m} \sum_{u=1}^{2^r} \sum_{v=1}^{2^m} \lambda_{1g}(k)\lambda_{2h}(k)\lambda_{1u}(k)\lambda_{2v}(k)\zeta_k^T \Big(\bar{H}_1^g(r_k) + \\
&\quad \bar{H}_1^h(r_k) \Big)^T F_k^T W_1(r_k) F_k \Big(\bar{H}_1^u(r_k) + \bar{H}_1^v(r_k) \Big)\zeta_k - w_k^T H_2^T F_k^T W_2(r_k) F_k H_2 w_k \\
&\qquad\qquad (13.14)
\end{aligned}$$

Using Lemma(6.2.2) and noting (6.10):

$$
\begin{aligned}
&\frac{1}{4}\sum_{g=1}^{2r}\sum_{h=1}^{2m}\sum_{u=1}^{2r}\sum_{v=1}^{2m}\lambda_{1g}(k)\lambda_{2h}(k)\lambda_{1u}(k)\lambda_{2v}(k)\Big\{\zeta_k^T\Big[\big(\bar{H}_1^g(r_k)+\bar{H}_1^h(r_k)\big)^T F_k^T W_1(r_k)F_k \\
&\big(\bar{H}_1^u(r_k)+\bar{H}_1^v(r_k)\big)\Big]\zeta_k + \tilde{\zeta}_k^T\Big[\big(\Gamma_1^{g,h}(r_k)+\Gamma_1^{h,g}(r_k)\big)^T\tilde{P}(r_k)\big(\Gamma_1^{u,v}(r_k)+\Gamma_1^{v,u}(r_k)\big)+ \\
&\big(\Gamma_2^g+\Gamma_2^h\big)^T\sum_{l=1}^{r}(\tilde{\tau}^l(r_k)R_1+\tau^l(s)R_2)\big(\Gamma_2^u+\Gamma_2^v\big)+\big(\Gamma_3^g+\Gamma_3^h\big)^T\big(\Gamma_3^u+\Gamma_3^v\big) \\
&+4\Upsilon_1(r_k)+4\Upsilon_1^T(r_k)+4\sum_{l=1}^{r}\tau^l(r_k)Z(r_k)\Big]\tilde{\zeta}_k\Big\} \\
\leq\ &\frac{1}{4}\sum_{g=1}^{2r}\sum_{h=1}^{2m}\lambda_{1g}(k)\lambda_{2h}(k)\Big\{\zeta_k^T\Big[\big(\bar{H}_1^g(r_k)+\bar{H}_1^h(r_k)\big)^T F_k^T W_1(r_k)F_k\big(\bar{H}_1^g(r_k)+\bar{H}_1^h(r_k)\big)\Big]\zeta_k \\
&+\tilde{\zeta}_k^T\Big[\big(\Gamma_1^{g,h}(r_k)+\Gamma_1^{h,g}(r_k)\big)^T\tilde{P}(r_k)\big(\Gamma_1^{g,h}(r_k)+\Gamma_1^{h,g}(r_k)\big)+\big(\Gamma_2^g+\Gamma_2^h\big)^T \\
&\sum_{l=1}^{r}(\tilde{\tau}^l(r_k)R_1+\tau^l(s)R_2)\big(\Gamma_2^g+\Gamma_2^h\big)+\big(\Gamma_3^g+\Gamma_3^h\big)^T\big(\Gamma_3^g+\Gamma_3^h\big)+4\Upsilon_1(r_k)+4\Upsilon_1^T(r_k)+ \\
&4\sum_{l=1}^{r}\tau^l(r_k)Z(r_k)\Big]\tilde{\zeta}_k\Big\}
\end{aligned}
\tag{13.15}
$$

Using (6.18) and(13.15), (13.14) can be rewritten as:

$$
\begin{aligned}
\Delta V(x_k,r_k)\ \leq\ &\frac{1}{4}\sum_{g=1}^{2r}\sum_{h=1}^{2m}\lambda_{1g}(k)\lambda_{2h}(k)\tilde{\zeta}_k^T\Big\{\Lambda^{g,h}(r_k)+\big(\Gamma_1^{g,h}(r_k)+\Gamma_1^{h,g}(r_k)\big)^T \\
&\tilde{P}(r_k)\big(\Gamma_1^{g,h}(r_k)+\Gamma_1^{h,g}(r_k)\big)+\big(\Gamma_2^g+\Gamma_2^h\big)^T\sum_{l=1}^{r}(\tilde{\tau}^l(r_k)R_1+\tau^l(s)R_2) \\
&\big(\Gamma_2^g+\Gamma_2^h\big)+\big(\Gamma_3^g+\Gamma_3^h\big)^T\big(\Gamma_3^g+\Gamma_3^h\big)\Big]+4\Upsilon_1(r_k)+4\Upsilon_1^T(r_k) \\
&+4\sum_{l=1}^{r}\tau^l(r_k)Z(r_k)\Big\}\tilde{\zeta}_k-z_k^Tz_k+\gamma^2 w_k^T w_k
\end{aligned}
\tag{13.16}
$$

Using (6.17), we have:

$$
\Delta V(\zeta_k,r_k)\leq -z_k^Tz_k+\gamma^2 w_k^T w_k
\tag{13.17}
$$

Taking expectation and sum from 0 to ∞ on both sides of (13.17) yields:

$$
E\{V(\zeta_\infty,r_\infty)\}-E\{V(\zeta_0,r_0)\}\leq -E\Big\{\sum_{\ell=0}^{\infty}z_\ell^Tz_\ell\Big\}+\gamma^2\sum_{\ell=0}^{\infty}w_\ell^T w_\ell
\tag{13.18}
$$

As initial conditions are considered zero i.e, $V(\zeta_0, r_0) = 0$, so

$$E\left\{ \sum_{\ell=0}^{\infty} z_\ell^T z_\ell \right\} \leq \gamma^2 \sum_{\ell=0}^{\infty} w_\ell^T w_\ell \qquad (13.19)$$

If $w(k) = 0, \forall k \geq 0$ closed-loop system should be stochastically stable. From (13.16) and (6.17), we learn that

$$V(\zeta_{(k+1)}, r_{(k+1)}) - V(\zeta_k, r_k) \leq -\beta \tilde{\zeta}_k^T \tilde{\zeta}_k \qquad (13.20)$$

where $\beta = \inf\{\Lambda^{g,h}(r_k)_{\min}[-\mathcal{M}(r_k)], i \in S\}$ with

$$
\begin{aligned}
\mathcal{M} = & \frac{1}{4} \sum_{g=1}^{2^r} \sum_{h=1}^{2^m} \lambda_{1g}(k) \lambda_{2h}(k) \tilde{\zeta}_k^T \left\{ \Lambda^{g,h}(r_k) + \left(\Gamma_1^{g,h}(r_k) + \Gamma_1^{h,g}(r_k) \right)^T \right. \\
& \tilde{P}(r_k) \left(\Gamma_1^{g,h}(r_k) + \Gamma_1^{h,g}(r_k) \right) + \left(\Gamma_2^g + \Gamma_2^h \right)^T \sum_{l=1}^{r} (\tilde{\tau}^l(r_k) R_1 + \tau^l(s) R_2) \left(\Gamma_2^g + \Gamma_2^h \right) + \\
& \left(\Gamma_3^g + \Gamma_3^h \right)^T \left(\Gamma_3^g + \Gamma_3^h \right) \right] + 4\Upsilon_1(r_k) + 4\Upsilon_1^T(r_k) + 4 \sum_{l=1}^{r} \tau^l(r_k) Z(r_k) \right\} \tilde{\zeta}_k - z_k^T z_k + \\
& \gamma^2 w_k^T w_k \qquad (13.21)
\end{aligned}
$$

Summing from 0 to ∞ and by taking expectation on both sides of (13.20) gives

$$
\begin{aligned}
E\{V(\zeta_\infty, r_\infty)\} - E\{V(\zeta_0, r_0)\} & \leq -\beta E\left\{ \sum_{k=0}^{\infty} \tilde{\zeta}_\ell^T \tilde{\zeta}_\ell \right\} \\
& \leq -\beta E\left\{ \sum_{k=0}^{\infty} \zeta_\ell^T \zeta_\ell \right\} \qquad (13.22)
\end{aligned}
$$

Re-arranging (13.22), we have

$$
\begin{aligned}
E\left\{ \sum_{k=0}^{\infty} \zeta_\ell^T \zeta_\ell \right\} & \leq \frac{1}{\beta} E\{V(\zeta_0, r_0)\} - \frac{1}{\beta} E\{V(\zeta_\infty, r_\infty)\} \\
& \leq \alpha \qquad (13.23)
\end{aligned}
$$

where $\alpha = \frac{1}{\beta} E\{V(\zeta_0, r_0)\} < \infty$. This shows that the closed loop system is stable and (6.13) holds. $\nabla\nabla\nabla$

Proof of Theorem 3.2:

Applying Schur complement on (6.17), we have

$$
\begin{bmatrix}
\Pi & \left(\Gamma_1^{g,h}(i)+\Gamma_1^{h,g}(i)\right)^T & \left(\Gamma_2^g(i)+\Gamma_2^h(i)\right)^T & \left(\Gamma_3^g(i)+\Gamma_3^h(i)\right)^T & \Gamma_4^T(i) & (\Gamma_5^{g,h})^T(i) \\
* & -\tilde{P}^{-1}(i) & 0 & 0 & 0 & 0 \\
* & * & -R^{-1} & 0 & 0 & 0 \\
* & * & * & -I & 0 & 0 \\
* & * & * & * & -4\tilde{Q}^{-1} & 0 \\
* & * & * & * & * & -\mathcal{W}_1(i)
\end{bmatrix} < 0
$$

(13.24)

where

$$
\begin{aligned}
\Pi &= 4\tilde{\Lambda}(i)+4\Upsilon_1(i)+4\Upsilon_1^T(i)+4\sum_{l=1}^{r}\tau^l(i)Z(i) \\
\tilde{\Lambda}(i) &= \mathrm{diag}\left\{-P(i),-Q^1,\cdots,-Q^r,\left(H_2^T W_2(i)H_2-\gamma^2 I\right),-W_1(i),-W_2(i)\right\} \\
\Gamma_4(i) &= \begin{bmatrix} I & 0 & 0 & 0 & 0 \end{bmatrix} \\
\Gamma_5^{g,h}(i) &= \begin{bmatrix} \bar{H}_1^g(i)+\bar{H}_1^h(i) & 0 & 0 & 0 & 0 \end{bmatrix} \\
\tilde{Q} &= \sum_{l=1}^{r}(\tau^l(s)-\tau^l(1)+1)Q^l
\end{aligned}
$$

(13.25)

Following from [85], with loss of generality, $P(i)$ and $\tilde{P}(i)$ are, respectively, partitioned as

$$
P(i) = \begin{bmatrix} X(i) & Y^{-1}(i)-X(i) \\ Y^{-1}(i)-X(i) & X(i)-Y^{-1}(i) \end{bmatrix}
$$

(13.26)

and

$$
\tilde{P}(i) = \begin{bmatrix} \tilde{X}(i) & \sum_{j=1}^{i+1}p_{ij}Y^{-1}(j)-\tilde{X}(i) \\ \sum_{j=1}^{i+1}p_{ij}Y^{-1}(j)-\tilde{X}(i) & \tilde{X}(i)-\sum_{j=1}^{i+1}p_{ij}Y^{-1}(j) \end{bmatrix}.
$$

(13.27)

Now define

$$
T_2(i) = \begin{bmatrix} I & \tilde{X}(i) \\ 0 & \sum_{j=1}^{i+1}p_{ij}Y^{-1}(j)-\tilde{X}(i) \end{bmatrix}
$$

(13.28)

Multiplying (13.24) to the right by the matrix $\mathrm{diag}\left\{\mathrm{diag}\left\{T(i),I,I,I,I\right\},T_2(i),I,I,I,I\right\}$ and the left by its transpose, we obtain (6.21) with $-\left(\sum_{j=1}^{i+1}p_{ij}Y^{-1}(j)\right)^{-1}$ at the place of $\tilde{S}(i)-J(i)-J^T(i)$ in $\tilde{\Xi}(i)$, $-\tilde{Q}^{-1}$ in place of $\tilde{\mathcal{D}}-\tilde{j}-\tilde{j}^T$, $\bar{Z}(i)=T^T(i)Z(i)T(i)$, $\bar{M}^T(i)=T^T(i)M^T(i)T(i)$, $\mathcal{R}=\mathrm{diag}\{R_1^{-1},R_2^{-1}\}$, $\mathcal{W}_1(i)=W_1^{-1}(i)$ and $\mathcal{A}(i),\mathcal{B}(i)$ and $\mathcal{C}(i)$ are given in Theorem 3.2.

Applying Schur complement on (6.22) and consequently multiplying these inequalities by p_{ij} and summing up for all $j = S$, we obtain

$$
\begin{aligned}
\tilde{S}(i) - J^T(i) - J(i) &= -J^T(i) - J(i) + \sum_{j=1}^{i+1} p_{ij} S(i,j) \qquad &(13.29)\\
&\geq -J^T(i) - J(i) + J^T(i)\tilde{Y}^{-1}(i)J(i) \\
&= -\Big(\sum_{j=1}^{i+1} p_{ij}Y^{-1}(j)\Big)^{-1} + \Big(J(i) - \Big(\sum_{j=1}^{i+1} p_{ij}Y^{-1}(j)\Big)^{-1}\Big)^T \\
&\quad \Big(\sum_{j=1}^{i+1} p_{ij}Y^{-1}(j)\Big)\Big(J(i) - \Big(\sum_{j=1}^{i+1} p_{ij}Y^{-1}(j)\Big)^{-1}\Big) \\
&\geq -\Big(\sum_{j=1}^{i+1} p_{ij}Y^{-1}(j)\Big)^{-1} \qquad &(13.30)
\end{aligned}
$$

It implies that (6.21) remains valid if $\tilde{S}(i) - J^T(i) - J(i)$ is replaced by $\Big(\sum_{j=1}^{i+1} p_{ij}Y^{-1}(j)\Big)^{-1}$.

Applying the Schur complement on (6.23) and consequently multiplying these inequalities by $(\tau^l(s) - \tau^l(1) + 1)$ and summing up for all l to r, we obtain

$$
\begin{aligned}
\tilde{\mathcal{D}} - \tilde{J}^T - \tilde{J} &= -\tilde{J}^T - \tilde{J} + \sum_{l=1}^{r}(\tau^l(s) - \tau^l(1) + 1)\mathcal{D}^l \qquad &(13.31)\\
&\geq -\tilde{J}^T - \tilde{J} + \tilde{J}^T\tilde{Q}\tilde{J} \\
&= -\tilde{Q}^{-1} + \Big(\tilde{J} - \tilde{Q}^{-1}\Big)^T\tilde{Q}\Big(\tilde{J} - \tilde{Q}^{-1}\Big) \\
&\geq -\tilde{Q}^{-1} \qquad &(13.32)
\end{aligned}
$$

So, (6.21) remains valid if we replace $\tilde{\mathcal{D}} - \tilde{J}^T - \tilde{J}$ by $-\tilde{Q}^{-1}$.

Multiplying (6.16) to the right by the matrix $\mathrm{diag}\{T(i), T(i)\}$ and the left by its transpose, we obtain (6.20) with $T^T(i)\Big((1 - p_{i(i+1)})R_1(i) + R_2(i)\Big)T(i)$ at the place of $N(i)$ where $\bar{Z}(i) = T^T(i)Z(i)T(i)$ and $\bar{M}^T(i) = T^T(i)M^T(i)T(i)$.

Applying Schur complement on (6.24) and consequently multiplying these inequalities by $T_1(i)$ to the right and its transpose to the left , we obtain

$$
T^T(i)\Big((1 - p_{i(i+1)})R_1(i) + R_2(i)\Big)T(i) > \mathcal{N}^{-1}(i) \qquad (13.33)
$$

which implies that (6.20) remains valid if $N(i)$ is replaced by $T^T(i)\Big((1 - p_{i(i+1)})R_1(i) + R_2(i)\Big)T(i)$ where $\mathcal{Y}(i) = Y^{-1}(i)$, $\mathcal{N}^{-1}(i) = N(i)$. This concludes the proof that the closed-loop system is stochastically stable with the prescribed $\mathcal{H}_\infty$ performance. $\nabla\nabla\nabla$

Using a cone complementary algorithm [86], the feasibility problem formulated by (6.19-6.25), which is not a convex problem, can be converted into following nonlinear minimization problem subject to LMIs:

Minimize $Tr\left(N(i)\mathcal{N}(i) + Y(i)\mathcal{Y}(i) + Q^l\mathcal{Q}^l + R_1\mathcal{R}_1 + R_2\mathcal{R}_2 + W_1(i)\mathcal{W}_1(i)\right)$ subject to (6.19)-(6.24) and

$$\begin{bmatrix} N(i) & I \\ I & \mathcal{N}(i) \end{bmatrix} \geq 0, \begin{bmatrix} Y(i) & I \\ I & \mathcal{Y}(i) \end{bmatrix} \geq 0, \begin{bmatrix} R_1 & I \\ I & \mathcal{R}_1 \end{bmatrix} \geq 0,$$

$$\begin{bmatrix} Q^l & I \\ I & \mathcal{Q}^l \end{bmatrix} \geq 0, \begin{bmatrix} R_2 & I \\ I & \mathcal{R}_2 \end{bmatrix} \geq 0, \begin{bmatrix} W_1(i) & I \\ I & \mathcal{W}_1(i) \end{bmatrix} \geq 0 \qquad (13.34)$$

To solve this optimization problem, the following algorithm is proposed:

Algorithm :

- Set $\jmath = 0$ and solve (6.19)-(6.24) and (13.34) to obtain the initial conditions:

$$\Big[\mathcal{A}(i), \mathcal{B}(i), \mathcal{C}(i), X(i), Y(i), \mathcal{Y}(i), W_1(i), \mathcal{W}_1(i), W_2(i), Q^1 \cdots Q^r, N(i), \mathcal{N}(i)$$
$$, R_1(i), R_1, \mathcal{R}_1(i), R_2, \mathcal{R}_2(i), S(i,j), J(i), \mathcal{Q}^1, \cdots, \mathcal{Q}^r, \tilde{\jmath}, \bar{M}(i), \bar{Z}(i) \Big]^0$$

- Solve the LMI problem:

  Minimize $Tr\Big(N(i)^{\jmath}\mathcal{N}(i) + Y(i)^{\jmath}\mathcal{Y}(i) + (Q^l)^{\jmath}\mathcal{Q}^l + R_1^{\jmath}\mathcal{R}_1 + R_2^{\jmath}\mathcal{R}_2 + W_1(i)^{\jmath}\mathcal{W}_1(i) + N(i)\mathcal{N}(i)^{\jmath} + Y(i)\mathcal{Y}(i)^{\jmath} + Q^l(\mathcal{Q}^l)^{\jmath} + R_1\mathcal{R}_1^{\jmath} + R_2\mathcal{R}_2^{\jmath} + W_1(i)\mathcal{W}_1(i)^{\jmath}\Big)$

  subject to (6.19)-(6.24) and (13.34).

  The obtained solutions are denoted as:

$$\Big[\mathcal{A}(i), \mathcal{C}(i), \mathcal{B}(i), X(i), Y(i), \mathcal{Y}(i), W_1(i), \mathcal{W}_1(i), W_2(i), Q^1 \cdots Q^r, N(i), \mathcal{N}(i),$$
$$R_1(i), R_1, \mathcal{R}_1(i), R_2(i), R_2, \mathcal{R}_2(i), S(i,j), J(i), \mathcal{Q}^1, \cdots, \mathcal{Q}^r, \tilde{\jmath}, \bar{M}(i), \bar{Z}(i) \Big]^{\jmath+1}$$

- Solve Theorem 3.1 with $A_c(i)^{\jmath+1}$, $B_c(i)^{\jmath+1}$ and $C_c(i)^{\jmath+1}$ obtained in Step 2, if there exist solutions, then $A_c(i)^{\jmath+1}$, $B_c(i)^{\jmath+1}$ and $C_c(i)^{\jmath+1}$ are the suitable controller matrices and EXIT. Otherwise, if

  $Tr\Big(N(i)^{\jmath}\mathcal{N}(i) + Y(i)^{\jmath}\mathcal{Y}(i) + (Q^l)^{\jmath}\mathcal{Q}^l + R_1^{\jmath}\mathcal{R}_1 + R_2^{\jmath}\mathcal{R}_2 + W_1(i)^{\jmath}\mathcal{W}_1(i) + N(i)\mathcal{N}(i)^{\jmath} + Y(i)\mathcal{Y}(i)^{\jmath} + Q^l(\mathcal{Q}^l)^{\jmath} + R_1\mathcal{R}_1^{\jmath} + R_2\mathcal{R}_2^{\jmath} + W_1(i)\mathcal{W}_1(i)^{\jmath}\Big) > \epsilon$, set $\jmath = \jmath + 1$ and return to Step 2 where ϵ is tolerant else EXIT and no solution will be possible.

Chapter 14

Appendix

Proof of Lemma 2.1: From (7.11), we learn that

$$\sum_{i=k-\bar{\tau}}^{k-1} \begin{bmatrix} \bar{x}(i) \\ \tilde{\zeta}(k) \end{bmatrix}^T \begin{bmatrix} R & M \\ M^T & Z \end{bmatrix} \begin{bmatrix} \bar{x}(i) \\ \tilde{\zeta}(k) \end{bmatrix} \geq 0 \tag{14.1}$$

It follows follows from (14.1) that:

$$\sum_{i=k-\bar{\tau}}^{k-1} \left[\bar{x}^T(i)R\bar{x}(i) + \tilde{\zeta}^T(k)M^T\bar{x}(i) + \bar{x}^T(i)M\tilde{\zeta}(k) + \tilde{\zeta}^T(k)Z\tilde{\zeta}(k) \right] \geq 0$$

$$\begin{array}{c} \sum_{i=k-\bar{\tau}}^{k-1} \bar{x}^T(i)R\bar{x}(i) + \sum_{i=k-\bar{\tau}}^{k-1} \tilde{\zeta}^T(k)M^T\bar{x}(i) + \sum_{i=k-\bar{\tau}}^{k-1} \bar{x}^T(i)M\tilde{\zeta}(k) \\ + \sum_{i=k-\bar{\tau}}^{k-1} \tilde{\zeta}^T(k)Z\tilde{\zeta}(k) \end{array} \geq 0$$

$$\begin{array}{c} \sum_{i=k-\bar{\tau}}^{k-1} \tilde{\zeta}^T(k)M^T\bar{x}(i) + \sum_{i=k-\bar{\tau}}^{k-1} \bar{x}^T(i)M\tilde{\zeta}(k) + \\ \sum_{i=k-\bar{\tau}}^{k-1} \tilde{\zeta}^T(k)Z\tilde{\zeta}(k) \end{array} \geq - \sum_{i=k-\bar{\tau}}^{k-1} \bar{x}^T(i)R\bar{x}(i)$$

$$\begin{array}{c} \tilde{\zeta}^T(k)M^T\{x(k) - x(k-\bar{\tau})\} + \{x(k) - x(k-\bar{\tau})\}^T M\tilde{\zeta}(k) + \\ \bar{\tau}\tilde{\zeta}^T(k)Z\tilde{\zeta}(k) \end{array} \geq - \sum_{i=k-\bar{\tau}}^{k-1} \bar{x}^T(i)R\bar{x}(i)$$

As

$$x(k) - x(k-\bar{\tau}) = \begin{bmatrix} \mathrm{diag}\{I,0\} & \mathrm{diag}\{-I,0\} & 0 & 0 & 0 & 0 & 0 & 0 \end{bmatrix} \tilde{\zeta}(k),$$

we can have:

$$\begin{bmatrix} \tilde{\zeta}^T(k)M^T \begin{bmatrix} \mathrm{diag}\{I,0\} & \mathrm{diag}\{-I,0\} & 0 & 0 & 0 & 0 & 0 & 0 \end{bmatrix} \tilde{\zeta}(k) \\ +\bar{\tau}\tilde{\zeta}^T(k)Z\tilde{\zeta}(k)+ \\ \tilde{\zeta}(k)^T \begin{bmatrix} \mathrm{diag}\{I,0\} & \mathrm{diag}\{-I,0\} & 0 & 0 & 0 & 0 & 0 & 0 \end{bmatrix}^T M\tilde{\zeta}(k) \end{bmatrix} \geq - \sum_{i=k-\bar{\tau}}^{k-1} \bar{x}^T(i)R\bar{x}(i).$$

Putting $\Upsilon_1 = M^T[\text{diag}\{I,0\} \quad \text{diag}\{-I,0\} \quad 0 \quad 0 \quad 0 \quad 0 \quad 0 \quad 0]$ in the above inequality gives (7.12). $\qquad\qquad\qquad\qquad\qquad\qquad\qquad\qquad\qquad\qquad\qquad\qquad\qquad\qquad\qquad$ $\nabla\nabla\nabla$

Proof of Theorem 3.1: The system (7.7) can be written as:

$$\begin{aligned}
\zeta_{k+1} &= \Gamma_1(r_k)\tilde{\zeta}_k \\
z_k &= \Xi(r_k)\tilde{\zeta}_k
\end{aligned} \tag{14.2}$$

where $\zeta(k+1) = \zeta_{k+1}$, $\Gamma_1(r_k)$ and $\Xi(r_k)$ are given in (7.16) and $\tilde{\zeta}_k$ is defined in Lemma 7.2.1.

Select the L-K candidate functional for the closed loop system as:

$$V(\zeta_k, r_k) = V_1(\zeta_k, r_k) + V_2(\zeta_k, r_k) + V_3(\zeta_k, r_k) \tag{14.3}$$

with

$$V_1(\zeta_k, r_k) = \zeta_k^T P(r_k)\zeta_k \tag{14.4}$$

$$V_2(\zeta_k, r_k) = \sum_{\ell=-\bar{\tau}}^{-1} \sum_{j=k+\ell}^{k-1} \bar{x}_j^T R_1 \bar{x}_j \tag{14.5}$$

$$V_3(\zeta_k, r_k) = \sum_{\ell=k-\tau(k)}^{k-1} \zeta_\ell^T Q\zeta_\ell + \sum_{\ell=-\bar{\tau}+2}^{-\underline{\tau}+1} \sum_{j=k+\ell-1}^{k-1} \zeta_j^T Q\zeta_j \tag{14.6}$$

First forward difference of $V(\zeta_k, r_k)$ is given as follows:

$$\Delta V(\zeta_k, r_k) = \Delta V_1(\zeta_k, r_k) + \Delta V_2(\zeta_k, r_k) + \Delta V_3(\zeta_k, r_k) \tag{14.7}$$

with

$$\begin{aligned}
\Delta V_1(\zeta_k, r_k) &= \zeta_{k+1}^T \tilde{P}(r_k)\zeta_{k+1} - \zeta_k^T P(r_k)\zeta_k \\
&= \tilde{\zeta}_k^T \Gamma_1^T \tilde{P}(r_k)\Gamma_1 \tilde{\zeta}_k - \zeta_k^T P(r_k)\zeta_k
\end{aligned} \tag{14.8}$$

$$\Delta V_2(\zeta_k, r_k) \leq \bar{x}_k^T \bar{\tau} R_1 \bar{x}_k - \sum_{\ell=k-\bar{\tau}}^{k-1} \bar{x}_\ell^T R_1 \bar{x}_\ell \tag{14.9}$$

and

$$\Delta V_3(\zeta_k, r_k) \leq (\bar{\tau} - \underline{\tau} + 1)\zeta_k^T Q\zeta_k - \zeta_{k-\tau(k)}^T Q\zeta_{k-\tau(k)}. \tag{14.10}$$

Using Lemma 7.2.1 and $\bar{x}_k = x_{k+1} - x_k = \Gamma_2(r_k)\tilde{\zeta}_k$, we have

$$\Delta V_2(\zeta_k, r_k) \;\leq\; \tilde{\zeta}_k^T\Big\{\Gamma_2^T\bar{\tau}R_1\Gamma_2 + \Upsilon_1(r_k) + \Upsilon_1^T(r_k) + \bar{\tau}Z(r_k)\Big\}\tilde{\zeta}_k \qquad (14.11)$$

where $\Gamma_2(r_k)$ is given in (7.16).

Therefore,

$$\begin{aligned}
\Delta V(\zeta_k, r_k) \;\leq\; & -\zeta_k^T\Big(P(r_k) - (\bar{\tau} - \underline{\tau} + 1)Q\Big)\zeta_k - \zeta_{k-\tau(k)}^T Q\zeta_{k-\tau(k)} + \tilde{\zeta}_k^T \\
& \Big\{\Gamma_1^T\tilde{P}(r_k)\Gamma_1 + \Gamma_2^T\bar{\tau}R_1\Gamma_2 + \Upsilon_1(r_k) + \Upsilon_1^T(r_k) + \bar{\tau}Z(r_k)\Big\}\tilde{\zeta}_k (14.12)
\end{aligned}$$

Using Assumption 3.2.1, and adding and subtracting $\zeta_k^T\bar{H}_1^T(r_k)F_k^T W_1(rk)F_k\bar{H}_1(r_k)\zeta_k$, $\zeta_{k-\tau(k)}^T\bar{C}_2^T\Delta_q^T(k)W_2(r_k)\Delta_q(k)\bar{C}_2\zeta_{k-\tau(k)}$, $w_k^T H_2^T F_k^T W_3(r_k)F_k H_2 w_k$, $z_k^T z_k$ and $\gamma^2 w_k^T w_k$ to and from (14.12), we obtain:

$$\begin{aligned}
\Delta V(\zeta_k, r_k) \;\leq\; & -\zeta_k^T\Big(P(r_k) - (\bar{\tau} - \underline{\tau} + 1)Q - \bar{H}_1^T(r_k)F_k^T W_1(rk)F_k\bar{H}_1(r_k)\Big)\zeta_k \\
& -\zeta_{k-\tau(k)}^T\Big(Q - \delta^2(i)\bar{C}_2^T W_2(r_k)\bar{C}_2\Big)\zeta_{k-\tau(k)} + \tilde{\zeta}_k^T\Big\{\Gamma_1^T(r_k)\tilde{P}(r_k)\Gamma_1(r_k) \\
& +\Gamma_2^T(r_k)\bar{\tau}R_1\Gamma_2(r_k) + \Upsilon_1(r_k) + \Upsilon_1^T(r_k) + \bar{\tau}Z(r_k) \\
& +\Xi^T(r_k)\Xi(r_k)\Big\}\tilde{\zeta}_k - z_k^T z_k + \gamma^2 w_k^T w_k - w_k^T\Big(\gamma^2 I - H_2^T W_3(r_k)H_2\Big)w_k - \\
& \zeta_{k-\tau(k)}^T\delta^2(i)\bar{C}_2^T W_2(r_k)\bar{C}_2\zeta_{k-\tau(k)} - \zeta_k^T\bar{H}_1^T(r_k)F_k^T W_1(r_k)F_k\bar{H}_1(r_k)\zeta_k \\
& -w_k^T H_2^T F_k^T W_3(r_k)F_k H_2 w_k \qquad (14.13)
\end{aligned}$$

Using (7.16), (14.13) can be rewritten as

$$\begin{aligned}
\Delta V(x_k, r_k) \;\leq\; & \tilde{\zeta}_k^T\Big\{\Lambda(r_k) + \Gamma_1^T(r_k)\tilde{P}(r_k)\Gamma_1(r_k) + \Gamma_2^T(r_k)\bar{\tau}R_1\Gamma_2(r_k) + \Upsilon_1(r_k) + \Upsilon_1^T(r_k) \\
& +\bar{\tau}Z(r_k) + \Xi^T(r_k)\Xi(r_k)\Big\}\tilde{\zeta}_k - z_k^T z_k + \gamma^2 w_k^T w_k \qquad (14.14)
\end{aligned}$$

Using (7.15), we have

$$\Delta V(\zeta_k, r_k) \leq -z_k^T z_k + \gamma^2 w_k^T w_k \qquad (14.15)$$

Taking expectation and sum from 0 to ∞ on both sides of (14.15) yields:

$$E\{V(\zeta_\infty, r_\infty)\} - E\{V(\zeta_0, r_0)\} \leq -E\Big\{\sum_{\ell=0}^{\infty} z_\ell^T z_\ell\Big\} + \gamma^2\sum_{\ell=0}^{\infty} w_\ell^T w_\ell. \qquad (14.16)$$

As initial conditions, which are given in problem formulation, are considered to be zero, i.e, $V(\zeta_0, r_0) = 0$, we get:

$$E\Big\{\sum_{\ell=0}^{\infty} z_\ell^T z_\ell\Big\} \leq \gamma^2\sum_{\ell=0}^{\infty} w_\ell^T w_\ell. \qquad (14.17)$$

If $w(k) = 0, \forall k \geq 0$ closed-loop system should be stochastically stable. From (14.14) and (7.15), we learn that

$$V(\zeta_{(k+1)}, r_{(k+1)}) - V(\zeta_k, r_k) \leq -\beta \tilde{\zeta}_k^T \tilde{\zeta}_k \qquad (14.18)$$

where $\beta = \inf\{\Lambda(r_k)_{\min}[-\mathcal{M}(r_k)], i \in S\}$ with

$$\begin{aligned}
\mathcal{M} &= \Lambda(r_k) + \Gamma_1^T(r_k)\tilde{P}(r_k)\Gamma_1(r_k) + \Gamma_2^T(r_k)\bar{\tau}R_1\Gamma_2(r_k) \\
&+ \Upsilon_1(r_k) + \Upsilon_1^T(r_k) + \bar{\tau}Z(r_k) + \Xi^T(r_k)\Xi(r_k).
\end{aligned} \qquad (14.19)$$

Summing from 0 to ∞ and by taking expectation on both sides of (14.18) gives

$$\begin{aligned}
E\{V(\zeta_\infty, r_\infty)\} - E\{V(\zeta_0, r_0)\} &\leq -\beta E\Big\{\sum_{k=0}^{\infty} \tilde{\zeta}_\ell^T \tilde{\zeta}_\ell\Big\} \\
&\leq -\beta E\Big\{\sum_{k=0}^{\infty} \zeta_\ell^T \zeta_\ell\Big\} \qquad (14.20)
\end{aligned}$$

Re-arranging (14.20), we have

$$\begin{aligned}
E\Big\{\sum_{k=0}^{\infty} \zeta_\ell^T \zeta_\ell\Big\} &\leq \frac{1}{\beta}E\{V(\zeta_0, r_0)\} - \frac{1}{\beta}E\{V(\zeta_\infty, r_\infty)\} \\
&\leq \alpha \qquad (14.21)
\end{aligned}$$

where $\alpha = \frac{1}{\beta}E\{V(\zeta_0, r_0)\} < \infty$. This shows that the closed loop system is stable. $\nabla\nabla\nabla$

Proof of Theorem 3.2:

Applying Schur complement on (7.15), we have

$$\begin{bmatrix}
\Pi(i) & \Gamma_1^T(i) & \Gamma_2^T(i) & \Gamma_3^T(i) & \Gamma_4^T(i) & \Gamma_5^T(i) & \Gamma_6^T(i) \\
* & -\tilde{P}^{-1}(i) & 0 & 0 & 0 & 0 & 0 \\
* & * & -R_1^{-1} & 0 & 0 & 0 & 0 \\
* & * & * & -I & 0 & 0 & 0 \\
* & * & * & * & -Q^{-1} & 0 & 0 \\
* & * & * & * & * & -\tilde{W}_1(i) & 0 \\
* & * & * & * & * & * & -\tilde{W}_2(i)
\end{bmatrix} < 0 \qquad (14.22)$$

where

$$
\begin{aligned}
\Pi(i) &= \tilde{\Lambda}(i) + \Upsilon_1(i) + \Upsilon_1^T(i) + \tau(k)Z(i) \\
\tilde{\Lambda}(i) &= \operatorname{diag}\left\{-\tilde{P}(i), -Q, \left(H_2^T W_3(i)H_2 - \gamma^2 I\right), -W_1(i), -W_2(i), -W_3(i)\right\}, \\
\Gamma_4(i) &= \left[\ (\sqrt{\bar{\tau} - \underline{\tau} + 1})I\ \ 0\ \ 0\ \ 0\ \ 0\ \ 0\ \right], \\
\Gamma_5(i) &= \left[\ \bar{H}_1(i)\ \ 0\ \ 0\ \ 0\ \ 0\ \ 0\ \right], \\
\Gamma_6(i) &= \left[\ 0\ \ \delta(i)\bar{C}_2\ \ 0\ \ 0\ \ 0\ \ 0\ \right].
\end{aligned}
\tag{14.23}
$$

Following from [85], without loss of generality, $P(i)$ and $\tilde{P}(i)$ are, respectively, partitioned as

$$
P(i) = \begin{bmatrix} X(i) & Y^{-1}(i) - X(i) \\ Y^{-1}(i) - X(i) & X(i) - Y^{-1}(i) \end{bmatrix}
\tag{14.24}
$$

and

$$
\tilde{P}(i) = \begin{bmatrix} \tilde{X}(i) & \sum_{j=1}^s p_{ij}Y^{-1}(j) - \tilde{X}(i) \\ \sum_{j=1}^s p_{ij}Y^{-1}(j) - \tilde{X}(i) & \tilde{X}(i) - \sum_{j=1}^s p_{ij}Y^{-1}(j) \end{bmatrix}.
\tag{14.25}
$$

Now define

$$
T_2(i) = \begin{bmatrix} I & \tilde{X}(i) \\ 0 & \sum_{j=1}^s p_{ij}Y^{-1}(j) - \tilde{X}(i) \end{bmatrix}
\tag{14.26}
$$

Multiplying (14.22) to the right by the matrix $\operatorname{diag}\left\{\operatorname{diag}\left\{T(i), I, I, I, I, I\right\}, T_2(i), I, I, I, I, I\right\}$ and the left by its transpose, we obtain (7.19) with $\left(\sum_{j=1}^s p_{ij}Y^{-1}(j)\right)^{-1}$ at the place of $\tilde{S}(i) - J(i) - J^T(i)$ in $\tilde{\Xi}(i)$, $\bar{Z}(i) = T^T(i)Z(i)T(i)$, $\bar{M}^T(i) = T^T(i)M^T(i)T(i)$, $\mathcal{R}_1 = R_1^{-1}$, $\mathcal{Q} = Q^{-1}$, $\mathcal{W}_1(i) = W_1^{-1}(i)$, $\mathcal{W}_2(i) = W_2^{-1}(i)$, and $\mathcal{A}(i), \mathcal{A}_f(i), \mathcal{B}(i)$ and $\mathcal{C}(i)$ are given in Theorem 3.2.

Applying the Schur complement on (7.20) and consequently multiplying these inequalities by p_{ij} and summing up for all $j = \mathcal{S}$, we obtain

$$
\begin{aligned}
\tilde{S}(i) - J^T(i) - J(i) &= -J^T(i) - J(i) + \sum_{j=1}^s p_{ij}S(i,j) \tag{14.27} \\
&\leq -J^T(i) - J(i) + J^T(i)\tilde{Y}^{-1}(i)J(i) \\
&= \left(\sum_{j=1}^s p_{ij}Y^{-1}(j)\right)^{-1} - \left(J(i) - \left(\sum_{j=1}^s p_{ij}Y^{-1}(j)\right)^{-1}\right)^T \\
&\quad \left(\sum_{j=1}^s p_{ij}Y^{-1}(j)\right)\left(J(i) - \left(\sum_{j=1}^s p_{ij}Y^{-1}(j)\right)^{-1}\right) \\
&\leq -\left(\sum_{j=1}^s p_{ij}Y^{-1}(j)\right)^{-1} \tag{14.28}
\end{aligned}
$$

which implies that (7.19) remains valid if $\tilde{S}(i) - J^T(i) - J(i)$ is replaced by $\left(\sum_{j=1}^{s} p_{ij} Y^{-1}(j) \right)^{-1}$.

Multiplying (7.14) to the right by the matrix $\text{diag}\{T(i), T(i)\}$ and the left by its transpose, we obtain (7.18) with $T^T(i) R_1(i) T(i)$ at the place of $N(i)$ where $\bar{Z}(i) = T^T(i) Z(i) T(i)$ and $\bar{M}^T(i) = T^T(i) M^T(i) T(i)$.

Applying the Schur complement on (7.21) and consequently multiplying these inequalities by $T(i)$ to the right and its transpose to the left, we obtain

$$T^T(i) R_1(i) T(i) > \mathcal{N}^{-1}(i) \tag{14.29}$$

which implies that (7.18) remains valid if $N(i)$ is replaced by $T^T(i) R_1(i) T(i)$ where $\mathcal{Y}(i) = Y^{-1}(i)$, $\mathcal{N}^{-1}(i) = N(i)$. This concludes the proof that the closed-loop system is stochastically stable with the prescribed $\mathcal{H}_\infty$ performance. $\nabla\nabla\nabla$

Using the cone complementary algorithm [127], the feasibility problem formulated by (7.17)-(7.23) which is not a convex problem can be converted into the following nonlinear minimization problem:

Minimize $Tr\Big(Y(i)\mathcal{Y}(i) + Q(i)\mathcal{Q}(i) + N(i)\mathcal{N}(i) + R_1\mathcal{R}_1 + W_1(i)\mathcal{W}_1(i) + W_2(i)\mathcal{W}_2(i) \Big)$

subject to (7.17)-(7.21) and

$$\begin{bmatrix} Y(i) & I \\ I & \mathcal{Y}(i) \end{bmatrix} \geq 0, \quad \begin{bmatrix} Q & I \\ I & \mathcal{Q} \end{bmatrix} \geq 0, \quad \begin{bmatrix} N(i) & I \\ I & \mathcal{N}(i) \end{bmatrix} \geq 0,$$

$$\begin{bmatrix} R_1 & I \\ I & \mathcal{R}_1 \end{bmatrix} \geq 0, \quad \begin{bmatrix} W_1(i) & I \\ I & \mathcal{W}_1(i) \end{bmatrix} \geq 0 \quad \begin{bmatrix} W_2(i) & I \\ I & \mathcal{W}_2(i) \end{bmatrix} \geq 0. \tag{14.30}$$

To solve this optimization problem, an algorithm is proposed as follows:

Algorithm:

Step 1: Set $\jmath = 0$ and solve (7.17)-(7.21) and (14.30) to obtain the initial conditions

$$\Big[\mathcal{A}(i), \mathcal{A}_{cf}, \mathcal{C}(i), \mathcal{B}(i), X(i), Y(i), \mathcal{Y}(i), W_1(i), \mathcal{W}_1(i),$$

$$W_2(i), \mathcal{W}_2(i), W_3(i), Q, \mathcal{Q}, N(i), \mathcal{N}(i), \mathcal{R}_1(i), R_1, \mathcal{R}_1(i), S(i,j), J(i), \bar{M}(i), \bar{Z}(i) \Big]^0$$

Step 2: Solve the LMI problem

Minimize $Tr\Big(N(i)^\jmath \mathcal{N}(i) + Y(i)^\jmath \mathcal{Y}(i) + R_1^\jmath \mathcal{R}_1 + W_1(i)^\jmath \mathcal{W}_1(i) + W_2(i)^\jmath \mathcal{W}_2(i) + Q(i)^\jmath \mathcal{Q}(i) +$

$N(i)\mathcal{N}(i)^\jmath + Y(i)\mathcal{Y}(i)^\jmath + R_1\mathcal{R}_1^\jmath + W_1(i)\mathcal{W}_1(i)^\jmath + W_2(i)\mathcal{W}_2(i)^\jmath + Q(i)\mathcal{Q}(i)^\jmath \Big)$

subject to (7.17)-(7.21) and (14.30).

The obtained solutions are denoted as

$$\Big[\mathcal{A}(i), \mathcal{A}_{cf}, \mathcal{C}(i), \mathcal{B}(i), X(i), Y(i), \mathcal{Y}(i), W_1(i), \mathcal{W}_1(i), W_2(i), \mathcal{W}_2(i), W_3(i), Q, \mathcal{Q},$$

$$N(i), \mathcal{N}(i), R_1(i), R_1, \mathcal{R}_1(i), S(i,j), J(i), \bar{M}(i), \bar{Z}(i)\Big]^{J+1}$$

Step 3: Solve Theorem 3.1 with $A_c(i)^{J+1}, B_c(i)^{J+1}$ and $C_c(i)^{J+1}$ obtained in Step 2. If there exist solutions, then $A_c(i)^{J+1}, A_{cf}(i)^{J+1}, B_c(i)^{J+1}$ and $C_c(i)^{J+1}$ are the suitable controller matrices and EXIT. Otherwise, set $J = J + 1$ and return to Step 2.

Bibliography

[1] T.C. Yang, "Networked control system: a brief survey", *Proceedings of IEE on Control Theory Applications*, vol. 153, no. 4, pp. 403–412, 2006.

[2] L. G. Bushnell, "Special Section on Networks and Control", *Control System Magazine*, vol. 21, no. 1, 2001.

[3] J-M. Fuertes, D. Catalunya, M-Y Chow, R. Villa, R. Gupta, and J. Ayza, "Network-Based Control", *Chapter–20, Taylor and Francis*, pp. 1–8, 2011.

[4] E. Fridman,"EDITORIAL: Special issue on time-delay systems", *International Journal of Robust Nonlinear Control*, vol. 13, pp. 791-792, 2003.

[5] M. Botts, and A. Robin, "Bringing the Sensor Web Together", *Geosciences*, pp. 46-53, 2007.

[6] P. Antsaklis, and J. Baillieul,"Guest Editorial: Special Issue on Networked Control Systems", *IEEE Transaction on Automatic Control*, vol. 49, No. 9, pp. 1421–1423, 2004.

[7] L. Zhang, H. Gao, and O. Kaynak, "Survey of Studies on Network-Induced Constraints in Networked Control Systems", *IEEE Transactions on Industrial Informatics*, vol. 9, no. 1, pp. 1-14, 2012.

[8] Y. Sun, and S. Qin, "Stability of networked control systems with packet dropout: an average dwell time approach", *IET Control Theory & Applications*, vol. 5 , no. 1, pp: 47–53, 2011.

[9] K. Gu, "$\mathcal{H}_\infty$ Control of Systems Under Norm Bounded Uncertainties in all System Matrices", *IEEE Transaction on Automatic Control*, vol. 39, no. 6, pp. 1320–1322, 1994.

[10] K. Johansson, M. Torngren, and L. Nielsen, "Vehicle applications of controller area network", in *D. Hristu-Varsakelis and W. S. Levine, Ed., Handbook of networked and embedded control systems*, Boston, MA: Birkhauser, 2005.

[11] http://www.moxa.com/industrial n ethernet/water wastewater.htm, "Home page of introduction of Moxas industrial Ethernets application in waste water treatment plants".

[12] P. Seiler, and R. Sengupta, "An $\mathcal{H}_\infty$ Approach to Networked Control", in *IEEE Transactions on Automatic Control*, vol. 50, no. 3, 2005.

[13] A. S. Arynova, S-K. Nguang, and G. Liu, "PI power control for CDMA cellular communication systems", in the proceedings of *IEEE International Conference on Control and Automation* , pp. 309–313, 2009.

[14] G. C. Walsh, and H. Ye, "Scheduling of networked control systems", *IEEE Control Systems Magazine*, 2001.

[15] S-K. Kweon, K G. Shin, and G. Workman, "Achieving real-time communication over ethernet with adaptive traffic smoothing", in the proceedings of *IEEE Real Time Technology and Applications Symposium*, 2000.

[16] F-L. Lian, J. R. Moyne, and D. M. Tilbury, "Performance evaluation of control networks: Ethernet, controlnet and devicenet", *IEEE Control Systems Magazine*, vol. 21, pp. 66-83, 2002.

[17] N. J. Ploplys, P. A. Kawka, and A. Alleyne, "Closed-loop control over wireless networks", *IEEE Control Systems Magazine*, vol. 24, pp. 58-71, 2004.

[18] G. C. Walsh, O. Beldiman, and L. Bushnell, "Predictors for networked control systems", in the Proceedings of *American Control Conference*, 2000.

[19] S. Chae, "Networked control systems", *Masters thesis*, Department of Electrical and Computer Engineering, UOA, New Zealand, 2008.

[20] W.-A. Zhang, L. Yu, and S. Yin, "A switched system approach to $\mathcal{H}_\infty$ control of networked control systems with time-varying delays", Journal of the Franklin Institute, vol. 348, no. 2, pp. 165- 178, 2011.

[21] E. G. Tian and D. Yue, "A new state feedback $\mathcal{H}_\infty$ control of networked control systems with time-varying network conditions", Journal of the Franklin Institute, vol. 349, no. 3,pp. 891-914, 2012.

[22] L. Qiu, B. G. Xu, and S. B. Li, "$\mathcal{L}_2$-$\mathcal{H}_\infty$ control of networked control system with random time delays", Science China, vol. 54, no. 12, pp. 2615-2630, 2011.

[23] J. Xiong and J. Lam, "Stabilization of linear systems over networks with bounded packet loss", Automatica, vol. 43, no. 1, pp. 80-87, 2007.

[24] Z. Wang, F. Yang, D. W. C. Ho, and X. Liu, "Robust $\mathcal{H}_\infty$ control for networked systemswith randompacket losses", IEEE Transactions on Systems, Man, and Cybernetics Part B, vol. 37, no. 4, pp. 916-924, 2007.

[25] J.Wu and T. Chen, "Design of networked control systems with packet dropouts", IEEE Transactions on Automatic Control, vol. 52, no. 7, pp. 1314-1319, 2007.

[26] C.-C. Hsieh and P.-L. Hsu, "Analysis and applications of the motion message estimator for network control systems", Asian Journal of Control, vol. 10, no. 1, pp. 45-54, 2008.

[27] T. Jia, Y. Niu, andX.Wang, "$\mathcal{H}_\infty$ control for networked systems with data packet dropout", International Journal of Control, Automation and Systems, vol. 8, no. 2, pp. 198-203, 2010.

[28] Q. G. Lu, L. X. Zhang, M. Basin, and H. Tian, "Analysis and synthesis for networked control systems with uncertain rate of packet losses", Journal of the Franklin Institute, vol. 349, no. 7, pp. 2500-2514, 2012.

[29] D. Liberzon, "On stabilization of linear systems with limited information", IEEE Transactions on Automatic Control, vol. 48, no. 2, pp. 304307, 2003.

[30] Y. Ishido, K. Takaba, and D. E. Quevedo, "Stability analysis of networked control systems subject to packet-dropouts and finite-level quantization", Systems & Control Letters, vol. 60, no. 5, pp. 325332, 2011.

[31] M. Iza, D. Gorges, and S. Liu, "Optimal control of networked control systems with uncertain time-varying transmission delay", in Proceedings of the 2nd IFAC Workshop on Distributed Estimation and Control in Networked Systems, pp. 1318, Annecy, France, 2010.

[32] H. Fujioka, "A discrete-time approach to stability analysis of systems with aperiodic sample-and-hold devices", IEEE Transactions on Automatic Control, vol. 54, no. 10, pp. 24402445, 2009.

[33] T. Suzuki, M. Kono, N. Takahashi, and O. Sato, "Controllability and stabilizability of a networked control system with periodic communication constraints", Systems & Control Letters, vol. 60, no. 12, pp. 977984, 2011.

[34] H. Rehbinder and M. Sanfridson, "Scheduling of a limited communication channel for optimal control", Automatica, vol. 40, no. 3, pp. 491500, 2004.

[35] T. Y. Yu, L. Wang, and M. Yu, "Switched system approach to stabilization of networked control systems", International Journal of Robust and Nonlinear Control, vol. 21, no. 17, pp. 1915- 1946, 2011.

[36] Y.-L. Wang and G.-H. Yang, "State feedback control synthesis for networked control systems with packet dropout", Asian Journal of Control, vol. 11, no. 1, pp. 4958, 2009.

[37] B. Yu and Y. Shi, "State feedback stabilization of networked control systems with random time delays and packet dropout", in Proceedings of the ASME Dynamic Systems and Control Conference (DSCC 08), pp. 127133, October 2008.

[38] H. Dong, Z. Wang, and H. Gao, "Robust $\mathcal{H}_\infty$ filtering for a class of nonlinear networked systems with multiple stochastic communication delays and packet dropouts", IEEE Transactions on Signal Processing, vol. 58, no. 4, pp. 19571966, 2010.

[39] A. Albert, "Comparison of Event-Triggered and Time-Triggered Concepts with Regard to Distributed Control Systems", presented at the *Embedded World Conference*, pp. 235-252, 2004.

[40] L. Almeida, P. Pedreiras, and J. A. G. Fonseca, "The FTT-CAN Protocol: Why and How", *IEEE Transaction on Industrial Electronics*, vol. 49, no. 6, pp. 1189–1201, 2002.

[41] H. Kopetz, "Real Time Systems- Design Principals for Distributed Embedded Applications", *Kluwer Academic Publishers, London*, 1997.

[42] W. Heemels, M. Donkers, and A. Teel, "Periodic event-triggered control: The state-feedback case", in the proceedings of *IEEE Joint Conference on Decision & Control and European Control Conference*, pp. 2571–2576, 2011.

[43] P. Tabuada, "Event-Triggered Real-Time Scheduling of Stabilizing Control Tasks", in *IEEE Transactions on Automatic Control*, vol. 52, no. 9, pp. 1680–685, 2007.

[44] M. C. F. Donkers, and W. P. M. H. Heemels, "Output-Based Event-Triggered Control With Guaranteed $\mathcal{L}_\infty$-Gain and Improved and Decentralized Event-Triggering", in *IEEE Transaction on Automatic Contrl.* vol. 57, no. 6, pp. 1362–1376, 2012.

[45] X. Wang, and M.D. Lemmon, "Event design in event-triggered feedback control systems", in the proceedings of *IEEE Conference on Decision and Control*, pp. 2105–2110, 2008.

[46] A. Albert, and W. Gerth, "Evaluation and Comparison of the Real-Time Performance of CAN and TTCAN", in the proceedings of 9th *International CAN Conference, Munich*, pp. 01–08, 2003.

[47] F. Rasool, S. K. Nguang, S. Saat, J. Wu, and G. Zeng, " Robust $\mathcal{H}_\infty$ State Feedback Control of Networked Control Systems with Congestion Control", accepted in *12th International Conference on Control, Automation, Robotics and Vision*, China, 2012.

[48] G. Leena, and D. Heffernanb, "TTCAN: a new time-triggered controller area network", *Microprocessors and Microsystems*, vol. 26, no. 2, pp. 77–94 , 2002.

[49] A. Cervin, D. Henriksson, B. Lincoln, J. Eker, and K-E. Arzen, "How Does Control Timing Affect Performance? Analysis and Simulation of Timing Using Jitterbug and TrueTime", *IEEE Control Systems Magazine*, vol. 23, no. 3, pp. 16-30, 2003.

[50] A. Cervin, D. Henriksson, and M. Ohlin, "TrueTime 2.0 beta 5 - Reference Manual", *Department of Automatic Control*, Lund University, Sweden, 2010.

[51] W. P. M. H. Heemels, A. R. Teel, N. van de Wouw, and D. Nesic, "Networked Control Systems with Communication Constraints: Trade offs between Transmission Intervals, Delays and Performance", *IEEE Transactions on Automatic Control*, vol. 55, pp. 1781–1796, 2010.

[52] W-A. Zhang, L. Yu, and S. Yin, "A switched system approach to $\mathcal{H}_\infty$ control of networked control systems with time-varying delays", *Journal of the Franklin Institute*, vol. 348, no. 04, pp. 165–178 , 2011.

[53] H-P. Pang, C-J. Liu, A-Z. Liu, and H-P. Pang, "Sliding Mode Control for Time-Delay Systems with Its Application to Networked Control Systems", in the proceedings of 6th *International Conference on Intelligent Systems Design and Applications* , vol. 2, pp. 192–197, 2006.

[54] H. Zhang, and L. Xie, "Linear Quadratic Regulation for Systems with Time-varying Delay", in the proceedings of 46th *IEEE Conference on Decision and Control, USA*, pp. 2974–2979, 2007.

[55] M. Nachidi, "Static output-feedback stabilization for time-delay Takagi-Sugeno fuzzy systems", in the proceedings of 46th *IEEE Conference on Decision and Control, USA*, pp. 1634–1639, 2007.

[56] A-N. Vargas, and J-B. R. do Val, "Asymptomatic Stability of Linear Stochastic Systems with Delay Driven by a Bernoulli Process", in the proceedings of 10th *Portuguese Conference on Automatic Control CONTROLO12*, Portugal, 2012.

[57] C. Guo, W. Zhang, and J. Bao, "Robust output feedback $\mathcal{H}_\infty$ control for networked control systems based on the occurrence probabilities of time delays", *International Journal of Systems Science*, vol. 2, pp. 192–197, 2010.

[58] F. Rasool, and S. K. Nguang, "A literature survey on the time triggered and event triggered mechanisms in networked control systems", accepted in *IET Control and Automation Conference*, 2013.

[59] F. Rasool, S-K. Nguang, F A. Bhatti, S. Rehman, and T. Shahzad,"Robust $\mathcal{H}_\infty$ Output Feedback Control of Networked Control Systems with Dynamic Quantizers", *International Multitopic Conference*, pp. 222–227, 2011.

[60] W. P. M. H. Heemels, K.H. Johansson, and P. Tabuada, "An Introduction to Event-triggered and Self-triggered Control", in the proceedings of *IEEE Conference on Decision and Control*, pp. 1–16, 2012.

[61] H. Yu, and P-J. Antsaklis, "Event-Triggered Output Feedback Control for Networked Control Systems using Passivity: Triggering Condition and Limitations ", in the proceedings of *IEEE Conference on Decision and Control and European Control Conference*, pp. 199–204, 2011.

[62] H. Yu and P J. Antsaklis, "Event-Triggered Output Feedback Control for Networked Control Systems using Passivity: Time-varying Network Induced Delays", in the proceedings of *IEEE Conference on Decision and Control and European Control Conference*, pp. 205–210, 2011.

[63] W. Zhang, M-S. Branicky, and S-M. Phillips,"Stability of Networked Control Systems", in *IEEE Control System Magazine*, pp. 84–99 , 2001.

[64] Y. Shi, and B. Yu,"Output Feedback Stabilization of Networked Control Systems With Random Delays Modelled by Markov Chains", *IEEE Transactions on Automatic Control*, vol. 54, pp. 1668–1674, 2009.

[65] Y. Y. Cao, J. Lam, and L. Hu "Delay-dependent stochastic stability and $\mathcal{H}_\infty$ analysis for time-delay systems with Markovian jumping parameters", *Journal of The Franklin Institute*, vol. 340, no. 7, pp. 423–434, 2003.

[66] H. Li, Q. Zhou, B. Chen, and H. Liu,"Parameter-dependent robust stability for uncertain Markovian jump systems with time delay", *Journal of the Franklin Institute*, vol. 348, no. 04, pp. 738-748 , 2011.

[67] P-G. Park, "A Delay-Dependent Stability Criterion for Systems with Uncertain Time-Invariant Delays", *IEEE Transaction on Automatic Control*, Vol. 44. no. 4, pp. 876–877, 1999.

[68] S. Zhou, and G. Feng,"$\mathcal{H}_\infty$ filtering for discrete-time systems with randomly varying sensor delays", *Automatica*, vol. 44, pp. 1918-1922, 2008.

[69] R. W. Brockett, and D. Liberzon, "Quantized Feedback Stabilization of Linear Systems", *IEEE Transactions on Automatic Control*, vol. 45, pp. 1279-1289, 2000.

[70] R. Kalman, "Nonlinear aspects of sampled data control systems", *In proceedings of the symposium on nonlinear circuit theory*, Brooklyn NY, 1956.

[71] R. K. Miller, A. N. Michel, and J. A. Farrel, "Quantizer effects on steady state error specifications of digital control systems", *IEEE Transactions on Automatic Control*, vol. 34, pp. 651-654, 1989.

[72] N. Elia, and S.K. Mitter, "Stabilization of linear systems with limited information ", *IEEE Transactions on Automatic Control*, vol. 46, pp. 1384–1400, 2001.

[73] L. Montestruque, and P. Antsaklis, "Static and dynamic quantization in model-based networked control systems", *International Journal of Control*, vol. 80, pp. 87–101, 2007.

[74] A. Bicchi, A. Marigo, and B. Piccoli, "On the reachability of quantized control systems", *IEEE Transactions on Automatic Control*, vol. 47, pp. 546-563, 2002.

[75] M. Fu, and L. Xie, "The sector bound approach to quantized feedback control", *IEEE Transactions on Automatic Control*, vol. 50, no. 11, pp. 1698–1711, 2005.

[76] N. Xiao, L. Xie, and M. Fu, "Quantized stabilization of Markov Jump Linear Systems via State Feedback ", in the proceedings of *American Control Conference*, pp. 4020–4025, 2009.

[77] G. N. Nair, and R. J. Evans, "Exponential Stabilization of multi dimensional Linear Systems", *Automatica*, vol. 35, pp. 916-924, 2003.

[78] M. Fu, and L. Xie, "Finite-level Quantized Feedback Control For Linear Systems", *45th IEEE Conference on Decision and Control*, pp. 1117–1122, 2006.

[79] H. Gao, and T. Chen, "A new approach to quantized feedback control systems", *Automatica*, vol. 44, pp. 534–542, 2008.

[80] F. Rasool, and S. K. Nguang, "Quantized robust $\mathcal{H}_\infty$ control of discrete-time systems with random communication delays", *International Journal of Systems Science*, vol. 42, no. 1, pp. 129–138 , 2011.

[81] J. Dai," A delay system approach to networked control systems with limited communication capacity", *Journal of the Franklin Institute*, vol. 347, no. 07, pp. 1334–1352, 2010.

[82] D. Coutinho, M. Fu, and C.E. de Souza, "Output Feedback Control of Linear Systems with Input and Output Quantization", 47th *IEEE Conference on Decision and Control*, pp. 4706–4711, 2008.

[83] H. Yan, X. Huang, M. Wang, and H. Zhang, "Delay-dependent stability criteria for a class of networked control systems with multi-input and multi-output", *Chaos, Solitons and Fractals*, vol. 24, pp. 997-1005, 2006.

[84] L. Xiao, A. Hassibi, and J. How, "Control with random communication delays via a discrete-time jump system approach", in the proceedings of *American Control Conference*, vol. 3, pp. 2199–2204, 2000.

[85] A. P. C. Goncalves, A. R. Fioravanti and J. C. Geromel, " Dynamic Output Feedback $\mathcal{H}_\infty$ Control of Discrete-Time Markov Jump Linear Systems Through Linear Matrix Inequalities", in the proceedings of the 47th *IEEE Conference on Decision and Control*, pp. 4787–4792, 2008.

[86] S. Chae, F. Rasool, S-K. Nguang, and A. Swain, "Robust mode delay-dependent $\mathcal{H}_\infty$ control of discrete-time systems with random communication delays", *IET Control Theory Applications*, vol. 04, no. 6, pp. 936–944, 2009.

[87] S. Zhou, J. Lame, and W. X. Zheng, "Control Design for Fuzzy Systems Based on Relaxed Non quadratic Stability and $\mathcal{H}_\infty$ Performance Conditions ", *IEEE Transactions On Fuzzy Systems*, vol. 15, no. 2, pp. 188–199, 2007.

[88] H. Haimovich, and M. M. Seron, "On Infimum Quantization density for Multiple-input system", in the proceedings of 44th *IEEE Conference on Decision and Control*, 2005.

[89] S. Yuksel, and T. Basar, "Optimal Signaling policies for Decentralized Multi Controller Stabilizability Over Communication channels", *IEEE Transactions on Automatic Control*, vol. 52, no. 10, pp. 1969–1975, 2007.

[90] L. Zhang, and C. Wang, " Stability and Stabilization of A Class of Multi-Mode Linear Discrete-Time Systems with Polytopic Uncertainties", *IEEE Transactions on Industrial Electronics*, vol. 56, no. 9, pp. 3684-3692, 2009.

[91] L. Zhang, and J. Lam, " Necessary and Sufficient Conditions for Analysis and Synthesis of Markov Jump Linear Systems with Incomplete Transition Descriptions", *IEEE Transactions on Automatic Control*, vol. 55, no. 7, pp. 1695-1701, 2010.

[92] G-N. Nair, F. Fagnani, S. Zampieri, and R-J. Evans, "Feedback Control Under Data Rate Constraints: An Overview", *Proceedings of the IEEE*, vol. 95, no. 1, pp. 108–137, 2007.

[93] L. Zhang, E. Boukas, and J. Lam, " Analysis and Synthesis of Markov Jump Linear Systems with Time-Varying delays and Partially Known Transition Probabilities", *IEEE Transactions on Automatic Control*, vol. 53, no. 10, pp. 2458–2464, 2008.

[94] P. Antsaklis, and J. Baillieul, "Special issue on technology of networked control systems", in *Proceedings of the IEEE*, vol. 95, no. 1, pp. 5–8, 2007.

[95] Y. Zhang, Q. Zhong, and L. Wei, "Stability of networked control systems with communication constraints", in the proceedings of *Chinese Control and Decision Conference*, pp. 335–339, 2008.

[96] D. Huang, and S. K. Nguang, "State feedback control of uncertain networked control systems with random time delays", *IEEE Transactions on Automatic Control*, vol. 53, no. 3, pp. 829–834, 2008.

[97] Y-Y. Cao, Y-X. Sun, and J. Lam, "Delay-dependent robust $\mathcal{H}_\infty$ control for uncertain systems with time-varying delays", IEE Proceedings of the *Control Theory and Applications*, vol. 145, no. 3, pp. 338-344, 1998.

[98] Q. Zhu, G. Lu, J. Cao, and S. Hu, "Stability analysis of networked control systems with markov delay", in the proceedings of *International Conference on Control and Automation*, vol. 2, pp. 720-724, 2005.

[99] Y-Y. Cao, and J. Lam, "Robust $\mathcal{H}_\infty$ control of uncertain markovian jump systems with time delay", *IEEE Transaction on Automatic Control*, vol. 45, pp. 77-83, 2000.

[100] I. V. Kolmanovsky, and T. L. Maizenberg, "Optimal control of continuous-time linear systems with a time-varying, random delay", *Systems & Control Letters*, vol. 44, no. 2, pp. 119126, 2001.

[101] F. Rasool, and S-K. Nguang, "Robust $\mathcal{H}_\infty$ State Feedback Control of NCSs with Poisson Noise and Successive Packet Dropouts", submitted in *International Journal of Control, Automation, and Systems*, 2013.

[102] F. Rasool, S-K. Nguang, and T. Shahzad, "Robust $\mathcal{H}_\infty$ State Feedback Control of NCSs with Poisson Noise and Successive Packet Dropouts", accepted in *IEEE International Conference on Networking, Sensing and Control*, 2013.

[103] F. Rasool, S. K. Nguang, and Chih-Min Lin " Robust $\mathcal{H}_\infty$ State Feedback Control of Networked Control Systems with Congestion Control", accepted in *Circuit System & Signal processing*, 2013.

[104] F. Rasool, S. K. Nguang, S. Saat, J. Wu, and G. Zeng, "Robust $\mathcal{H}_\infty$ State Feedback Control of Networked Control Systems with Congestion Control", accepted in *12th International Conference on Control, Automation, Robotics and Vision*, China, 2012.

[105] F. Rasool, and S. K. Nguang, "Robust $\mathcal{H}_\infty$ Output Feedback Control of Networked Control Systems with Congestion Control", accepted with revisions in *International Journal of systems Science*, 2013.

[106] F. Rasool, S. K. Nguang, and T. Shahzad, "Robust $\mathcal{H}_\infty$ Output Feedback Control of Networked Control Systems with Congestion Control", accepted in *International Conference on Innovative Engineering Systems*, 2012.

[107] F. Rasool, D. Huang and S. K. Nguang, "Robust $\mathcal{H}_\infty$ output feedback control of networked control systems with multiple quantizers", accepted in *Journal of the Franklin Institute*, vol. 349, no. 3, pp. 1153-1173, 2012.

[108] F. Rasool, S. K. Nguang and M. Krug, "Robust $\mathcal{H}_\infty$ output feedback control of networked control systems with multiple quantizers", accepted in *6th IEEE Conference on Industrial Electronics and Applications*, pp. 1541–1546, 2011.

[109] F. Rasool, D. Huang and S. K. Nguang, "Robust $\mathcal{H}_\infty$ output feedback control of discrete-time networked systems with limited information", accepted in *Systems & Control Letters*, vol. 60, no. 10, pp. 845–853, 2011.

[110] F. Rasool, D. Huang, S. K. Nguang, "Robust $\mathcal{H}_\infty$ output feedback control of discrete-time networked systems with adaptive quantizers", accepted in *CDC-ECC*, pp: 2381–2386, 2011.

[111] F. Rasool, and S. K. Nguang, "Quantized robust $\mathcal{H}_\infty$ output feedback control of discrete-time systems with random communication delays", in *Proceedings of 2009 IEEE International Conference on Control and Automation*, Christchurch, New Zealand, pp. 1399–1404, 2009.

[112] Y. Y. Cao, J. Lam, and L. Hu, "Delay-dependent stochastic stability and $\mathcal{H}_\infty$ analysis for time-delay systems with Markovian jumping parameters", *Journal of The Franklin Institute*, vol. 340, no. 7, pp. 423–434, 2003.

[113] Z. D. Wang, J. Lam and X. H. Liu, "Exponential filtering for uncertain Markovian jump time-delay systems with nonlinear disturbances", *IEEE Transactions on Circuits and Systems*, vol. 51, no. 1, pp. 262–268, 2004.

[114] Z. Wang, and F. Yang, "Robust filtering for uncertain linear systems with delayed states and outputs", *IEEE Transactions on Circuits and Systems I: Fundamental Theory and Applications*, vol. 49, no. 1, pp. 125–130, 2002.

[115] H. Gao, T. Chen, and J. Lam, "A new model for time-delay systems with application to network based control", in *Proceedings of 2006 Chinese Control Conference*, pp. 56–61, 2006.

[116] L. Zhou, and G. Lu, "Quantized feedback stabilization for networked control systems with nonlinear perturbation", *International Journal of Innovative Computing, Information and Control*, vol. 6, no. 6, pp. 2485–2496, 2010.

[117] V. Vesely, and T. N. Quang, "Robust output networked control system design", *ICIC Express Letters*, vol. 4, no. 4, pp. 1399–1404, 2010.

[118] G. Wang, Q. Zhang, and V. Sreeram, "Partially mode-dependent $\mathcal{H}_\infty$ filtering for discrete-time Markovian jump systems with partly unknown transition probabilities", *Signal Processing*, vol. 90, no. 2, pp. 548–556, 2010.

[119] S. Hu, and W. Yan, "Stability robustness of networked control systems with respect to packet loss", *Automatica*, vol. 43, no. 7, pp. 1243–1248, 2007.

[120] R. Yang, P. Shi, and G-P. Liu, "Filtering for Discrete-Time Networked Nonlinear Systems With Mixed Random Delays and Packet Dropouts", *IEEE Transactionon Automatic Control*, vol. 56 , no. 11, pp. 2655–2660, 2011.

[121] C. Peng and Y-C. Tian, "Networked $\mathcal{H}_\infty$ control of linear systems with state quantization", *Information Sciences*, vol. 177, no. 24, pp. 5763–5774, 2007.

[122] E. Tian, D. Yue, and X. Zhao, "Quantized control design for networked control systems", *IET Control Theory and Applications*, vol. 16, no. 6, pp. 1693–1699, 2007.

[123] E. Tian, D. Yue, and C. Peng, "Quantized output feedback control for networked control systems", *Information sciences*, vol. 178, no. 12, pp. 2734–2749, 2008.

[124] L. Sheng, and Y-J. Pan, "Stochastic stabilization of sampled-data networked control systems", *International Journal of Innovative Computing, Information and Control*, vol. 6, no. 4, pp. 1949–1972, 2010.

[125] S. Chae, F. Rasool, S-K. Nguang, and A. Swain, "Robust mode delay-dependent $\mathcal{H}_\infty$ control of discrete-time systems with random communication delays", *IET Control Theory and Applications*, vol. 04, no. 6, pp. 936–944, 2009.

[126] K. Zhou, and P. Khargonekar, "Robust stabilization of linear systems with norm-bounded time-varying uncertainty", *Systems & Control Letters*, vol. 10, pp. 17–20, 1988.

[127] L. Ghaoui, F. Oustry, and M. AitRami, "A cone complementarity linearization algorithm for static output-feedback and related problems", *IEEE Transactions on Automatic Control*, vol. 42, no. 8, pp. 1171–1176, 1997.

[128] F. Rasool, D. Huang, and S-K. Nguang, " Robust $\mathcal{H}_\infty$ output feedback control of discrete-time networked systems with adaptive quantizers", in the proceedings of *Conference on Decision & Conference-European Control Conference*, pp: 2381–2386, 2011.

[129] F. Yang, W. Wang, and Y. Li, "An iterative LMI approach to $\mathcal{H}_\infty$ networked control with random communication delays", *International Journal of Systems, Control and Communications*, vol. 1, no. 3, pp. 325-341, 2009.

[130] D. Huang, and S-K. Nguang, "State feedback control of uncertain networked control systems with random time-delays", *IEEE Transactions on Automatic Control*, vol. 53, pp. 829–834, 2008.

[131] L. Ma, F. Da, and K-J. Zhang, "Exponential $\mathcal{H}_\infty$ Filter Design for Discrete Time-Delay Stochastic Systems With Markovian Jump Parameters and Missing Measurements", *IEEE Transaction on Circuits and Systems-I: Regular Papers*, vol. 58, no. 5, pp. 994–1007, 2011.

[132] L. Teng, P. Wen, and W. Xiang, "Model-Based Networked Control System stability based on packet drop distributions", in the proceedings of 10th *International Conference on Control, Automation, Robotics and Vision*, pp.488–493, 2008.

[133] J. J. Westman, and F. B. Hanson, "State dependent jump models in optimal control I", *IEEE Confernce on Decision and Control*, vol. 3, pp: 2378–2383, 1999.

[134] I. Kolmanovsky, Ford Motor Co Res Lab, M. I. Dearborn, and T. L. Maizenberg, "Optimal containment control for a class of stochastic systems perturbed by Poisson and Wiener processes", in the proceedings of *American Control Conference*, vol. 1, pp. 322-327, 2002.

[135] S. Kalpakama, and K. P. Sapnaa, "A control policy of an inventory system with compound poisson demand", *Stochastic Analysis and Apllication*, vol. 11, pp. 459–482, 1993.

[136] A. P. C. Goncalves, A. R. Fioravanti, and J. C. Geromel, "Dynamic output feedback $\mathcal{H}_\infty$ control of discrete-time Markov jump linear systems through linear matrix inequalities", in the proceedings of 47th *IEEE Conference on Decision and Control*, pp. 4787–4792, 2008.

[137] H. Hamidian, and A. Jalali, "Calculation of PID Controller Parameters for Unstable First Order Time Delay Systems", *International Journal of Scientific and Engineering Research*, vol. 2, no. 3, 2011.

[138] E. Konaka, "Stability of Networked Control System with Dynamic Quantizer and Data-Driven Zero-Order Hold", in *Electronics and Communications in Japan*, vol. 94, no. 2, pp. 46-52, 2011.

[139] M.B.G. Cloosterman, L. Hetel, N. van de Wouwa, W.P.M.H. Heemels, J. Daafouz, and H. Nijmeijer, "Controller synthesis for networked control systems", *Automatica*, vol. 46, pp. 1584–1594, 2010.

[140] H. Gao, T. Chen, and J. Lam, " A new delay system approach to network-based control", in *Automatica*, vol. 44. no. 1, pp. 39–52, 2008.

[141] E. Fridman, A. Seuret, and J. P. Richard, "Robust sampled-data stabilization of linear systems: an input delay approach", *Automatica*, vol. 40, pp. 1441–1446, 2004.

[142] L. Mirkin, "Some remarks on the use of time-varying delay to model sample and hold circuits", *IEEE Transactions on Automatic Control*, vol 52, no. 6, pp. 1109–1112, 2007.

[143] H. Fujioka, "Stability analysis for a class of networked/embedded control systems: output feedback case", in the proceedings of 17th *IFAC world congress*, pp. 4210–4215, 2008.

[144] F. Rasool, S-K. Nguang, and M. Krug, "Robust $\mathcal{H}_\infty$ Output Feedback Control of Discrete-Time Networked Systems With Adaptive Quantizers", in the proceedings of 6th *IEEE Conference on Industrial Electronics and Applications* , pp. 1535–1540, 2011.

[145] J. Wu, and T. Chen, "Design of networked control systems with packet dropouts", *IEEE Transactions on Automatic Control*, vol. 52, no. 7, pp. 1314-1319, 2007.

[146] Y. Wang, and G. Yang, "Multiple communication channels-based packet dropout compensation for networked control systems", *IET Control Theory and Applications*, vol. 2, pp. 717-727, 2008.

[147] A. Bemporad, W. P. M. H Heemels, and M. Johansson, " Networked Control Systems", *Lecture Notes in Control and Information Sciences*, 2010.

[148] D. Delchamps, "Stabilizing a linear system with quantized state feedback," *IEEE Transactions on Automatic Control*, vol. 35, pp. 916–924, 1990.

[149] K. Ji, and W. J. Kim, "Real-time control of networked control systems via ethernet", *Interanational Journal of Control, Automation and Systems*, vol. 3, pp. 591–599, 2005.

[150] F. Rasool, D. Huang, and S. K. Nguang, "Robust $\mathcal{H}_\infty$ output feedback control of discrete-time networked systems with limited information", *Systems & Control Letters*, vol. 60, no. 10. pp. 845–853, 2011.

[151] F. Rasool, and S. K. Nguang, "Quantized robust control of discrete-time systems with random communication delays", *International Journal of Systems Science*, vol. 42, no. 1, pp.129–138, 2011.

[152] F. Rasool, D. Huang and S. K. Nguang, "Robust $\mathcal{H}_\infty$ output feedback control of networked control systems with multiple quantizers", *Journal of the Franklin Institute*, vol. 349, no. 3, pp. 1153-1173, 2012.

[153] E. K. Boukas, and Z. K. Liu, "Robust Stability and Stabilizability of Markov Jump Linear Uncertain Systems with Mode-Dependent Time Delays", *Journal of Optimization Theory and Applications*, vol. 109, no. 3, pp. 587–600, 2001.

[154] E. K. Boukas, P. Shi, M. Karan, and C. Y. Kaya, "Linear Discrete-time Systems with Markovian Jumps and Mode Dependent Time-delay: Stability and Stabilizability", *Mathematical Problems in Engineering*, vol. 8, no. 2, pp. 123–133, 2002.

[155] Z. H. Guan, W. H. Chen, and J. X. Xu, "Delay-dependent stability and stabilizability of uncertain jump bilinear stochastic systems with mode-dependent time-delays", *International Journal of Systems Science*, vol. 36, no. 5, pp. 275–285, 2005.

[156] W. H. Chen and W. X. Zheng, "Robust Stabilization of Delayed Markovian Jump Systems Subject to Parametric Uncertainties," in *Proceedings of the 46th IEEE Conference on Decision and Control, New Orleans, LA, USA*, pp. 3054–3059, 2007.

[157] X. Wang, and M D. Lemmon, "Event-Triggering in Distributed Networked Control Systems", *IEEE Transaction On Automatic Control*, vol. 56, no. 3, pp. 586–601, 2011.

[158] X. Meng, and T. Chen, "Event based stabilization over networks with time-varying transmission delays", in press for the *Journal of Control Science and Engineering*, 2012.

[159] K. J. Astrom, and B. M. Bernhardsson, "Comparison of Riemann and Lebesgue sampling for first order stochastic systems", in the proceedings of 41st *IEEE Conference on Decision and Control*, vol. 2, pp. 2011–2016, 2002.

[160] T. Henningsson, E. Johannesson, and A. Cervin, "Sporadic event-based control of first-order linear stochastic systems", *Automatica*, vol. 44, pp. 2890-2895, 2008.

[161] J. Lunze and D. Lehmann, "A state-feedback approach to event-based control", *Automatica*, vol. 46, pp. 211-215, 2010.

[162] P. J. Gawthrop and L. B. Wang, "Event-driven intermittent control", *International Journal Control*, vol. 82, pp. 2235-2248, 2009.

[163] T. Estrada and P. J. Antsaklis, "Stability of discrete-time plants using model-based control with intermittent feedback", in proceedings of *Mediterranean Conference on Automatic Control*, pp. 11301136, 2008.

[164] W. P. M. H. Heemels, J. H. Sandee, and P. P. J. van den Bosch, "Analysis of event-driven controllers for linear systems", International Journal of Control, vol. 81, pp. 571-590, 2008.

[165] P. G. Otanez, J. R. Moyne, and D. M. Tilbury, "Using deadbands to reduce communication in networked control systems", in the proceedings of *American Control Conference*, pp. 3015–3020, 2002.

[166] T. Fuhrer, B. Muller, W. Dieterle, F. Hartwich, R. Hugel, and M. Walther, "Time Triggered Communication on CAN (Time Triggered CAN - TTCAN)", 7th *international CAN in Automation Conference*, pp 92-98, 2000.

[167] R. Goebel, R. G. Sanfelice, and A. R. Teel, "Hybrid dynamical systems", *Control System Magazine*, vol. 2, pp. 2893, 2009.

[168] H. K. Khalil, "Nonlinear Systems", *Prentice-Hall, Upper Saddle River, NJ, Second Ed.*, 1996.

[169] J. C. Willems, "Dissipative dynamical systems, Part 1: General Theory, Part II: Linear System with quadratic supply rates", *Arch. Rational Mech. Analysis*, vol. 45, pp. 321–393, 1972.

[170] A. D. Sontag, "A universal construction of Arteins theorem on nonlinear stabilization", *Systems and Control Letters*, vol. 13, no. 2, pp. 117–123, 1989.

[171] P. A. Parrilo, "Structured semidefinite programs and semialgebraic geometry methods in robustness and optimization", *Ph.D dissertation, California Inst. Technology., Pasadena*, 2000.

[172] L. Vandennerghe, and S. Boyd, "Semi-definite programming", *SIAM Review*, vol. 38, no. 1, pp. 49–95, 1996.

[173] M. Krug, M-S. Saat, and S-K. Nguang, "Nonlinear robust $\mathcal{H}_\infty$ static output feedback controller design for parameter dependent polynomial systems: An iterative sum of squares approach", *CDC-ECE*, pp. 3502–3507, 2011.

[174] M-S. Saat, M. Krug, and S-K. Nguang, "A nonlinear static output controller design for polynomial systems: An iterative sums of squares approach", 4th *International Conference On Mechatronics (ICOM)*, pp. 1–6, 2011.

[175] R.A Gupta, M-Y. Chow, "Performance Assessment and Compensation for Secure Networked Control Systems", $34^t h$ *Annual Conference of IEEE on Industrial Electronics*, pp. 2929–2934, 2008.

List of Author's Publications

- Peer-reviewed journal papers

    1. S. Chae, F. Rasool, S-K. Nguang, and A. Swain, "Robust mode delay-dependent $\mathcal{H}_\infty$ control of discrete-time systems with random communication delays", *IET Control Theory Applications*, vol. 04, no. 6, pp. 936–944, 2009.

    2. F. Rasool and S.K. Nguang, "Quantized Robust $\mathcal{H}_\infty$ Output Feedback Control of Discrete-Time Systems with Random Communication Delays", *IET Control Theory and Applications,* 2009.

    3. F. Rasool, and S. K. Nguang, "Quantized robust $\mathcal{H}_\infty$ control of discrete-time systems with random communication delays", *International Journal of Systems Science*, vol. 42, no. 1, pp. 129–138 , 2011.

    4. F. Rasool, D. Huang and S. K. Nguang, "Robust $\mathcal{H}_\infty$ output feedback control of discrete-time networked systems with limited information", accepted in *Systems & Control Letters*, vol. 60, no. 10, pp. 845–853, 2011.

    5. F. Rasool, D. Huang and S. K. Nguang, "Robust $\mathcal{H}_\infty$ output feedback control of networked control systems with multiple quantizers", accepted in *Journal of the Franklin Institute*, vol. 349, no. 3, pp. 1153-1173, 2012.

    6. F. Rasool, S. K. Nguang, and Chih-Min Lin " Robust $\mathcal{H}_\infty$ State Feedback Control of Networked Control Systems with Congestion Control", accepted in *Circuit System & Signal processing*, 2013.

    7. F. Rasool, and S. K. Nguang, "Robust $\mathcal{H}_\infty$ Output Feedback Control of Networked Control Systems with Congestion Control", accepted in *International Journal of systems Science*, 2013.

    8. F. Rasool, and S-K. Nguang, "Robust $\mathcal{H}_\infty$ State Feedback Control of NCSs with Poisson Noise and Successive Packet Dropouts", submitted in *International Journal of Control, Automation, and Systems*, 2013.

- Conference Papers

    1. F. Rasool, and S. K. Nguang, "Quantized robust $\mathcal{H}_\infty$ output feedback control of discrete-time systems with random communication delays", in *Proceedings of 2009 IEEE International Conference on Control and Automation*, Christchurch, New Zealand, pp. 1399–1404, 2009.

    2. F. Rasool, S.K. Nguang, D. Huang and L. Zhang, "Quantized robust $\mathcal{H}_\infty$ control of discrete-time systems with random communication delays", *Conference on Decision and Control,* pp. 4081-4086, 2009.

3. F. Rasool and S.K. Nguang, "Robust $\mathcal{H}_\infty$ dynamic Output Feedback Control of NCSs with Adaptive Quantizers", published in *American Control Conference,* 2011.

4. F. Rasool and S.K. Nguang, "Robust $\mathcal{H}_\infty$ dynamic Output Feedback Control of NCSs with Multiple Quantizers", published in *American Control Conference,* 2011.

5. F. Rasool, S-K. Nguang, F A. Bhatti, S. Rehman, and T. Shahzad, "Robust $\mathcal{H}_\infty$ Output Feedback Control of Networked Control Systems with Dynamic Quantizers", *International Multitopic Conference*, pp. 222–227, 2011.

6. F. Rasool, S-K. Nguang, F A. Bhatti, S. Rehman, and T. Shahzad, "Robust $\mathcal{H}_\infty$ Output Feedback Control of Networked Control Systems with Dynamic Quantizers", *International Multitopic Conference*, pp. 222–227, 2011.

7. F. Rasool, S. K. Nguang, and T. Shahzad, "Robust $\mathcal{H}_\infty$ Output Feedback Control of Networked Control Systems with Congestion Control", accepted in *International Conference on Innovative Engineering Systems*, 2012.

8. F. Rasool, S. K. Nguang, S. Saat, J. Wu, and G. Zeng, " Robust $\mathcal{H}_\infty$ State Feedback Control of Networked Control Systems with Congestion Control", accepted in *12th International Conference on Control, Automation, Robotics and Vision*, China, 2012.

9. F. Rasool, S. K. Nguang, and T. Shahzad, "Robust $\mathcal{H}_\infty$ Output Feedback Control of Networked Control Systems with Congestion Control", accepted in *International Conference on Innovative Engineering Systems*, 2012

10. F. Rasool, S-K. Nguang, and T. Shahzad, "Robust $\mathcal{H}_\infty$ State Feedback Control of NCSs with Poisson Noise and Successive Packet Dropouts", submitted in *IEEE International Conference on Networking, Sensing and Control*, 2013.

11. F. Rasool, and S. K. Nguang, "A literature survey on the time triggered and event triggered mechanisms in networked control systems", accepted in *IET Control and Automation Conference*, 2013.

VITA

Faiz Rasool was born in Taunsa Sharif, Pakistan on January 15, 1983. He received his B. Eng from COMSATS Institute of Information Technology (CIIT), Lahore Pakistan in 2006 and M. Eng from The University of Auckland (UOA), New Zealand in 2009. He started his Ph. D. program with the department of Electrical and Computer Engineering at the University of Auckland, New Zealand , from September 2009. He is currently employed by the CIIT, Pakistan as a lecturer and now he is on study leave. His Ph. D. study is sponsored by The Higher Education Commission of Pakistan and Doctoral PReSS accounts from the University of Auckland. His research interest includes discrete-time NCSs, event-triggered control, polynomial systems and numerical computing techniques in system and control.